Chapter 4

Temporal and spatial frequency domain representation

4.1 Interpretation of the temporal transform

When a field is represented by a continuous superposition of elemental components, the resulting decomposition can simplify computation and provide physical insight. Such representation is usually accomplished through the use of an integral transform. Although several different transforms are used in electromagnetics, we shall concentrate on the powerful and efficient Fourier transform.

Let us consider the Fourier transform of the electromagnetic field. The field depends on x, y, z, t, and we can transform with respect to any or all of these variables. However, a consideration of units leads us to consider a transform over t separately. Let $\psi(\mathbf{r}, t)$ represent any rectangular component of the electric or magnetic field. Then the temporal transform will be designated by $\tilde{\psi}(\mathbf{r}, \omega)$:

$$\psi(\mathbf{r}, t) \leftrightarrow \tilde{\psi}(\mathbf{r}, \omega).$$

Here ω is the transform variable. The transform field $\tilde{\psi}$ is calculated using (A.1):

$$\tilde{\psi}(\mathbf{r}, \omega) = \int_{-\infty}^{\infty} \psi(\mathbf{r}, t)\, e^{-j\omega t}\, dt. \tag{4.1}$$

The inverse transform is, by (A.2),

$$\psi(\mathbf{r}, t) = \frac{1}{2\pi} \int_{-\infty}^{\infty} \tilde{\psi}(\mathbf{r}, \omega)\, e^{j\omega t}\, d\omega. \tag{4.2}$$

Since $\tilde{\psi}$ is complex it may be written in amplitude–phase form:

$$\tilde{\psi}(\mathbf{r}, \omega) = |\tilde{\psi}(\mathbf{r}, \omega)| e^{j\xi^{\psi}(\mathbf{r}, \omega)},$$

where we take $-\pi < \xi^{\psi}(\mathbf{r}, \omega) \le \pi$.

Since $\psi(\mathbf{r}, t)$ must be real, (4.1) shows that

$$\tilde{\psi}(\mathbf{r}, -\omega) = \tilde{\psi}^*(\mathbf{r}, \omega). \tag{4.3}$$

Furthermore, the transform of the derivative of ψ may be found by differentiating (4.2). We have

$$\frac{\partial}{\partial t}\psi(\mathbf{r}, t) = \frac{1}{2\pi} \int_{-\infty}^{\infty} j\omega\tilde{\psi}(\mathbf{r}, \omega)\, e^{j\omega t}\, d\omega,$$

hence

$$\frac{\partial}{\partial t}\psi(\mathbf{r},t) \leftrightarrow j\omega\tilde{\psi}(\mathbf{r},\omega). \tag{4.4}$$

By virtue of (4.2), any electromagnetic field component can be decomposed into a continuous, weighted superposition of elemental temporal terms $e^{j\omega t}$. Note that the weighting factor $\tilde{\psi}(\mathbf{r},\omega)$, often called the *frequency spectrum* of $\psi(\mathbf{r},t)$, is not arbitrary because $\psi(\mathbf{r},t)$ must obey a scalar wave equation such as (2.327). For a source-free region of space we have

$$\left(\nabla^2 - \mu\sigma\frac{\partial}{\partial t} - \mu\epsilon\frac{\partial^2}{\partial t^2}\right)\frac{1}{2\pi}\int_{-\infty}^{\infty}\tilde{\psi}(\mathbf{r},\omega)\,e^{j\omega t}\,d\omega = 0.$$

Differentiating under the integral sign we have

$$\frac{1}{2\pi}\int_{-\infty}^{\infty}\left[\left(\nabla^2 - j\omega\mu\sigma + \omega^2\mu\epsilon\right)\tilde{\psi}(\mathbf{r},\omega)\right]e^{j\omega t}\,d\omega = 0,$$

hence by the Fourier integral theorem

$$\left(\nabla^2 + k^2\right)\tilde{\psi}(\mathbf{r},\omega) = 0 \tag{4.5}$$

where

$$k = \omega\sqrt{\mu\epsilon}\sqrt{1 - j\frac{\sigma}{\omega\epsilon}}$$

is the *wavenumber*. Equation (4.5) is called the *scalar Helmholtz equation*, and represents the wave equation in the temporal frequency domain.

4.2 The frequency-domain Maxwell equations

If the region of interest contains sources, we can return to Maxwell's equations and represent all quantities using the temporal inverse Fourier transform. We have, for example,

$$\mathbf{E}(\mathbf{r},t) = \frac{1}{2\pi}\int_{-\infty}^{\infty}\tilde{\mathbf{E}}(\mathbf{r},\omega)\,e^{j\omega t}\,d\omega$$

where

$$\tilde{\mathbf{E}}(\mathbf{r},\omega) = \sum_{i=1}^{3}\hat{\mathbf{i}}_i\tilde{E}_i(\mathbf{r},\omega) = \sum_{i=1}^{3}\hat{\mathbf{i}}_i|\tilde{E}_i(\mathbf{r},\omega)|e^{j\xi_i^E(\mathbf{r},\omega)}. \tag{4.6}$$

All other field quantities will be written similarly with an appropriate superscript on the phase. Substitution into Ampere's law gives

$$\nabla\times\frac{1}{2\pi}\int_{-\infty}^{\infty}\tilde{\mathbf{H}}(\mathbf{r},\omega)\,e^{j\omega t}\,d\omega = \frac{\partial}{\partial t}\frac{1}{2\pi}\int_{-\infty}^{\infty}\tilde{\mathbf{D}}(\mathbf{r},\omega)\,e^{j\omega t}\,d\omega + \frac{1}{2\pi}\int_{-\infty}^{\infty}\tilde{\mathbf{J}}(\mathbf{r},\omega)\,e^{j\omega t}\,d\omega,$$

hence

$$\frac{1}{2\pi}\int_{-\infty}^{\infty}[\nabla\times\tilde{\mathbf{H}}(\mathbf{r},\omega) - j\omega\tilde{\mathbf{D}}(\mathbf{r},\omega) - \tilde{\mathbf{J}}(\mathbf{r},\omega)]e^{j\omega t}\,d\omega = 0$$

after we differentiate under the integral signs and combine terms. So

$$\nabla \times \tilde{\mathbf{H}} = j\omega\tilde{\mathbf{D}} + \tilde{\mathbf{J}} \tag{4.7}$$

by the Fourier integral theorem. This version of Ampere's law involves only the frequency-domain fields. By similar reasoning we have

$$\nabla \times \tilde{\mathbf{E}} = -j\omega\tilde{\mathbf{B}}, \tag{4.8}$$
$$\nabla \cdot \tilde{\mathbf{D}} = \tilde{\rho}, \tag{4.9}$$
$$\nabla \cdot \tilde{\mathbf{B}}(\mathbf{r}, \omega) = 0, \tag{4.10}$$

and

$$\nabla \cdot \tilde{\mathbf{J}} + j\omega\tilde{\rho} = 0.$$

Equations (4.7)–(4.10) govern the temporal spectra of the electromagnetic fields. We may manipulate them to obtain wave equations, and apply the boundary conditions from the following section. After finding the frequency-domain fields we may find the temporal fields by Fourier inversion. The frequency-domain equations involve one fewer derivative (the time derivative has been replaced by multiplication by $j\omega$), hence may be easier to solve. However, the inverse transform may be difficult to compute.

4.3 Boundary conditions on the frequency-domain fields

Several boundary conditions on the source and mediating fields were derived in § 2.8.2. For example, we found that the tangential electric field must obey

$$\hat{\mathbf{n}}_{12} \times \mathbf{E}_1(\mathbf{r}, t) - \hat{\mathbf{n}}_{12} \times \mathbf{E}_2(\mathbf{r}, t) = -\mathbf{J}_{ms}(\mathbf{r}, t).$$

The technique of the previous section gives us

$$\hat{\mathbf{n}}_{12} \times [\tilde{\mathbf{E}}_1(\mathbf{r}, \omega) - \tilde{\mathbf{E}}_2(\mathbf{r}, \omega)] = -\tilde{\mathbf{J}}_{ms}(\mathbf{r}, \omega)$$

as the condition satisfied by the frequency-domain electric field. The remaining boundary conditions are treated similarly. Let us summarize the results, including the effects of fictitious magnetic sources:

$$\hat{\mathbf{n}}_{12} \times (\tilde{\mathbf{H}}_1 - \tilde{\mathbf{H}}_2) = \tilde{\mathbf{J}}_s,$$
$$\hat{\mathbf{n}}_{12} \times (\tilde{\mathbf{E}}_1 - \tilde{\mathbf{E}}_2) = -\tilde{\mathbf{J}}_{ms},$$
$$\hat{\mathbf{n}}_{12} \cdot (\tilde{\mathbf{D}}_1 - \tilde{\mathbf{D}}_2) = \tilde{\rho}_s,$$
$$\hat{\mathbf{n}}_{12} \cdot (\tilde{\mathbf{B}}_1 - \tilde{\mathbf{B}}_2) = \tilde{\rho}_{ms},$$

and

$$\hat{\mathbf{n}}_{12} \cdot (\tilde{\mathbf{J}}_1 - \tilde{\mathbf{J}}_2) = -\nabla_s \cdot \tilde{\mathbf{J}}_s - j\omega\tilde{\rho}_s,$$
$$\hat{\mathbf{n}}_{12} \cdot (\tilde{\mathbf{J}}_{m1} - \tilde{\mathbf{J}}_{m2}) = -\nabla_s \cdot \tilde{\mathbf{J}}_{ms} - j\omega\tilde{\rho}_{ms}.$$

Here $\hat{\mathbf{n}}_{12}$ points into region 1 from region 2.

4.4 Constitutive relations in the frequency domain and the Kronig–Kramers relations

All materials are to some extent dispersive. If a field applied to a material undergoes a sufficiently rapid change, there is a time lag in the response of the polarization or magnetization of the atoms. It has been found that such materials have constitutive relations involving products in the frequency domain, and that the frequency-domain constitutive parameters are complex, frequency-dependent quantities. We shall restrict ourselves to the special case of anisotropic materials and refer the reader to Kong [101] and Lindell [113] for the more general case. For anisotropic materials we write

$$\tilde{\mathbf{P}} = \epsilon_0 \tilde{\bar{\boldsymbol{\chi}}}_e \cdot \tilde{\mathbf{E}}, \tag{4.11}$$

$$\tilde{\mathbf{M}} = \tilde{\bar{\boldsymbol{\chi}}}_m \cdot \tilde{\mathbf{H}}, \tag{4.12}$$

$$\tilde{\mathbf{D}} = \tilde{\bar{\boldsymbol{\epsilon}}} \cdot \tilde{\mathbf{E}} = \epsilon_0 [\bar{\mathbf{I}} + \tilde{\bar{\boldsymbol{\chi}}}_e] \cdot \tilde{\mathbf{E}}, \tag{4.13}$$

$$\tilde{\mathbf{B}} = \tilde{\bar{\boldsymbol{\mu}}} \cdot \tilde{\mathbf{H}} = \mu_0 [\bar{\mathbf{I}} + \tilde{\bar{\boldsymbol{\chi}}}_m] \cdot \tilde{\mathbf{H}}, \tag{4.14}$$

$$\tilde{\mathbf{J}} = \tilde{\bar{\boldsymbol{\sigma}}} \cdot \tilde{\mathbf{E}}. \tag{4.15}$$

By the convolution theorem and the assumption of causality we immediately obtain the dyadic versions of (2.29)–(2.31):

$$\mathbf{D}(\mathbf{r}, t) = \epsilon_0 \left(\mathbf{E}(\mathbf{r}, t) + \int_{-\infty}^{t} \bar{\chi}_e(\mathbf{r}, t - t') \cdot \mathbf{E}(\mathbf{r}, t')\, dt' \right),$$

$$\mathbf{B}(\mathbf{r}, t) = \mu_0 \left(\mathbf{H}(\mathbf{r}, t) + \int_{-\infty}^{t} \bar{\chi}_m(\mathbf{r}, t - t') \cdot \mathbf{H}(\mathbf{r}, t')\, dt' \right),$$

$$\mathbf{J}(\mathbf{r}, t) = \int_{-\infty}^{t} \bar{\boldsymbol{\sigma}}(\mathbf{r}, t - t') \cdot \mathbf{E}(\mathbf{r}, t')\, dt'.$$

These describe the essential behavior of a dispersive material. The susceptances and conductivity, describing the response of the atomic structure to an applied field, depend not only on the present value of the applied field but on all past values as well.

Now since $\mathbf{D}(\mathbf{r}, t)$, $\mathbf{B}(\mathbf{r}, t)$, and $\mathbf{J}(\mathbf{r}, t)$ are all real, so are the entries in the dyadic matrices $\bar{\boldsymbol{\epsilon}}(\mathbf{r}, t)$, $\bar{\boldsymbol{\mu}}(\mathbf{r}, t)$, and $\bar{\boldsymbol{\sigma}}(\mathbf{r}, t)$. Thus, applying (4.3) to each entry we must have

$$\tilde{\bar{\boldsymbol{\chi}}}_e(\mathbf{r}, -\omega) = \tilde{\bar{\boldsymbol{\chi}}}_e^*(\mathbf{r}, \omega), \quad \tilde{\bar{\boldsymbol{\chi}}}_m(\mathbf{r}, -\omega) = \tilde{\bar{\boldsymbol{\chi}}}_m^*(\mathbf{r}, \omega), \quad \tilde{\bar{\boldsymbol{\sigma}}}(\mathbf{r}, -\omega) = \tilde{\bar{\boldsymbol{\sigma}}}^*(\mathbf{r}, \omega), \tag{4.16}$$

and hence

$$\tilde{\bar{\boldsymbol{\epsilon}}}(\mathbf{r}, -\omega) = \tilde{\bar{\boldsymbol{\epsilon}}}^*(\mathbf{r}, \omega), \qquad \tilde{\bar{\boldsymbol{\mu}}}(\mathbf{r}, -\omega) = \tilde{\bar{\boldsymbol{\mu}}}^*(\mathbf{r}, \omega). \tag{4.17}$$

If we write the constitutive parameters in terms of real and imaginary parts as

$$\tilde{\epsilon}_{ij} = \tilde{\epsilon}'_{ij} + j\tilde{\epsilon}''_{ij}, \qquad \tilde{\mu}_{ij} = \tilde{\mu}'_{ij} + j\tilde{\mu}''_{ij}, \qquad \tilde{\sigma}_{ij} = \tilde{\sigma}'_{ij} + j\tilde{\sigma}''_{ij},$$

these conditions become

$$\tilde{\epsilon}'_{ij}(\mathbf{r}, -\omega) = \tilde{\epsilon}'_{ij}(\mathbf{r}, \omega), \qquad \tilde{\epsilon}''_{ij}(\mathbf{r}, -\omega) = -\tilde{\epsilon}''_{ij}(\mathbf{r}, \omega),$$

and so on. Therefore the real parts of the constitutive parameters are even functions of frequency, and the imaginary parts are odd functions of frequency.

In most instances, the presence of an imaginary part in the constitutive parameters implies that the material is either *dissipative* (*lossy*), transforming some of the electromagnetic energy in the fields into thermal energy, or *active*, transforming the chemical or mechanical energy of the material into energy in the fields. We investigate this further in § 4.5 and § 4.8.3.

We can also write the constitutive equations in amplitude–phase form. Letting

$$\tilde{\epsilon}_{ij} = |\tilde{\epsilon}_{ij}|e^{j\xi^{\epsilon}_{ij}}, \qquad \tilde{\mu}_{ij} = |\tilde{\mu}_{ij}|e^{j\xi^{\mu}_{ij}}, \qquad \tilde{\sigma}_{ij} = |\tilde{\sigma}_{ij}|e^{j\xi^{\sigma}_{ij}},$$

and using the field notation (4.6), we can write (4.13)–(4.15) as

$$\tilde{D}_i = |\tilde{D}_i|e^{j\xi^D_i} = \sum_{j=1}^{3} |\tilde{\epsilon}_{ij}||\tilde{E}_j|e^{j[\xi^E_j + \xi^{\epsilon}_{ij}]}, \tag{4.18}$$

$$\tilde{B}_i = |\tilde{B}_i|e^{j\xi^B_i} = \sum_{j=1}^{3} |\tilde{\mu}_{ij}||\tilde{H}_j|e^{j[\xi^H_j + \xi^{\mu}_{ij}]}, \tag{4.19}$$

$$\tilde{J}_i = |\tilde{J}_i|e^{j\xi^J_i} = \sum_{j=1}^{3} |\tilde{\sigma}_{ij}||\tilde{E}_j|e^{j[\xi^E_j + \xi^{\sigma}_{ij}]}. \tag{4.20}$$

Here we remember that the amplitudes and phases may be functions of both $\mathbf{r}$ and ω. For isotropic materials these reduce to

$$\tilde{D}_i = |\tilde{D}_i|e^{j\xi^D_i} = |\tilde{\epsilon}||\tilde{E}_i|e^{j(\xi^E_i + \xi^{\epsilon})}, \tag{4.21}$$

$$\tilde{B}_i = |\tilde{B}_i|e^{j\xi^B_i} = |\tilde{\mu}||\tilde{H}_i|e^{j(\xi^H_i + \xi^{\mu})}, \tag{4.22}$$

$$\tilde{J}_i = |\tilde{J}_i|e^{j\xi^J_i} = |\tilde{\sigma}||\tilde{E}_i|e^{j(\xi^E_i + \xi^{\sigma})}. \tag{4.23}$$

4.4.1 The complex permittivity

As mentioned above, dissipative effects may be associated with complex entries in the permittivity matrix. Since conduction effects can also lead to dissipation, the permittivity and conductivity matrices are often combined to form a *complex permittivity*. Writing the current as a sum of impressed and secondary conduction terms ($\tilde{\mathbf{J}} = \tilde{\mathbf{J}}^i + \tilde{\mathbf{J}}^c$) and substituting (4.13) and (4.15) into Ampere's law, we find

$$\nabla \times \tilde{\mathbf{H}} = \tilde{\mathbf{J}}^i + \tilde{\bar{\boldsymbol{\sigma}}} \cdot \tilde{\mathbf{E}} + j\omega\tilde{\bar{\boldsymbol{\epsilon}}} \cdot \tilde{\mathbf{E}}.$$

Defining the complex permittivity

$$\tilde{\bar{\boldsymbol{\epsilon}}}^c(\mathbf{r},\omega) = \frac{\tilde{\bar{\boldsymbol{\sigma}}}(\mathbf{r},\omega)}{j\omega} + \tilde{\bar{\boldsymbol{\epsilon}}}(\mathbf{r},\omega), \tag{4.24}$$

we have

$$\nabla \times \tilde{\mathbf{H}} = \tilde{\mathbf{J}}^i + j\omega\tilde{\bar{\boldsymbol{\epsilon}}}^c \cdot \tilde{\mathbf{E}}.$$

Using the complex permittivity we can include the effects of conduction current by merely replacing the total current with the impressed current. Since Faraday's law is unaffected, any equation (such as the wave equation) derived previously using total current retains its form with the same substitution.

By (4.16) and (4.17) the complex permittivity obeys

$$\tilde{\bar{\boldsymbol{\epsilon}}}^c(\mathbf{r},-\omega) = \tilde{\bar{\boldsymbol{\epsilon}}}^{c*}(\mathbf{r},\omega) \tag{4.25}$$

or

$$\tilde{\epsilon}^{c\prime}_{ij}(\mathbf{r},-\omega) = \tilde{\epsilon}^{c\prime}_{ij}(\mathbf{r},\omega), \qquad \tilde{\epsilon}^{c\prime\prime}_{ij}(\mathbf{r},-\omega) = -\tilde{\epsilon}^{c\prime\prime}_{ij}(\mathbf{r},\omega).$$

For an isotropic material it takes the particularly simple form

$$\tilde{\epsilon}^c = \frac{\tilde{\sigma}}{j\omega} + \tilde{\epsilon} = \frac{\tilde{\sigma}}{j\omega} + \epsilon_0 + \epsilon_0\tilde{\chi}_e, \tag{4.26}$$

and we have

$$\tilde{\epsilon}^{c\prime}(\mathbf{r},-\omega) = \tilde{\epsilon}^{c\prime}(\mathbf{r},\omega), \qquad \tilde{\epsilon}^{c\prime\prime}(\mathbf{r},-\omega) = -\tilde{\epsilon}^{c\prime\prime}(\mathbf{r},\omega). \tag{4.27}$$

4.4.2 High and low frequency behavior of constitutive parameters

At low frequencies the permittivity reduces to the electrostatic permittivity. Since $\tilde{\epsilon}'$ is even in ω and $\tilde{\epsilon}''$ is odd, we have for small ω

$$\tilde{\epsilon}' \sim \epsilon_0\epsilon_r, \qquad \tilde{\epsilon}'' \sim \omega.$$

If the material has some dc conductivity σ_0, then for low frequencies the complex permittivity behaves as

$$\tilde{\epsilon}^{c\prime} \sim \epsilon_0\epsilon_r, \qquad \tilde{\epsilon}^{c\prime\prime} \sim \sigma_0/\omega. \tag{4.28}$$

If **E** or **H** changes very rapidly, there may be no polarization or magnetization effect at all. This occurs at frequencies so high that the atomic structure of the material cannot respond to the rapidly oscillating applied field. Above some frequency then, we can assume $\tilde{\bar{\boldsymbol{\chi}}}_e = 0$ and $\tilde{\bar{\boldsymbol{\chi}}}_m = 0$ so that

$$\tilde{\mathbf{P}} = 0, \qquad \tilde{\mathbf{M}} = 0,$$

and

$$\tilde{\mathbf{D}} = \epsilon_0\tilde{\mathbf{E}}, \qquad \tilde{\mathbf{B}} = \mu_0\tilde{\mathbf{H}}.$$

In our simple models of dielectric materials (§ 4.6) we find that as ω becomes large

$$\tilde{\epsilon}' - \epsilon_0 \sim 1/\omega^2, \qquad \tilde{\epsilon}'' \sim 1/\omega^3. \tag{4.29}$$

Our assumption of a macroscopic model of matter provides a fairly strict upper frequency limit to the range of validity of the constitutive parameters. We must assume that the wavelength of the electromagnetic field is large compared to the size of the atomic structure. This limit suggests that permittivity and permeability might remain meaningful even at optical frequencies, and for dielectrics this is indeed the case since the values of $\tilde{\mathbf{P}}$ remain significant. However, $\tilde{\mathbf{M}}$ becomes insignificant at much lower frequencies, and at optical frequencies we may use $\tilde{\mathbf{B}} = \mu_0\tilde{\mathbf{H}}$ [107].

4.4.3 The Kronig–Kramers relations

The principle of causality is clearly implicit in (2.29)–(2.31). We shall demonstrate that causality leads to explicit relationships between the real and imaginary parts of the frequency-domain constitutive parameters. For simplicity we concentrate on the isotropic case and merely note that the present analysis may be applied to all the dyadic components of an anisotropic constitutive parameter. We also concentrate on the complex permittivity and extend the results to permeability by induction.

The implications of causality on the behavior of the constitutive parameters in the time domain can be easily identified. Writing (2.29) and (2.31) after setting $u = t - t'$ and then $u = t'$, we have

$$\mathbf{D}(\mathbf{r}, t) = \epsilon_0 \mathbf{E}(\mathbf{r}, t) + \epsilon_0 \int_0^\infty \chi_e(\mathbf{r}, t')\mathbf{E}(\mathbf{r}, t - t')\, dt',$$

$$\mathbf{J}(\mathbf{r}, t) = \int_0^\infty \sigma(\mathbf{r}, t')\mathbf{E}(\mathbf{r}, t - t')\, dt'.$$

We see that there is no contribution from values of $\chi_e(\mathbf{r}, t)$ or $\sigma(\mathbf{r}, t)$ for times $t < 0$. So we can write

$$\mathbf{D}(\mathbf{r}, t) = \epsilon_0 \mathbf{E}(\mathbf{r}, t) + \epsilon_0 \int_{-\infty}^\infty \chi_e(\mathbf{r}, t')\mathbf{E}(\mathbf{r}, t - t')\, dt',$$

$$\mathbf{J}(\mathbf{r}, t) = \int_{-\infty}^\infty \sigma(\mathbf{r}, t')\mathbf{E}(\mathbf{r}, t - t')\, dt',$$

with the additional assumption

$$\chi_e(\mathbf{r}, t) = 0, \quad t < 0, \qquad\qquad \sigma(\mathbf{r}, t) = 0, \quad t < 0. \tag{4.30}$$

By (4.30) we can write the frequency-domain complex permittivity (4.26) as

$$\tilde{\epsilon}^c(\mathbf{r}, \omega) - \epsilon_0 = \frac{1}{j\omega} \int_0^\infty \sigma(\mathbf{r}, t')e^{-j\omega t'}\, dt' + \epsilon_0 \int_0^\infty \chi_e(\mathbf{r}, t')e^{-j\omega t'}\, dt'. \tag{4.31}$$

In order to derive the Kronig–Kramers relations we must understand the behavior of $\tilde{\epsilon}^c(\mathbf{r}, \omega) - \epsilon_0$ in the complex ω-plane. Writing $\omega = \omega_r + j\omega_i$, we need to establish the following two properties.

Property 1: The function $\tilde{\epsilon}^c(\mathbf{r}, \omega) - \epsilon_0$ is analytic in the lower half-plane ($\omega_i < 0$) except at $\omega = 0$ where it has a simple pole.

We can establish the analyticity of $\tilde{\sigma}(\mathbf{r}, \omega)$ by integrating over any closed contour in the lower half-plane. We have

$$\oint_\Gamma \tilde{\sigma}(\mathbf{r}, \omega)\, d\omega = \oint_\Gamma \left[\int_0^\infty \sigma(\mathbf{r}, t')e^{-j\omega t'}\, dt'\right] d\omega = \int_0^\infty \sigma(\mathbf{r}, t') \left[\oint_\Gamma e^{-j\omega t'}\, d\omega\right] dt'. \tag{4.32}$$

Note that an exchange in the order of integration in the above expression is only valid for ω in the lower half-plane where $\lim_{t' \to \infty} e^{-j\omega t'} = 0$. Since the function $f(\omega) = e^{-j\omega t'}$ is analytic in the lower half-plane, its closed contour integral is zero by the Cauchy–Goursat theorem. Thus, by (4.32) we have

$$\oint_\Gamma \tilde{\sigma}(\mathbf{r}, \omega)\, d\omega = 0.$$

Then, since $\tilde{\sigma}$ may be assumed to be continuous in the lower half-plane for a physical medium, and since its closed path integral is zero for all possible paths Γ, it is by Morera's theorem [110] analytic in the lower half-plane. By similar reasoning $\chi_e(\mathbf{r}, \omega)$ is analytic in the lower half-plane. Since the function $1/\omega$ has a simple pole at $\omega = 0$, the composite function $\tilde{\epsilon}^c(\mathbf{r}, \omega) - \epsilon_0$ given by (4.31) is analytic in the lower half-plane excluding $\omega = 0$ where it has a simple pole.

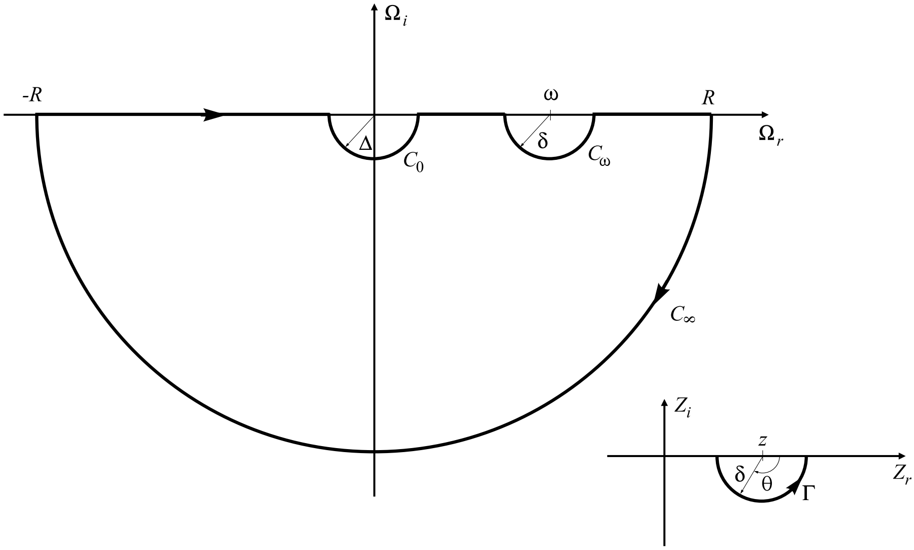

Figure 4.1: Complex integration contour used to establish the Kronig–Kramers relations.

Property 2: We have

$$\lim_{\omega\to\pm\infty} \tilde{\epsilon}^c(\mathbf{r},\omega) - \epsilon_0 = 0.$$

To establish this property we need the *Riemann–Lebesgue lemma* [142], which states that if $f(t)$ is absolutely integrable on the interval (a, b) where a and b are finite or infinite constants, then

$$\lim_{\omega\to\pm\infty} \int_a^b f(t)e^{-j\omega t}\, dt = 0.$$

From this we see that

$$\lim_{\omega\to\pm\infty} \frac{\tilde{\sigma}(\mathbf{r},\omega)}{j\omega} = \lim_{\omega\to\pm\infty} \frac{1}{j\omega} \int_0^\infty \sigma(\mathbf{r},t')e^{-j\omega t'}\, dt' = 0,$$

$$\lim_{\omega\to\pm\infty} \epsilon_0\chi_e(\mathbf{r},\omega) = \lim_{\omega\to\pm\infty} \epsilon_0 \int_0^\infty \chi_e(\mathbf{r},t')e^{-j\omega t'}\, dt' = 0,$$

and thus

$$\lim_{\omega\to\pm\infty} \tilde{\epsilon}^c(\mathbf{r},\omega) - \epsilon_0 = 0.$$

To establish the Kronig–Kramers relations we examine the integral

$$\oint_\Gamma \frac{\tilde{\epsilon}^c(\mathbf{r},\Omega) - \epsilon_0}{\Omega - \omega}\, d\Omega$$

where Γ is the contour shown in Figure 4.1. Since the points $\Omega = 0, \omega$ are excluded, the integrand is analytic everywhere within and on Γ, hence the integral vanishes by the Cauchy–Goursat theorem. By Property 2 we have

$$\lim_{R\to\infty} \int_{C_\infty} \frac{\tilde{\epsilon}^c(\mathbf{r},\Omega) - \epsilon_0}{\Omega - \omega}\, d\Omega = 0,$$

hence

$$\int_{C_0+C_\omega} \frac{\tilde{\epsilon}^c(\mathbf{r},\Omega)-\epsilon_0}{\Omega-\omega}\,d\Omega + \text{P.V.}\int_{-\infty}^{\infty} \frac{\tilde{\epsilon}^c(\mathbf{r},\Omega)-\epsilon_0}{\Omega-\omega}\,d\Omega = 0. \tag{4.33}$$

Here "P.V." indicates that the integral is computed in the Cauchy principal value sense (see Appendix A). To evaluate the integrals over C_0 and C_ω, consider a function $f(Z)$ analytic in the lower half of the Z-plane ($Z = Z_r + jZ_i$). If the point z lies on the real axis as shown in Figure 4.1, we can calculate the integral

$$F(z) = \lim_{\delta\to 0}\int_\Gamma \frac{f(Z)}{Z-z}\,dZ$$

through the parameterization $Z - z = \delta e^{j\theta}$. Since $dZ = j\delta e^{j\theta}\,d\theta$ we have

$$F(z) = \lim_{\delta\to 0}\int_{-\pi}^{0} \frac{f\left(z+\delta e^{j\theta}\right)}{\delta e^{j\theta}}\left[j\delta e^{j\theta}\right]d\theta = jf(z)\int_{-\pi}^{0} d\theta = j\pi f(z).$$

Replacing Z by Ω and z by 0 we can compute

$$\begin{aligned}
&\lim_{\Delta\to 0}\int_{C_0} \frac{\tilde{\epsilon}^c(\mathbf{r},\Omega)-\epsilon_0}{\Omega-\omega}\,d\Omega \\
&\quad= \lim_{\Delta\to 0}\int_{C_0} \frac{\left[\frac{1}{j}\int_0^\infty \sigma(\mathbf{r},t')e^{-j\Omega t'}\,dt' + \Omega\epsilon_0\int_0^\infty \chi_e(\mathbf{r},t')e^{-j\Omega t'}\,dt'\right]\frac{1}{\Omega-\omega}}{\Omega}\,d\Omega \\
&\quad= -\frac{\pi\int_0^\infty \sigma(\mathbf{r},t')\,dt'}{\omega}.
\end{aligned}$$

We recognize

$$\int_0^\infty \sigma(\mathbf{r},t')\,dt' = \sigma_0(\mathbf{r})$$

as the dc conductivity and write

$$\lim_{\Delta\to 0}\int_{C_0} \frac{\tilde{\epsilon}^c(\mathbf{r},\Omega)-\epsilon_0}{\Omega-\omega}\,d\Omega = -\frac{\pi\sigma_0(\mathbf{r})}{\omega}.$$

If we replace Z by Ω and z by ω we get

$$\lim_{\delta\to 0}\int_{C_\omega} \frac{\tilde{\epsilon}^c(\mathbf{r},\Omega)-\epsilon_0}{\Omega-\omega}\,d\Omega = j\pi\tilde{\epsilon}^c(\mathbf{r},\omega) - j\pi\epsilon_0.$$

Substituting these into (4.33) we have

$$\tilde{\epsilon}^c(\mathbf{r},\omega)-\epsilon_0 = -\frac{1}{j\pi}\,\text{P.V.}\int_{-\infty}^{\infty} \frac{\tilde{\epsilon}^c(\mathbf{r},\Omega)-\epsilon_0}{\Omega-\omega}\,d\Omega + \frac{\sigma_0(\mathbf{r})}{j\omega}. \tag{4.34}$$

If we write $\tilde{\epsilon}^c(\mathbf{r},\omega) = \tilde{\epsilon}^{c\prime}(\mathbf{r},\omega) + j\tilde{\epsilon}^{c\prime\prime}(\mathbf{r},\omega)$ and equate real and imaginary parts in (4.34) we find that

$$\tilde{\epsilon}^{c\prime}(\mathbf{r},\omega)-\epsilon_0 = -\frac{1}{\pi}\,\text{P.V.}\int_{-\infty}^{\infty} \frac{\tilde{\epsilon}^{c\prime\prime}(\mathbf{r},\Omega)}{\Omega-\omega}\,d\Omega, \tag{4.35}$$

$$\tilde{\epsilon}^{c\prime\prime}(\mathbf{r},\omega) = \frac{1}{\pi}\,\text{P.V.}\int_{-\infty}^{\infty} \frac{\tilde{\epsilon}^{c\prime}(\mathbf{r},\Omega)-\epsilon_0}{\Omega-\omega}\,d\Omega - \frac{\sigma_0(\mathbf{r})}{\omega}. \tag{4.36}$$

These are the *Kronig–Kramers relations*, named after R. de L. Kronig and H.A. Kramers who derived them independently. The expressions show that causality requires the real and imaginary parts of the permittivity to depend upon each other through the Hilbert transform pair [142].

It is often more convenient to write the Kronig–Kramers relations in a form that employs only positive frequencies. This can be accomplished using the even–odd behavior of the real and imaginary parts of $\tilde{\epsilon}^c$. Breaking the integrals in (4.35)–(4.36) into the ranges $(-\infty, 0)$ and $(0, \infty)$, and substituting from (4.27), we can show that

$$\tilde{\epsilon}^{c\prime}(\mathbf{r}, \omega) - \epsilon_0 = -\frac{2}{\pi} \text{P.V.} \int_0^\infty \frac{\Omega \tilde{\epsilon}^{c\prime\prime}(\mathbf{r}, \Omega)}{\Omega^2 - \omega^2} \, d\Omega, \tag{4.37}$$

$$\tilde{\epsilon}^{c\prime\prime}(\mathbf{r}, \omega) = \frac{2\omega}{\pi} \text{P.V.} \int_0^\infty \frac{\tilde{\epsilon}^{c\prime}(\mathbf{r}, \Omega)}{\Omega^2 - \omega^2} \, d\Omega - \frac{\sigma_0(\mathbf{r})}{\omega}. \tag{4.38}$$

The symbol P.V. in this case indicates that values of the integrand around both $\Omega = 0$ and $\Omega = \omega$ must be excluded from the integration. The details of the derivation of (4.37)–(4.38) are left as an exercise. We shall use (4.37) in § 4.6 to demonstrate the Kronig–Kramers relationship for a model of complex permittivity of an actual material.

We cannot specify $\tilde{\epsilon}^{c\prime}$ arbitrarily; for a passive medium $\tilde{\epsilon}^{c\prime\prime}$ must be zero or negative at all values of ω, and (4.36) will not necessarily return these required values. However, if we have a good measurement or physical model for $\tilde{\epsilon}^{c\prime\prime}$, as might come from studies of the absorbing properties of the material, we can approximate the real part of the permittivity using (4.35). We shall demonstrate this using simple models for permittivity in § 4.6.

The Kronig–Kramers properties hold for μ as well. We must for practical reasons consider the fact that magnetization becomes unimportant at a much lower frequency than does polarization, so that the infinite integrals in the Kronig–Kramers relations should be truncated at some upper frequency ω_{max}. If we use a model or measured values of $\tilde{\mu}''$ to determine $\tilde{\mu}'$, the form of the relation (4.37) should be [107]

$$\tilde{\mu}'(\mathbf{r}, \omega) - \mu_0 = -\frac{2}{\pi} \text{P.V.} \int_0^{\omega_{\text{max}}} \frac{\Omega \tilde{\mu}''(\mathbf{r}, \Omega)}{\Omega^2 - \omega^2} d\Omega,$$

where ω_{max} is the frequency at which magnetization ceases to be important, and above which $\tilde{\mu} = \mu_0$.

4.5 Dissipated and stored energy in a dispersive medium

Let us write down Poynting's power balance theorem for a dispersive medium. Writing $\mathbf{J} = \mathbf{J}^i + \mathbf{J}^c$ we have (§ 2.9.5)

$$-\mathbf{J}^i \cdot \mathbf{E} = \mathbf{J}^c \cdot \mathbf{E} + \nabla \cdot [\mathbf{E} \times \mathbf{H}] + \left[\mathbf{E} \cdot \frac{\partial \mathbf{D}}{\partial t} + \mathbf{H} \cdot \frac{\partial \mathbf{B}}{\partial t} \right]. \tag{4.39}$$

We cannot express this in terms of the time rate of change of a stored energy density because of the difficulty in interpreting the term

$$\mathbf{E} \cdot \frac{\partial \mathbf{D}}{\partial t} + \mathbf{H} \cdot \frac{\partial \mathbf{B}}{\partial t} \tag{4.40}$$

when the constitutive parameters have the form (2.29)–(2.31). Physically, this term describes both the energy stored in the electromagnetic field *and* the energy dissipated by the material because of time lags between the application of **E** and **H** and the polarization or magnetization of the atoms (and thus the response fields **D** and **B**). In principle this term can also be used to describe *active* media that transfer mechanical or chemical energy of the material into field energy.

Instead of attempting to interpret (4.40), we concentrate on the physical meaning of

$$-\nabla \cdot \mathbf{S}(\mathbf{r}, t) = -\nabla \cdot [\mathbf{E}(\mathbf{r}, t) \times \mathbf{H}(\mathbf{r}, t)].$$

We shall postulate that this term describes the net flow of electromagnetic energy into the point $\mathbf{r}$ at time t. Then (4.39) shows that in the absence of impressed sources the energy flow must act to (1) increase or decrease the stored energy density at $\mathbf{r}$, (2) dissipate energy in ohmic losses through the term involving $\mathbf{J}^c$, or (3) dissipate (or provide) energy through the term (40). Assuming linearity we may write

$$-\nabla \cdot \mathbf{S}(\mathbf{r}, t) = \frac{\partial}{\partial t} w_e(\mathbf{r}, t) + \frac{\partial}{\partial t} w_m(\mathbf{r}, t) + \frac{\partial}{\partial t} w_Q(\mathbf{r}, t), \tag{4.41}$$

where the terms on the right-hand side represent the time rates of change of, respectively, stored electric, stored magnetic, and dissipated energies.

4.5.1 Dissipation in a dispersive material

Although we may, in general, be unable to separate the individual terms in (4.41), we can examine these terms under certain conditions. For example, consider a field that builds from zero starting from time $t = -\infty$ and then decays back to zero at $t = \infty$. Then by direct integration[1]

$$-\int_{-\infty}^{\infty} \nabla \cdot \mathbf{S}(t)\, dt = w_{em}(t = \infty) - w_{em}(t = -\infty) + w_Q(t = \infty) - w_Q(t = -\infty)$$

where $w_{em} = w_e + w_m$ is the volume density of stored electromagnetic energy. This stored energy is zero at $t = \pm\infty$ since the fields are zero at those times. Thus,

$$\Delta w_Q = -\int_{-\infty}^{\infty} \nabla \cdot \mathbf{S}(t)\, dt = w_Q(t = \infty) - w_Q(t = -\infty)$$

represents the volume density of the net energy dissipated by a lossy medium (or supplied by an active medium). We may thus classify materials according to the scheme

$$\begin{aligned} \Delta w_Q &= 0, && \text{lossless}, \\ \Delta w_Q &> 0, && \text{lossy}, \\ \Delta w_Q &\geq 0, && \text{passive}, \\ \Delta w_Q &< 0, && \text{active}. \end{aligned}$$

For an anisotropic material with the constitutive relations

$$\tilde{\mathbf{D}} = \tilde{\bar{\epsilon}} \cdot \tilde{\mathbf{E}}, \qquad \tilde{\mathbf{B}} = \tilde{\bar{\mu}} \cdot \tilde{\mathbf{H}}, \qquad \tilde{\mathbf{J}}^c = \tilde{\bar{\sigma}} \cdot \tilde{\mathbf{E}},$$

[1]Note that in this section we suppress the $\mathbf{r}$-dependence of most quantities for clarity of presentation.

we find that dissipation is associated with negative imaginary parts of the constitutive parameters. To see this we write

$$\mathbf{E}(\mathbf{r},t) = \frac{1}{2\pi}\int_{-\infty}^{\infty} \tilde{\mathbf{E}}(\mathbf{r},\omega)e^{j\omega t}\,d\omega, \qquad \mathbf{D}(\mathbf{r},t) = \frac{1}{2\pi}\int_{-\infty}^{\infty} \tilde{\mathbf{D}}(\mathbf{r},\omega')e^{j\omega' t}\,d\omega',$$

and thus find

$$\mathbf{J}^c\cdot\mathbf{E} + \mathbf{E}\cdot\frac{\partial\mathbf{D}}{\partial t} = \frac{1}{(2\pi)^2}\int_{-\infty}^{\infty}\int_{-\infty}^{\infty}\tilde{\mathbf{E}}(\omega)\cdot\tilde{\bar{\boldsymbol{\epsilon}}}^c(\omega')\cdot\tilde{\mathbf{E}}(\omega')e^{j(\omega+\omega')t}j\omega'\,d\omega\,d\omega'$$

where $\tilde{\bar{\boldsymbol{\epsilon}}}^c$ is the complex dyadic permittivity (4.24). Then

$$\Delta w_Q = \frac{1}{(2\pi)^2}\int_{-\infty}^{\infty}\int_{-\infty}^{\infty}\left[\tilde{\mathbf{E}}(\omega)\cdot\tilde{\bar{\boldsymbol{\epsilon}}}^c(\omega')\cdot\tilde{\mathbf{E}}(\omega') + \tilde{\mathbf{H}}(\omega)\cdot\tilde{\bar{\boldsymbol{\mu}}}(\omega')\cdot\tilde{\mathbf{H}}(\omega')\right]\cdot \\ \cdot\left[\int_{-\infty}^{\infty}e^{j(\omega+\omega')t}\,dt\right]j\omega'\,d\omega\,d\omega'. \tag{4.42}$$

Using (A.4) and integrating over ω we obtain

$$\Delta w_Q = \frac{1}{2\pi}\int_{-\infty}^{\infty}\left[\tilde{\mathbf{E}}(-\omega')\cdot\tilde{\bar{\boldsymbol{\epsilon}}}^c(\omega')\cdot\tilde{\mathbf{E}}(\omega') + \tilde{\mathbf{H}}(-\omega')\cdot\tilde{\bar{\boldsymbol{\mu}}}(\omega')\cdot\tilde{\mathbf{H}}(\omega')\right]j\omega'\,d\omega'. \tag{4.43}$$

Let us examine (4.43) more closely for the simple case of an isotropic material for which

$$\Delta w_Q = \frac{1}{2\pi}\int_{-\infty}^{\infty}\left\{\left[j\tilde{\epsilon}^{c\prime}(\omega') - \tilde{\epsilon}^{c\prime\prime}(\omega')\right]\tilde{\mathbf{E}}(-\omega')\cdot\tilde{\mathbf{E}}(\omega') + \right. \\ \left. + \left[j\tilde{\mu}'(\omega') - \tilde{\mu}''(\omega')\right]\tilde{\mathbf{H}}(-\omega')\cdot\tilde{\mathbf{H}}(\omega')\right\}\omega'\,d\omega'.$$

Using the frequency symmetry property for complex permittivity (4.17) (which also holds for permeability), we find that for isotropic materials

$$\tilde{\epsilon}^{c\prime}(\mathbf{r},\omega) = \tilde{\epsilon}^{c\prime}(\mathbf{r},-\omega), \qquad \tilde{\epsilon}^{c\prime\prime}(\mathbf{r},\omega) = -\tilde{\epsilon}^{c\prime\prime}(\mathbf{r},-\omega), \tag{4.44}$$

$$\tilde{\mu}'(\mathbf{r},\omega) = \tilde{\mu}'(\mathbf{r},-\omega), \qquad \tilde{\mu}''(\mathbf{r},\omega) = -\tilde{\mu}''(\mathbf{r},-\omega). \tag{4.45}$$

Thus, the products of ω' and the real parts of the constitutive parameters are odd functions, while for the imaginary parts these products are even. Since the dot products of the vector fields are even functions, we find that the integrals of the terms containing the real parts of the constitutive parameters vanish, leaving

$$\Delta w_Q = 2\frac{1}{2\pi}\int_0^{\infty}\left[-\tilde{\epsilon}^{c\prime\prime}|\tilde{\mathbf{E}}|^2 - \tilde{\mu}''|\tilde{\mathbf{H}}|^2\right]\omega\,d\omega. \tag{4.46}$$

Here we have used (4.3) in the form

$$\tilde{\mathbf{E}}(\mathbf{r},-\omega) = \tilde{\mathbf{E}}^*(\mathbf{r},\omega), \qquad \tilde{\mathbf{H}}(\mathbf{r},-\omega) = \tilde{\mathbf{H}}^*(\mathbf{r},\omega). \tag{4.47}$$

Equation (4.46) leads us to associate the imaginary parts of the constitutive parameters with dissipation. Moreover, a lossy isotropic material for which $\Delta w_Q > 0$ must have at least one of $\epsilon^{c\prime\prime}$ and μ'' less than zero over some range of positive frequencies, while an active isotropic medium must have at least one of these greater than zero. In general, we speak of a lossy material as having negative imaginary constitutive parameters:

$$\tilde{\epsilon}^{c\prime\prime} < 0, \qquad \tilde{\mu}'' < 0, \qquad \omega > 0. \tag{4.48}$$

A *lossless* medium must have

$$\tilde{\epsilon}'' = \tilde{\mu}'' = \tilde{\sigma} = 0$$

for all ω.

Things are not as simple in the more general anisotropic case. An integration of (4.42) over ω' instead of ω produces

$$\Delta w_Q = -\frac{1}{2\pi}\int_{-\infty}^{\infty}\left[\tilde{\mathbf{E}}(\omega)\cdot\tilde{\bar{\boldsymbol{\epsilon}}}^c(-\omega)\cdot\tilde{\mathbf{E}}(-\omega)+\tilde{\mathbf{H}}(\omega)\cdot\tilde{\bar{\boldsymbol{\mu}}}(-\omega)\cdot\tilde{\mathbf{H}}(-\omega)\right]j\omega\,d\omega.$$

Adding half of this expression to half of (4.43) and using (4.25), (4.17), and (4.47), we obtain

$$\Delta w_Q = \frac{1}{4\pi}\int_{-\infty}^{\infty}\left[\tilde{\mathbf{E}}^*\cdot\tilde{\bar{\boldsymbol{\epsilon}}}^c\cdot\tilde{\mathbf{E}}-\tilde{\mathbf{E}}\cdot\tilde{\bar{\boldsymbol{\epsilon}}}^{c*}\cdot\tilde{\mathbf{E}}^*+\tilde{\mathbf{H}}^*\cdot\tilde{\bar{\boldsymbol{\mu}}}\cdot\tilde{\mathbf{H}}-\tilde{\mathbf{H}}\cdot\tilde{\bar{\boldsymbol{\mu}}}^*\cdot\tilde{\mathbf{H}}^*\right]j\omega\,d\omega.$$

Finally, using the dyadic identity (A.76), we have

$$\Delta w_Q = \frac{1}{4\pi}\int_{-\infty}^{\infty}\left[\tilde{\mathbf{E}}^*\cdot\left(\tilde{\bar{\boldsymbol{\epsilon}}}^c-\tilde{\bar{\boldsymbol{\epsilon}}}^{c\dagger}\right)\cdot\tilde{\mathbf{E}}+\tilde{\mathbf{H}}^*\cdot\left(\tilde{\bar{\boldsymbol{\mu}}}-\tilde{\bar{\boldsymbol{\mu}}}^{\dagger}\right)\cdot\tilde{\mathbf{H}}\right]j\omega\,d\omega$$

where the dagger (†) denotes the hermitian (conjugate-transpose) operation. The condition for a lossless anisotropic material is

$$\tilde{\bar{\boldsymbol{\epsilon}}}^c = \tilde{\bar{\boldsymbol{\epsilon}}}^{c\dagger}, \qquad \tilde{\bar{\boldsymbol{\mu}}} = \tilde{\bar{\boldsymbol{\mu}}}^{\dagger}, \tag{4.49}$$

or

$$\tilde{\epsilon}_{ij} = \tilde{\epsilon}^*_{ji}, \qquad \tilde{\mu}_{ij} = \tilde{\mu}^*_{ji}, \qquad \tilde{\sigma}_{ij} = \tilde{\sigma}^*_{ji}. \tag{4.50}$$

These relationships imply that in the lossless case the diagonal entries of the constitutive dyadics are purely real.

Equations (4.50) show that complex entries in a permittivity or permeability matrix do not necessarily imply loss. For example, we will show in § 4.6.2 that an electron plasma exposed to a z-directed dc magnetic field has a permittivity of the form

$$[\tilde{\bar{\boldsymbol{\epsilon}}}] = \begin{bmatrix} \epsilon & -j\delta & 0 \\ j\delta & \epsilon & 0 \\ 0 & 0 & \epsilon_z \end{bmatrix}$$

where ϵ, ϵ_z, and δ are real functions of space and frequency. Since $\tilde{\bar{\boldsymbol{\epsilon}}}$ is hermitian it describes a lossless plasma. Similarly, a gyrotropic medium such as a ferrite exposed to a z-directed magnetic field has a permeability dyadic

$$[\tilde{\bar{\boldsymbol{\mu}}}] = \begin{bmatrix} \mu & -j\kappa & 0 \\ j\kappa & \mu & 0 \\ 0 & 0 & \mu_0 \end{bmatrix},$$

which also describes a lossless material.

4.5.2 Energy stored in a dispersive material

In the previous section we were able to isolate the dissipative effects for a dispersive material under special circumstances. It is not generally possible, however, to isolate a term describing the stored energy. The Kronig–Kramers relations imply that if the constitutive parameters of a material are frequency-dependent, they must have both real and imaginary parts; such a material, if isotropic, must be lossy. So dispersive materials are generally lossy and must have both dissipative and energy-storage characteristics. However, many materials have frequency ranges called *transparency ranges* over which $\tilde{\epsilon}^{c\prime\prime}$ and $\tilde{\mu}''$ are small compared to $\tilde{\epsilon}^{c\prime}$ and $\tilde{\mu}'$. If we restrict our interest to these ranges, we may approximate the material as lossless and compute a stored energy. An important special case involves a monochromatic field oscillating at a frequency within this range.

To study the energy stored by a monochromatic field in a dispersive material we must consider the transient period during which energy accumulates in the fields. The assumption of a purely sinusoidal field variation would not include the effects described by the temporal constitutive relations (2.29)–(2.31), which show that as the field builds the energy must be added with a time lag. Instead we shall assume fields with the temporal variation

$$\mathbf{E}(\mathbf{r},t) = f(t)\sum_{i=1}^{3}\hat{\mathbf{i}}_i|E_i(\mathbf{r})|\cos[\omega_0 t + \xi_i^E(\mathbf{r})] \tag{4.51}$$

where $f(t)$ is an appropriate function describing the build-up of the sinusoidal field. To compute the stored energy of a sinusoidal wave we must parameterize $f(t)$ so that we may drive it to unity as a limiting case of the parameter. A simple choice is

$$f(t) = e^{-\alpha^2 t^2} \leftrightarrow \tilde{F}(\omega) = \sqrt{\frac{\pi}{\alpha^2}}e^{-\frac{\omega^2}{4\alpha^2}}. \tag{4.52}$$

Note that since $f(t)$ approaches unity as $\alpha \to 0$, we have the generalized Fourier transform relation

$$\lim_{\alpha\to 0}\tilde{F}(\omega) = 2\pi\delta(\omega). \tag{4.53}$$

Substituting (4.51) into the Fourier transform formula (4.1) we find that

$$\tilde{\mathbf{E}}(\mathbf{r},\omega) = \frac{1}{2}\sum_{i=1}^{3}\hat{\mathbf{i}}_i|E_i(\mathbf{r})|e^{j\xi_i^E(\mathbf{r})}\tilde{F}(\omega-\omega_0) + \frac{1}{2}\sum_{i=1}^{3}\hat{\mathbf{i}}_i|E_i(\mathbf{r})|e^{-j\xi_i^E(\mathbf{r})}\tilde{F}(\omega+\omega_0).$$

We can simplify this by defining

$$\check{\mathbf{E}}(\mathbf{r}) = \sum_{i=1}^{3}\hat{\mathbf{i}}_i|E_i(\mathbf{r})|e^{j\xi_i^E(\mathbf{r})} \tag{4.54}$$

as the *phasor* vector field to obtain

$$\tilde{\mathbf{E}}(\mathbf{r},\omega) = \frac{1}{2}\left[\check{\mathbf{E}}(\mathbf{r})\tilde{F}(\omega-\omega_0) + \check{\mathbf{E}}^*(\mathbf{r})\tilde{F}(\omega+\omega_0)\right]. \tag{4.55}$$

We shall discuss the phasor concept in detail in § 4.7.

The field $\mathbf{E}(\mathbf{r},t)$ is shown in Figure 4.2 as a function of t, while $\tilde{\mathbf{E}}(\mathbf{r},\omega)$ is shown in Figure 4.2 as a function of ω. As α becomes small the spectrum of $\mathbf{E}(\mathbf{r},t)$ concentrates around $\omega = \pm\omega_0$. We assume the material is transparent for all values α of interest so

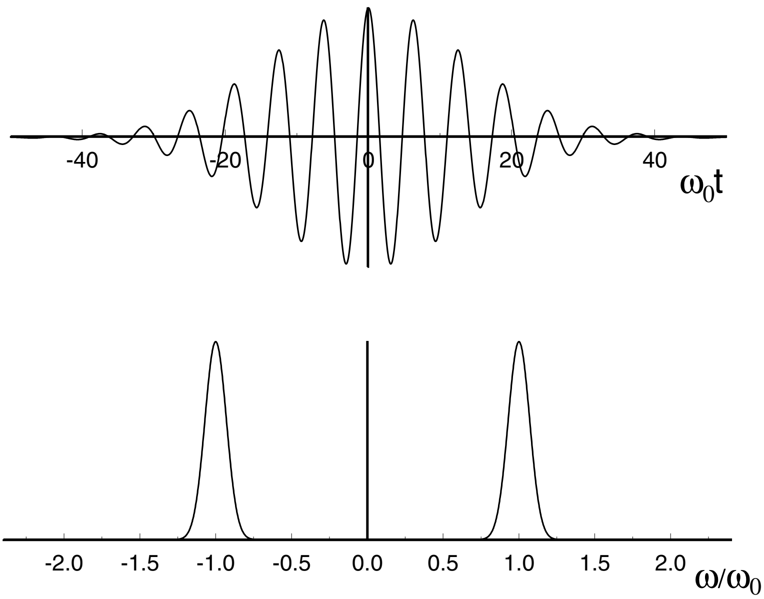

Figure 4.2: Temporal (top) and spectral magnitude (bottom) dependences of **E** used to compute energy stored in a dispersive material.

that we may treat ϵ as real. Then, since there is no dissipation, we conclude that the term (4.40) represents the time rate of change of stored energy at time t, including the effects of field build-up. Hence the interpretation[2]

$$\mathbf{E} \cdot \frac{\partial \mathbf{D}}{\partial t} = \frac{\partial w_e}{\partial t}, \qquad \mathbf{H} \cdot \frac{\partial \mathbf{B}}{\partial t} = \frac{\partial w_m}{\partial t}.$$

We shall concentrate on the electric field term and later obtain the magnetic field term by induction.

Since for periodic signals it is more convenient to deal with the time-averaged stored energy than with the instantaneous stored energy, we compute the time average of $w_e(\mathbf{r}, t)$ over the period of the sinusoid centered at the time origin. That is, we compute

$$\langle w_e \rangle = \frac{1}{T} \int_{-T/2}^{T/2} w_e(t)\, dt \tag{4.56}$$

where $T = 2\pi/\omega_0$. With $\alpha \to 0$, this time-average value is accurate for all periods of the sinusoidal wave.

Because the most expedient approach to the computation of (4.56) is to employ the Fourier spectrum of **E**, we use

$$\mathbf{E}(\mathbf{r}, t) = \frac{1}{2\pi} \int_{-\infty}^{\infty} \tilde{\mathbf{E}}(\mathbf{r}, \omega) e^{j\omega t}\, d\omega = \frac{1}{2\pi} \int_{-\infty}^{\infty} \tilde{\mathbf{E}}^*(\mathbf{r}, \omega') e^{-j\omega' t}\, d\omega',$$

$$\frac{\partial \mathbf{D}(\mathbf{r}, t)}{\partial t} = \frac{1}{2\pi} \int_{-\infty}^{\infty} (j\omega) \tilde{\mathbf{D}}(\mathbf{r}, \omega) e^{j\omega t}\, d\omega = \frac{1}{2\pi} \int_{-\infty}^{\infty} (-j\omega') \tilde{\mathbf{D}}^*(\mathbf{r}, \omega') e^{-j\omega' t}\, d\omega'.$$

[2]Note that in this section we suppress the **r**-dependence of most quantities for clarity of presentation.

We have obtained the second form of each of these expressions using the property (4.3) for the transform of a real function, and by using the change of variables $\omega' = -\omega$. Multiplying the two forms of the expressions and adding half of each, we find that

$$\frac{\partial w_e}{\partial t} = \frac{1}{2}\int_{-\infty}^{\infty}\frac{d\omega}{2\pi}\int_{-\infty}^{\infty}\frac{d\omega'}{2\pi}\left[j\omega\tilde{\mathbf{E}}^*(\omega')\cdot\tilde{\mathbf{D}}(\omega) - j\omega'\tilde{\mathbf{E}}(\omega)\cdot\tilde{\mathbf{D}}^*(\omega')\right]e^{-j(\omega'-\omega)t}. \qquad (4.57)$$

Now let us consider a dispersive isotropic medium described by the constitutive relations $\tilde{\mathbf{D}} = \tilde{\epsilon}\tilde{\mathbf{E}}$, $\tilde{\mathbf{B}} = \tilde{\mu}\tilde{\mathbf{H}}$. Since the imaginary parts of $\tilde{\epsilon}$ and $\tilde{\mu}$ are associated with power dissipation in the medium, we shall approximate $\tilde{\epsilon}$ and $\tilde{\mu}$ as purely real. Then (4.57) becomes

$$\frac{\partial w_e}{\partial t} = \frac{1}{2}\int_{-\infty}^{\infty}\frac{d\omega}{2\pi}\int_{-\infty}^{\infty}\frac{d\omega'}{2\pi}\tilde{\mathbf{E}}^*(\omega')\cdot\tilde{\mathbf{E}}(\omega)\left[j\omega\tilde{\epsilon}(\omega) - j\omega'\tilde{\epsilon}(\omega')\right]e^{-j(\omega'-\omega)t}.$$

Substitution from (4.55) now gives

$$\begin{aligned}\frac{\partial w_e}{\partial t} = \frac{1}{8}\int_{-\infty}^{\infty}\frac{d\omega}{2\pi}\int_{-\infty}^{\infty}\frac{d\omega'}{2\pi}&\left[j\omega\tilde{\epsilon}(\omega) - j\omega'\tilde{\epsilon}(\omega')\right]\cdot\\ &\cdot\left[\check{\mathbf{E}}\cdot\check{\mathbf{E}}^*\tilde{F}(\omega-\omega_0)\tilde{F}(\omega'-\omega_0) + \check{\mathbf{E}}\cdot\check{\mathbf{E}}^*\tilde{F}(\omega+\omega_0)\tilde{F}(\omega'+\omega_0) + \right.\\ &\left.+\ \check{\mathbf{E}}\cdot\check{\mathbf{E}}\tilde{F}(\omega-\omega_0)\tilde{F}(\omega'+\omega_0) + \check{\mathbf{E}}^*\cdot\check{\mathbf{E}}^*\tilde{F}(\omega+\omega_0)\tilde{F}(\omega'-\omega_0)\right]e^{-j(\omega'-\omega)t}.\end{aligned}$$

Let $\omega \to -\omega$ wherever the term $\tilde{F}(\omega+\omega_0)$ appears, and $\omega' \to -\omega'$ wherever the term $\tilde{F}(\omega'+\omega_0)$ appears. Since $\tilde{F}(-\omega) = \tilde{F}(\omega)$ and $\tilde{\epsilon}(-\omega) = \tilde{\epsilon}(\omega)$, we find that

$$\begin{aligned}\frac{\partial w_e}{\partial t} = \frac{1}{8}\int_{-\infty}^{\infty}\frac{d\omega}{2\pi}\int_{-\infty}^{\infty}\frac{d\omega'}{2\pi}&\tilde{F}(\omega-\omega_0)\tilde{F}(\omega'-\omega_0)\cdot\\ \cdot\Big[&\check{\mathbf{E}}\cdot\check{\mathbf{E}}^*[j\omega\tilde{\epsilon}(\omega) - j\omega'\tilde{\epsilon}(\omega')]e^{j(\omega-\omega')t} + \check{\mathbf{E}}\cdot\check{\mathbf{E}}^*[j\omega'\tilde{\epsilon}(\omega') - j\omega\tilde{\epsilon}(\omega)]e^{j(\omega'-\omega)t} + \\ +\ &\check{\mathbf{E}}\cdot\check{\mathbf{E}}[j\omega\tilde{\epsilon}(\omega) + j\omega'\tilde{\epsilon}(\omega')]e^{j(\omega+\omega')t} + \check{\mathbf{E}}^*\cdot\check{\mathbf{E}}^*[-j\omega\tilde{\epsilon}(\omega) - j\omega'\tilde{\epsilon}(\omega')]e^{-j(\omega+\omega')t}\Big].\end{aligned} \qquad (4.58)$$

For small α the spectra are concentrated near $\omega = \omega_0$ or $\omega' = \omega_0$. For terms involving the difference in the permittivities we can expand $g(\omega) = \omega\tilde{\epsilon}(\omega)$ in a Taylor series about ω_0 to obtain the approximation

$$\omega\tilde{\epsilon}(\omega) \approx \omega_0\tilde{\epsilon}(\omega_0) + (\omega-\omega_0)g'(\omega_0)$$

where

$$g'(\omega_0) = \left.\frac{\partial[\omega\tilde{\epsilon}(\omega)]}{\partial\omega}\right|_{\omega=\omega_0}.$$

This is not required for terms involving a sum of permittivities since these will not tend to cancel. For such terms we merely substitute $\omega = \omega_0$ or $\omega' = \omega_0$. With these (4.58) becomes

$$\begin{aligned}\frac{\partial w_e}{\partial t} = \frac{1}{8}\int_{-\infty}^{\infty}\frac{d\omega}{2\pi}\int_{-\infty}^{\infty}\frac{d\omega'}{2\pi}&\tilde{F}(\omega-\omega_0)\tilde{F}(\omega'-\omega_0)\cdot\\ \cdot\Big[&\check{\mathbf{E}}\cdot\check{\mathbf{E}}^*g'(\omega_0)[j(\omega-\omega')]e^{j(\omega-\omega')t} + \check{\mathbf{E}}\cdot\check{\mathbf{E}}^*g'(\omega_0)[j(\omega'-\omega)]e^{j(\omega'-\omega)t} + \\ +\ &\check{\mathbf{E}}\cdot\check{\mathbf{E}}\tilde{\epsilon}(\omega_0)[j(\omega+\omega')]e^{j(\omega+\omega')t} + \check{\mathbf{E}}^*\cdot\check{\mathbf{E}}^*\tilde{\epsilon}(\omega_0)[-j(\omega+\omega')]e^{-j(\omega+\omega')t}\Big].\end{aligned}$$

By integration

$$w_e(t) = \frac{1}{8}\int_{-\infty}^{\infty}\frac{d\omega}{2\pi}\int_{-\infty}^{\infty}\frac{d\omega'}{2\pi}\tilde{F}(\omega-\omega_0)\tilde{F}(\omega'-\omega_0)\cdot$$
$$\cdot\Big[\check{\mathbf{E}}\cdot\check{\mathbf{E}}^* g'(\omega_0)e^{j(\omega-\omega')t} + \check{\mathbf{E}}\cdot\check{\mathbf{E}}^* g'(\omega_0)e^{j(\omega'-\omega)t} +$$
$$+ \check{\mathbf{E}}\cdot\check{\mathbf{E}}\tilde{\epsilon}(\omega_0)e^{j(\omega+\omega')t} + \check{\mathbf{E}}^*\cdot\check{\mathbf{E}}^*\tilde{\epsilon}(\omega_0)e^{-j(\omega+\omega')t}\Big].$$

Our last step is to compute the time-average value of w_e and let $\alpha \to 0$. Applying (4.56) we find

$$\langle w_e\rangle = \frac{1}{8}\int_{-\infty}^{\infty}\frac{d\omega}{2\pi}\int_{-\infty}^{\infty}\frac{d\omega'}{2\pi}\tilde{F}(\omega-\omega_0)\tilde{F}(\omega'-\omega_0)\cdot$$
$$\cdot\left[2\check{\mathbf{E}}\cdot\check{\mathbf{E}}^* g'(\omega_0)\,\mathrm{sinc}\left([\omega-\omega']\frac{\pi}{\omega_0}\right) + \left\{\check{\mathbf{E}}^*\cdot\check{\mathbf{E}}^* + \check{\mathbf{E}}\cdot\check{\mathbf{E}}\right\}\tilde{\epsilon}(\omega_0)\,\mathrm{sinc}\left([\omega+\omega']\frac{\pi}{\omega_0}\right)\right]$$

where $\mathrm{sinc}(x)$ is defined in (A.9) and we note that $\mathrm{sinc}(-x) = \mathrm{sinc}(x)$. Finally we let $\alpha \to 0$ and use (4.53) to replace $\tilde{F}(\omega)$ by a δ-function. Upon integration these δ-functions set $\omega = \omega_0$ and $\omega' = \omega_0$. Since $\mathrm{sinc}(0) = 1$ and $\mathrm{sinc}(2\pi) = 0$, the time-average stored electric energy density becomes simply

$$\langle w_e\rangle = \frac{1}{4}|\check{\mathbf{E}}|^2\frac{\partial[\omega\tilde{\epsilon}]}{\partial\omega}\bigg|_{\omega=\omega_0}. \tag{4.59}$$

Similarly,

$$\langle w_m\rangle = \frac{1}{4}|\check{\mathbf{H}}|^2\frac{\partial[\omega\tilde{\mu}]}{\partial\omega}\bigg|_{\omega=\omega_0}.$$

This approach can also be applied to anisotropic materials to give

$$\langle w_e\rangle = \frac{1}{4}\check{\mathbf{E}}^*\cdot\frac{\partial[\omega\tilde{\bar{\boldsymbol{\epsilon}}}]}{\partial\omega}\bigg|_{\omega=\omega_0}\cdot\check{\mathbf{E}}, \tag{4.60}$$

$$\langle w_m\rangle = \frac{1}{4}\check{\mathbf{H}}^*\cdot\frac{\partial[\omega\tilde{\bar{\boldsymbol{\mu}}}]}{\partial\omega}\bigg|_{\omega=\omega_0}\cdot\check{\mathbf{H}}. \tag{4.61}$$

See Collin [39] for details. For the case of a lossless, nondispersive material where the constitutive parameters are frequency independent, we can use (4.49) and (A.76) to simplify this and obtain

$$\langle w_e\rangle = \frac{1}{4}\check{\mathbf{E}}^*\cdot\bar{\boldsymbol{\epsilon}}\cdot\check{\mathbf{E}} = \frac{1}{4}\check{\mathbf{E}}\cdot\check{\mathbf{D}}^*, \tag{4.62}$$

$$\langle w_m\rangle = \frac{1}{4}\check{\mathbf{H}}^*\cdot\bar{\boldsymbol{\mu}}\cdot\check{\mathbf{H}} = \frac{1}{4}\check{\mathbf{H}}\cdot\check{\mathbf{B}}^*, \tag{4.63}$$

in the anisotropic case and

$$\langle w_e\rangle = \frac{1}{4}\epsilon|\check{\mathbf{E}}|^2 = \frac{1}{4}\check{\mathbf{E}}\cdot\check{\mathbf{D}}^*, \tag{4.64}$$

$$\langle w_m\rangle = \frac{1}{4}\mu|\check{\mathbf{H}}|^2 = \frac{1}{4}\check{\mathbf{H}}\cdot\check{\mathbf{B}}^*, \tag{4.65}$$

in the isotropic case. Here $\check{\mathbf{E}}$, $\check{\mathbf{D}}$, $\check{\mathbf{B}}$, $\check{\mathbf{H}}$ are all phasor fields as defined by (4.54).

4.5.3 The energy theorem

A convenient expression for the time-average stored energies (4.60) and (4.61) is found by manipulating the frequency-domain Maxwell equations. Beginning with the complex conjugates of the two frequency-domain curl equations for anisotropic media,

$$\nabla \times \tilde{\mathbf{E}}^* = j\omega\tilde{\bar{\boldsymbol{\mu}}}^* \cdot \tilde{\mathbf{H}}^*,$$

$$\nabla \times \tilde{\mathbf{H}}^* = \tilde{\mathbf{J}}^* - j\omega\tilde{\bar{\boldsymbol{\epsilon}}}^* \cdot \tilde{\mathbf{E}}^*,$$

we differentiate with respect to frequency:

$$\nabla \times \frac{\partial \tilde{\mathbf{E}}^*}{\partial\omega} = j\frac{\partial[\omega\tilde{\bar{\boldsymbol{\mu}}}^*]}{\partial\omega} \cdot \tilde{\mathbf{H}}^* + j\omega\tilde{\bar{\boldsymbol{\mu}}}^* \cdot \frac{\partial \tilde{\mathbf{H}}^*}{\partial\omega}, \tag{4.66}$$

$$\nabla \times \frac{\partial \tilde{\mathbf{H}}^*}{\partial\omega} = \frac{\partial \tilde{\mathbf{J}}^*}{\partial\omega} - j\frac{\partial[\omega\tilde{\bar{\boldsymbol{\epsilon}}}^*]}{\partial\omega} \cdot \tilde{\mathbf{E}}^* - j\omega\tilde{\bar{\boldsymbol{\epsilon}}}^* \cdot \frac{\partial \tilde{\mathbf{E}}^*}{\partial\omega}. \tag{4.67}$$

These terms also appear as a part of the expansion

$$\nabla \cdot \left[\tilde{\mathbf{E}} \times \frac{\partial \tilde{\mathbf{H}}^*}{\partial\omega} + \frac{\partial \tilde{\mathbf{E}}^*}{\partial\omega} \times \tilde{\mathbf{H}}\right] =$$

$$\frac{\partial \tilde{\mathbf{H}}^*}{\partial\omega} \cdot [\nabla \times \tilde{\mathbf{E}}] - \tilde{\mathbf{E}} \cdot \nabla \times \frac{\partial \tilde{\mathbf{H}}^*}{\partial\omega} + \tilde{\mathbf{H}} \cdot \nabla \times \frac{\partial \tilde{\mathbf{E}}^*}{\partial\omega} - \frac{\partial \tilde{\mathbf{E}}^*}{\partial\omega} \cdot [\nabla \times \tilde{\mathbf{H}}]$$

where we have used (B.44). Substituting from (4.66)–(4.67) and eliminating $\nabla \times \tilde{\mathbf{E}}$ and $\nabla \times \tilde{\mathbf{H}}$ by Maxwell's equations we have

$$\frac{1}{4}\nabla \cdot \left(\tilde{\mathbf{E}} \times \frac{\partial \tilde{\mathbf{H}}^*}{\partial\omega} + \frac{\partial \tilde{\mathbf{E}}^*}{\partial\omega} \times \tilde{\mathbf{H}}\right) =$$

$$j\frac{1}{4}\omega\left(\tilde{\mathbf{E}} \cdot \tilde{\bar{\boldsymbol{\epsilon}}}^* \cdot \frac{\partial \tilde{\mathbf{E}}^*}{\partial\omega} - \frac{\partial \tilde{\mathbf{E}}^*}{\partial\omega} \cdot \tilde{\bar{\boldsymbol{\epsilon}}} \cdot \tilde{\mathbf{E}}\right) + j\frac{1}{4}\omega\left(\tilde{\mathbf{H}} \cdot \tilde{\bar{\boldsymbol{\mu}}}^* \cdot \frac{\partial \tilde{\mathbf{H}}^*}{\partial\omega} - \frac{\partial \tilde{\mathbf{H}}^*}{\partial\omega} \cdot \tilde{\bar{\boldsymbol{\mu}}} \cdot \tilde{\mathbf{H}}\right) +$$

$$+j\frac{1}{4}\left(\tilde{\mathbf{E}} \cdot \frac{\partial[\omega\tilde{\bar{\boldsymbol{\epsilon}}}^*]}{\partial\omega} \cdot \tilde{\mathbf{E}}^* + \tilde{\mathbf{H}} \cdot \frac{\partial[\omega\tilde{\bar{\boldsymbol{\mu}}}^*]}{\partial\omega} \cdot \tilde{\mathbf{H}}^*\right) - \frac{1}{4}\left(\tilde{\mathbf{E}} \cdot \frac{\partial \tilde{\mathbf{J}}^*}{\partial\omega} + \tilde{\mathbf{J}} \cdot \frac{\partial \tilde{\mathbf{E}}^*}{\partial\omega}\right).$$

Let us assume that the sources and fields are narrowband, centered on ω_0, and that ω_0 lies within a transparency range so that within the band the material may be considered lossless. Invoking from (4.49) the facts that $\tilde{\bar{\boldsymbol{\epsilon}}} = \tilde{\bar{\boldsymbol{\epsilon}}}^\dagger$ and $\tilde{\bar{\boldsymbol{\mu}}} = \tilde{\bar{\boldsymbol{\mu}}}^\dagger$, we find that the first two terms on the right are zero. Integrating over a volume and taking the complex conjugate of both sides we obtain

$$\frac{1}{4}\oint_S \left(\tilde{\mathbf{E}}^* \times \frac{\partial \tilde{\mathbf{H}}}{\partial\omega} + \frac{\partial \tilde{\mathbf{E}}}{\partial\omega} \times \tilde{\mathbf{H}}^*\right) \cdot \mathbf{dS} =$$

$$-j\frac{1}{4}\int_V \left(\tilde{\mathbf{E}}^* \cdot \frac{\partial[\omega\tilde{\bar{\boldsymbol{\epsilon}}}]}{\partial\omega} \cdot \tilde{\mathbf{E}} + \tilde{\mathbf{H}}^* \cdot \frac{\partial[\omega\tilde{\bar{\boldsymbol{\mu}}}]}{\partial\omega} \cdot \tilde{\mathbf{H}}\right) dV - \frac{1}{4}\int_V \left(\tilde{\mathbf{E}}^* \cdot \frac{\partial \tilde{\mathbf{J}}}{\partial\omega} + \tilde{\mathbf{J}}^* \cdot \frac{\partial \tilde{\mathbf{E}}}{\partial\omega}\right) dV.$$

Evaluating each of the terms at $\omega = \omega_0$ and using (4.60)–(4.61) we have

$$\frac{1}{4}\oint_S \left(\tilde{\mathbf{E}}^* \times \frac{\partial \tilde{\mathbf{H}}}{\partial\omega} + \frac{\partial \tilde{\mathbf{E}}}{\partial\omega} \times \tilde{\mathbf{H}}^*\right)\bigg|_{\omega=\omega_0} \cdot \mathbf{dS} =$$

$$-j\left[\langle W_e\rangle + \langle W_m\rangle\right] - \frac{1}{4}\int_V \left(\tilde{\mathbf{E}}^* \cdot \frac{\partial \tilde{\mathbf{J}}}{\partial\omega} + \tilde{\mathbf{J}}^* \cdot \frac{\partial \tilde{\mathbf{E}}}{\partial\omega}\right)\bigg|_{\omega=\omega_0} dV \tag{4.68}$$

where $\langle W_e \rangle + \langle W_m \rangle$ is the total time-average electromagnetic energy stored in the volume region V. This is known as the *energy theorem.* We shall use it in § 4.11.3 to determine the velocity of energy transport for a plane wave.

4.6 Some simple models for constitutive parameters

Thus far our discussion of electromagnetic fields has been restricted to macroscopic phenomena. Although we recognize that matter is composed of microscopic constituents, we have chosen to describe materials using constitutive relationships whose parameters, such as permittivity, conductivity, and permeability, are viewed in the macroscopic sense. By performing experiments on the laboratory scale we can measure the constitutive parameters to the precision required for engineering applications.

At some point it becomes useful to establish models of the macroscopic behavior of materials based on microscopic considerations, formulating expressions for the constitutive parameters using atomic descriptors such as number density, atomic charge, and molecular dipole moment. These models allow us to predict the behavior of broad classes of materials, such as dielectrics and conductors, over wide ranges of frequency and field strength.

Accurate models for the behavior of materials under the influence of electromagnetic fields must account for many complicated effects, including those best described by quantum mechanics. However, many simple models can be obtained using classical mechanics and field theory. We shall investigate several of the most useful of these, and in the process try to gain a feeling for the relationship between the field applied to a material and the resulting polarization or magnetization of the underlying atomic structure.

For simplicity we shall consider only homogeneous materials. The fundamental atomic descriptor of "number density," N, is thus taken to be independent of position and time. The result may be more generally applicable since we may think of an inhomogeneous material in terms of the spatial variation of constitutive parameters originally determined assuming homogeneity. However, we shall not attempt to study the microscopic conditions that give rise to inhomogeneities.

4.6.1 Complex permittivity of a non-magnetized plasma

A plasma is an ionized gas in which the charged particles are free to move under the influence of an applied field and through particle-particle interactions. A plasma differs from other materials in that there is no atomic lattice restricting the motion of the particles. However, even in a gas the interactions between the particles and the fields give rise to a polarization effect, causing the permittivity of the gas to differ from that of free space. In addition, exposing the gas to an external field will cause a secondary current to flow as a result of the Lorentz force on the particles. As the moving particles collide with one another they relinquish their momentum, an effect describable in terms of a conductivity. In this section we shall perform a simple analysis to determine the complex permittivity of a non-magnetized plasma.

To make our analysis tractable, we shall make several assumptions.

1. We assume that the plasma is *neutral*: i.e., that the free electrons and positive ions are of equal number and distributed in like manner. If the particles are sufficiently

dense to be considered in the macroscopic sense, then there is no net field produced by the gas and thus no electromagnetic interaction between the particles. We also assume that the plasma is homogeneous and that the number density of the electrons N (number of electrons per m^3) is independent of time and position. In contrast to this are *electron beams*, whose properties differ significantly from neutral plasmas because of bunching of electrons by the applied field [148].

2. We ignore the motion of the positive ions in the computation of the secondary current, since the ratio of the mass of an ion to that of an electron is at least as large as the ratio of a proton to an electron ($m_p/m_e = 1837$) and thus the ions accelerate much more slowly.
3. We assume that the applied field is that of an electromagnetic wave. In § 2.10.6 we found that for a wave in free space the ratio of magnetic to electric field is $|\mathbf{H}|/|\mathbf{E}| = \sqrt{\epsilon_0/\mu_0}$, so that

$$\frac{|\mathbf{B}|}{|\mathbf{E}|} = \mu_0\sqrt{\frac{\epsilon_0}{\mu_0}} = \sqrt{\mu_0\epsilon_0} = \frac{1}{c}.$$

   Thus, in the Lorentz force equation we may approximate the force on an electron as

$$\mathbf{F} = -q_e(\mathbf{E} + \mathbf{v} \times \mathbf{B}) \approx -q_e\mathbf{E}$$

   as long as $v \ll c$. Here q_e is the *unsigned* charge on an electron, $q_e = 1.6021 \times 10^{-19}$ C. Note that when an external static magnetic field accompanies the field of the wave, as is the case in the earth's ionosphere for example, we cannot ignore the magnetic component of the Lorentz force. This case will be considered in § 4.6.2.
4. We assume that the mechanical interactions between particles can be described using a *collision frequency* ν, which describes the rate at which a directed plasma velocity becomes random in the absence of external forces.

With these assumptions we can write the equation of motion for the plasma medium. Let $\mathbf{v}(\mathbf{r}, t)$ represent the macroscopic velocity of the plasma medium. Then, by Newton's second law, the force acting at each point on the medium is balanced by the time-rate of change in momentum at that point. Because of collisions, the total change in momentum density is described by

$$\mathbf{F}(\mathbf{r}, t) = -Nq_e\mathbf{E}(\mathbf{r}, t) = \frac{d\wp(\mathbf{r}, t)}{dt} + \nu\wp(\mathbf{r}, t) \tag{4.69}$$

where

$$\wp(\mathbf{r}, t) = Nm_e\mathbf{v}(\mathbf{r}, t)$$

is the volume density of momentum. Note that if there is no externally-applied electromagnetic force, then (4.69) becomes

$$\frac{d\wp(\mathbf{r}, t)}{dt} + \nu\wp(\mathbf{r}, t) = 0.$$

Hence

$$\wp(\mathbf{r}, t) = \wp_0(\mathbf{r})e^{-\nu t},$$

and we see that ν describes the rate at which the electron velocities move toward a random state, producing a macroscopic plasma velocity $\mathbf{v}$ of zero.

The time derivative in (4.69) is the total derivative as defined in (A.58):

$$\frac{d\wp(\mathbf{r},t)}{dt} = \frac{\partial\wp(\mathbf{r},t)}{\partial t} + (\mathbf{v}\cdot\nabla)\wp(\mathbf{r},t). \tag{4.70}$$

The second term on the right accounts for the time-rate of change of momentum perceived as the observer moves through regions of spatially-changing momentum. Since the electron velocity is induced by the electromagnetic field, we anticipate that for a sinusoidal wave the spatial variation will be on the order of the wavelength of the field: $\lambda = 2\pi c/\omega$. Thus, while the first term in (4.70) is proportional to ω, the second term is proportional to $\omega v/c$ and can be neglected for non-relativistic particle velocities. Then, writing $\mathbf{E}(\mathbf{r},t)$ and $\mathbf{v}(\mathbf{r},t)$ as inverse Fourier transforms, we see that (4.69) yields

$$-q_e\tilde{\mathbf{E}} = j\omega m_e\tilde{\mathbf{v}} + m_e\nu\tilde{\mathbf{v}} \tag{4.71}$$

and thus

$$\tilde{\mathbf{v}} = -\frac{\frac{q_e}{m_e}\tilde{\mathbf{E}}}{\nu + j\omega}. \tag{4.72}$$

The secondary current associated with the moving electrons is (since q_e is unsigned)

$$\tilde{\mathbf{J}}^s = -Nq_e\tilde{\mathbf{v}} = \frac{\epsilon_0\omega_p^2}{\omega^2+\nu^2}(\nu - j\omega)\tilde{\mathbf{E}} \tag{4.73}$$

where

$$\omega_p^2 = \frac{Nq_e^2}{\epsilon_0 m_e} \tag{4.74}$$

is called the *plasma frequency*.

The frequency-domain Ampere's law for primary and secondary currents in free space is merely

$$\nabla\times\tilde{\mathbf{H}} = \tilde{\mathbf{J}}^i + \tilde{\mathbf{J}}^s + j\omega\epsilon_0\tilde{\mathbf{E}}.$$

Substitution from (4.73) gives

$$\nabla\times\tilde{\mathbf{H}} = \tilde{\mathbf{J}}^i + \frac{\epsilon_0\omega_p^2\nu}{\omega^2+\nu^2}\tilde{\mathbf{E}} + j\omega\epsilon_0\left[1 - \frac{\omega_p^2}{\omega^2+\nu^2}\right]\tilde{\mathbf{E}}.$$

We can determine the material properties of the plasma by realizing that the above expression can be written as

$$\nabla\times\tilde{\mathbf{H}} = \tilde{\mathbf{J}}^i + \tilde{\mathbf{J}}^s + j\omega\tilde{\mathbf{D}}$$

with the constitutive relations

$$\tilde{\mathbf{J}}^s = \tilde{\sigma}\tilde{\mathbf{E}}, \qquad \tilde{\mathbf{D}} = \tilde{\epsilon}\tilde{\mathbf{E}}.$$

Here we identify the conductivity of the plasma as

$$\tilde{\sigma}(\omega) = \frac{\epsilon_0\omega_p^2\nu}{\omega^2+\nu^2} \tag{4.75}$$

and the permittivity as

$$\tilde{\epsilon}(\omega) = \epsilon_0\left[1 - \frac{\omega_p^2}{\omega^2+\nu^2}\right].$$

We can also write Ampere's law as

$$\nabla \times \tilde{\mathbf{H}} = \tilde{\mathbf{J}}^i + j\omega\tilde{\epsilon}^c\tilde{\mathbf{E}}$$

where $\tilde{\epsilon}^c$ is the complex permittivity

$$\tilde{\epsilon}^c(\omega) = \tilde{\epsilon}(\omega) + \frac{\tilde{\sigma}(\omega)}{j\omega} = \epsilon_0\left[1 - \frac{\omega_p^2}{\omega^2 + \nu^2}\right] - j\frac{\epsilon_0\omega_p^2\nu}{\omega(\omega^2 + \nu^2)}. \tag{4.76}$$

If we wish to describe the plasma in terms of a polarization vector, we merely use $\tilde{\mathbf{D}} = \epsilon_0\tilde{\mathbf{E}} + \tilde{\mathbf{P}} = \tilde{\epsilon}\tilde{\mathbf{E}}$ to obtain the polarization vector $\tilde{\mathbf{P}} = (\tilde{\epsilon} - \epsilon_0)\tilde{\mathbf{E}} = \epsilon_0\tilde{\chi}_e\tilde{\mathbf{E}}$, where $\tilde{\chi}_e$ is the electric susceptibility

$$\tilde{\chi}_e(\omega) = -\frac{\omega_p^2}{\omega^2 + \nu^2}.$$

We note that $\tilde{\mathbf{P}}$ is directed opposite the applied field $\tilde{\mathbf{E}}$, resulting in $\tilde{\epsilon} < \epsilon_0$.

The plasma is dispersive since both its permittivity and conductivity depend on ω. As $\omega \to 0$ we have $\tilde{\epsilon}^{c\prime} \to \epsilon_0\epsilon_r$ where $\epsilon_r = 1 - \omega_p^2/\nu^2$, and also $\tilde{\epsilon}^{c\prime\prime} \sim 1/\omega$, as remarked in (4.28). As $\omega \to \infty$ we have $\tilde{\epsilon}^{c\prime} - \epsilon_0 \sim 1/\omega^2$ and $\tilde{\epsilon}^{c\prime\prime} \sim 1/\omega^3$, as mentioned in (4.29). When a transient plane wave propagates through a dispersive medium, the frequency dependence of the constitutive parameters tends to cause spreading of the waveshape.

We see that the plasma conductivity (4.75) is proportional to the collision frequency ν, and that, since $\tilde{\epsilon}^{c\prime\prime} < 0$ by the arguments of § 4.5, the plasma must be lossy. Loss arises from the transfer of electromagnetic energy into heat through electron collisions. If there are no collisions ($\nu = 0$), there is no mechanism for the transfer of energy into heat, and the conductivity of a lossless (or "collisionless") plasma reduces to zero as expected.

In a lowloss plasma ($\nu \to 0$) we may determine the time-average stored electromagnetic energy for sinusoidal excitation at frequency $\check{\omega}$. We must be careful to use (4.59), which holds for materials with dispersion. If we apply the simpler formula (4.64), we find that for $\nu \to 0$

$$\langle w_e \rangle = \frac{1}{4}\epsilon_0|\check{\mathbf{E}}|^2 - \frac{1}{4}\epsilon_0|\check{\mathbf{E}}|^2\frac{\omega_p^2}{\check{\omega}^2}.$$

For those excitation frequencies obeying $\check{\omega} < \omega_p$ we have $\langle w_e \rangle < 0$, implying that the material is active. Since there is no mechanism for the plasma to produce energy, this is obviously not valid. But an application of (4.59) gives

$$\langle w_e \rangle = \frac{1}{4}|\check{\mathbf{E}}|^2\frac{\partial}{\partial\omega}\left[\epsilon_0\omega\left(1 - \frac{\omega_p^2}{\omega^2}\right)\right]\Bigg|_{\omega=\check{\omega}} = \frac{1}{4}\epsilon_0|\check{\mathbf{E}}|^2 + \frac{1}{4}\epsilon_0|\check{\mathbf{E}}|^2\frac{\omega_p^2}{\check{\omega}^2}, \tag{4.77}$$

which is always positive. In this expression the first term represents the time-average energy stored in the vacuum, while the second term represents the energy stored in the kinetic energy of the electrons. For harmonic excitation, the time-average electron kinetic energy density is

$$\langle w_q \rangle = \frac{1}{4}Nm_e\check{\mathbf{v}} \cdot \check{\mathbf{v}}^*.$$

Substituting $\check{\mathbf{v}}$ from (4.72) with $\nu = 0$ we see that

$$\frac{1}{4}Nm_e\check{\mathbf{v}} \cdot \check{\mathbf{v}}^* = \frac{1}{4}\frac{Nq_e^2}{m_e\check{\omega}^2}|\check{\mathbf{E}}|^2 = \frac{1}{4}\epsilon_0|\check{\mathbf{E}}|^2\frac{\omega_p^2}{\check{\omega}^2},$$

which matches the second term of (4.77).

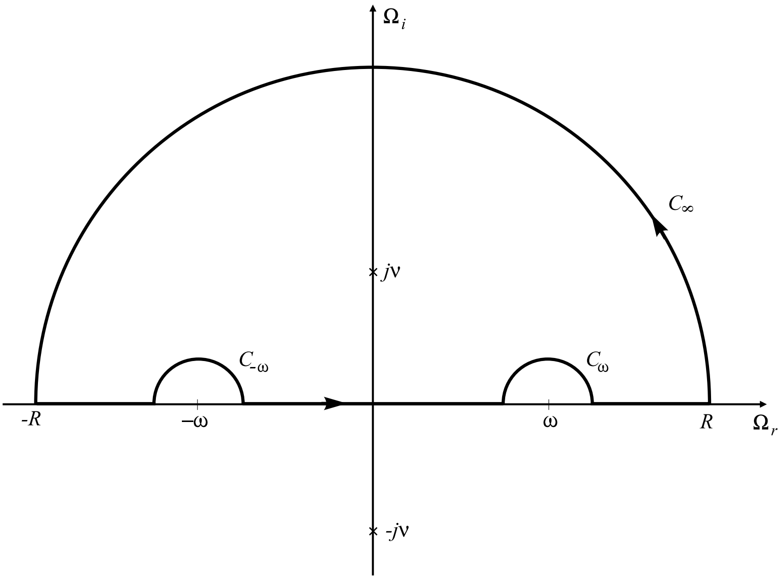

Figure 4.3: Integration contour used in Kronig–Kramers relations to find $\tilde{\epsilon}^{c\prime}$ from $\tilde{\epsilon}^{c\prime\prime}$ for a non-magnetized plasma.

The complex permittivity of a plasma (4.76) obviously obeys the required frequency-symmetry conditions (4.27). It also obeys the Kronig–Kramers relations required for a causal material. From (4.76) we see that the imaginary part of the complex plasma permittivity is

$$\tilde{\epsilon}^{c\prime\prime}(\omega) = -\frac{\epsilon_0 \omega_p^2 \nu}{\omega(\omega^2 + \nu^2)}.$$

Substituting this into (4.37) we have

$$\tilde{\epsilon}^{c\prime}(\omega) - \epsilon_0 = -\frac{2}{\pi}\,\text{P.V.}\int_0^\infty \left[-\frac{\epsilon_0 \omega_p^2 \nu}{\Omega(\Omega^2 + \nu^2)}\right] \frac{\Omega}{\Omega^2 - \omega^2} d\Omega.$$

We can evaluate the principal value integral and thus verify that it produces $\tilde{\epsilon}^{c\prime}$ by using the contour method of § A.1. Because the integrand is even we can extend the domain of integration to $(-\infty, \infty)$ and divide the result by two. Thus

$$\tilde{\epsilon}^{c\prime}(\omega) - \epsilon_0 = \frac{1}{\pi}\,\text{P.V.}\int_{-\infty}^\infty \frac{\epsilon_0 \omega_p^2 \nu}{(\Omega - j\nu)(\Omega + j\nu)} \frac{d\Omega}{(\Omega - \omega)(\Omega + \omega)}.$$

We integrate around the closed contour shown in Figure 4.3. Since the integrand falls off as $1/\Omega^4$ the contribution from C_∞ is zero. The contributions from the semicircles C_ω and $C_{-\omega}$ are given by πj times the residues of the integrand at $\Omega = \omega$ and at $\Omega = -\omega$, respectively, which are identical but of opposite sign. Thus, the semicircle contributions cancel and leave only the contribution from the residue at the upper-half-plane pole $\Omega = j\nu$. Evaluation of the residue gives

$$\tilde{\epsilon}^{c\prime}(\omega) - \epsilon_0 = \frac{1}{\pi} 2\pi j \frac{\epsilon_0 \omega_p^2 \nu}{j\nu + j\nu} \frac{1}{(j\nu - \omega)(j\nu + \omega)} = -\frac{\epsilon_0 \omega_p^2}{\nu^2 + \omega^2}$$

and thus

$$\tilde{\epsilon}^{c\prime}(\omega) = \epsilon_0\left(1 - \frac{\omega_p^2}{\nu^2+\omega^2}\right),$$

which matches (4.76) as expected.

4.6.2 Complex dyadic permittivity of a magnetized plasma

When an electron plasma is exposed to a magnetostatic field, as occurs in the earth's ionosphere, the behavior of the plasma is altered so that the secondary current is no longer aligned with the electric field, requiring the constitutive relationships to be written in terms of a complex dyadic permittivity. If the static field is $\mathbf{B}_0$, the velocity field of the plasma is determined by adding the magnetic component of the Lorentz force to (4.71), giving

$$-q_e[\tilde{\mathbf{E}} + \tilde{\mathbf{v}} \times \mathbf{B}_0] = \tilde{\mathbf{v}}(j\omega m_e + m_e\nu)$$

or equivalently

$$\tilde{\mathbf{v}} - j\frac{q_e}{m_e(\omega - j\nu)}\tilde{\mathbf{v}} \times \mathbf{B}_0 = j\frac{q_e}{m_e(\omega - j\nu)}\tilde{\mathbf{E}}. \tag{4.78}$$

Writing this expression generically as

$$\mathbf{v} + \mathbf{v} \times \mathbf{C} = \mathbf{A}, \tag{4.79}$$

we can solve for $\mathbf{v}$ as follows. Dotting both sides of the equation with $\mathbf{C}$ we quickly establish that $\mathbf{C}\cdot\mathbf{v} = \mathbf{C}\cdot\mathbf{A}$. Crossing both sides of the equation with $\mathbf{C}$, using (B.7), and substituting $\mathbf{C}\cdot\mathbf{A}$ for $\mathbf{C}\cdot\mathbf{v}$, we have

$$\mathbf{v} \times \mathbf{C} = \mathbf{A} \times \mathbf{C} + \mathbf{v}(\mathbf{C}\cdot\mathbf{C}) - \mathbf{C}(\mathbf{A}\cdot\mathbf{C}).$$

Finally, substituting $\mathbf{v} \times \mathbf{C}$ back into (4.79) we obtain

$$\mathbf{v} = \frac{\mathbf{A} - \mathbf{A} \times \mathbf{C} + (\mathbf{A}\cdot\mathbf{C})\mathbf{C}}{1 + \mathbf{C}\cdot\mathbf{C}}. \tag{4.80}$$

Let us first consider a lossless plasma for which $\nu = 0$. We can solve (4.78) for $\tilde{\mathbf{v}}$ by setting

$$\mathbf{C} = -j\frac{\boldsymbol{\omega}_c}{\omega}, \qquad \mathbf{A} = j\frac{\epsilon_0\omega_p^2}{\omega N q_e}\tilde{\mathbf{E}},$$

where

$$\boldsymbol{\omega}_c = \frac{q_e}{m_e}\mathbf{B}_0.$$

Here $\omega_c = q_e B_0/m_e = |\boldsymbol{\omega}_c|$ is called the *electron cyclotron frequency*. Substituting these into (4.80) we have

$$\left(\omega^2 - \omega_c^2\right)\tilde{\mathbf{v}} = j\frac{\epsilon_0\omega\omega_p^2}{Nq_e}\tilde{\mathbf{E}} + \frac{\epsilon_0\omega_p^2}{Nq_e}\boldsymbol{\omega}_c \times \tilde{\mathbf{E}} - j\frac{\boldsymbol{\omega}_c}{\omega}\frac{\epsilon_0\omega_p^2}{Nq_e}\boldsymbol{\omega}_c \cdot \tilde{\mathbf{E}}.$$

Since the secondary current produced by the moving electrons is just $\tilde{\mathbf{J}}^s = -Nq_e\tilde{\mathbf{v}}$, we have

$$\tilde{\mathbf{J}}^s = j\omega\left[-\frac{\epsilon_0\omega_p^2}{\omega^2 - \omega_c^2}\tilde{\mathbf{E}} + j\frac{\epsilon_0\omega_p^2}{\omega(\omega^2 - \omega_c^2)}\boldsymbol{\omega}_c \times \tilde{\mathbf{E}} + \frac{\boldsymbol{\omega}_c}{\omega^2}\frac{\epsilon_0\omega_p^2}{\omega^2 - \omega_c^2}\boldsymbol{\omega}_c \cdot \tilde{\mathbf{E}}\right]. \tag{4.81}$$

Now, by the Ampere–Maxwell law we can write for currents in free space

$$\nabla \times \tilde{\mathbf{H}} = \tilde{\mathbf{J}}^i + \tilde{\mathbf{J}}^s + j\omega\epsilon_0\tilde{\mathbf{E}}. \tag{4.82}$$

Considering the plasma to be a material implies that we can describe the gas in terms of a complex permittivity dyadic $\tilde{\bar{\boldsymbol{\epsilon}}}^c$ such that the Ampere–Maxwell law is

$$\nabla \times \tilde{\mathbf{H}} = \tilde{\mathbf{J}}^i + j\omega\tilde{\bar{\boldsymbol{\epsilon}}}^c \cdot \tilde{\mathbf{E}}.$$

Substituting (4.81) into (4.82), and defining the dyadic $\bar{\boldsymbol{\omega}}_c$ so that $\bar{\boldsymbol{\omega}}_c \cdot \tilde{\mathbf{E}} = \boldsymbol{\omega}_c \times \tilde{\mathbf{E}}$, we identify the dyadic permittivity

$$\tilde{\bar{\boldsymbol{\epsilon}}}^c(\omega) = \left[\epsilon_0 - \epsilon_0\frac{\omega_p^2}{\omega^2 - \omega_c^2}\right]\bar{\mathbf{I}} + j\frac{\epsilon_0\omega_p^2}{\omega(\omega^2 - \omega_c^2)}\bar{\boldsymbol{\omega}}_c + \frac{\epsilon_0\omega_p^2}{\omega^2(\omega^2 - \omega_c^2)}\boldsymbol{\omega}_c\boldsymbol{\omega}_c. \tag{4.83}$$

Note that in rectangular coordinates

$$[\bar{\boldsymbol{\omega}}_c] = \begin{bmatrix} 0 & -\omega_{cz} & \omega_{cy} \\ \omega_{cz} & 0 & -\omega_{cx} \\ -\omega_{cy} & \omega_{cx} & 0 \end{bmatrix}. \tag{4.84}$$

To examine the properties of the dyadic permittivity it is useful to write it in matrix form. To do this we must choose a coordinate system. We shall assume that $\mathbf{B}_0$ is aligned along the z-axis such that $\mathbf{B}_0 = \hat{\mathbf{z}}B_0$ and $\boldsymbol{\omega}_c = \hat{\mathbf{z}}\omega_c$. Then (4.84) becomes

$$[\bar{\boldsymbol{\omega}}_c] = \begin{bmatrix} 0 & -\omega_c & 0 \\ \omega_c & 0 & 0 \\ 0 & 0 & 0 \end{bmatrix} \tag{4.85}$$

and we can write the permittivity dyadic (4.83) as

$$[\tilde{\bar{\boldsymbol{\epsilon}}}(\omega)] = \begin{bmatrix} \epsilon & -j\delta & 0 \\ j\delta & \epsilon & 0 \\ 0 & 0 & \epsilon_z \end{bmatrix} \tag{4.86}$$

where

$$\epsilon = \epsilon_0\left(1 - \frac{\omega_p^2}{\omega^2 - \omega_c^2}\right), \qquad \epsilon_z = \epsilon_0\left(1 - \frac{\omega_p^2}{\omega^2}\right), \qquad \delta = \frac{\epsilon_0\omega_c\omega_p^2}{\omega(\omega^2 - \omega_c^2)}.$$

Note that the form of the permittivity dyadic is that for a lossless *gyrotropic* material (2.33).

Since the plasma is lossless, equation (4.49) shows that the dyadic permittivity must be hermitian. Equation (4.86) confirms this. We also note that since the sign of $\boldsymbol{\omega}_c$ is determined by the sign of $\mathbf{B}_0$, the dyadic permittivity obeys the symmetry relation

$$\tilde{\epsilon}_{ij}^c(\mathbf{B}_0) = \tilde{\epsilon}_{ji}^c(-\mathbf{B}_0) \tag{4.87}$$

as does the permittivity matrix of any material that has anisotropic properties dependent on an externally applied magnetic field [141]. We will find later in this section that the permeability matrix of a magnetized ferrite also obeys such a symmetry condition.

We can let $\omega \to \omega - j\nu$ in (4.81) to obtain the secondary current in a plasma with collisions:

$$\tilde{\mathbf{J}}^s(\mathbf{r},\omega) = j\omega\left[-\frac{\epsilon_0\omega_p^2(\omega - j\nu)}{\omega[(\omega-j\nu)^2-\omega_c^2]}\tilde{\mathbf{E}}(\mathbf{r},\omega) + \right.$$
$$+ j\frac{\epsilon_0\omega_p^2(\omega - j\nu)}{\omega(\omega-j\nu)[(\omega-j\nu)^2-\omega_c^2)]}\boldsymbol{\omega}_c \times \tilde{\mathbf{E}}(\mathbf{r},\omega) +$$
$$\left. + \frac{\boldsymbol{\omega}_c}{(\omega-j\nu)^2}\frac{\epsilon_0\omega_p^2(\omega - j\nu)}{\omega[(\omega-j\nu)^2-\omega_c^2]}\boldsymbol{\omega}_c \cdot \tilde{\mathbf{E}}(\mathbf{r},\omega)\right].$$

From this we find the dyadic permittivity

$$\tilde{\bar{\boldsymbol{\epsilon}}}^c(\omega) = \left[\epsilon_0 - \frac{\epsilon_0\omega_p^2(\omega-j\nu)}{\omega[(\omega-j\nu)^2-\omega_c^2]}\right]\bar{\mathbf{I}} + j\frac{\epsilon_0\omega_p^2}{\omega[(\omega-j\nu)^2-\omega_c^2)]}\bar{\boldsymbol{\omega}}_c +$$
$$+ \frac{1}{(\omega-j\nu)}\frac{\epsilon_0\omega_p^2}{\omega[(\omega-j\nu)^2-\omega_c^2]}\boldsymbol{\omega}_c\boldsymbol{\omega}_c.$$

Assuming that $\mathbf{B}_0$ is aligned with the z-axis we can use (4.85) to find the components of the dyadic permittivity matrix:

$$\tilde{\epsilon}^c_{xx}(\omega) = \tilde{\epsilon}^c_{yy}(\omega) = \epsilon_0\left(1 - \frac{\omega_p^2(\omega-j\nu)}{\omega[(\omega-j\nu)^2-\omega_c^2]}\right), \tag{4.88}$$

$$\tilde{\epsilon}^c_{xy}(\omega) = -\tilde{\epsilon}^c_{yx}(\omega) = -j\epsilon_0\frac{\omega_p^2\omega_c}{\omega[(\omega-j\nu)^2-\omega_c^2)]}, \tag{4.89}$$

$$\tilde{\epsilon}^c_{zz}(\omega) = \epsilon_0\left(1 - \frac{\omega_p^2}{\omega(\omega-j\nu)}\right), \tag{4.90}$$

and

$$\tilde{\epsilon}^c_{zx} = \tilde{\epsilon}^c_{xz} = \tilde{\epsilon}^c_{zy} = \tilde{\epsilon}^c_{yz} = 0. \tag{4.91}$$

We see that $[\tilde{\epsilon}^c]$ is not hermitian when $\nu \neq 0$. We expect this since the plasma is lossy when collisions occur. However, we can decompose $[\tilde{\bar{\boldsymbol{\epsilon}}}^c]$ as a sum of two matrices:

$$[\tilde{\bar{\boldsymbol{\epsilon}}}^c] = [\tilde{\bar{\boldsymbol{\epsilon}}}] + \frac{[\tilde{\bar{\boldsymbol{\sigma}}}]}{j\omega},$$

where $[\tilde{\bar{\boldsymbol{\epsilon}}}]$ and $[\tilde{\bar{\boldsymbol{\sigma}}}]$ are hermitian [141]. The details are left as an exercise. We also note that, as in the case of the lossless plasma, the permittivity dyadic obeys the symmetry condition $\tilde{\epsilon}^c_{ij}(\mathbf{B}_0) = \tilde{\epsilon}^c_{ji}(-\mathbf{B}_0)$.

4.6.3 Simple models of dielectrics

We define an isotropic dielectric material (also called an *insulator*) as one that obeys the macroscopic frequency-domain constitutive relationship

$$\tilde{\mathbf{D}}(\mathbf{r},\omega) = \tilde{\epsilon}(\mathbf{r},\omega)\tilde{\mathbf{E}}(\mathbf{r},\omega).$$

Since the polarization vector $\mathbf{P}$ was defined in Chapter 2 as $\mathbf{P}(\mathbf{r},t) = \mathbf{D}(\mathbf{r},t) - \epsilon_0\mathbf{E}(\mathbf{r},t)$, an isotropic dielectric can also be described through

$$\tilde{\mathbf{P}}(\mathbf{r},\omega) = (\tilde{\epsilon}(\mathbf{r},\omega) - \epsilon_0)\tilde{\mathbf{E}}(\mathbf{r},\omega) = \tilde{\chi}_e(\mathbf{r},\omega)\epsilon_0\tilde{\mathbf{E}}(\mathbf{r},\omega)$$

where $\tilde{\chi}_e$ is the dielectric susceptibility. In this section we shall model a homogeneous dielectric consisting of a single, uniform material type.

We found in Chapter 3 that for a dielectric material immersed in a static electric field, the polarization vector $\mathbf{P}$ can be viewed as a volume density of dipole moments. We choose to retain this view as the fundamental link between microscopic dipole moments and the macroscopic polarization vector. Within the framework of our model we thus describe the polarization through the expression

$$\mathbf{P}(\mathbf{r}, t) = \frac{1}{\Delta V} \sum_{\mathbf{r}-\mathbf{r}_i(t)\in B} \mathbf{p}_i. \tag{4.92}$$

Here $\mathbf{p}_i$ is the dipole moment of the ith elementary microscopic constituent, and we form the macroscopic density function as in § 1.3.1.

We may also write (4.92) as

$$\mathbf{P}(\mathbf{r}, t) = \left[\frac{N_B}{\Delta V}\right]\left[\frac{1}{N_B}\sum_{i=1}^{N_B} \mathbf{p}_i\right] = N(\mathbf{r}, t)\mathbf{p}(\mathbf{r}, t) \tag{4.93}$$

where N_B is the number of constituent particles within ΔV. We identify

$$\mathbf{p}(\mathbf{r}, t) = \frac{1}{N_B}\sum_{i=1}^{N_B} \mathbf{p}_i(\mathbf{r}, t)$$

as the average dipole moment within ΔV, and

$$N(\mathbf{r}, t) = \frac{N_B}{\Delta V}$$

as the dipole moment number density. In this model a dielectric material does not require higher-order multipole moments to describe its behavior. Since we are only interested in homogeneous materials in this section we shall assume that the number density is constant: $N(\mathbf{r}, t) = N$.

To understand how dipole moments arise, we choose to adopt the simple idea that matter consists of atomic particles, each of which has a positively charged nucleus surrounded by a negatively charged electron cloud. Isolated, these particles have no net charge and no net electric dipole moment. However, there are several ways in which individual particles, or aggregates of particles, may take on a dipole moment. When exposed to an external electric field the electron cloud of an individual atom may be displaced, resulting in an *induced* dipole moment which gives rise to *electronic polarization*. When groups of atoms form a molecule, the individual electron clouds may combine to form an asymmetric structure having a *permanent* dipole moment. In some materials these molecules are randomly distributed and no net dipole moment results. However, upon application of an external field the torque acting on the molecules may tend to align them, creating an *induced* dipole moment and *orientation*, or *dipole*, polarization. In other materials, the asymmetric structure of the molecules may be weak until an external field causes the displacement of atoms within each molecule, resulting in an *induced* dipole moment causing *atomic*, or *molecular*, polarization. If a material maintains a permanent polarization without the application of an external field, it is called an *electret* (and is thus similar in behavior to a permanently magnetized magnet).

To describe the constitutive relations, we must establish a link between $\mathbf{P}$ (now describable in microscopic terms) and $\mathbf{E}$. We do this by postulating that the average constituent dipole moment is proportional to the *local electric field strength* $\mathbf{E}'$:

$$\mathbf{p} = \alpha \mathbf{E}', \tag{4.94}$$

where α is called the *polarizability* of the elementary constituent. Each of the polarization effects listed above may have its own polarizability: α_e for electronic polarization, α_a for atomic polarization, and α_d for dipole polarization. The total polarizability is merely the sum $\alpha = \alpha_e + \alpha_a + \alpha_d$.

In a rarefied gas the particles are so far apart that their interaction can be neglected. Here the localized field $\mathbf{E}'$ is the same as the applied field $\mathbf{E}$. In liquids and solids where particles are tightly packed, $\mathbf{E}'$ depends on the manner in which the material is polarized and may differ from $\mathbf{E}$. We therefore proceed to determine a relationship between $\mathbf{E}'$ and $\mathbf{P}$.

The Clausius–Mosotti equation. We seek the local field at an observation point within a polarized material. Let us first assume that the fields are static. We surround the observation point with an artificial spherical surface of radius a and write the field at the observation point as a superposition of the field $\mathbf{E}$ applied, the field $\mathbf{E}_2$ of the polarized molecules external to the sphere, and the field $\mathbf{E}_3$ of the polarized molecules within the sphere. We take a large enough that we may describe the molecules outside the sphere in terms of the macroscopic dipole moment density $\mathbf{P}$, but small enough to assume that $\mathbf{P}$ is uniform over the surface of the sphere. We also assume that the major contribution to $\mathbf{E}_2$ comes from the dipoles nearest the observation point. We then approximate $\mathbf{E}_2$ using the electrostatic potential produced by the equivalent polarization surface charge on the sphere $\rho_{Ps} = \hat{\mathbf{n}} \cdot \mathbf{P}$ (where $\hat{\mathbf{n}}$ points toward the center of the sphere). Placing the origin of coordinates at the observation point and orienting the z-axis with the polarization $\mathbf{P}$ so that $\mathbf{P} = P_0 \hat{\mathbf{z}}$, we find that $\hat{\mathbf{n}} \cdot \mathbf{P} = -\cos\theta$ and thus the electrostatic potential at any point $\mathbf{r}$ within the sphere is merely

$$\Phi(\mathbf{r}) = -\frac{1}{4\pi\epsilon_0} \oint_S \frac{P_0 \cos\theta'}{|\mathbf{r} - \mathbf{r}'|}\, dS'.$$

This integral has been computed in § 3.2.7 with the result given by (3.103) Hence

$$\Phi(\mathbf{r}) = -\frac{P_0}{3\epsilon_0} r \cos\theta = -\frac{P_0}{3\epsilon_0} z$$

and therefore

$$\mathbf{E}_2 = \frac{\mathbf{P}}{3\epsilon_0}. \tag{4.95}$$

Note that this is uniform and independent of a.

The assumption that the localized field varies spatially as the electrostatic field, even when $\mathbf{P}$ may depend on frequency, is quite good. In Chapter 5 we will find that for a frequency-dependent source (or, equivalently, a time-varying source), the fields very near the source have a spatial dependence nearly identical to that of the electrostatic case.

We now have the seemingly more difficult task of determining the field $\mathbf{E}_3$ produced by the dipoles within the sphere. This would seem difficult since the field produced by dipoles near the observation point should be highly-dependent on the particular dipole arrangement. As mentioned above, there are various mechanisms for polarization, and the distribution of charge near any particular point depends on the molecular arrangement. However, Lorentz showed [115] that for crystalline solids with cubical symmetry, or for a randomly-structured gas, the contribution from dipoles within the sphere is zero. Indeed, it is convenient and reasonable to assume that for most dielectrics the effects of the dipoles immediately surrounding the observation point cancel so that $\mathbf{E}_3 = 0$. This was first suggested by O.F. Mosotti in 1850 [52].

With $\mathbf{E}_2$ approximated as (4.95) and $\mathbf{E}_3$ assumed to be zero, we have the value of the resulting local field:

$$\mathbf{E}'(\mathbf{r}) = \mathbf{E}(\mathbf{r}) + \frac{\mathbf{P}(\mathbf{r})}{3\epsilon_0}. \tag{4.96}$$

This is called the *Mosotti field*. Substituting the Mosotti field into (4.94) and using $\mathbf{P} = N\mathbf{p}$, we obtain

$$\mathbf{P}(\mathbf{r}) = N\alpha\mathbf{E}'(\mathbf{r}) = N\alpha\left(\mathbf{E}(\mathbf{r}) + \frac{\mathbf{P}(\mathbf{r})}{3\epsilon_0}\right).$$

Solving for $\mathbf{P}$ we obtain

$$\mathbf{P}(\mathbf{r}) = \left(\frac{3\epsilon_0 N\alpha}{3\epsilon_0 - N\alpha}\right)\mathbf{E}(\mathbf{r}) = \chi_e\epsilon_0\mathbf{E}(\mathbf{r}).$$

So the electric susceptibility of a dielectric may be expressed as

$$\chi_e = \frac{3N\alpha}{3\epsilon_0 - N\alpha}. \tag{4.97}$$

Using $\chi_e = \epsilon_r - 1$ we can rewrite (4.97) as

$$\epsilon = \epsilon_0\epsilon_r = \epsilon_0\frac{3 + 2N\alpha/\epsilon_0}{3 - N\alpha/\epsilon_0}, \tag{4.98}$$

which we can arrange to obtain

$$\alpha = \alpha_e + \alpha_a + \alpha_d = \frac{3\epsilon_0}{N}\frac{\epsilon_r - 1}{\epsilon_r + 2}.$$

This has been named the *Clausius–Mosotti formula*, after O.F. Mosotti who proposed it in 1850 and R. Clausius who proposed it independently in 1879. When written in terms of the index of refraction n (where $n^2 = \epsilon_r$), it is also known as the *Lorentz–Lorenz formula*, after H. Lorentz and L. Lorenz who proposed it independently for optical materials in 1880. The Clausius–Mosotti formula allows us to determine the dielectric constant from the polarizability and number density of a material. It is reasonably accurate for certain simple gases (with pressures up to 1000 atmospheres) but becomes less reliable for liquids and solids, especially for those with large dielectric constants.

The response of the microscopic structure of matter to an applied field is not instantaneous. When exposed to a rapidly oscillating sinusoidal field, the induced dipole moments may lag in time. This results in a loss mechanism that can be described macroscopically by a complex permittivity. We can modify the Clausius–Mosotti formula by assuming that both the relative permittivity and polarizability are complex numbers, but this will not model the dependence of these parameters on frequency. Instead we shall (in later paragraphs) model the time response of the dipole moments to the applied field.

An interesting application of the Clausius–Mosotti formula is to determine the permittivity of a mixture of dielectrics with different permittivities. Consider the simple case in which many small spheres of permittivity ϵ_2, radius a, and volume V are embedded within a dielectric matrix of permittivity ϵ_1. If we assume that a is much smaller than the wavelength of the electromagnetic field, and that the spheres are sparsely distributed within the matrix, then we may ignore any mutual interaction between the spheres. Since the expression for the permittivity of a uniform dielectric given by (4.98) describes the effect produced by dipoles in free space, we can use the Clausius–Mosotti formula to define an *effective* permittivity ϵ_e for a material consisting of spheres in a background dielectric by replacing ϵ_0 with ϵ_1 to obtain

$$\epsilon_e = \epsilon_1 \frac{3 + 2N\alpha/\epsilon_1}{3 - N\alpha/\epsilon_1}. \tag{4.99}$$

In this expression α is the polarizability of a single dielectric sphere embedded in the background dielectric, and N is the number density of dielectric spheres. To find α we use the static field solution for a dielectric sphere immersed in a field (§ 3.2.10). Remembering that $\mathbf{p} = \alpha\mathbf{E}$ and that for a uniform region of volume V we have $\mathbf{p} = V\mathbf{P}$, we can make the replacements $\epsilon_0 \to \epsilon_1$ and $\epsilon \to \epsilon_2$ in (3.117) to get

$$\alpha = 3\epsilon_1 V \frac{\epsilon_2 - \epsilon_1}{\epsilon_2 + 2\epsilon_1}. \tag{4.100}$$

Defining $f = NV$ as the *fractional volume* occupied by the spheres, we can substitute (4.100) into (4.99) to find that

$$\epsilon_e = \epsilon_1 \frac{1 + 2fy}{1 - fy}$$

where

$$y = \frac{\epsilon_2 - \epsilon_1}{\epsilon_2 + 2\epsilon_1}.$$

This is known as the *Maxwell–Garnett mixing formula.* Rearranging we obtain

$$\frac{\epsilon_e - \epsilon_1}{\epsilon_e + 2\epsilon_1} = f \frac{\epsilon_2 - \epsilon_1}{\epsilon_2 + 2\epsilon_1},$$

which is known as the *Rayleigh mixing formula.* As expected, $\epsilon_e \to \epsilon_1$ as $f \to 0$. Even though as $f \to 1$ the formula also reduces to $\epsilon_e = \epsilon_2$, our initial assumption that $f \ll 1$ (sparsely distributed spheres) is violated and the result is inaccurate for non-spherical inhomogeneities [90]. For a discussion of more accurate mixing formulas, see Ishimaru [90] or Sihvola [175].

The dispersion formula of classical physics. We may determine the frequency dependence of the permittivity by modeling the time response of induced dipole moments. This was done by H. Lorentz using the simple atomic model we introduced earlier. Consider what happens when a molecule consisting of heavy particles (nuclei) surrounded by clouds of electrons is exposed to a time-harmonic electromagnetic wave. Using the same arguments we made when we studied the interactions of fields with a plasma in § 4.6.1, we assume that each electron experiences a Lorentz force $\mathbf{F}_e = -q_e\mathbf{E}'$. We neglect the magnetic component of the force for nonrelativistic charge velocities, and ignore the motion of the much heavier nuclei in favor of studying the motion of the electron cloud. However, several important distinctions exist between the behavior of charges within a plasma and those within a solid or liquid material. Because of the surrounding polarized matter, any molecule responds to the local field $\mathbf{E}'$ instead of the applied field $\mathbf{E}$. Also, as the electron cloud is displaced by the Lorentz force, the attraction from the positive nuclei provides a restoring force $\mathbf{F}_r$. In the absence of loss the restoring force causes the electron cloud (and thus the induced dipole moment) to oscillate in phase with the applied field. In addition, there will be loss due to radiation by the oscillating molecules and collisions between charges that can be modeled using a "frictional force" $\mathbf{F}_s$ in the same manner as for a mechanical harmonic oscillator.

We can express the restoring and frictional forces by the use of a mechanical analogue. The restoring force acting on each electron is taken to be proportional to the displacement from equilibrium $\mathbf{l}$:

$$\mathbf{F}_r(\mathbf{r},t) = -m_e\omega_r^2\mathbf{l}(\mathbf{r},t),$$

where m_e is the mass of an electron and ω_r is a material constant that depends on the molecular structure. The frictional force is similar to the collisional term in § 4.6.1 in that it is assumed to be proportional to the electron momentum $m_e\mathbf{v}$:

$$\mathbf{F}_s(\mathbf{r},t) = -2\Gamma m_e\mathbf{v}(\mathbf{r},t)$$

where Γ is a material constant. With these we can apply Newton's second law to obtain

$$\mathbf{F}(\mathbf{r},t) = -q_e\mathbf{E}'(\mathbf{r},t) - m_e\omega_r^2\mathbf{l}(\mathbf{r},t) - 2\Gamma m_e\mathbf{v}(\mathbf{r},t) = m_e\frac{d\mathbf{v}(\mathbf{r},t)}{dt}.$$

Using $\mathbf{v} = d\mathbf{l}/dt$ we find that the equation of motion for the electron is

$$\frac{d^2\mathbf{l}(\mathbf{r},t)}{dt^2} + 2\Gamma\frac{d\mathbf{l}(\mathbf{r},t)}{dt} + \omega_r^2\mathbf{l}(\mathbf{r},t) = -\frac{q_e}{m_e}\mathbf{E}'(\mathbf{r},t). \tag{4.101}$$

We recognize this differential equation as the damped harmonic equation. When $\mathbf{E}' = 0$ we have the homogeneous solution

$$\mathbf{l}(\mathbf{r},t) = \mathbf{l}_0(\mathbf{r})e^{-\Gamma t}\cos\left(t\sqrt{\omega_r^2 - \Gamma^2}\right).$$

Thus the electron position is a damped oscillation. The resonant frequency $\sqrt{\omega_r^2 - \Gamma^2}$ is usually only slightly reduced from ω_r since radiation damping is generally quite low.

Since the dipole moment for an electron displaced from equilibrium by $\mathbf{l}$ is $\mathbf{p} = -q_e\mathbf{l}$, and the polarization density is $\mathbf{P} = N\mathbf{p}$ from (93), we can write

$$\mathbf{P}(\mathbf{r},t) = -Nq_e\mathbf{l}(\mathbf{r},t).$$

Multiplying (4.101) by $-Nq_e$ and substituting the above expression, we have a differential equation for the polarization:

$$\frac{d^2\mathbf{P}}{dt^2} + 2\Gamma\frac{d\mathbf{P}}{dt} + \omega_r^2\mathbf{P} = \frac{Nq_e^2}{m_e}\mathbf{E}'.$$

To obtain a constitutive equation we must relate the polarization to the applied field $\mathbf{E}$. We can accomplish this by relating the local field $\mathbf{E}'$ to the polarization using the Mosotti field (4.96). Substitution gives

$$\frac{d^2\mathbf{P}}{dt^2} + 2\Gamma\frac{d\mathbf{P}}{dt} + \omega_0^2\mathbf{P} = \frac{Nq_e^2}{m_e}\mathbf{E} \tag{4.102}$$

where

$$\omega_0 = \sqrt{\omega_r^2 - \frac{Nq_e^2}{3m_e\epsilon_0}}$$

is the resonance frequency of the dipole moments. We see that this frequency is reduced from the resonance frequency of the electron oscillation because of the polarization of the surrounding medium.

We can now obtain a dispersion equation for the electrical susceptibility by taking the Fourier transform of (4.102). We have

$$-\omega^2\tilde{\mathbf{P}} + j\omega 2\Gamma\tilde{\mathbf{P}} + \omega_0^2\tilde{\mathbf{P}} = \frac{Nq_e^2}{m_e}\tilde{\mathbf{E}}.$$

Thus we obtain the dispersion relation

$$\tilde{\chi}_e(\omega) = \frac{\tilde{\mathbf{P}}}{\epsilon_0\tilde{\mathbf{E}}} = \frac{\omega_p^2}{\omega_0^2 - \omega^2 + j\omega 2\Gamma}$$

where ω_p is the plasma frequency (4.74). Since $\tilde{\epsilon}_r(\omega) = 1 + \tilde{\chi}_e(\omega)$ we also have

$$\tilde{\epsilon}(\omega) = \epsilon_0 + \epsilon_0\frac{\omega_p^2}{\omega_0^2 - \omega^2 + j\omega 2\Gamma}. \tag{4.103}$$

If more than one type of oscillating moment contributes to the permittivity, we may extend (4.103) to

$$\tilde{\epsilon}(\omega) = \epsilon_0 + \sum_i \epsilon_0\frac{\omega_{pi}^2}{\omega_i^2 - \omega^2 + j\omega 2\Gamma_i} \tag{4.104}$$

where $\omega_{pi} = N_i q_e^2/\epsilon_0 m_i$ is the plasma frequency of the ith resonance component, and ω_i and Γ_i are the oscillation frequency and damping coefficient, respectively, of this component. This expression is the *dispersion formula for classical physics*, so called because it neglects quantum effects. When losses are negligible, (4.104) reduces to the *Sellmeier equation*

$$\tilde{\epsilon}(\omega) = \epsilon_0 + \sum_i \epsilon_0\frac{\omega_{pi}^2}{\omega_i^2 - \omega^2}. \tag{4.105}$$

Let us now study the frequency behavior of the dispersion relation (4.104). Splitting the permittivity into real and imaginary parts we have

$$\tilde{\epsilon}'(\omega) - \epsilon_0 = \epsilon_0\sum_i \omega_{pi}^2\frac{\omega_i^2 - \omega^2}{[\omega_i^2 - \omega^2]^2 + 4\omega^2\Gamma_i^2},$$
$$\tilde{\epsilon}''(\omega) = -\epsilon_0\sum_i \omega_{pi}^2\frac{2\omega\Gamma_i}{[\omega_i^2 - \omega^2]^2 + 4\omega^2\Gamma_i^2}.$$

As $\omega \to 0$ the permittivity reduces to

$$\epsilon = \epsilon_0\left(1 + \sum_i \frac{\omega_{pi}^2}{\omega_i^2}\right),$$

which is the static permittivity of the material. As $\omega \to \infty$ the permittivity behaves as

$$\tilde{\epsilon}'(\omega) \to \epsilon_0\left(1 - \frac{\sum_i \omega_{pi}^2}{\omega^2}\right), \qquad \tilde{\epsilon}''(\omega) \to -\epsilon_0\frac{2\sum_i \omega_{pi}^2\Gamma_i}{\omega^3}.$$

This high frequency behavior is identical to that of a plasma as described by (4.76).

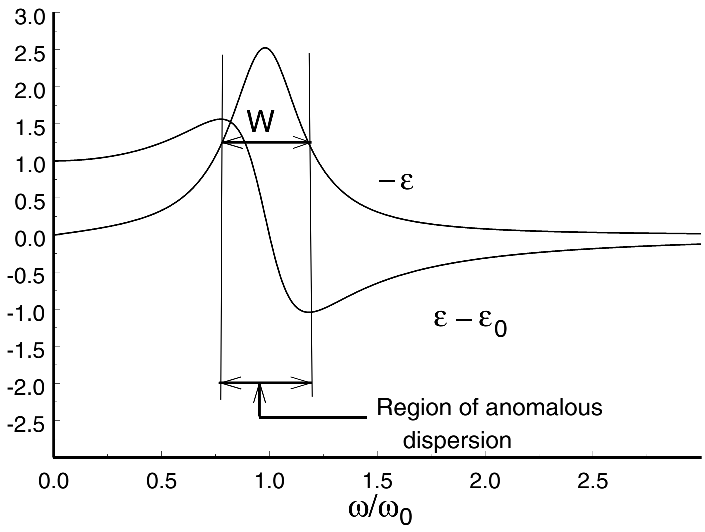

Figure 4.4: Real and imaginary parts of permittivity for a single resonance model of a dielectric with $\Gamma/\omega_0 = 0.2$. Permittivity normalized by dividing by $\epsilon_0(\omega_p/\omega_0)^2$.

The major characteristic of the dispersion relation (4.104) is the presence of one or more *resonances*. Figure 4.4 shows a plot of a single resonance component, where we have normalized the permittivity as

$$(\tilde{\epsilon}'(\omega) - \epsilon_0)/(\epsilon_0\bar{\omega}_p^2) = \frac{1-\bar{\omega}^2}{\left[1-\bar{\omega}^2\right]^2 + 4\bar{\omega}^2\bar{\Gamma}^2},$$

$$-\tilde{\epsilon}''(\omega)/(\epsilon_0\bar{\omega}_p^2) = \frac{2\bar{\omega}\bar{\Gamma}}{\left[1-\bar{\omega}^2\right]^2 + 4\bar{\omega}^2\bar{\Gamma}^2},$$

with $\bar{\omega} = \omega/\omega_0$, $\bar{\omega}_p = \omega_p/\omega_0$, and $\bar{\Gamma} = \Gamma/\omega_0$. We see a distinct resonance centered at $\omega = \omega_0$. Approaching this resonance through frequencies less than ω_0, we see that $\tilde{\epsilon}'$ increases slowly until peaking at $\omega_{\text{max}} = \omega_0\sqrt{1 - 2\Gamma/\omega_0}$ where it attains a value of

$$\tilde{\epsilon}'_{\text{max}} = \epsilon_0 + \frac{1}{4}\epsilon_0\frac{\bar{\omega}_p^2}{\bar{\Gamma}(1-\bar{\Gamma})}.$$

After peaking, $\tilde{\epsilon}'$ undergoes a rapid decrease, passing through $\tilde{\epsilon}' = \epsilon_0$ at $\omega = \omega_0$, and then continuing to decrease until reaching a minimum value of

$$\tilde{\epsilon}'_{\text{min}} = \epsilon_0 - \frac{1}{4}\epsilon_0\frac{\bar{\omega}_p^2}{\bar{\Gamma}(1+\bar{\Gamma})}$$

at $\omega_{\text{min}} = \omega_0\sqrt{1 + 2\Gamma/\omega_0}$. As ω continues to increase, $\tilde{\epsilon}'$ again increases slowly toward a final value of $\tilde{\epsilon}' = \epsilon_0$. The regions of slow variation of $\tilde{\epsilon}'$ are called regions of *normal dispersion*, while the region where $\tilde{\epsilon}'$ decreases abruptly is called the region of *anomalous dispersion*. Anomalous dispersion is unusual only in the sense that it occurs over a narrower range of frequencies than normal dispersion.

The imaginary part of the permittivity peaks near the resonant frequency, dropping off monotonically in each direction away from the peak. The width of the curve is an important parameter that we can most easily determine by approximating the behavior of $\tilde{\epsilon}''$ near ω_0. Letting $\Delta\bar{\omega} = (\omega_0 - \omega)/\omega_0$ and using

$$\omega_0^2 - \omega^2 = (\omega_0 - \omega)(\omega_0 + \omega) \approx 2\omega_0^2 \Delta\bar{\omega},$$

we get

$$\tilde{\epsilon}''(\omega) \approx -\frac{1}{2}\epsilon_0 \bar{\omega}_p^2 \frac{\bar{\Gamma}}{(\Delta\bar{\omega})^2 + \bar{\Gamma}^2}.$$

This approximation has a maximum value of

$$\tilde{\epsilon}''_{\text{max}} = \tilde{\epsilon}''(\omega_0) = -\frac{1}{2}\epsilon_0 \bar{\omega}_p^2 \frac{1}{\bar{\Gamma}}$$

located at $\omega = \omega_0$, and has half-amplitude points located at $\Delta\bar{\omega} = \pm\bar{\Gamma}$. Thus the width of the resonance curve is

$$W = 2\Gamma.$$

Note that for a material characterized by a low-loss resonance ($\Gamma \ll \omega_0$), the location of $\tilde{\epsilon}'_{\text{max}}$ can be approximated as

$$\omega_{\text{max}} = \omega_0 \sqrt{1 - 2\Gamma/\omega_0} \approx \omega_0 - \Gamma$$

while $\tilde{\epsilon}'_{\text{min}}$ is located at

$$\omega_{\text{min}} = \omega_0 \sqrt{1 + 2\Gamma/\omega_0} \approx \omega_0 + \Gamma.$$

The region of anomalous dispersion thus lies between the half amplitude points of $\tilde{\epsilon}''$: $\omega_0 - \Gamma < \omega < \omega_0 + \Gamma$.

As $\Gamma \to 0$ the resonance curve becomes narrower and taller. Thus, a material characterized by a very low-loss resonance may be modeled very simply using $\tilde{\epsilon}'' = A\delta(\omega - \omega_0)$, where A is a constant to be determined. We can find A by applying the Kronig–Kramers formula (4.37):

$$\tilde{\epsilon}'(\omega) - \epsilon_0 = -\frac{2}{\pi} \text{P.V.} \int_0^\infty A\delta(\Omega - \omega_0) \frac{\Omega \, d\Omega}{\Omega^2 - \omega^2} = -\frac{2}{\pi} A \frac{\omega_0}{\omega_0^2 - \omega^2}.$$

Since the material approaches the lossless case, this expression should match the Sellmeier equation (4.105):

$$-\frac{2}{\pi} A \frac{\omega_0}{\omega_0^2 - \omega^2} = \epsilon_0 \frac{\omega_p^2}{\omega_0^2 - \omega^2},$$

giving $A = -\pi\epsilon_0 \omega_p^2 / 2\omega_0$. Hence the permittivity of a material characterized by a low-loss resonance may be approximated as

$$\tilde{\epsilon}^c(\omega) = \epsilon_0 \left(1 + \frac{\omega_p^2}{\omega_0^2 - \omega^2}\right) - j\epsilon_0 \frac{\pi}{2} \frac{\omega_p^2}{\omega_0} \delta(\omega - \omega_0).$$

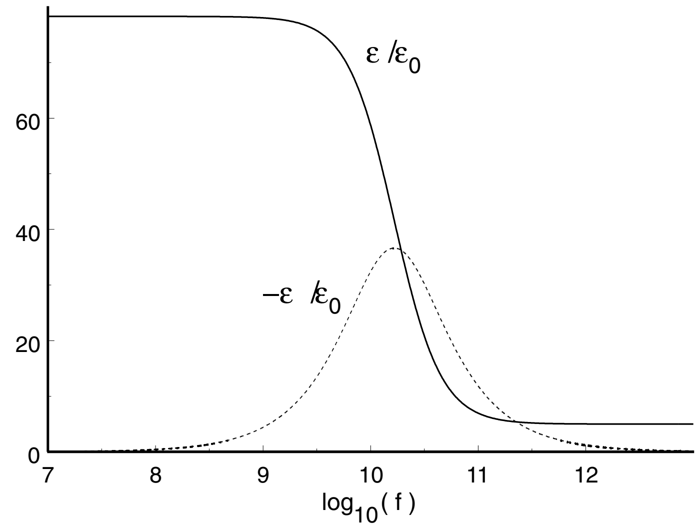

Figure 4.5: Relaxation spectrum for water at 20° C found using Debye equation.

Debye relaxation and the Cole–Cole equation. In solids or liquids consisting of *polar molecules* (those retaining a permanent dipole moment, e.g., water), the resonance effect is replaced by *relaxation.* We can view the molecule as attempting to rotate in response to an applied field within a background medium dominated by the frictional term in (4.101). The rotating molecule experiences many weak collisions which continuously drain off energy, preventing it from accelerating under the force of the applied field. J.W.P. Debye proposed that such materials are described by an exponential damping of their polarization and a complete absence of oscillations. If we neglect the acceleration term in (4.101) we have the equation of motion

$$2\Gamma \frac{d\mathbf{l}(\mathbf{r},t)}{dt} + \omega_r^2 \mathbf{l}(\mathbf{r},t) = -\frac{q_e}{m_e}\mathbf{E}'(\mathbf{r},t),$$

which has homogeneous solution

$$\mathbf{l}(\mathbf{r},t) = \mathbf{l}_0(\mathbf{r}) e^{-\frac{\omega_r^2}{2\Gamma}t} = \mathbf{l}_0(\mathbf{r}) e^{-t/\tau}$$

where τ is Debye's *relaxation time.*

By neglecting the acceleration term in (4.102) we obtain from (4.103) the dispersion equation, or *relaxation spectrum*

$$\tilde{\epsilon}(\omega) = \epsilon_0 + \epsilon_0 \frac{\omega_p^2}{\omega_0^2 + j\omega 2\Gamma}.$$

Debye proposed a relaxation spectrum a bit more general than this, now called the *Debye equation*:

$$\tilde{\epsilon}(\omega) = \epsilon_\infty + \frac{\epsilon_s - \epsilon_\infty}{1 + j\omega\tau}. \qquad (4.106)$$

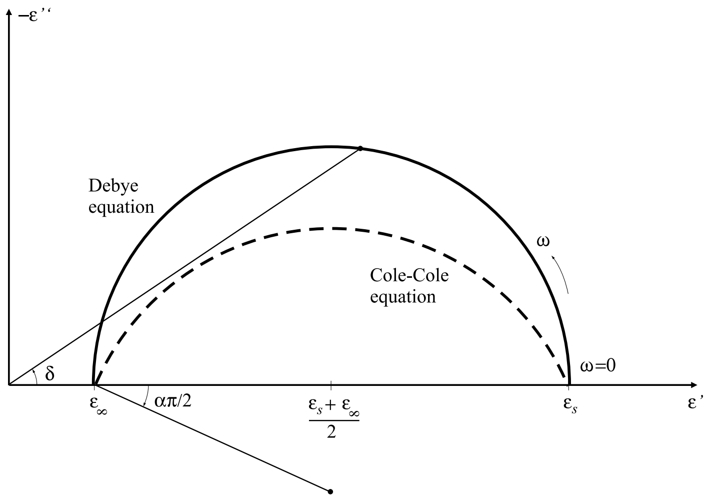

Figure 4.6: Arc plots for Debye and Cole–Cole descriptions of a polar material.

Here ϵ_s is the real static permittivity obtained when $\omega \to 0$, while ϵ_∞ is the real "optical" permittivity describing the high frequency behavior of $\tilde{\epsilon}$. If we split (4.106) into real and imaginary parts we find that

$$\tilde{\epsilon}'(\omega) - \epsilon_\infty = \frac{\epsilon_s - \epsilon_\infty}{1 + \omega^2\tau^2}, \qquad \tilde{\epsilon}''(\omega) = -\frac{\omega\tau(\epsilon_s - \epsilon_\infty)}{1 + \omega^2\tau^2}.$$

For a passive material we must have $\tilde{\epsilon}'' < 0$, which requires $\epsilon_s > \epsilon_\infty$. It is straightforward to show that these expressions obey the Kronig–Kramers relationships. The details are left as an exercise.

A plot of the Debye spectrum of water at $T = 20^\circ$ C is shown in Figure 4.5, where we have used $\epsilon_s = 78.3\epsilon_0$, $\epsilon_\infty = 5\epsilon_0$, and $\tau = 9.6 \times 10^{-12}$ s [49]. We see that $\tilde{\epsilon}'$ decreases over the entire frequency range. The frequency dependence of the imaginary part of the permittivity is similar to that found in the resonance model, forming a curve which peaks at the *critical frequency*

$$\omega_{\text{max}} = 1/\tau$$

where it obtains a maximum value of

$$-\tilde{\epsilon}''_{\text{max}} = \frac{\epsilon_s - \epsilon_\infty}{2}.$$

At this point $\tilde{\epsilon}'$ achieves the average value of ϵ_s and ϵ_∞:

$$\epsilon'(\omega_{\text{max}}) = \frac{\epsilon_s + \epsilon_\infty}{2}.$$

Since the frequency label is logarithmic, we see that the peak is far broader than that for the resonance model.

Interestingly, a plot of $-\tilde{\epsilon}''$ versus $\tilde{\epsilon}'$ traces out a semicircle centered along the real axis at $(\epsilon_s + \epsilon_\infty)/2$ and with radius $(\epsilon_s - \epsilon_\infty)/2$. Such a plot, shown in Figure 4.6, was first described by K.S. Cole and R.H. Cole [38] and is thus called a *Cole–Cole diagram* or "arc

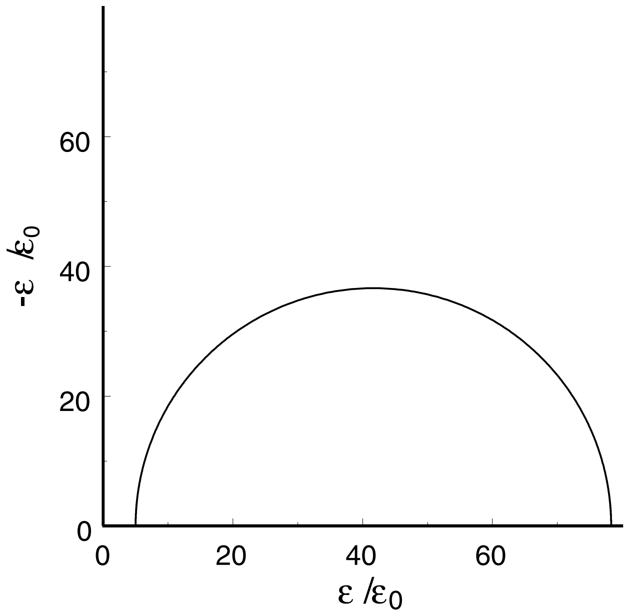

Figure 4.7: Cole–Cole diagram for water at 20° C.

plot." We can think of the vector extending from the origin to a point on the semicircle as a phasor whose phase angle δ is described by the *loss tangent* of the material:

$$\tan\delta = -\frac{\tilde{\epsilon}''}{\tilde{\epsilon}'} = \frac{\omega\tau(\epsilon_s - \epsilon_\infty)}{\epsilon_s + \epsilon_\infty\omega^2\tau^2}. \tag{4.107}$$

The Cole–Cole plot shows that the maximum value of $-\tilde{\epsilon}''$ is $(\epsilon_s - \epsilon_\infty)/2$ and that $\tilde{\epsilon}' = (\epsilon_s + \epsilon_\infty)/2$ at this point.

A Cole–Cole plot for water, shown in Figure 4.7, displays the typical semicircular nature of the arc plot. However, not all polar materials have a relaxation spectrum that follows the Debye equation as closely as water. Cole and Cole found that for many materials the arc plot traces a circular arc centered *below* the real axis, and that the line through its center makes an angle of $\alpha(\pi/2)$ with the real axis as shown in Figure 4.6. This relaxation spectrum can be described in terms of a modified Debye equation

$$\tilde{\epsilon}(\omega) = \epsilon_\infty + \frac{\epsilon_s - \epsilon_\infty}{1 + (j\omega\tau)^{1-\alpha}},$$

called the *Cole–Cole equation*. A nonzero Cole–Cole parameter α tends to broaden the relaxation spectrum, and results from a spread of relaxation times centered around τ [4]. For water the Cole–Cole parameter is only $\alpha = 0.02$, suggesting that a Debye description is sufficient, but for other materials α may be much higher. For instance, consider a transformer oil with a measured Cole–Cole parameter of $\alpha = 0.23$, along with a measured relaxation time of $\tau = 2.3 \times 10^{-9}$ s, a static permittivity of $\epsilon_s = 5.9\epsilon_0$, and an optical permittivity of $\epsilon_\infty = 2.9\epsilon_0$ [4]. Figure 4.8 shows the Cole–Cole plot calculated using both $\alpha = 0$ and $\alpha = 0.23$, demonstrating a significant divergence from the Debye model. Figure 4.9 shows the relaxation spectrum for the transformer oil calculated with these same two parameters.

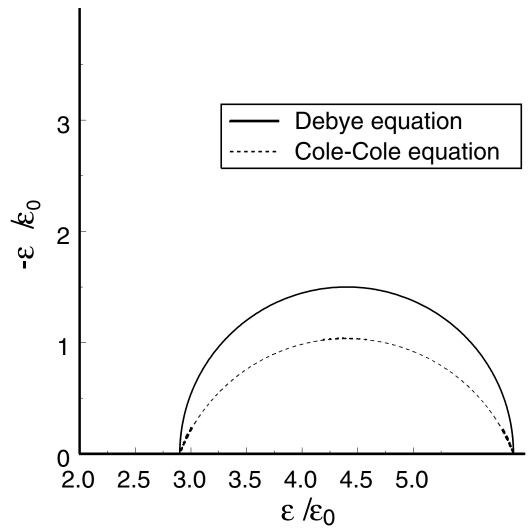

Figure 4.8: Cole–Cole diagram for transformer oil found using Debye equation and Cole–Cole equation with $\alpha = 0.23$.

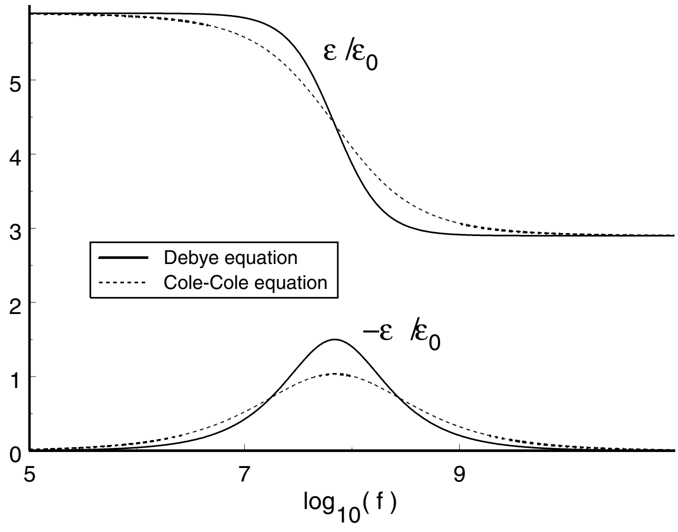

Figure 4.9: Relaxation spectrum for transformer oil found using Debye equation and Cole–Cole equation with $\alpha = 0.23$.

4.6.4 Permittivity and conductivity of a conductor

The free electrons within a conductor may be considered as an electron gas which is free to move under the influence of an applied field. Since the electrons are not bound to the atoms of the conductor, there is no restoring force acting on them. However, there is a damping term associated with electron collisions. We therefore model a conductor as a plasma, but with a very high collision frequency; in a good metallic conductor ν is typically in the range 10^{13}–10^{14} Hz.

We therefore have the conductivity of a conductor from (4.75) as

$$\tilde{\sigma}(\omega) = \frac{\epsilon_0 \omega_p^2 \nu}{\omega^2 + \nu^2}$$

and the permittivity as

$$\tilde{\epsilon}(\omega) = \epsilon_0 \left[1 - \frac{\omega_p^2}{\omega^2 + \nu^2} \right].$$

Since ν is so large, the conductivity is approximately

$$\tilde{\sigma}(\omega) \approx \frac{\epsilon_0 \omega_p^2}{\nu} = \frac{N q_e^2}{m_e \nu}$$

and the permittivity is

$$\tilde{\epsilon}(\omega) \approx \epsilon_0$$

well past microwave frequencies and into the infrared. Hence the dc conductivity is often employed by engineers throughout the communications bands. When approaching the visible spectrum the permittivity and conductivity begin to show a strong frequency dependence. In the violet and ultraviolet frequency ranges the free-charge conductivity becomes proportional to $1/\omega$ and is driven toward zero. However, at these frequencies the resonances of the bound electrons of the metal become important and the permittivity behaves more like that of a dielectric. At these frequencies the permittivity is best described using the resonance formula (4.104).

4.6.5 Permeability dyadic of a ferrite

The magnetic properties of materials are complicated and diverse. The formation of accurate models based on atomic behavior requires an understanding of quantum mechanics, but simple models may be constructed using classical mechanics along with very simple quantum-mechanical assumptions, such as the existence of a spin moment. For an excellent review of the magnetic properties of materials, see Elliott [65].

The magnetic properties of matter ultimately result from atomic currents. In our simple microscopic view these currents arise from the spin and orbital motion of negatively charged electrons. These atomic currents potentially give each atom a *magnetic moment* $\mathbf{m}$. In *diamagnetic* materials the orbital and spin moments cancel unless the material is exposed to an external magnetic field, in which case the orbital electron velocity changes to produce a net moment opposite the applied field. In *paramagnetic* materials the spin moments are greater than the orbital moments, leaving the atoms with a net permanent magnetic moment. When exposed to an external magnetic field, these moments align in the same direction as an applied field. In either case, the density of magnetic moments $\mathbf{M}$ is zero in the absence of an applied field.

In most paramagnetic materials the alignment of the permanent moment of neighboring atoms is random. However, in the subsets of paramagnetic materials known as *ferromagnetic*, *anti-ferromagnetic*, and *ferrimagnetic* materials, there is a strong coupling between the spin moments of neighboring atoms resulting in either parallel or antiparallel alignment of moments. The most familiar case is the parallel alignment of moments within the domains of ferromagnetic permanent magnets made of iron, nickel, and cobalt. Anti-ferromagnetic materials, such as chromium and manganese, have strongly coupled moments that alternate in direction between small domains, resulting in zero net magnetic moment. Ferrimagnetic materials also have alternating moments, but these are unequal and thus do not cancel completely.

Ferrites form a particularly useful subgroup of ferrimagnetic materials. They were first developed during the 1940s by researchers at the Phillips Laboratories as low-loss magnetic media for supporting electromagnetic waves [65]. Typically, ferrites have conductivities ranging from 10^{-4} to 10^0 S/m (compared to 10^7 for iron), relative permeabilities in the thousands, and dielectric constants in the range 10–15. Their low loss makes them useful for constructing transformer cores and for a variety of microwave applications. Their chemical formula is $XO \cdot Fe_2O_3$, where X is a divalent metal or mixture of metals, such as cadmium, copper, iron, or zinc. When exposed to static magnetic fields, ferrites exhibit gyrotropic magnetic (or *gyromagnetic*) properties and have permeability matrices of the form (2.32). The properties of a wide variety of ferrites are given by von Aulock [204].

To determine the permeability matrix of a ferrite we will model its electrons as simple spinning tops and examine the torque exerted on the magnetic moment by the application of an external field. Each electron has an angular momentum $\mathbf{L}$ and a magnetic dipole moment $\mathbf{m}$, with these two vectors anti-parallel:

$$\mathbf{m}(\mathbf{r}, t) = -\gamma \mathbf{L}(\mathbf{r}, t)$$

where

$$\gamma = \frac{q_e}{m_e} = 1.7592 \times 10^{11} \text{ C/kg}$$

is called the *gyromagnetic ratio*.

Let us first consider a single spinning electron immersed in an applied static magnetic field $\mathbf{B}_0$. Any torque applied to the electron results in a change of angular momentum as given by Newton's second law

$$\mathbf{T}(\mathbf{r}, t) = \frac{d\mathbf{L}(\mathbf{r}, t)}{dt}.$$

We found in (3.179) that a very small loop of current in a magnetic field experiences a torque $\mathbf{m} \times \mathbf{B}$. Thus, when first placed into a static magnetic field $\mathbf{B}_0$ an electron's angular momentum obeys the equation

$$\frac{d\mathbf{L}(\mathbf{r}, t)}{dt} = -\gamma \mathbf{L}(\mathbf{r}, t) \times \mathbf{B}_0(\mathbf{r}) = \boldsymbol{\omega}_0(\mathbf{r}) \times \mathbf{L}(\mathbf{r}, t) \tag{4.108}$$

where $\boldsymbol{\omega}_0 = \gamma \mathbf{B}_0$. This equation of motion describes the *precession* of the electron spin axis about the direction of the applied field, which is analogous to the precession of a gyroscope [129]. The spin axis rotates at the *Larmor precessional frequency* $\omega_0 = \gamma B_0 = \gamma \mu_0 H_0$.

We can use this to understand what happens when we insert a homogeneous ferrite material into a uniform static magnetic field $\mathbf{B}_0 = \mu_0 \mathbf{H}_0$. The internal field $\mathbf{H}_i$ experienced by any magnetic dipole is not the same as the external field $\mathbf{H}_0$, and need not even be in the same direction. In general we write

$$\mathbf{H}_0(\mathbf{r}, t) - \mathbf{H}_i(\mathbf{r}, t) = \mathbf{H}_d(\mathbf{r}, t)$$

where $\mathbf{H}_d$ is the *demagnetizing field* produced by the magnetic dipole moments of the material. Each electron responds to the internal field by precessing as described above until the precession damps out and the electron moments align with the magnetic field. At this point the ferrite is *saturated*. Because the demagnetizing field depends strongly on the shape of the material we choose to ignore it as a first approximation, and this allows us to concentrate our study on the fundamental atomic properties of the ferrite.

For purposes of understanding its magnetic properties, we view the ferrite as a dense collection of electrons and write

$$\mathbf{M}(\mathbf{r}, t) = N\mathbf{m}(\mathbf{r}, t)$$

where N is the number density of electrons. Since we are assuming the ferrite is homogeneous, we take N to be independent of time and position. Multiplying (4.108) by $-N\gamma$, we obtain an equation describing the evolution of $\mathbf{M}$:

$$\frac{d\mathbf{M}(\mathbf{r}, t)}{dt} = -\gamma \mathbf{M}(\mathbf{r}, t) \times \mathbf{B}_i(\mathbf{r}, t). \tag{4.109}$$

To determine the temporal response of the ferrite we must include a time-dependent component of the applied field. We now let

$$\mathbf{H}_0(\mathbf{r}, t) = \mathbf{H}_i(\mathbf{r}, t) = \mathbf{H}_T(\mathbf{r}, t) + \mathbf{H}_{dc}$$

where $\mathbf{H}_T$ is the time-dependent component superimposed with the uniform static component $\mathbf{H}_{dc}$. Using $\mathbf{B} = \mu_0(\mathbf{H} + \mathbf{M})$ we have from (4.109)

$$\frac{d\mathbf{M}(\mathbf{r}, t)}{dt} = -\gamma \mu_0 \mathbf{M}(\mathbf{r}, t) \times [\mathbf{H}_T(\mathbf{r}, t) + \mathbf{H}_{dc} + \mathbf{M}(\mathbf{r}, t)].$$

With $\mathbf{M} = \mathbf{M}_T(\mathbf{r}, t) + \mathbf{M}_{dc}$ and $\mathbf{M} \times \mathbf{M} = 0$ this becomes

$$\frac{d\mathbf{M}_T(\mathbf{r}, t)}{dt} + \frac{d\mathbf{M}_{dc}}{dt} = -\gamma \mu_0 [\mathbf{M}_T(\mathbf{r}, t) \times \mathbf{H}_T(\mathbf{r}, t) + \mathbf{M}_T(\mathbf{r}, t) \times \mathbf{H}_{dc} + + \mathbf{M}_{dc} \times \mathbf{H}_T(\mathbf{r}, t) + \mathbf{M}_{dc} \times \mathbf{H}_{dc}. \tag{4.110}$$

Let us assume that the ferrite is saturated. Then $\mathbf{M}_{dc}$ is aligned with $\mathbf{H}_{dc}$ and their cross product vanishes. Let us further assume that the spectrum of H_T is small compared to H_{dc} at all frequencies: $|\tilde{H}_T(\mathbf{r}, \omega)| \ll H_{dc}$. This small-signal assumption allows us to neglect $\mathbf{M}_T \times \mathbf{H}_T$. Using these and noting that the time derivative of $\mathbf{M}_{dc}$ is zero, we see that (4.110) reduces to

$$\frac{d\mathbf{M}_T(\mathbf{r}, t)}{dt} = -\gamma \mu_0 [\mathbf{M}_T(\mathbf{r}, t) \times \mathbf{H}_{dc} + \mathbf{M}_{dc} \times \mathbf{H}_T(\mathbf{r}, t)]. \tag{4.111}$$

To determine the frequency response we write (4.111) in terms of inverse Fourier transforms and invoke the Fourier integral theorem to find that

$$j\omega \tilde{\mathbf{M}}_T(\mathbf{r}, \omega) = -\gamma \mu_0 [\tilde{\mathbf{M}}_T(\mathbf{r}, \omega) \times \mathbf{H}_{dc} + \mathbf{M}_{dc} \times \tilde{\mathbf{H}}_T(\mathbf{r}, \omega)].$$

Defining

$$\gamma \mu_0 \mathbf{M}_{dc} = \boldsymbol{\omega}_M,$$

where $\omega_M = |\boldsymbol{\omega}_M|$ is the *saturation magnetization frequency*, we find that

$$\tilde{\mathbf{M}}_T + \tilde{\mathbf{M}}_T \times \left[\frac{\boldsymbol{\omega}_0}{j\omega}\right] = \left[-\frac{1}{j\omega}\boldsymbol{\omega}_M \times \tilde{\mathbf{H}}_T\right], \tag{4.112}$$

where $\boldsymbol{\omega}_0 = \gamma\mu_0\mathbf{H}_{dc}$ with ω_0 now called the *gyromagnetic response frequency*. This has the form $\mathbf{v} + \mathbf{v} \times \mathbf{C} = \mathbf{A}$, which has solution (4.80). Substituting into this expression and remembering that $\boldsymbol{\omega}_0$ is parallel to $\boldsymbol{\omega}_M$, we find that

$$\tilde{\mathbf{M}}_T = \frac{-\frac{1}{j\omega}\boldsymbol{\omega}_M \times \tilde{\mathbf{H}}_T + \frac{1}{\omega^2}\left\{\boldsymbol{\omega}_M[\boldsymbol{\omega}_0 \cdot \tilde{\mathbf{H}}_T] - (\boldsymbol{\omega}_0 \cdot \boldsymbol{\omega}_M)\tilde{\mathbf{H}}_T\right\}}{1 - \frac{\omega_0^2}{\omega^2}}.$$

If we define the dyadic $\bar{\boldsymbol{\omega}}_M$ such that $\bar{\boldsymbol{\omega}}_M \cdot \tilde{\mathbf{H}}_T = \boldsymbol{\omega}_M \times \tilde{\mathbf{H}}_T$, then we identify the dyadic magnetic susceptibility

$$\tilde{\bar{\chi}}_m(\omega) = \frac{j\omega\bar{\boldsymbol{\omega}}_M + \boldsymbol{\omega}_M\boldsymbol{\omega}_0 - \omega_M\omega_0\bar{\mathbf{I}}}{\omega^2 - \omega_0^2} \tag{4.113}$$

with which we can write $\tilde{\mathbf{M}}(\mathbf{r},\omega) = \tilde{\bar{\chi}}_m(\omega) \cdot \tilde{\mathbf{H}}(\mathbf{r},\omega)$. In rectangular coordinates $\bar{\boldsymbol{\omega}}_M$ is represented by

$$[\bar{\boldsymbol{\omega}}_M] = \begin{bmatrix} 0 & -\omega_{Mz} & \omega_{My} \\ \omega_{Mz} & 0 & -\omega_{Mx} \\ -\omega_{My} & \omega_{Mx} & 0 \end{bmatrix}. \tag{4.114}$$

Finally, using $\tilde{\mathbf{B}} = \mu_0(\tilde{\mathbf{H}} + \tilde{\mathbf{M}}) = \mu_0(\bar{\mathbf{I}} + \tilde{\bar{\chi}}_m) \cdot \tilde{\mathbf{H}} = \tilde{\bar{\boldsymbol{\mu}}} \cdot \tilde{\mathbf{H}}$ we find that

$$\tilde{\bar{\boldsymbol{\mu}}}(\omega) = \mu_0[\bar{\mathbf{I}} + \tilde{\bar{\chi}}_m(\omega)].$$

To examine the properties of the dyadic permeability it is useful to write it in matrix form. To do this we must choose a coordinate system. We shall assume that $\mathbf{H}_{dc}$ is aligned with the z-axis so that $\mathbf{H}_{dc} = \hat{\mathbf{z}}H_{dc}$ and thus $\boldsymbol{\omega}_M = \hat{\mathbf{z}}\omega_M$ and $\boldsymbol{\omega}_0 = \hat{\mathbf{z}}\omega_0$. Then (4.114) becomes

$$[\bar{\boldsymbol{\omega}}_M] = \begin{bmatrix} 0 & -\omega_M & 0 \\ \omega_M & 0 & 0 \\ 0 & 0 & 0 \end{bmatrix}$$

and we can write the susceptibility dyadic (4.113) as

$$[\tilde{\bar{\chi}}_m(\omega)] = \frac{\omega_M}{\omega^2 - \omega_0^2}\begin{bmatrix} -\omega_0 & -j\omega & 0 \\ j\omega & -\omega_0 & 0 \\ 0 & 0 & 0 \end{bmatrix}.$$

The permeability dyadic becomes

$$[\tilde{\bar{\boldsymbol{\mu}}}(\omega)] = \begin{bmatrix} \mu & -j\kappa & 0 \\ j\kappa & \mu & 0 \\ 0 & 0 & \mu_0 \end{bmatrix} \tag{4.115}$$

where

$$\mu = \mu_0\left(1 - \frac{\omega_0\omega_M}{\omega^2 - \omega_0^2}\right), \tag{4.116}$$

$$\kappa = \mu_0\frac{\omega\omega_M}{\omega^2 - \omega_0^2}. \tag{4.117}$$

Because its permeability dyadic is that for a lossless *gyrotropic* material (2.33), we call the ferrite *gyromagnetic*.

Since the ferrite is lossless, the dyadic permeability must be hermitian according to (4.49). The specific form of (4.115) shows this explicitly. We also note that since the sign of $\boldsymbol{\omega}_M$ is determined by that of $\mathbf{H}_{dc}$, the dyadic permittivity obeys the symmetry relation

$$\tilde{\mu}_{ij}(\mathbf{H}_{dc}) = \tilde{\mu}_{ji}(-\mathbf{H}_{dc}),$$

which is the symmetry condition observed for a plasma in (4.87).

A lossy ferrite material can be modeled by adding a damping term to (4.111):

$$\frac{d\mathbf{M}(\mathbf{r},t)}{dt} = -\gamma\mu_0 \left[\mathbf{M}_T(\mathbf{r},t) \times \mathbf{H}_{dc} + \mathbf{M}_{dc} \times \mathbf{H}_T(\mathbf{r},t)\right] + \alpha \frac{\mathbf{M}_{dc}}{M_{dc}} \times \frac{d\mathbf{M}_T(\mathbf{r},t)}{dt},$$

where α is the damping parameter [40, 204]. This term tends to reduce the angle of precession. Fourier transformation gives

$$j\omega\tilde{\mathbf{M}}_T = \boldsymbol{\omega}_0 \times \tilde{\mathbf{M}}_T - \boldsymbol{\omega}_M \times \tilde{\mathbf{H}}_T + \alpha \frac{\boldsymbol{\omega}_M}{\omega_M} \times j\omega\tilde{\mathbf{M}}_T.$$

Remembering that $\boldsymbol{\omega}_0$ and $\boldsymbol{\omega}_M$ are aligned we can write this as

$$\tilde{\mathbf{M}}_T + \tilde{\mathbf{M}}_T \times \left[\frac{\boldsymbol{\omega}_0\left(1 + j\alpha\frac{\omega}{\omega_0}\right)}{j\omega}\right] = \left[-\frac{1}{j\omega}\boldsymbol{\omega}_M \times \tilde{\mathbf{H}}_T\right].$$

This is identical to (4.112) with

$$\boldsymbol{\omega}_0 \to \boldsymbol{\omega}_0\left(1 + j\alpha\frac{\omega}{\omega_0}\right).$$

Thus, we merely substitute this into (4.113) to find the susceptibility dyadic for a lossy ferrite:

$$\tilde{\bar{\chi}}_m(\omega) = \frac{j\omega\bar{\boldsymbol{\omega}}_M + \boldsymbol{\omega}_M\boldsymbol{\omega}_0\left(1 + j\alpha\omega/\omega_0\right) - \omega_M\omega_0\left(1 + j\alpha\omega/\omega_0\right)\bar{\mathbf{I}}}{\omega^2(1+\alpha^2) - \omega_0^2 - 2j\alpha\omega\omega_0}.$$

Making the same substitution into (4.115) we can write the dyadic permeability matrix as

$$[\tilde{\bar{\boldsymbol{\mu}}}(\omega)] = \begin{bmatrix} \tilde{\mu}_{xx} & \tilde{\mu}_{xy} & 0 \\ \tilde{\mu}_{yx} & \tilde{\mu}_{yy} & 0 \\ 0 & 0 & \mu_0 \end{bmatrix} \tag{4.118}$$

where

$$\tilde{\mu}_{xx} = \tilde{\mu}_{yy} = \mu_0 - \mu_0\omega_M \frac{\omega_0\left[\omega^2(1-\alpha^2) - \omega_0^2\right] + j\omega\alpha\left[\omega^2(1+\alpha^2) + \omega_0^2\right]}{\left[\omega^2(1+\alpha^2) - \omega_0^2\right]^2 + 4\alpha^2\omega^2\omega_0^2} \tag{4.119}$$

and

$$\tilde{\mu}_{xy} = -\tilde{\mu}_{yx} = \frac{2\mu_0\alpha\omega^2\omega_0\omega_M - j\mu_0\omega\omega_M\left[\omega^2(1+\alpha^2) - \omega_0^2\right]}{\left[\omega^2(1+\alpha^2) - \omega_0^2\right]^2 + 4\alpha^2\omega^2\omega_0^2}. \tag{4.120}$$

In the case of a lossy ferrite, the hermitian nature of the permeability dyadic is lost.

4.7 Monochromatic fields and the phasor domain

The Fourier transform is very efficient for representing the nearly sinusoidal signals produced by electronic systems such as oscillators. However, we should realize that the elemental term $e^{j\omega t}$ by itself cannot represent any physical quantity; only a continuous superposition of such terms can have physical meaning, because no physical process can be truly monochromatic. All events must have transient periods during which they are established. Even "monochromatic" light appears in bundles called quanta, interpreted as containing finite numbers of oscillations.

Arguments about whether "monochromatic" or "sinusoidal steady-state" fields can actually exist may sound purely academic. After all, a microwave oscillator can create a wave train of 10^{10} oscillations within the first second after being turned on. Such a waveform is surely as close to monochromatic as we would care to measure. But as with all mathematical models of physical systems, we can get into trouble by making non-physical assumptions, in this instance by assuming a physical system has always been in the steady state. Sinusoidal steady-state solutions to Maxwell's equations can lead to troublesome infinities linked to the infinite energy content of each elemental component. For example, an attempt to compute the energy stored within a lossless microwave cavity under steady-state conditions gives an infinite result since the cavity has been building up energy since $t = -\infty$. We handle this by considering time-averaged quantities, but even then must be careful when materials are dispersive (§ 4.5). Nevertheless, the steady-state concept is valuable because of its simplicity and finds widespread application in electromagnetics.

Since the elemental term is complex, we may use its real part, its imaginary part, or some combination of both to represent a monochromatic (or *time-harmonic*) field. We choose the representation

$$\psi(\mathbf{r}, t) = \psi_0(\mathbf{r}) \cos[\check{\omega} t + \xi(\mathbf{r})], \tag{4.121}$$

where ξ is the temporal phase angle of the sinusoidal function. The Fourier transform is

$$\tilde{\psi}(\mathbf{r}, \omega) = \int_{-\infty}^{\infty} \psi_0(\mathbf{r}) \cos[\check{\omega} t + \xi(\mathbf{r})] e^{-j\omega t}\, dt. \tag{4.122}$$

Here we run into an immediate problem: the transform in (4.122) does not exist in the ordinary sense since $\cos(\check{\omega} t + \xi)$ is not absolutely integrable on $(-\infty, \infty)$. We should not be surprised by this: the cosine function cannot describe an actual physical process (it extends in time to $\pm\infty$), so it lacks a classical Fourier transform. One way out of this predicament is to extend the meaning of the Fourier transform as we do in § A.1. Then the monochromatic field (4.121) is viewed as having the generalized transform

$$\tilde{\psi}(\mathbf{r}, \omega) = \psi_0(\mathbf{r}) \pi \left[e^{j\xi(\mathbf{r})} \delta(\omega - \check{\omega}) + e^{-j\xi(\mathbf{r})} \delta(\omega + \check{\omega}) \right]. \tag{4.123}$$

We can compute the inverse Fourier transform by substituting (123) into (2):

$$\psi(\mathbf{r}, t) = \frac{1}{2\pi} \int_{-\infty}^{\infty} \psi_0(\mathbf{r}) \pi \left[e^{j\xi(\mathbf{r})} \delta(\omega - \check{\omega}) + e^{-j\xi(\mathbf{r})} \delta(\omega + \check{\omega}) \right] e^{j\omega t}\, d\omega. \tag{4.124}$$

By our interpretation of the Dirac delta, we see that the decomposition of the cosine function has only two discrete components, located at $\omega = \pm\check{\omega}$. So we have realized our initial intention of having only a single elemental function present. The sifting property gives

$$\psi(\mathbf{r}, t) = \psi_0(\mathbf{r}) \frac{e^{j\check{\omega}t} e^{j\xi(\mathbf{r})} + e^{-j\check{\omega}t} e^{-j\xi(\mathbf{r})}}{2} = \psi_0(\mathbf{r}) \cos[\check{\omega}t + \xi(\mathbf{r})]$$

as expected.

4.7.1 The time-harmonic EM fields and constitutive relations

The time-harmonic fields are described using the representation (4.121) for each field component. The electric field is

$$\mathbf{E}(\mathbf{r}, t) = \sum_{i=1}^{3} \hat{\mathbf{i}}_i |E_i(\mathbf{r})| \cos[\check{\omega}t + \xi_i^E(\mathbf{r})]$$

for example. Here $|E_i|$ is the complex magnitude of the ith vector component, and ξ_i^E is the phase angle ($-\pi < \xi_i^E \leq \pi$). Similar terminology is used for the remaining fields.

The frequency-domain constitutive relations (4.11)–(4.15) may be written for the time-harmonic fields by employing (4.124). For instance, for an isotropic material where

$$\tilde{\mathbf{D}}(\mathbf{r}, \omega) = \tilde{\epsilon}(\mathbf{r}, \omega)\tilde{\mathbf{E}}(\mathbf{r}, \omega), \qquad \tilde{\mathbf{B}}(\mathbf{r}, \omega) = \tilde{\mu}(\mathbf{r}, \omega)\tilde{\mathbf{H}}(\mathbf{r}, \omega),$$

with

$$\tilde{\epsilon}(\mathbf{r}, \omega) = |\tilde{\epsilon}(\mathbf{r}, \omega)| e^{\xi^\epsilon(\mathbf{r}, \omega)}, \qquad \tilde{\mu}(\mathbf{r}, \omega) = |\tilde{\mu}(\mathbf{r}, \omega)| e^{\xi^\mu(\mathbf{r}, \omega)},$$

we can write

$$\begin{aligned}
\mathbf{D}(\mathbf{r}, t) &= \sum_{i=1}^{3} \hat{\mathbf{i}}_i |D_i(\mathbf{r})| \cos[\check{\omega}t + \xi_i^D(\mathbf{r})] \\
&= \frac{1}{2\pi} \int_{-\infty}^{\infty} \sum_{i=1}^{3} \hat{\mathbf{i}}_i \tilde{\epsilon}(\mathbf{r}, \omega) |E_i(\mathbf{r})| \pi \left[e^{j\xi_i^E(\mathbf{r})} \delta(\omega - \check{\omega}) + e^{-j\xi_i^E(\mathbf{r})} \delta(\omega + \check{\omega}) \right] e^{j\omega t} \, d\omega \\
&= \frac{1}{2} \sum_{i=1}^{3} \hat{\mathbf{i}}_i |E_i(\mathbf{r})| \left[\tilde{\epsilon}(\mathbf{r}, \check{\omega}) e^{j(\check{\omega}t + j\xi_i^E(\mathbf{r}))} + \tilde{\epsilon}(\mathbf{r}, -\check{\omega}) e^{-j(\check{\omega}t + j\xi_i^E(\mathbf{r}))} \right].
\end{aligned}$$

Since (4.25) shows that $\tilde{\epsilon}(\mathbf{r}, -\check{\omega}) = \tilde{\epsilon}^*(\mathbf{r}, \check{\omega})$, we have

$$\begin{aligned}
\mathbf{D}(\mathbf{r}, t) &= \frac{1}{2} \sum_{i=1}^{3} \hat{\mathbf{i}}_i |E_i(\mathbf{r})| |\tilde{\epsilon}(\mathbf{r}, \check{\omega})| \left[e^{j(\check{\omega}t + j\xi_i^E(\mathbf{r}) + j\xi^\epsilon(\mathbf{r}, \check{\omega}))} + e^{-j(\check{\omega}t + j\xi_i^E(\mathbf{r}) + j\xi^\epsilon(\mathbf{r}, \check{\omega}))} \right] \\
&= \sum_{i=1}^{3} \hat{\mathbf{i}}_i |\tilde{\epsilon}(\mathbf{r}, \check{\omega})| |E_i(\mathbf{r})| \cos[\check{\omega}t + \xi_i^E(\mathbf{r}) + \xi^\epsilon(\mathbf{r}, \check{\omega})]. \qquad (4.125)
\end{aligned}$$

Similarly

$$\begin{aligned}
\mathbf{B}(\mathbf{r}, t) &= \sum_{i=1}^{3} \hat{\mathbf{i}}_i |B_i(\mathbf{r})| \cos[\check{\omega}t + \xi_i^B(\mathbf{r})] \\
&= \sum_{i=1}^{3} \hat{\mathbf{i}}_i |\tilde{\mu}(\mathbf{r}, \check{\omega})| |H_i(\mathbf{r})| \cos[\check{\omega}t + \xi_i^H(\mathbf{r}) + \xi^\mu(\mathbf{r}, \check{\omega})].
\end{aligned}$$

4.7.2 The phasor fields and Maxwell's equations

Sinusoidal steady-state computations using the forward and inverse transform formulas are unnecessarily cumbersome. A much more efficient approach is to use the *phasor* concept. If we define the complex function

$$\check{\psi}(\mathbf{r}) = \psi_0(\mathbf{r}) e^{j\xi(\mathbf{r})}$$

as the *phasor form* of the monochromatic field $\tilde{\psi}(\mathbf{r}, \omega)$, then the inverse Fourier transform is easily computed by multiplying $\check{\psi}(\mathbf{r})$ by $e^{j\check{\omega}t}$ and taking the real part. That is,

$$\psi(\mathbf{r}, t) = \text{Re}\left\{\check{\psi}(\mathbf{r}) e^{j\check{\omega}t}\right\} = \psi_0(\mathbf{r}) \cos[\check{\omega}t + \xi(\mathbf{r})]. \tag{4.126}$$

Using the phasor representation of the fields, we can obtain a set of Maxwell equations relating the phasor components. Let

$$\check{\mathbf{E}}(\mathbf{r}) = \sum_{i=1}^{3} \hat{\mathbf{i}}_i \check{E}_i(\mathbf{r}) = \sum_{i=1}^{3} \hat{\mathbf{i}}_i |E_i(\mathbf{r})| e^{j\xi_i^E(\mathbf{r})}$$

represent the phasor monochromatic electric field, with similar formulas for the other fields. Then

$$\mathbf{E}(\mathbf{r}, t) = \text{Re}\left\{\check{\mathbf{E}}(\mathbf{r}) e^{j\check{\omega}t}\right\} = \sum_{i=1}^{3} \hat{\mathbf{i}}_i |E_i(\mathbf{r})| \cos[\check{\omega}t + \xi_i^E(\mathbf{r})].$$

Substituting these expressions into Ampere's law (2.2), we have

$$\nabla \times \text{Re}\left\{\check{\mathbf{H}}(\mathbf{r}) e^{j\check{\omega}t}\right\} = \frac{\partial}{\partial t} \text{Re}\left\{\check{\mathbf{D}}(\mathbf{r}) e^{j\check{\omega}t}\right\} + \text{Re}\left\{\check{\mathbf{J}}(\mathbf{r}) e^{j\check{\omega}t}\right\}.$$

Since the real part of a sum of complex variables equals the sum of the real parts, we can write

$$\text{Re}\left\{\nabla \times \check{\mathbf{H}}(\mathbf{r}) e^{j\check{\omega}t} - \check{\mathbf{D}}(\mathbf{r}) \frac{\partial}{\partial t} e^{j\check{\omega}t} - \check{\mathbf{J}}(\mathbf{r}) e^{j\check{\omega}t}\right\} = 0. \tag{4.127}$$

If we examine for an arbitrary complex function $F = F_r + jF_i$ the quantity

$$\text{Re}\left\{(F_r + jF_i) e^{j\check{\omega}t}\right\} = \text{Re}\left\{(F_r \cos\check{\omega}t - F_i \sin\check{\omega}t) + j(F_r \sin\check{\omega}t + F_i \cos\check{\omega}t)\right\},$$

we see that both F_r and F_i must be zero for the expression to vanish for all t. Thus (4.127) requires that

$$\nabla \times \check{\mathbf{H}}(\mathbf{r}) = j\check{\omega}\check{\mathbf{D}}(\mathbf{r}) + \check{\mathbf{J}}(\mathbf{r}), \tag{4.128}$$

which is the phasor Ampere's law. Similarly we have

$$\nabla \times \check{\mathbf{E}}(\mathbf{r}) = -j\check{\omega}\check{\mathbf{B}}(\mathbf{r}), \tag{4.129}$$

$$\nabla \cdot \check{\mathbf{D}}(\mathbf{r}) = \check{\rho}(\mathbf{r}), \tag{4.130}$$

$$\nabla \cdot \check{\mathbf{B}}(\mathbf{r}) = 0, \tag{4.131}$$

and

$$\nabla \cdot \check{\mathbf{J}}(\mathbf{r}) = -j\check{\omega}\check{\rho}(\mathbf{r}). \tag{4.132}$$

The constitutive relations may be easily incorporated into the phasor concept. If we use

$$\check{D}_i(\mathbf{r}) = \tilde{\epsilon}(\mathbf{r}, \check{\omega}) \check{E}_i(\mathbf{r}) = |\tilde{\epsilon}(\mathbf{r}, \check{\omega})| e^{j\xi^\epsilon(\mathbf{r},\check{\omega})} |E_i(\mathbf{r})| e^{j\xi_i^E(\mathbf{r})},$$

then forming

$$D_i(\mathbf{r},t) = \text{Re}\left\{\check{D}_i(\mathbf{r})e^{j\check{\omega}t}\right\}$$

we reproduce (4.125). Thus we may write

$$\check{\mathbf{D}}(\mathbf{r}) = \tilde{\epsilon}(\mathbf{r},\check{\omega})\check{\mathbf{E}}(\mathbf{r}).$$

Note that we never write $\check{\epsilon}$ or refer to a "phasor permittivity" since the permittivity does not vary sinusoidally in the time domain.

An obvious benefit of the phasor method is that we can manipulate field quantities without involving the sinusoidal time dependence. When our manipulations are complete, we return to the time domain using (4.126).

The phasor Maxwell equations (4.128)–(4.131) are identical in form to the temporal frequency-domain Maxwell equations (4.7)–(4.10), except that $\omega = \check{\omega}$ in the phasor equations. This is sensible, since the phasor fields represent a single component of the complete frequency-domain spectrum of the arbitrary time-varying fields. Thus, if the phasor fields are calculated for some $\check{\omega}$, we can make the replacements

$$\check{\omega} \to \omega, \qquad \check{\mathbf{E}}(\mathbf{r}) \to \tilde{\mathbf{E}}(\mathbf{r},\omega), \qquad \check{\mathbf{H}}(\mathbf{r}) \to \tilde{\mathbf{H}}(\mathbf{r},\omega), \qquad \dots,$$

and obtain the general time-domain expressions by performing the inversion (4.2). Similarly, if we evaluate the frequency-domain field $\tilde{\mathbf{E}}(\mathbf{r},\omega)$ at $\omega = \check{\omega}$, we produce the phasor field $\check{\mathbf{E}}(\mathbf{r}) = \tilde{\mathbf{E}}(\mathbf{r},\check{\omega})$ for this frequency. That is

$$\text{Re}\left\{\tilde{\mathbf{E}}(\mathbf{r},\check{\omega})e^{j\check{\omega}t}\right\} = \sum_{i=1}^{3} \hat{\mathbf{i}}_i |\tilde{\mathbf{E}}_i(\mathbf{r},\check{\omega})| \cos\left(\check{\omega}t + \xi^E(\mathbf{r},\check{\omega})\right).$$

4.7.3 Boundary conditions on the phasor fields

The boundary conditions developed in § 4.3 for the frequency-domain fields may be adapted for use with the phasor fields by selecting $\omega = \check{\omega}$. Let us include the effects of fictitious magnetic sources and write

$$\hat{\mathbf{n}}_{12} \times (\check{\mathbf{H}}_1 - \check{\mathbf{H}}_2) = \check{\mathbf{J}}_s, \tag{4.133}$$

$$\hat{\mathbf{n}}_{12} \times (\check{\mathbf{E}}_1 - \check{\mathbf{E}}_2) = -\check{\mathbf{J}}_{ms}, \tag{4.134}$$

$$\hat{\mathbf{n}}_{12} \cdot (\check{\mathbf{D}}_1 - \check{\mathbf{D}}_2) = \check{\rho}_s, \tag{4.135}$$

$$\hat{\mathbf{n}}_{12} \cdot (\check{\mathbf{B}}_1 - \check{\mathbf{B}}_2) = \check{\rho}_{ms}, \tag{4.136}$$

and

$$\hat{\mathbf{n}}_{12} \cdot (\check{\mathbf{J}}_1 - \check{\mathbf{J}}_2) = -\nabla_s \cdot \check{\mathbf{J}}_s - j\check{\omega}\check{\rho}_s, \tag{4.137}$$

$$\hat{\mathbf{n}}_{12} \cdot (\check{\mathbf{J}}_{m1} - \check{\mathbf{J}}_{m2}) = -\nabla_s \cdot \check{\mathbf{J}}_{ms} - j\check{\omega}\check{\rho}_{ms}, \tag{4.138}$$

where $\hat{\mathbf{n}}_{12}$ points into region 1 from region 2.

4.8 Poynting's theorem for time-harmonic fields

We can specialize Poynting's theorem to time-harmonic form by substituting the time-harmonic field representations. The result depends on whether we use the general form

(2.301), which is valid for dispersive materials, or (2.299). For nondispersive materials (2.299) allows us to interpret the volume integral term as the time rate of change of stored energy. But if the operating frequency lies within the realm of material dispersion and loss, then we can no longer identify an explicit stored energy term.

4.8.1 General form of Poynting's theorem

We begin with (2.301). Substituting the time-harmonic representations we obtain the term

$$\mathbf{E}(\mathbf{r},t)\cdot\frac{\partial\mathbf{D}(\mathbf{r},t)}{\partial t} = \left[\sum_{i=1}^{3}\hat{\mathbf{i}}_i|E_i|\cos[\check{\omega}t+\xi_i^E]\right]\cdot\frac{\partial}{\partial t}\left[\sum_{i=1}^{3}\hat{\mathbf{i}}_i|D_i|\cos[\check{\omega}t+\xi_i^D]\right]$$
$$= -\check{\omega}\sum_{i=1}^{3}|E_i||D_i|\cos[\check{\omega}t+\xi_i^E]\sin[\check{\omega}t+\xi_i^D].$$

Since $2\sin A\cos B \equiv \sin(A+B)+\sin(A-B)$ we have

$$\mathbf{E}(\mathbf{r},t)\cdot\frac{\partial}{\partial t}\mathbf{D}(\mathbf{r},t) = -\frac{1}{2}\sum_{i=1}^{3}\check{\omega}|E_i||D_i|S_{ii}^{DE}(t),$$

where

$$S_{ii}^{DE}(t) = \sin(2\check{\omega}t+\xi_i^D+\xi_i^E)+\sin(\xi_i^D-\xi_i^E)$$

describes the temporal dependence of the field product. Separating the current into an impressed term $\mathbf{J}^i$ and a secondary term $\mathbf{J}^c$ (assumed to be the conduction current) as $\mathbf{J} = \mathbf{J}^i + \mathbf{J}^c$ and repeating the above steps with the other terms, we obtain

$$-\frac{1}{2}\int_V\sum_{i=1}^{3}|J_i^i||E_i|C_{ii}^{J^iE}(t)\,dV = \frac{1}{2}\oint_S\sum_{i,j=1}^{3}|E_i||H_j|(\hat{\mathbf{i}}_i\times\hat{\mathbf{i}}_j)\cdot\hat{\mathbf{n}}C_{ij}^{EH}(t)\,dS +$$
$$+\frac{1}{2}\int_V\sum_{i=1}^{3}\left\{-\check{\omega}|D_i||E_i|S_{ii}^{DE}(t)-\check{\omega}|B_i||H_i|S_{ii}^{BH}(t)+|J_i^c||E_i|C_{ii}^{J^cE}(t)\right\}dV, \qquad (4.139)$$

where

$$S_{ii}^{BH}(t) = \sin(2\check{\omega}t+\xi_i^B+\xi_i^H)+\sin(\xi_i^B-\xi_i^H),$$
$$C_{ij}^{EH}(t) = \cos(2\check{\omega}t+\xi_i^E+\xi_j^H)+\cos(\xi_i^E-\xi_j^H),$$

and so on.

We see that each power term has two temporal components: one oscillating at frequency $2\check{\omega}$, and one constant with time. The oscillating component describes power that cycles through the various mechanisms of energy storage, dissipation, and transfer across the boundary. Dissipation may be produced through conduction processes or through polarization and magnetization phase lag, as described by the volume term on the right-hand side of (4.139). Power may also be delivered to the fields either from the sources, as described by the volume term on the left-hand side, or from an active medium, as described by the volume term on the right-hand side. The time-average balance of power supplied to the fields and extracted from the fields throughout each cycle, including that transported across the surface S, is given by the constant terms in (4.139):

$$-\frac{1}{2}\int_V \sum_{i=1}^{3} |J_i^i||E_i| \cos(\xi_i^{J^i} - \xi_i^E)\, dV = \frac{1}{2}\int_V \sum_{i=1}^{3} \{\check{\omega}|E_i||D_i| \sin(\xi_i^E - \xi_i^D) +$$
$$+\check{\omega}|B_i||H_i| \sin(\xi_i^H - \xi_i^B) + |J_i^c||E_i| \cos(\xi_i^{J^c} - \xi_i^E)\}\, dV +$$
$$+\frac{1}{2}\oint_S \sum_{i,j=1}^{3} |E_i||H_j|(\hat{\mathbf{i}}_i \times \hat{\mathbf{i}}_j)\cdot \hat{\mathbf{n}} \cos(\xi_i^E - \xi_j^H)\, dS. \tag{4.140}$$

We associate one mechanism for time-average power loss with the phase lag between applied field and resulting polarization or magnetization. We can see this more clearly if we use the alternative form of the Poynting theorem (2.302) written in terms of the polarization and magnetization vectors. Writing

$$\mathbf{P}(\mathbf{r}, t) = \sum_{i=1}^{3} |P_i(\mathbf{r})| \cos[\check{\omega}t + \xi_i^P(\mathbf{r})], \qquad \mathbf{M}(\mathbf{r}, t) = \sum_{i=1}^{3} |M_i(\mathbf{r})| \cos[\check{\omega}t + \xi_i^M(\mathbf{r})],$$

and substituting the time-harmonic fields, we see that

$$-\frac{1}{2}\int_V \sum_{i=1}^{3} |J_i||E_i| C_{ii}^{JE}(t)\, dV + \frac{\check{\omega}}{2}\int_V \sum_{i=1}^{3} \left[|P_i||E_i| S_{ii}^{PE}(t) + \mu_0 |M_i||H_i| S_{ii}^{MH}(t)\right] dV$$
$$= -\frac{\check{\omega}}{2}\int_V \sum_{i=1}^{3} \left[\epsilon_0 |E_i|^2 S_{ii}^{EE}(t) + \mu_0 |H_i|^2 S_{ii}^{HH}(t)\right] dV +$$
$$+\frac{1}{2}\oint_S \sum_{i,j=1}^{3} |E_i||H_j|(\hat{\mathbf{i}}_i \times \hat{\mathbf{i}}_j)\cdot \hat{\mathbf{n}} C_{ij}^{EH}(t)\, dS. \tag{4.141}$$

Selection of the constant part gives the balance of time-average power:

$$-\frac{1}{2}\int_V \sum_{i=1}^{3} |J_i||E_i| \cos(\xi_i^J - \xi_i^E)\, dV$$
$$= \frac{\check{\omega}}{2}\int_V \sum_{i=1}^{3} \left[|E_i||P_i| \sin(\xi_i^E - \xi_i^P) + \mu_0 |H_i||M_i| \sin(\xi_i^H - \xi_i^M)\right] dV +$$
$$+\frac{1}{2}\oint_S \sum_{i,j=1}^{3} |E_i||H_j|(\hat{\mathbf{i}}_i \times \hat{\mathbf{i}}_j)\cdot \hat{\mathbf{n}} \cos(\xi_i^E - \xi_j^H)\, dS. \tag{4.142}$$

Here the power loss associated with the lag in alignment of the electric and magnetic dipoles is easily identified as the volume term on the right-hand side, and is seen to arise through the interaction of the fields with the equivalent sources as described through the phase difference between **E** and **P** and between **H** and **M**. If these pairs are in phase, then the time-average power balance reduces to that for a dispersionless material, equation (4.146).

4.8.2 Poynting's theorem for nondispersive materials

For nondispersive materials (2.299) is appropriate. We shall carry out the details here so that we may examine the power-balance implications of nondispersive media. We have, substituting the field expressions,

$$-\frac{1}{2}\int_V \sum_{i=1}^{3} |J_i^i||E_i|C_{ii}^{J^iE}(t)\,dV = \frac{1}{2}\int_V \sum_{i=1}^{3} |J_i^c||E_i|C_{ii}^{J^cE}(t)\,dV +$$
$$+\frac{\partial}{\partial t}\int_V \sum_{i=1}^{3}\left\{\frac{1}{4}|D_i||E_i|C_{ii}^{DE}(t) + \frac{1}{4}|B_i||H_i|C_{ii}^{BH}(t)\right\} dV +$$
$$+\frac{1}{2}\oint_S \sum_{i,j=1}^{3} |E_i||H_j|(\hat{\mathbf{i}}_i \times \hat{\mathbf{i}}_j)\cdot\hat{\mathbf{n}}C_{ij}^{EH}(t)\,dS. \tag{4.143}$$

Here we remember that the conductivity relating $\mathbf{E}$ to $\mathbf{J}^c$ must also be nondispersive. Note that the electric and magnetic energy densities $w_e(\mathbf{r},t)$ and $w_m(\mathbf{r},t)$ have the time-average values $\langle w_e(\mathbf{r},t)\rangle$ and $\langle w_m(\mathbf{r},t)\rangle$ given by

$$\langle w_e(\mathbf{r},t)\rangle = \frac{1}{T}\int_{-T/2}^{T/2}\frac{1}{2}\mathbf{E}(\mathbf{r},t)\cdot\mathbf{D}(\mathbf{r},t)\,dt = \frac{1}{4}\sum_{i=1}^{3}|E_i||D_i|\cos(\xi_i^E - \xi_i^D)$$
$$= \frac{1}{4}\,\mathrm{Re}\left\{\check{\mathbf{E}}(\mathbf{r})\cdot\check{\mathbf{D}}^*(\mathbf{r})\right\} \tag{4.144}$$

and

$$\langle w_m(\mathbf{r},t)\rangle = \frac{1}{T}\int_{-T/2}^{T/2}\frac{1}{2}\mathbf{B}(\mathbf{r},t)\cdot\mathbf{H}(\mathbf{r},t)\,dt = \frac{1}{4}\sum_{i=1}^{3}|B_i||H_i|\cos(\xi_i^H - \xi_i^B)$$
$$= \frac{1}{4}\,\mathrm{Re}\left\{\check{\mathbf{H}}(\mathbf{r})\cdot\check{\mathbf{B}}^*(\mathbf{r})\right\}, \tag{4.145}$$

where $T = 2\pi/\check{\omega}$. We have already identified the energy stored in a nondispersive material (§ 4.5.2). If (4.144) is to match with (4.62), the phases of $\check{\mathbf{E}}$ and $\check{\mathbf{D}}$ must match: $\xi_i^E = \xi_i^D$. We must also have $\xi_i^H = \xi_i^B$. Since in a dispersionless material σ must be independent of frequency, from $\check{\mathbf{J}}^c = \sigma\check{\mathbf{E}}$ we also see that $\xi_i^{J^c} = \xi_i^E$.

Upon differentiation the time-average stored energy terms in (4.143) disappear, giving

$$-\frac{1}{2}\int_V \sum_{i=1}^{3} |J_i^i||E_i|C_{ii}^{J^iE}(t)\,dV = \frac{1}{2}\int_V \sum_{i=1}^{3} |J_i^c||E_i|C_{ii}^{EE}(t)\,dV -$$
$$-2\check{\omega}\int_V \sum_{i=1}^{3}\left\{\frac{1}{4}|D_i||E_i|S_{ii}^{EE}(t) + \frac{1}{4}|B_i||H_i|S_{ii}^{BB}(t)\right\} dV +$$
$$+\frac{1}{2}\oint_S \sum_{i,j=1}^{3} |E_i||H_j|(\hat{\mathbf{i}}_i \times \hat{\mathbf{i}}_j)\cdot\hat{\mathbf{n}}C_{ij}^{EH}(t)\,dS.$$

Equating the constant terms, we find the time-average power balance expression

$$-\frac{1}{2}\int_V \sum_{i=1}^{3} |J_i^i||E_i|\cos(\xi_i^{J^i} - \xi_i^E)\,dV = \frac{1}{2}\int_V \sum_{i=1}^{3} |J_i^c||E_i|\,dV +$$
$$+\frac{1}{2}\oint_S \sum_{i,j=1}^{3} |E_i||H_j|(\hat{\mathbf{i}}_i \times \hat{\mathbf{i}}_j)\cdot\hat{\mathbf{n}}\cos(\xi_i^E - \xi_j^H)\,dS. \tag{4.146}$$

This can be written more compactly using phasor notation as

$$\int_V p_J(\mathbf{r})\,dV = \int_V p_\sigma(\mathbf{r})\,dV + \oint_S \mathbf{S}_{av}(\mathbf{r})\cdot\hat{\mathbf{n}}\,dS \tag{4.147}$$

where

$$p_J(\mathbf{r}) = -\frac{1}{2}\operatorname{Re}\left\{\check{\mathbf{E}}(\mathbf{r})\cdot\check{\mathbf{J}}^{i*}(\mathbf{r})\right\}$$

is the time-average density of power delivered by the sources to the fields in V,

$$p_\sigma(\mathbf{r}) = \frac{1}{2}\check{\mathbf{E}}(\mathbf{r})\cdot\check{\mathbf{J}}^{c*}(\mathbf{r})$$

is the time-average density of power transferred to the conducting material as heat, and

$$\mathbf{S}_{av}(\mathbf{r})\cdot\hat{\mathbf{n}} = \frac{1}{2}\operatorname{Re}\left\{\check{\mathbf{E}}(\mathbf{r})\times\check{\mathbf{H}}^*(\mathbf{r})\right\}\cdot\hat{\mathbf{n}}$$

is the density of time-average power transferred across the boundary surface S. Here

$$\mathbf{S}^c = \check{\mathbf{E}}(\mathbf{r})\times\check{\mathbf{H}}^*(\mathbf{r})$$

is called the *complex Poynting vector* and $\mathbf{S}_{av}$ is called the *time-average Poynting vector.*

Comparison of (4.146) with (4.140) shows that nondispersive materials cannot manifest the dissipative (or active) properties determined by the term

$$\frac{1}{2}\int_V \sum_{i=1}^{3}\left\{\check{\omega}|E_i||D_i|\sin(\xi_i^E-\xi_i^D)+\check{\omega}|B_i||H_i|\sin(\xi_i^H-\xi_i^B)+|J_i^c||E_i|\cos(\xi_i^{J^c}-\xi_i^E)\right\}\,dV.$$

This term can be used to classify materials as lossless, lossy, or active, as shown next.

4.8.3 Lossless, lossy, and active media

In § 4.5.1 we classified materials based on whether they dissipate (or provide) energy over the period of a transient event. We can provide the same classification based on their steady-state behavior.

We classify a material as *lossless* if the time-average flow of power entering a homogeneous body is zero when there are sources external to the body, but no sources internal to the body. This implies that the mechanisms within the body either do not dissipate power that enters, or that there is a mechanism that creates energy to exactly balance the dissipation. If the time-average power entering is positive, then the material dissipates power and is termed *lossy.* If the time-average power entering is negative, then power must originate from within the body and the material is termed *active.* (Note that the power associated with an active body is not described as arising from sources, but is rather described through the constitutive relations.)

Since materials are generally inhomogeneous we may apply this concept to a vanishingly small volume, thus invoking the point-form of Poynting's theorem. From (4.140) we see that the time-average influx of power density is given by

$$-\nabla\cdot\mathbf{S}_{av}(\mathbf{r}) = p_{in}(\mathbf{r}) = \frac{1}{2}\sum_{i=1}^{3}\left\{\check{\omega}|E_i||D_i|\sin(\xi_i^E-\xi_i^D)+\check{\omega}|B_i||H_i|\sin(\xi_i^H-\xi_i^B)+\right.$$
$$\left. + \;|J_i^c||E_i|\cos(\xi_i^{J^c}-\xi_i^E)\right\}.$$

Materials are then classified as follows:

$$\begin{aligned} p_{in}(\mathbf{r}) &= 0, && \text{lossless,}\\ p_{in}(\mathbf{r}) &> 0, && \text{lossy,}\\ p_{in}(\mathbf{r}) &\geq 0, && \text{passive,}\\ p_{in}(\mathbf{r}) &< 0, && \text{active.} \end{aligned}$$

We see that if $\xi_i^E = \xi_i^D$, $\xi_i^H = \xi_i^B$, and $\mathbf{J}^c = 0$, then the material is lossless. This implies that (**D**,**E**) and (**B**,**H**) are exactly in phase and there is no conduction current. If the material is isotropic, we may substitute from the constitutive relations (4.21)–(4.23) to obtain

$$p_{in}(\mathbf{r}) = -\frac{\check{\omega}}{2}\sum_{i=1}^{3}\left\{|E_i|^2\left[|\tilde{\epsilon}|\sin(\xi^{\epsilon}) - \frac{|\tilde{\sigma}|}{\check{\omega}}\cos(\xi^{\sigma})\right] + |\tilde{\mu}||H_i|^2\sin(\xi^{\mu})\right\}. \tag{4.148}$$

The first two terms can be regarded as resulting from a single complex permittivity (4.26). Then (4.148) simplifies to

$$p_{in}(\mathbf{r}) = -\frac{\check{\omega}}{2}\sum_{i=1}^{3}\left\{|\tilde{\epsilon}^c||E_i|^2\sin(\xi^{\epsilon^c}) + |\tilde{\mu}||H_i|^2\sin(\xi^{\mu})\right\}. \tag{4.149}$$

Now we can see that a lossless medium, which requires (4.149) to vanish, has $\xi^{\epsilon^c} = \xi^{\mu} = 0$ (or perhaps the unlikely condition that dissipative and active effects within the electric and magnetic terms exactly cancel). To have $\xi^{\mu} = 0$ we need **B** and **H** to be in phase, hence we need $\tilde{\mu}(\mathbf{r},\omega)$ to be real. To have $\xi^{\epsilon^c} = 0$ we need $\xi^{\epsilon} = 0$ ($\tilde{\epsilon}(\mathbf{r},\omega)$ real) and $\tilde{\sigma}(\mathbf{r},\omega) = 0$ (or perhaps the unlikely condition that the active and dissipative effects of the permittivity and conductivity exactly cancel).

A lossy medium requires (4.149) to be positive. This occurs when $\xi^{\mu} < 0$ or $\xi^{\epsilon^c} < 0$, meaning that the imaginary part of the permeability or complex permittivity is negative. The complex permittivity has a negative imaginary part if the imaginary part of $\tilde{\epsilon}$ is negative or if the real part of $\tilde{\sigma}$ is positive. Physically, $\xi^{\epsilon} < 0$ means that $\xi^D < \xi^E$ and thus the phase of the response field **D** lags that of the excitation field **E**. This results from a delay in the polarization alignment of the atoms, and leads to dissipation of power within the material.

An active medium requires (4.149) to be negative. This occurs when $\xi^{\mu} > 0$ or $\xi^{\epsilon^c} > 0$, meaning that the imaginary part of the permeability or complex permittivity is positive. The complex permittivity has a positive imaginary part if the imaginary part of $\tilde{\epsilon}$ is positive or if the real part of $\tilde{\sigma}$ is negative.

In summary, a passive isotropic medium is lossless when the permittivity and permeability are real and when the conductivity is zero. A passive isotropic medium is lossy when one or more of the following holds: the permittivity is complex with negative imaginary part, the permeability is complex with negative imaginary part, or the conductivity has a positive real part. Finally, a complex permittivity or permeability with positive imaginary part or a conductivity with negative real part indicates an *active* medium.

For anisotropic materials the interpretation of p_{in} is not as simple. Here we find that the permittivity or permeability dyadic may be complex, and yet the material may still be lossless. To determine the condition for a lossless medium, let us recompute p_{in} using the constitutive relations (4.18)–(4.20). With these we have

$$\mathbf{E}\cdot\left[\frac{\partial\mathbf{D}}{\partial t} + \mathbf{J}^c\right] + \mathbf{H}\cdot\frac{\partial\mathbf{B}}{\partial t} = \check{\omega}\sum_{i,j=1}^{3}|E_i||E_j|\Bigg[-|\tilde{\epsilon}_{ij}|\sin(\check{\omega}t + \xi_j^E + \xi_{ij}^{\epsilon})\cos(\check{\omega}t + \xi_i^E) +$$

$$+\frac{|\tilde{\sigma}_{ij}|}{\check{\omega}}\cos(\check{\omega}t+\xi_j^E+\xi_{ij}^{\sigma})\cos(\check{\omega}t+\xi_i^E)\Bigg]+$$
$$+\check{\omega}\sum_{i,j=1}^{3}|H_i||H_j|\Big[-|\tilde{\mu}_{ij}|\sin(\check{\omega}t+\xi_j^H+\xi_{ij}^{\mu})\cos(\check{\omega}t+\xi_i^H)\Big].$$

Using the angle-sum formulas and discarding the time-varying quantities, we may obtain the time-average input power density:

$$p_{in}(\mathbf{r})=-\frac{\check{\omega}}{2}\sum_{i,j=1}^{3}|E_i||E_j|\left[|\tilde{\epsilon}_{ij}|\sin(\xi_j^E-\xi_i^E+\xi_{ij}^{\epsilon})-\frac{|\tilde{\sigma}_{ij}|}{\check{\omega}}\cos(\xi_j^E-\xi_i^E+\xi_{ij}^{\sigma})\right]-$$
$$-\frac{\check{\omega}}{2}\sum_{i,j=1}^{3}|H_i||H_j||\tilde{\mu}_{ij}|\sin(\xi_j^H-\xi_i^H+\xi_{ij}^{\mu}).$$

The reader can easily verify that the conditions that make this quantity vanish, thus describing a lossless material, are

$$|\tilde{\epsilon}_{ij}|=|\tilde{\epsilon}_{ji}|,\qquad \xi_{ij}^{\epsilon}=-\xi_{ji}^{\epsilon}, \tag{4.150}$$
$$|\tilde{\sigma}_{ij}|=|\tilde{\sigma}_{ji}|,\qquad \xi_{ij}^{\sigma}=-\xi_{ji}^{\sigma}+\pi, \tag{4.151}$$
$$|\tilde{\mu}_{ij}|=|\tilde{\mu}_{ji}|,\qquad \xi_{ij}^{\mu}=-\xi_{ji}^{\mu}. \tag{4.152}$$

Note that this requires $\xi_{ii}^{\epsilon}=\xi_{ii}^{\mu}=\xi_{ii}^{\sigma}=0$.

The condition (4.152) is easily written in dyadic form as

$$\tilde{\bar{\boldsymbol{\mu}}}(\mathbf{r},\check{\omega})^{\dagger}=\tilde{\bar{\boldsymbol{\mu}}}(\mathbf{r},\check{\omega}) \tag{4.153}$$

where "†" stands for the conjugate-transpose operation. The dyadic permeability $\tilde{\bar{\boldsymbol{\mu}}}$ is hermitian. The set of conditions (4.150)–(4.151) can also be written quite simply using the complex permittivity dyadic (4.24):

$$\tilde{\bar{\boldsymbol{\epsilon}}}^{c}(\mathbf{r},\check{\omega})^{\dagger}=\tilde{\bar{\boldsymbol{\epsilon}}}^{c}(\mathbf{r},\check{\omega}). \tag{4.154}$$

Thus, an anisotropic material is lossless when the both the dyadic permeability and the complex dyadic permittivity are hermitian. Since $\check{\omega}$ is arbitrary, these results are exactly those obtained in § 4.5.1. Note that in the special case of an isotropic material the conditions (4.153) and (4.154) can only hold if $\tilde{\epsilon}$ and $\tilde{\mu}$ are real and $\tilde{\sigma}$ is zero, agreeing with our earlier conclusions.

4.9 The complex Poynting theorem

An equation having a striking resemblance to Poynting's theorem can be obtained by direct manipulation of the phasor-domain Maxwell equations. The result, although certainly satisfied by the phasor fields, does *not* replace Poynting's theorem as the power-balance equation for time-harmonic fields. We shall be careful to contrast the interpretation of the phasor expression with the actual time-harmonic Poynting theorem.

We begin by dotting both sides of the phasor-domain Faraday's law with $\check{\mathbf{H}}^*$ to obtain

$$\check{\mathbf{H}}^*\cdot(\nabla\times\check{\mathbf{E}})=-j\check{\omega}\check{\mathbf{H}}^*\cdot\check{\mathbf{B}}.$$

Taking the complex conjugate of the phasor-domain Ampere's law and dotting with $\check{\mathbf{E}}$, we have

$$\check{\mathbf{E}} \cdot (\nabla \times \check{\mathbf{H}}^*) = \check{\mathbf{E}} \cdot \check{\mathbf{J}}^* - j\check{\omega}\check{\mathbf{E}} \cdot \check{\mathbf{D}}^*.$$

We subtract these expressions and use (B.44) to write

$$-\check{\mathbf{E}} \cdot \check{\mathbf{J}}^* = \nabla \cdot (\check{\mathbf{E}} \times \check{\mathbf{H}}^*) - j\check{\omega}[\check{\mathbf{E}} \cdot \check{\mathbf{D}}^* - \check{\mathbf{B}} \cdot \check{\mathbf{H}}^*].$$

Finally, integrating over the volume region V and dividing by two, we have

$$-\frac{1}{2}\int_V \check{\mathbf{E}} \cdot \check{\mathbf{J}}^*\, dV = \frac{1}{2}\oint_S (\check{\mathbf{E}} \times \check{\mathbf{H}}^*) \cdot \mathbf{dS} - 2j\check{\omega}\int_V \left[\frac{1}{4}\check{\mathbf{E}} \cdot \check{\mathbf{D}}^* - \frac{1}{4}\check{\mathbf{B}} \cdot \check{\mathbf{H}}^*\right] dV. \tag{4.155}$$

This is known as the *complex Poynting theorem*, and is an expression that must be obeyed by the phasor fields.

As a power balance theorem, the complex Poynting theorem has meaning only for dispersionless materials. If we let $\mathbf{J} = \mathbf{J}^i + \mathbf{J}^c$ and assume no dispersion, (4.155) becomes

$$-\frac{1}{2}\int_V \check{\mathbf{E}} \cdot \check{\mathbf{J}}^{i*}\, dV = \frac{1}{2}\int_V \check{\mathbf{E}} \cdot \check{\mathbf{J}}^{c*}\, dV + \frac{1}{2}\oint_S (\check{\mathbf{E}} \times \check{\mathbf{H}}^*) \cdot \mathbf{dS} - \\ - 2j\omega \int_V [\langle w_e \rangle - \langle w_m \rangle]\, dV \tag{4.156}$$

where $\langle w_e \rangle$ and $\langle w_m \rangle$ are the time-average stored electric and magnetic energy densities as described in (4.62)–(4.63). Selection of the real part now gives

$$-\frac{1}{2}\int_V \text{Re}\left\{\check{\mathbf{E}} \cdot \check{\mathbf{J}}^{i*}\right\} dV = \frac{1}{2}\int_V \check{\mathbf{E}} \cdot \check{\mathbf{J}}^{c*}\, dV + \frac{1}{2}\oint_S \text{Re}\left\{\check{\mathbf{E}} \times \check{\mathbf{H}}^*\right\} \cdot \mathbf{dS}, \tag{4.157}$$

which is identical to (4.147). Thus the real part of the complex Poynting theorem gives the balance of time-average power for a dispersionless material.

Selection of the imaginary part of (4.156) gives the balance of imaginary, or *reactive* power:

$$-\frac{1}{2}\int_V \text{Im}\left\{\check{\mathbf{E}} \cdot \check{\mathbf{J}}^{i*}\right\} dV = \frac{1}{2}\oint_S \text{Im}\left\{\check{\mathbf{E}} \times \check{\mathbf{H}}^*\right\} \cdot \mathbf{dS} - 2\check{\omega}\int_V [\langle w_e \rangle - \langle w_m \rangle]\, dV. \tag{4.158}$$

In general, the reactive power balance does not have a simple physical interpretation (it is *not* the balance of the oscillating terms in (4.139)). However, an interesting concept can be gleaned from it. If the source current and electric field are in phase, and there is no reactive power leaving S, then the time-average stored electric energy is equal to the time-average stored magnetic energy:

$$\int_V \langle w_e \rangle\, dV = \int_V \langle w_m \rangle\, dV.$$

This is the condition for "resonance." An example is a series RLC circuit with the source current and voltage in phase. Here the stored energy in the capacitor is equal to the stored energy in the inductor and the input impedance (ratio of voltage to current) is real. Such a resonance occurs at only one value of frequency. In more complicated electromagnetic systems resonance may occur at many discrete eigenfrequencies.

4.9.1 Boundary condition for the time-average Poynting vector

In § 2.9.5 we developed a boundary condition for the normal component of the time-domain Poynting vector. For time-harmonic fields we can derive a similar boundary condition using the time-average Poynting vector. Consider a surface S across which the electromagnetic sources and constitutive parameters are discontinuous, as shown in Figure 2.6. Let $\hat{\mathbf{n}}_{12}$ be the unit normal to the surface pointing into region 1 from region 2. If we apply the large-scale form of the complex Poynting theorem (4.155) to the two separate surfaces shown in Figure 2.6, we obtain

$$\frac{1}{2}\int_V \left[\check{\mathbf{E}}\cdot\check{\mathbf{J}}^* - 2j\check{\omega}\left(\frac{1}{4}\check{\mathbf{E}}\cdot\check{\mathbf{D}}^* - \frac{1}{4}\check{\mathbf{B}}\cdot\check{\mathbf{H}}^*\right)\right]dV + \frac{1}{2}\oint_S \mathbf{S}^c\cdot\hat{\mathbf{n}}\,dS$$
$$= \frac{1}{2}\int_{S_{10}} \hat{\mathbf{n}}_{12}\cdot(\mathbf{S}_1^c - \mathbf{S}_2^c)\,dS \tag{4.159}$$

where $\mathbf{S}^c = \check{\mathbf{E}}\times\check{\mathbf{H}}^*$ is the complex Poynting vector. If, on the other hand, we apply the large-scale form of Poynting's theorem to the entire volume region including the surface of discontinuity, and include the surface current contribution, we have

$$\frac{1}{2}\int_V \left[\check{\mathbf{E}}\cdot\check{\mathbf{J}}^* - 2j\check{\omega}\int_V\left(\frac{1}{4}\check{\mathbf{E}}\cdot\check{\mathbf{D}}^* - \frac{1}{4}\check{\mathbf{B}}\cdot\check{\mathbf{H}}^*\right)\right]dV + \frac{1}{2}\oint_S \mathbf{S}^c\cdot\hat{\mathbf{n}}\,dS$$
$$= -\frac{1}{2}\int_{S_{10}} \check{\mathbf{J}}_s^*\cdot\check{\mathbf{E}}\,dS. \tag{4.160}$$

If we wish to have the integrals over V and S in (4.159) and (4.160) produce identical results, then we must postulate the two conditions

$$\hat{\mathbf{n}}_{12}\times(\check{\mathbf{E}}_1 - \check{\mathbf{E}}_2) = 0$$

and

$$\hat{\mathbf{n}}_{12}\cdot(\mathbf{S}_1^c - \mathbf{S}_2^c) = -\check{\mathbf{J}}_s^*\cdot\check{\mathbf{E}}. \tag{4.161}$$

The first condition is merely the continuity of tangential electric field; it allows us to be nonspecific as to which value of $\mathbf{E}$ we use in the second condition. If we take the real part of the second condition we have

$$\hat{\mathbf{n}}_{12}\cdot(\mathbf{S}_{av,1} - \mathbf{S}_{av,2}) = p_{J^s}, \tag{4.162}$$

where $\mathbf{S}_{av} = \frac{1}{2}\,\mathrm{Re}\{\check{\mathbf{E}}\times\check{\mathbf{H}}^*\}$ is the time-average Poynting power flow density and $p_{J^s} = -\frac{1}{2}\,\mathrm{Re}\{\check{\mathbf{J}}_s^*\cdot\check{\mathbf{E}}\}$ is the time-average density of power delivered by the surface sources. This is the desired boundary condition on the time-average power flow density.

4.10 Fundamental theorems for time-harmonic fields

4.10.1 Uniqueness

If we think of a sinusoidal electromagnetic field as the steady-state culmination of a transient event that has an identifiable starting time, then the conditions for uniqueness established in § 2.2.1 are applicable. However, a true time-harmonic wave, which has existed since $t = -\infty$ and thus has infinite energy, must be interpreted differently.

Our approach is similar to that of § 2.2.1. Consider a simply-connected region of space V bounded by surface S, where both V and S contain only ordinary points. The phasor-domain fields within V are associated with a phasor current distribution $\check{\mathbf{J}}$, which may be internal to V (entirely or in part). We seek conditions under which the phasor electromagnetic fields are uniquely determined. Let the field set $(\check{\mathbf{E}}_1, \check{\mathbf{D}}_1, \check{\mathbf{B}}_1, \check{\mathbf{H}}_1)$ satisfy Maxwell's equations (4.128) and (4.129) associated with the current $\check{\mathbf{J}}$ (along with an appropriate set of constitutive relations), and let $(\check{\mathbf{E}}_2, \check{\mathbf{D}}_2, \check{\mathbf{B}}_2, \check{\mathbf{H}}_2)$ be a second solution. To determine the conditions for uniqueness of the fields, we look for a situation that results in $\check{\mathbf{E}}_1 = \check{\mathbf{E}}_2$, $\check{\mathbf{H}}_1 = \check{\mathbf{H}}_2$, and so on. The electromagnetic fields must obey

$$\begin{aligned}
\nabla \times \check{\mathbf{H}}_1 &= j\check{\omega}\check{\mathbf{D}}_1 + \check{\mathbf{J}},\\
\nabla \times \check{\mathbf{E}}_1 &= -j\check{\omega}\check{\mathbf{B}}_1,\\
\nabla \times \check{\mathbf{H}}_2 &= j\check{\omega}\check{\mathbf{D}}_2 + \check{\mathbf{J}},\\
\nabla \times \check{\mathbf{E}}_2 &= -j\check{\omega}\check{\mathbf{B}}_2.
\end{aligned}$$

Subtracting these and defining the difference fields $\check{\mathbf{E}}_0 = \check{\mathbf{E}}_1 - \check{\mathbf{E}}_2$, $\check{\mathbf{H}}_0 = \check{\mathbf{H}}_1 - \check{\mathbf{H}}_2$, and so on, we find that

$$\nabla \times \check{\mathbf{H}}_0 = j\check{\omega}\check{\mathbf{D}}_0, \tag{4.163}$$

$$\nabla \times \check{\mathbf{E}}_0 = -j\check{\omega}\check{\mathbf{B}}_0. \tag{4.164}$$

Establishing the conditions under which the difference fields vanish throughout V, we shall determine the conditions for uniqueness.

Dotting (4.164) by $\check{\mathbf{H}}_0^*$ and dotting the complex conjugate of (4.163) by $\check{\mathbf{E}}_0$, we have

$$\begin{aligned}
\check{\mathbf{H}}_0^* \cdot \left(\nabla \times \check{\mathbf{E}}_0\right) &= -j\check{\omega}\check{\mathbf{B}}_0 \cdot \check{\mathbf{H}}_0^*,\\
\check{\mathbf{E}}_0 \cdot \left(\nabla \times \check{\mathbf{H}}_0^*\right) &= -j\check{\omega}\check{\mathbf{D}}_0^* \cdot \check{\mathbf{E}}_0.
\end{aligned}$$

Subtraction yields

$$\check{\mathbf{H}}_0^* \cdot \left(\nabla \times \check{\mathbf{E}}_0\right) - \check{\mathbf{E}}_0 \cdot \left(\nabla \times \check{\mathbf{H}}_0^*\right) = -j\check{\omega}\check{\mathbf{B}}_0 \cdot \check{\mathbf{H}}_0^* + j\check{\omega}\check{\mathbf{D}}_0^* \cdot \check{\mathbf{E}}_0$$

which, by (B.44), can be written as

$$\nabla \cdot \left(\check{\mathbf{E}}_0 \times \check{\mathbf{H}}_0^*\right) = j\check{\omega}\left[\check{\mathbf{E}}_0 \cdot \check{\mathbf{D}}_0^* - \check{\mathbf{B}}_0 \cdot \check{\mathbf{H}}_0^*\right].$$

Adding this expression to its complex conjugate, integrating over V, and using the divergence theorem, we obtain

$$\mathrm{Re}\oint_S \left[\check{\mathbf{E}}_0 \times \check{\mathbf{H}}_0^*\right] \cdot \mathbf{dS} = -j\frac{\check{\omega}}{2}\int_V \left[\left(\check{\mathbf{E}}_0^* \cdot \check{\mathbf{D}}_0 - \check{\mathbf{E}}_0 \cdot \check{\mathbf{D}}_0^*\right) + \left(\check{\mathbf{H}}_0^* \cdot \check{\mathbf{B}}_0 - \check{\mathbf{H}}_0 \cdot \check{\mathbf{B}}_0^*\right)\right] dV.$$

Breaking S into two arbitrary portions and using (**??**), we obtain

$$\begin{aligned}
&\mathrm{Re}\oint_{S_1} \check{\mathbf{H}}_0^* \cdot (\hat{\mathbf{n}} \times \check{\mathbf{E}}_0)\, dS - \mathrm{Re}\oint_{S_2} \check{\mathbf{E}}_0 \cdot (\hat{\mathbf{n}} \times \check{\mathbf{H}}_0^*)\, dS = \\
&-j\frac{\check{\omega}}{2}\int_V \left[\left(\check{\mathbf{E}}_0^* \cdot \check{\mathbf{D}}_0 - \check{\mathbf{E}}_0 \cdot \check{\mathbf{D}}_0^*\right) + \left(\check{\mathbf{H}}_0^* \cdot \check{\mathbf{B}}_0 - \check{\mathbf{H}}_0 \cdot \check{\mathbf{B}}_0^*\right)\right] dV.
\end{aligned} \tag{4.165}$$

Now if $\hat{\mathbf{n}} \times \mathbf{E}_0 = 0$ or $\hat{\mathbf{n}} \times \mathbf{H}_0 = 0$ over all of S, or some combination of these conditions holds over all of S, then

$$\int_V \left[\left(\check{\mathbf{E}}_0^* \cdot \check{\mathbf{D}}_0 - \check{\mathbf{E}}_0 \cdot \check{\mathbf{D}}_0^*\right) + \left(\check{\mathbf{H}}_0^* \cdot \check{\mathbf{B}}_0 - \check{\mathbf{H}}_0 \cdot \check{\mathbf{B}}_0^*\right)\right] dV = 0. \tag{4.166}$$

This implies a relationship between $\check{\mathbf{E}}_0$, $\check{\mathbf{D}}_0$, $\check{\mathbf{B}}_0$, and $\check{\mathbf{H}}_0$. Since V is arbitrary we see that one possible relationship is simply to have one of each pair $(\check{\mathbf{E}}_0, \check{\mathbf{D}}_0)$ and $(\check{\mathbf{H}}_0, \check{\mathbf{B}}_0)$ equal to zero. Then, by (4.163) and (4.164), $\check{\mathbf{E}}_0 = 0$ implies $\check{\mathbf{B}}_0 = 0$, and $\check{\mathbf{D}}_0 = 0$ implies $\check{\mathbf{H}}_0 = 0$. Thus $\check{\mathbf{E}}_1 = \check{\mathbf{E}}_2$, etc., and the solution is unique throughout V. However, we cannot in general rule out more complicated relationships. The number of possibilities depends on the additional constraints on the relationship between $\check{\mathbf{E}}_0$, $\check{\mathbf{D}}_0$, $\check{\mathbf{B}}_0$, and $\check{\mathbf{H}}_0$ that we must supply to describe the material supporting the field — i.e., the constitutive relationships. For a simple medium described by $\tilde{\mu}(\omega)$ and $\tilde{\epsilon}^c(\omega)$, equation (4.166) becomes

$$\int_V \left(|\check{\mathbf{E}}_0|^2[\tilde{\epsilon}^c(\check{\omega}) - \tilde{\epsilon}^{c*}(\check{\omega})] + |\check{\mathbf{H}}_0|^2[\tilde{\mu}(\check{\omega}) - \tilde{\mu}^*(\check{\omega})]\right) dV = 0$$

or

$$\int_V \left[|\check{\mathbf{E}}_0|^2\tilde{\epsilon}^{c\prime\prime}(\check{\omega}) + |\check{\mathbf{H}}_0|^2\tilde{\mu}^{\prime\prime}(\check{\omega})\right] dV = 0.$$

For a lossy medium, $\tilde{\epsilon}^{c\prime\prime} < 0$ and $\tilde{\mu}^{\prime\prime} < 0$ as shown in § 4.5.1. So both terms in the integral must be negative. For the integral to be zero each term must vanish, requiring $\check{\mathbf{E}}_0 = \check{\mathbf{H}}_0 = 0$, and uniqueness is guaranteed.

When establishing more complicated constitutive relations we must be careful to ensure that they lead to a unique solution, and that the condition for uniqueness is understood. In the case above, the assumption $\hat{\mathbf{n}} \times \check{\mathbf{E}}_0\big|_S = 0$ implies that the tangential components of $\check{\mathbf{E}}_1$ and $\check{\mathbf{E}}_2$ are identical over S — that is, we must give specific values of these quantities on S to ensure uniqueness. A similar statement holds for the condition $\hat{\mathbf{n}} \times \check{\mathbf{H}}_0\big|_S = 0$.

In summary, the conditions for the fields within a region V containing lossy isotropic materials to be unique are as follows:

1. the sources within V must be specified;
2. the tangential component of the electric field must be specified over all or part of the bounding surface S;
3. the tangential component of the magnetic field must be specified over the remainder of S.

We may question the requirement of a *lossy* medium to demonstrate uniqueness of the phasor fields. Does this mean that within a vacuum the specification of tangential fields is insufficient? Experience shows that the fields in such a region are indeed properly described by the surface fields, and it is just a case of the mathematical model being slightly out of sync with the physics. As long as we recognize that the sinusoidal steady state requires an initial transient period, we know that specification of the tangential fields is sufficient. We must be careful, however, to understand the restrictions of the mathematical model. Any attempt to describe the fields within a lossless cavity, for instance, is fraught with difficulty if true time-harmonic fields are used to model the actual physical fields. A helpful mathematical strategy is to think of free space as the limit of a lossy medium as the loss recedes to zero. Of course this does not represent the physical state of "empty" space. Although even interstellar space may have a few particles for every cubic meter to interact with the electromagnetic field, the density of these particles invalidates our initial macroscopic assumptions.

Another important concern is whether we can extend the uniqueness argument to all of space. If we let S recede to infinity, must we continue to specify the fields over S, or is it sufficient to merely specify the sources within S? Since the boundary fields provide information to the internal region about sources that exist outside S, it is sensible to assume that as $S \to \infty$ there are no sources external to S and thus no need for the boundary fields. This is indeed the case. If all sources are localized, the fields they produce behave in just the right manner for the surface integral in (4.165) to vanish, and thus uniqueness is again guaranteed. Later we will find that the electric and magnetic fields produced by a localized source at great distance have the form of a spherical wave:

$$\check{\mathbf{E}} \sim \check{\mathbf{H}} \sim \frac{e^{-jkr}}{r}.$$

If space is taken to be slightly lossy, then k is complex with negative imaginary part, and thus the fields decrease exponentially with distance from the source. As we argued above, it may not be physically meaningful to assume that space is lossy. Sommerfeld postulated that even for lossless space the surface integral in (4.165) vanishes as $S \to \infty$. This has been verified experimentally, and provides the following restrictions on the free-space fields known as the *Sommerfeld radiation condition*:

$$\lim_{r\to\infty} r\left[\eta_0 \hat{\mathbf{r}} \times \check{\mathbf{H}}(\mathbf{r}) + \check{\mathbf{E}}(\mathbf{r})\right] = 0, \tag{4.167}$$

$$\lim_{r\to\infty} r\left[\hat{\mathbf{r}} \times \check{\mathbf{E}}(\mathbf{r}) - \eta_0 \check{\mathbf{H}}(\mathbf{r})\right] = 0, \tag{4.168}$$

where $\eta_0 = (\mu_0/\epsilon_0)^{1/2}$. Later we shall see how these expressions arise from the integral solutions to Maxwell's equations.

4.10.2 Reciprocity revisited

In § 2.9.3 we discussed the basic concept of reciprocity, but were unable to examine its real potential since we had not yet developed the theory of time-harmonic fields. In this section we shall apply the reciprocity concept to time-harmonic sources and fields, and investigate the properties a material must display to be reciprocal.

The general form of the reciprocity theorem. As in § 2.9.3, we consider a closed surface S enclosing a volume V. Sources of an electromagnetic field are located either inside or outside S. Material media may lie within S, and their properties are described in terms of the constitutive relations. To obtain the time-harmonic (phasor) form of the reciprocity theorem we proceed as in § 2.9.3 but begin with the phasor forms of Maxwell's equations. We find

$$\nabla \cdot (\check{\mathbf{E}}_a \times \check{\mathbf{H}}_b - \check{\mathbf{E}}_b \times \check{\mathbf{H}}_a) = j\check{\omega}[\check{\mathbf{H}}_a \cdot \check{\mathbf{B}}_b - \check{\mathbf{H}}_b \cdot \check{\mathbf{B}}_a] - j\check{\omega}[\check{\mathbf{E}}_a \cdot \check{\mathbf{D}}_b - \check{\mathbf{E}}_b \cdot \check{\mathbf{D}}_a] + \\ + [\check{\mathbf{E}}_b \cdot \check{\mathbf{J}}_a - \check{\mathbf{E}}_a \cdot \check{\mathbf{J}}_b - \check{\mathbf{H}}_b \cdot \check{\mathbf{J}}_{ma} + \check{\mathbf{H}}_a \cdot \check{\mathbf{J}}_{mb}], \tag{4.169}$$

where $(\check{\mathbf{E}}_a, \check{\mathbf{D}}_a, \check{\mathbf{B}}_a, \check{\mathbf{H}}_a)$ are the fields produced by the phasor sources $(\check{\mathbf{J}}_a, \check{\mathbf{J}}_{ma})$ and $(\check{\mathbf{E}}_b, \check{\mathbf{D}}_b, \check{\mathbf{B}}_b, \check{\mathbf{H}}_b)$ are the fields produced by an independent set of sources $(\check{\mathbf{J}}_b, \check{\mathbf{J}}_{mb})$.

As in § 2.9.3, we are interested in the case in which the first two terms on the right-hand side of (4.169) are zero. To see the conditions under which this might occur, we substitute the constitutive equations for a bianisotropic medium

$$\check{\mathbf{D}} = \tilde{\bar{\bar{\boldsymbol{\xi}}}} \cdot \check{\mathbf{H}} + \tilde{\bar{\bar{\boldsymbol{\epsilon}}}} \cdot \check{\mathbf{E}},$$

$$\check{\mathbf{B}} = \tilde{\bar{\bar{\boldsymbol{\mu}}}} \cdot \check{\mathbf{H}} + \tilde{\bar{\bar{\boldsymbol{\zeta}}}} \cdot \check{\mathbf{E}},$$

into (4.169), where each of the constitutive parameters is evaluated at $\check{\omega}$. Setting the two terms to zero gives

$$j\check{\omega}\left[\check{\mathbf{H}}_a \cdot \left(\tilde{\bar{\bar{\boldsymbol{\mu}}}} \cdot \check{\mathbf{H}}_b + \tilde{\bar{\bar{\boldsymbol{\zeta}}}} \cdot \check{\mathbf{E}}_b\right) - \check{\mathbf{H}}_b \cdot \left(\tilde{\bar{\bar{\boldsymbol{\mu}}}} \cdot \check{\mathbf{H}}_a + \tilde{\bar{\bar{\boldsymbol{\zeta}}}} \cdot \check{\mathbf{E}}_a\right)\right] -$$

$$-j\check{\omega}\left[\check{\mathbf{E}}_a \cdot \left(\tilde{\bar{\boldsymbol{\xi}}} \cdot \check{\mathbf{H}}_b + \tilde{\bar{\boldsymbol{\epsilon}}} \cdot \check{\mathbf{E}}_b\right) - \check{\mathbf{E}}_b \cdot \left(\tilde{\bar{\boldsymbol{\xi}}} \cdot \check{\mathbf{H}}_a + \tilde{\bar{\boldsymbol{\epsilon}}} \cdot \check{\mathbf{E}}_a\right)\right] = 0,$$

which holds if

$$\begin{aligned}
\check{\mathbf{H}}_a \cdot \tilde{\bar{\boldsymbol{\mu}}} \cdot \check{\mathbf{H}}_b - \check{\mathbf{H}}_b \cdot \tilde{\bar{\boldsymbol{\mu}}} \cdot \check{\mathbf{H}}_a &= 0,\\
\check{\mathbf{H}}_a \cdot \tilde{\bar{\boldsymbol{\zeta}}} \cdot \check{\mathbf{E}}_b + \check{\mathbf{E}}_b \cdot \tilde{\bar{\boldsymbol{\xi}}} \cdot \check{\mathbf{H}}_a &= 0,\\
\check{\mathbf{E}}_a \cdot \tilde{\bar{\boldsymbol{\xi}}} \cdot \check{\mathbf{H}}_b + \check{\mathbf{H}}_b \cdot \tilde{\bar{\boldsymbol{\zeta}}} \cdot \check{\mathbf{E}}_a &= 0,\\
\check{\mathbf{E}}_a \cdot \tilde{\bar{\boldsymbol{\epsilon}}} \cdot \check{\mathbf{E}}_b - \check{\mathbf{E}}_b \cdot \tilde{\bar{\boldsymbol{\epsilon}}} \cdot \check{\mathbf{E}}_a &= 0.
\end{aligned}$$

These in turn hold if

$$\tilde{\bar{\boldsymbol{\epsilon}}} = \tilde{\bar{\boldsymbol{\epsilon}}}^T, \qquad \tilde{\bar{\boldsymbol{\mu}}} = \tilde{\bar{\boldsymbol{\mu}}}^T, \qquad \tilde{\bar{\boldsymbol{\xi}}} = -\tilde{\bar{\boldsymbol{\zeta}}}^T, \qquad \tilde{\bar{\boldsymbol{\zeta}}} = -\tilde{\bar{\boldsymbol{\xi}}}^T. \tag{4.170}$$

These are the conditions for a *reciprocal medium*. For example, an anisotropic dielectric is a reciprocal medium if its permittivity dyadic is symmetric. An isotropic medium described by scalar quantities μ and ϵ is certainly reciprocal. In contrast, lossless Gyrotropic media are nonreciprocal since the constitutive parameters obey $\tilde{\bar{\boldsymbol{\epsilon}}} = \tilde{\bar{\boldsymbol{\epsilon}}}^\dagger$ or $\tilde{\bar{\boldsymbol{\mu}}} = \tilde{\bar{\boldsymbol{\mu}}}^\dagger$ rather than $\tilde{\bar{\boldsymbol{\epsilon}}} = \tilde{\bar{\boldsymbol{\epsilon}}}^T$ or $\tilde{\bar{\boldsymbol{\mu}}} = \tilde{\bar{\boldsymbol{\mu}}}^T$.

For a reciprocal medium (4.169) reduces to

$$\nabla \cdot (\check{\mathbf{E}}_a \times \check{\mathbf{H}}_b - \check{\mathbf{E}}_b \times \check{\mathbf{H}}_a) = \left[\check{\mathbf{E}}_b \cdot \check{\mathbf{J}}_a - \check{\mathbf{E}}_a \cdot \check{\mathbf{J}}_b - \check{\mathbf{H}}_b \cdot \check{\mathbf{J}}_{ma} + \check{\mathbf{H}}_a \cdot \check{\mathbf{J}}_{mb}\right]. \tag{4.171}$$

At points where the sources are zero, or are conduction currents described entirely by Ohm's law $\check{\mathbf{J}} = \sigma\check{\mathbf{E}}$, we have

$$\nabla \cdot (\check{\mathbf{E}}_a \times \check{\mathbf{H}}_b - \check{\mathbf{E}}_b \times \check{\mathbf{H}}_a) = 0, \tag{4.172}$$

known as *Lorentz's lemma*. If we integrate (4.171) over V and use the divergence theorem we obtain

$$\oint_S \left[\check{\mathbf{E}}_a \times \check{\mathbf{H}}_b - \check{\mathbf{E}}_b \times \check{\mathbf{H}}_a\right] \cdot \mathbf{dS} = \int_V \left[\check{\mathbf{E}}_b \cdot \check{\mathbf{J}}_a - \check{\mathbf{E}}_a \cdot \check{\mathbf{J}}_b - \check{\mathbf{H}}_b \cdot \check{\mathbf{J}}_{ma} + \check{\mathbf{H}}_a \cdot \check{\mathbf{J}}_{mb}\right] dV. \tag{4.173}$$

This is the general form of the *Lorentz reciprocity theorem*, and is valid when V contains reciprocal media as defined in (4.170).

Note that by an identical set of steps we find that the frequency-domain fields obey an identical Lorentz lemma and reciprocity theorem.

The condition for reciprocal systems. The quantity

$$\langle \check{\mathbf{f}}_a, \check{\mathbf{g}}_b \rangle = \int_V \left[\check{\mathbf{E}}_a \cdot \check{\mathbf{J}}_b - \check{\mathbf{H}}_a \cdot \check{\mathbf{J}}_{mb}\right] dV$$

is called the *reaction* between the source fields $\check{\mathbf{g}}$ of set b and the mediating fields $\check{\mathbf{f}}$ of an independent set a. Note that $\check{\mathbf{E}}_a \cdot \check{\mathbf{J}}_b$ is not quite a power density, since the current lacks a complex conjugate. Using this reaction concept, first introduced by Rumsey [161], we can write (4.173) as

$$\langle \check{\mathbf{f}}_b, \check{\mathbf{g}}_a \rangle - \langle \check{\mathbf{f}}_a, \check{\mathbf{g}}_b \rangle = \oint_S \left[\check{\mathbf{E}}_a \times \check{\mathbf{H}}_b - \check{\mathbf{E}}_b \times \check{\mathbf{H}}_a\right] \cdot \mathbf{dS}. \tag{4.174}$$

We see that if there are no sources within S then

$$\oint_S \left[\check{\mathbf{E}}_a \times \check{\mathbf{H}}_b - \check{\mathbf{E}}_b \times \check{\mathbf{H}}_a\right] \cdot \mathbf{dS} = 0. \tag{4.175}$$

Whenever (4.175) holds we say that the "system" within S is *reciprocal*. Thus, for instance, a region of empty space is a reciprocal system.

A system need not be source-free in order for (4.175) to hold. Suppose the relationship between $\check{\mathbf{E}}$ and $\check{\mathbf{H}}$ on S is given by the *impedance boundary condition*

$$\check{\mathbf{E}}_t = -Z(\hat{\mathbf{n}} \times \check{\mathbf{H}}), \tag{4.176}$$

where $\check{\mathbf{E}}_t$ is the component of $\check{\mathbf{E}}$ tangential to S so that $\hat{\mathbf{n}} \times \mathbf{E} = \hat{\mathbf{n}} \times \mathbf{E}_t$, and the complex *wall impedance* Z may depend on position. By (4.176) we can write

$$\begin{aligned}(\check{\mathbf{E}}_a \times \check{\mathbf{H}}_b - \check{\mathbf{E}}_b \times \check{\mathbf{H}}_a) \cdot \hat{\mathbf{n}} &= \check{\mathbf{H}}_b \cdot (\hat{\mathbf{n}} \times \check{\mathbf{E}}_a) - \check{\mathbf{H}}_a \cdot (\hat{\mathbf{n}} \times \check{\mathbf{E}}_b) \\ &= -Z\check{\mathbf{H}}_b \cdot [\hat{\mathbf{n}} \times (\hat{\mathbf{n}} \times \check{\mathbf{H}}_a)] + Z\check{\mathbf{H}}_a \cdot [\hat{\mathbf{n}} \times (\hat{\mathbf{n}} \times \check{\mathbf{H}}_b)].\end{aligned}$$

Since $\hat{\mathbf{n}} \times (\hat{\mathbf{n}} \times \check{\mathbf{H}}) = \hat{\mathbf{n}}(\hat{\mathbf{n}} \cdot \check{\mathbf{H}}) - \check{\mathbf{H}}$, the right-hand side vanishes. Hence (4.175) still holds even though there are sources within S.

The reaction theorem. When sources lie within the surface S, and the fields on S obey (4.176), we obtain an important corollary of the Lorentz reciprocity theorem. We have from (4.174) the additional result

$$\langle \check{\mathbf{f}}_a, \check{\mathbf{g}}_b \rangle - \langle \check{\mathbf{f}}_b, \check{\mathbf{g}}_a \rangle = 0.$$

Hence a reciprocal system has

$$\langle \check{\mathbf{f}}_a, \check{\mathbf{g}}_b \rangle = \langle \check{\mathbf{f}}_b, \check{\mathbf{g}}_a \rangle \tag{4.177}$$

(which holds even if there are no sources within S, since then the reactions would be identically zero). This condition for reciprocity is sometimes called the *reaction theorem* and has an important physical meaning which we shall explore below in the form of the Rayleigh–Carson reciprocity theorem. Note that in obtaining this relation we must assume that the medium is reciprocal in order to eliminate the terms in (4.169). Thus, in order for a system to be reciprocal, it must involve *both* a reciprocal medium and a boundary over which (4.176) holds.

It is important to note that the impedance boundary condition (4.176) is widely applicable. If $Z \to 0$, then the boundary condition is that for a PEC: $\hat{\mathbf{n}} \times \check{\mathbf{E}} = 0$. If $Z \to \infty$, a PMC is described: $\hat{\mathbf{n}} \times \check{\mathbf{H}} = 0$. Suppose S represents a sphere of infinite radius. We know from (4.168) that if the sources and material media within S are spatially finite, the fields far removed from these sources are described by the Sommerfeld radiation condition

$$\hat{\mathbf{r}} \times \check{\mathbf{E}} = \eta_0 \check{\mathbf{H}}$$

where $\hat{\mathbf{r}}$ is the radial unit vector of spherical coordinates. This condition is of the type (4.176) since $\hat{\mathbf{r}} = \hat{\mathbf{n}}$ on S, hence the unbounded region that results from S receding to infinity is also reciprocal.

Summary of reciprocity for reciprocal systems. We can summarize reciprocity as follows. Unbounded space containing sources and materials of finite size is a reciprocal system if the media are reciprocal; a bounded region of space is a reciprocal system only if the materials within are reciprocal and the boundary fields obey (4.176), or if the region is source-free. In each of these cases

$$\oint_S \left[\check{\mathbf{E}}_a \times \check{\mathbf{H}}_b - \check{\mathbf{E}}_b \times \check{\mathbf{H}}_a\right] \cdot \mathbf{dS} = 0 \tag{4.178}$$

and

$$\langle \check{\mathbf{f}}_a, \check{\mathbf{g}}_b \rangle - \langle \check{\mathbf{f}}_b, \check{\mathbf{g}}_a \rangle = 0. \tag{4.179}$$

Rayleigh–Carson reciprocity theorem. The physical meaning behind reciprocity can be made clear with a simple example. Consider two electric Hertzian dipoles, each oscillating with frequency $\check{\omega}$ and located within an empty box consisting of PEC walls. These dipoles can be described in terms of volume current density as

$$\check{\mathbf{J}}_a(\mathbf{r}) = \check{\mathbf{I}}_a \delta(\mathbf{r} - \mathbf{r}'_a),$$
$$\check{\mathbf{J}}_b(\mathbf{r}) = \check{\mathbf{I}}_b \delta(\mathbf{r} - \mathbf{r}'_b).$$

Since the fields on the surface obey (4.176) (specifically, $\hat{\mathbf{n}} \times \check{\mathbf{E}} = 0$), and since the medium within the box is empty space (a reciprocal medium), the fields produced by the sources must obey (4.179). We have

$$\int_V \check{\mathbf{E}}_b(\mathbf{r}) \cdot \left[\check{\mathbf{I}}_a \delta(\mathbf{r} - \mathbf{r}'_a)\right] dV = \int_V \check{\mathbf{E}}_a(\mathbf{r}) \cdot \left[\check{\mathbf{I}}_b \delta(\mathbf{r} - \mathbf{r}'_b)\right] dV,$$

hence

$$\check{\mathbf{I}}_a \cdot \check{\mathbf{E}}_b(\mathbf{r}'_a) = \check{\mathbf{I}}_b \cdot \check{\mathbf{E}}_a(\mathbf{r}'_b). \tag{4.180}$$

This is the *Rayleigh–Carson reciprocity theorem*. It also holds for two Hertzian dipoles located in unbounded free space, because in that case the Sommerfeld radiation condition satisfies (4.176).

As an important application of this principle, consider a closed PEC body located in free space. Reciprocity holds in the region external to the body since we have $\hat{\mathbf{n}} \times \check{\mathbf{E}} = 0$ at the boundary of the perfect conductor and the Sommerfeld radiation condition on the boundary at infinity. Now let us place dipole a somewhere external to the body, and dipole b adjacent and tangential to the perfectly conducting body. We regard dipole a as the source of an electromagnetic field and dipole b as "sampling" that field. Since the tangential electric field is zero at the surface of the conductor, the reaction between the two dipoles is zero. Now let us switch the roles of the dipoles so that b is regarded as the source and a is regarded as the sampler. By reciprocity the reaction is again zero and thus there is no field produced by b at the position of a. Now the position and orientation of a are arbitrary, so we conclude that an impressed electric source current placed tangentially to a perfectly conducting body produces no field external to the body. This result is used in Chapter 6 to develop a field equivalence principle useful in the study of antennas and scattering.

4.10.3 Duality

A duality principle analogous to that found for time-domain fields in § 2.9.2 may be established for frequency-domain and time-harmonic fields. Consider a closed surface S enclosing a region of space that includes a frequency-domain electric source current $\tilde{\mathbf{J}}$

and a frequency-domain magnetic source current $\tilde{\mathbf{J}}_m$. The fields ($\tilde{\mathbf{E}}_1$,$\tilde{\mathbf{D}}_1$,$\tilde{\mathbf{B}}_1$,$\tilde{\mathbf{H}}_1$) within the region (which may also contain arbitrary media) are described by

$$\nabla \times \tilde{\mathbf{E}}_1 = -\tilde{\mathbf{J}}_m - j\omega\tilde{\mathbf{B}}_1, \tag{4.181}$$
$$\nabla \times \tilde{\mathbf{H}}_1 = \tilde{\mathbf{J}} + j\omega\tilde{\mathbf{D}}_1, \tag{4.182}$$
$$\nabla \cdot \tilde{\mathbf{D}}_1 = \tilde{\rho}, \tag{4.183}$$
$$\nabla \cdot \tilde{\mathbf{B}}_1 = \tilde{\rho}_m. \tag{4.184}$$

Suppose we have been given a mathematical description of the sources ($\tilde{\mathbf{J}}, \tilde{\mathbf{J}}_m$) and have solved for the field vectors ($\tilde{\mathbf{E}}_1, \tilde{\mathbf{D}}_1, \tilde{\mathbf{B}}_1, \tilde{\mathbf{H}}_1$). Of course, we must also have been supplied with a set of boundary values and constitutive relations in order to make the solution unique. We note that if we replace the formula for $\tilde{\mathbf{J}}$ with the formula for $\tilde{\mathbf{J}}_m$ in (4.182) (and $\tilde{\rho}$ with $\tilde{\rho}_m$ in (4.183)) and also replace $\tilde{\mathbf{J}}_m$ with $-\tilde{\mathbf{J}}$ in (4.181) (and $\tilde{\rho}_m$ with $-\tilde{\rho}$ in (4.184)) we get a new problem. However, the symmetry of the equations allows us to specify the solution immediately. The new set of curl equations requires

$$\nabla \times \tilde{\mathbf{E}}_2 = \tilde{\mathbf{J}} - j\omega\tilde{\mathbf{B}}_2, \tag{4.185}$$
$$\nabla \times \tilde{\mathbf{H}}_2 = \tilde{\mathbf{J}}_m + j\omega\tilde{\mathbf{D}}_2. \tag{4.186}$$

If we can resolve the question of how the constitutive parameters must be altered to reflect these replacements, then we can conclude by comparing (4.185) with (4.182) and (4.186) with (4.181) that

$$\tilde{\mathbf{E}}_2 = \tilde{\mathbf{H}}_1, \qquad \tilde{\mathbf{B}}_2 = -\tilde{\mathbf{D}}_1, \qquad \tilde{\mathbf{D}}_2 = \tilde{\mathbf{B}}_1, \qquad \tilde{\mathbf{H}}_2 = -\tilde{\mathbf{E}}_1.$$

The discussion regarding units in § 2.9.2 carries over to the present case. Multiplying Ampere's law by $\eta_0 = (\mu_0/\epsilon_0)^{1/2}$, we have

$$\nabla \times \tilde{\mathbf{E}} = -\tilde{\mathbf{J}}_m - j\omega\tilde{\mathbf{B}}, \qquad \nabla \times (\eta_0\tilde{\mathbf{H}}) = (\eta_0\tilde{\mathbf{J}}) + j\omega(\eta_0\tilde{\mathbf{D}}).$$

Thus if the original problem has solution ($\tilde{\mathbf{E}}_1, \eta_0\tilde{\mathbf{D}}_1, \tilde{\mathbf{B}}_1, \eta_0\tilde{\mathbf{H}}_1$), then the dual problem with $\tilde{\mathbf{J}}$ replaced by $\tilde{\mathbf{J}}_m/\eta_0$ and $\tilde{\mathbf{J}}_m$ replaced by $-\eta_0\tilde{\mathbf{J}}$ has solution

$$\tilde{\mathbf{E}}_2 = \eta_0\tilde{\mathbf{H}}_1, \tag{4.187}$$
$$\tilde{\mathbf{B}}_2 = -\eta_0\tilde{\mathbf{D}}_1, \tag{4.188}$$
$$\eta_0\tilde{\mathbf{D}}_2 = \tilde{\mathbf{B}}_1, \tag{4.189}$$
$$\eta_0\tilde{\mathbf{H}}_2 = -\tilde{\mathbf{E}}_1. \tag{4.190}$$

As with duality in the time domain, the constitutive parameters for the dual problem must be altered from those of the original problem. For linear anisotropic media we have from (4.13) and (4.14) the constitutive relationships

$$\tilde{\mathbf{D}}_1 = \tilde{\bar{\epsilon}}_1 \cdot \tilde{\mathbf{E}}_1, \tag{4.191}$$
$$\tilde{\mathbf{B}}_1 = \tilde{\bar{\boldsymbol{\mu}}}_1 \cdot \tilde{\mathbf{H}}_1, \tag{4.192}$$

for the original problem, and

$$\tilde{\mathbf{D}}_2 = \tilde{\bar{\epsilon}}_2 \cdot \tilde{\mathbf{E}}_2, \tag{4.193}$$
$$\tilde{\mathbf{B}}_2 = \tilde{\bar{\boldsymbol{\mu}}}_2 \cdot \tilde{\mathbf{H}}_2, \tag{4.194}$$

for the dual problem. Substitution of (4.187)–(4.190) into (4.191) and (4.192) gives

$$\tilde{\mathbf{D}}_2 = \left(\frac{\tilde{\bar{\boldsymbol{\mu}}}_1}{\eta_0^2}\right) \cdot \tilde{\mathbf{E}}_2, \tag{4.195}$$

$$\tilde{\mathbf{B}}_2 = \left(\eta_0^2 \tilde{\bar{\boldsymbol{\epsilon}}}_1\right) \cdot \tilde{\mathbf{H}}_2. \tag{4.196}$$

Comparing (4.195) with (4.193) and (4.196) with (4.194), we conclude that

$$\tilde{\bar{\boldsymbol{\mu}}}_2 = \eta_0^2 \tilde{\bar{\boldsymbol{\epsilon}}}_1, \qquad \tilde{\bar{\boldsymbol{\epsilon}}}_2 = \tilde{\bar{\boldsymbol{\mu}}}_1/\eta_0^2. \tag{4.197}$$

For a linear, isotropic medium specified by $\tilde{\epsilon}$ and $\tilde{\mu}$, the dual problem is obtained by replacing $\tilde{\epsilon}_r$ with $\tilde{\mu}_r$ and $\tilde{\mu}_r$ with $\tilde{\epsilon}_r$. The solution to the dual problem is then

$$\tilde{\mathbf{E}}_2 = \eta_0 \tilde{\mathbf{H}}_1, \qquad \eta_0 \tilde{\mathbf{H}}_2 = -\tilde{\mathbf{E}}_1,$$

as before. The medium in the dual problem must have electric properties numerically equal to the magnetic properties of the medium in the original problem, and magnetic properties numerically equal to the electric properties of the medium in the original problem. Alternatively we may divide Ampere's law by $\eta = (\tilde{\mu}/\tilde{\epsilon})^{1/2}$ instead of η_0. Then the dual problem has $\tilde{\mathbf{J}}$ replaced by $\tilde{\mathbf{J}}_m/\eta$, and $\tilde{\mathbf{J}}_m$ replaced by $-\eta\tilde{\mathbf{J}}$, and the solution is

$$\tilde{\mathbf{E}}_2 = \eta \tilde{\mathbf{H}}_1, \qquad \eta \tilde{\mathbf{H}}_2 = -\tilde{\mathbf{E}}_1. \tag{4.198}$$

There is no need to swap $\tilde{\epsilon}_r$ and $\tilde{\mu}_r$ since information about these parameters is incorporated into the replacement sources.

We may also apply duality to a problem where we have separated the impressed and secondary sources. In a homogeneous, isotropic, conducting medium we may let $\tilde{\mathbf{J}} = \tilde{\mathbf{J}}^i + \tilde{\sigma}\tilde{\mathbf{E}}$. With this the curl equations become

$$\nabla \times \eta \tilde{\mathbf{H}} = \eta \tilde{\mathbf{J}}^i + j\omega\eta\tilde{\epsilon}^c \tilde{\mathbf{E}},$$

$$\nabla \times \tilde{\mathbf{E}} = -\tilde{\mathbf{J}}_m - j\omega\tilde{\mu}\tilde{\mathbf{H}}.$$

The solution to the dual problem is again given by (4.198), except that now $\eta = (\tilde{\mu}/\tilde{\epsilon}^c)^{1/2}$.

As we did near the end of § 2.9.2, we can consider duality in a source-free region. We let S enclose a source-free region of space and, for simplicity, assume that the medium within S is linear, isotropic, and homogeneous. The fields within S are described by

$$\nabla \times \tilde{\mathbf{E}}_1 = -j\omega\tilde{\mu}\tilde{\mathbf{H}}_1,$$

$$\nabla \times \eta\tilde{\mathbf{H}}_1 = j\omega\tilde{\epsilon}\eta\tilde{\mathbf{E}}_1,$$

$$\nabla \cdot \tilde{\epsilon}\tilde{\mathbf{E}}_1 = 0,$$

$$\nabla \cdot \tilde{\mu}\tilde{\mathbf{H}}_1 = 0.$$

The symmetry of the equations is such that the mathematical form of the solution for $\tilde{\mathbf{E}}$ is the same as that for $\eta\tilde{\mathbf{H}}$. Since the fields

$$\tilde{\mathbf{E}}_2 = \eta\tilde{\mathbf{H}}_1, \qquad \tilde{\mathbf{H}}_2 = -\tilde{\mathbf{E}}_1/\eta,$$

also satisfy Maxwell's equations, the dual problem merely involves replacing $\tilde{\mathbf{E}}$ by $\eta\tilde{\mathbf{H}}$ and $\tilde{\mathbf{H}}$ by $-\tilde{\mathbf{E}}/\eta$.

4.11 The wave nature of the time-harmonic EM field

Time-harmonic electromagnetic waves have been studied in great detail. Narrowband waves are widely used for signal transmission, heating, power transfer, and radar. They share many of the properties of more general transient waves, and the discussions of § 2.10.1 are applicable. Here we shall investigate some of the unique properties of time-harmonic waves and introduce such fundamental quantities as wavelength, phase and group velocity, and polarization.

4.11.1 The frequency-domain wave equation

We begin by deriving the frequency-domain wave equation for dispersive bianisotropic materials. A solution to this equation may be viewed as the transform of a general time-dependent field. If one specific frequency is considered the time-harmonic solution is produced.

In § 2.10.2 we derived the time-domain wave equation for bianisotropic materials. There it was necessary to consider only time-independent constitutive parameters. We can overcome this requirement, and thus deal with dispersive materials, by using a Fourier transform approach. We solve a frequency-domain wave equation that includes the frequency dependence of the constitutive parameters, and then use an inverse transform to return to the time domain.

The derivation of the equation parallels that of § 2.10.2. We substitute the frequency-domain constitutive relationships

$$\tilde{\mathbf{D}} = \tilde{\bar{\boldsymbol{\epsilon}}} \cdot \tilde{\mathbf{E}} + \tilde{\bar{\boldsymbol{\xi}}} \cdot \tilde{\mathbf{H}},$$
$$\tilde{\mathbf{B}} = \tilde{\bar{\boldsymbol{\zeta}}} \cdot \tilde{\mathbf{E}} + \tilde{\bar{\boldsymbol{\mu}}} \cdot \tilde{\mathbf{H}},$$

into Maxwell's curl equations (4.7) and (4.8) to get the coupled differential equations

$$\nabla \times \tilde{\mathbf{E}} = -j\omega[\tilde{\bar{\boldsymbol{\zeta}}} \cdot \tilde{\mathbf{E}} + \tilde{\bar{\boldsymbol{\mu}}} \cdot \tilde{\mathbf{H}}] - \tilde{\mathbf{J}}_m,$$
$$\nabla \times \tilde{\mathbf{H}} = j\omega[\tilde{\bar{\boldsymbol{\epsilon}}} \cdot \tilde{\mathbf{E}} + \tilde{\bar{\boldsymbol{\xi}}} \cdot \tilde{\mathbf{H}}] + \tilde{\mathbf{J}},$$

for $\tilde{\mathbf{E}}$ and $\tilde{\mathbf{H}}$. Here we have included magnetic sources $\tilde{\mathbf{J}}_m$ in Faraday's law. Using the dyadic operator $\bar{\nabla}$ defined in (2.308) we can write these equations as

$$\left(\bar{\nabla} + j\omega\tilde{\bar{\boldsymbol{\zeta}}}\right) \cdot \tilde{\mathbf{E}} = -j\omega\tilde{\bar{\boldsymbol{\mu}}} \cdot \tilde{\mathbf{H}} - \tilde{\mathbf{J}}_m, \tag{4.199}$$

$$\left(\bar{\nabla} - j\omega\tilde{\bar{\boldsymbol{\xi}}}\right) \cdot \tilde{\mathbf{H}} = j\omega\tilde{\bar{\boldsymbol{\epsilon}}} \cdot \tilde{\mathbf{E}} + \tilde{\mathbf{J}}. \tag{4.200}$$

We can obtain separate equations for $\tilde{\mathbf{E}}$ and $\tilde{\mathbf{H}}$ by defining the inverse dyadics

$$\tilde{\bar{\boldsymbol{\epsilon}}} \cdot \tilde{\bar{\boldsymbol{\epsilon}}}^{-1} = \bar{\mathbf{I}}, \qquad \tilde{\bar{\boldsymbol{\mu}}} \cdot \tilde{\bar{\boldsymbol{\mu}}}^{-1} = \bar{\mathbf{I}}.$$

Using $\tilde{\bar{\boldsymbol{\mu}}}^{-1}$ we can write (4.199) as

$$-j\omega\tilde{\mathbf{H}} = \tilde{\bar{\boldsymbol{\mu}}}^{-1} \cdot \left(\bar{\nabla} + j\omega\tilde{\bar{\boldsymbol{\zeta}}}\right) \cdot \tilde{\mathbf{E}} + \tilde{\bar{\boldsymbol{\mu}}}^{-1} \cdot \tilde{\mathbf{J}}_m.$$

Substituting this into (4.200) we get

$$\left[\left(\bar{\nabla} - j\omega\tilde{\bar{\boldsymbol{\xi}}}\right) \cdot \tilde{\bar{\boldsymbol{\mu}}}^{-1} \cdot \left(\bar{\nabla} + j\omega\tilde{\bar{\boldsymbol{\zeta}}}\right) - \omega^2\tilde{\bar{\boldsymbol{\epsilon}}}\right] \cdot \tilde{\mathbf{E}} = -\left(\bar{\nabla} - j\omega\tilde{\bar{\boldsymbol{\xi}}}\right) \cdot \tilde{\bar{\boldsymbol{\mu}}}^{-1} \cdot \tilde{\mathbf{J}}_m - j\omega\tilde{\mathbf{J}}. \tag{4.201}$$

This is the general frequency-domain wave equation for $\tilde{\mathbf{E}}$. Using $\tilde{\bar{\bar{\boldsymbol{\epsilon}}}}^{-1}$ we can write (4.200) as

$$j\omega\tilde{\mathbf{E}} = \tilde{\bar{\bar{\boldsymbol{\epsilon}}}}^{-1} \cdot \left(\bar{\nabla} - j\omega\tilde{\bar{\bar{\boldsymbol{\xi}}}}\right) \cdot \tilde{\mathbf{H}} - \tilde{\bar{\bar{\boldsymbol{\epsilon}}}}^{-1} \cdot \tilde{\mathbf{J}}.$$

Substituting this into (4.199) we get

$$\left[\left(\bar{\nabla} + j\omega\tilde{\bar{\bar{\boldsymbol{\zeta}}}}\right) \cdot \tilde{\bar{\bar{\boldsymbol{\epsilon}}}}^{-1} \cdot \left(\bar{\nabla} - j\omega\tilde{\bar{\bar{\boldsymbol{\xi}}}}\right) - \omega^2\tilde{\bar{\bar{\boldsymbol{\mu}}}}\right] \cdot \tilde{\mathbf{H}} = \left(\bar{\nabla} + j\omega\tilde{\bar{\bar{\boldsymbol{\zeta}}}}\right) \cdot \tilde{\bar{\bar{\boldsymbol{\epsilon}}}}^{-1} \cdot \tilde{\mathbf{J}} - j\omega\tilde{\mathbf{J}}_m. \qquad (4.202)$$

This is the general frequency-domain wave equation for $\tilde{\mathbf{H}}$.

Wave equation for a homogeneous, lossy, isotropic medium. We may specialize (4.201) and (4.202) to the case of a homogeneous, lossy, isotropic medium by setting $\tilde{\bar{\bar{\boldsymbol{\zeta}}}} = \tilde{\bar{\bar{\boldsymbol{\xi}}}} = 0$, $\tilde{\bar{\bar{\boldsymbol{\mu}}}} = \tilde{\mu}\bar{\mathbf{I}}$, $\tilde{\bar{\bar{\boldsymbol{\epsilon}}}} = \tilde{\epsilon}\bar{\mathbf{I}}$, and $\tilde{\mathbf{J}} = \tilde{\mathbf{J}}^i + \tilde{\mathbf{J}}^c$:

$$\nabla \times (\nabla \times \tilde{\mathbf{E}}) - \omega^2\tilde{\mu}\tilde{\epsilon}\tilde{\mathbf{E}} = -\nabla \times \tilde{\mathbf{J}}_m - j\omega\tilde{\mu}(\tilde{\mathbf{J}}^i + \tilde{\mathbf{J}}^c), \qquad (4.203)$$

$$\nabla \times (\nabla \times \tilde{\mathbf{H}}) - \omega^2\tilde{\mu}\tilde{\epsilon}\tilde{\mathbf{H}} = \nabla \times (\tilde{\mathbf{J}}^i + \tilde{\mathbf{J}}^c) - j\omega\tilde{\epsilon}\tilde{\mathbf{J}}_m. \qquad (4.204)$$

Using (B.47) and using Ohm's law $\tilde{\mathbf{J}}^c = \tilde{\sigma}\tilde{\mathbf{E}}$ to describe the secondary current, we get from (4.203)

$$\nabla(\nabla \cdot \tilde{\mathbf{E}}) - \nabla^2\tilde{\mathbf{E}} - \omega^2\tilde{\mu}\tilde{\epsilon}\tilde{\mathbf{E}} = -\nabla \times \tilde{\mathbf{J}}_m - j\omega\tilde{\mu}\tilde{\mathbf{J}}^i - j\omega\tilde{\mu}\tilde{\sigma}\tilde{\mathbf{E}}$$

which, using $\nabla \cdot \tilde{\mathbf{E}} = \tilde{\rho}/\tilde{\epsilon}$, can be simplified to

$$(\nabla^2 + k^2)\tilde{\mathbf{E}} = \nabla \times \tilde{\mathbf{J}}_m + j\omega\tilde{\mu}\tilde{\mathbf{J}}^i + \frac{1}{\tilde{\epsilon}}\nabla\tilde{\rho}. \qquad (4.205)$$

This is the *vector Helmholtz equation* for $\tilde{\mathbf{E}}$. Here k is the *complex wavenumber* defined through

$$k^2 = \omega^2\tilde{\mu}\tilde{\epsilon} - j\omega\tilde{\mu}\tilde{\sigma} = \omega^2\tilde{\mu}\left[\tilde{\epsilon} + \frac{\tilde{\sigma}}{j\omega}\right] = \omega^2\tilde{\mu}\tilde{\epsilon}^c \qquad (4.206)$$

where $\tilde{\epsilon}^c$ is the complex permittivity (4.26).

By (4.204) we have

$$\nabla(\nabla \cdot \tilde{\mathbf{H}}) - \nabla^2\tilde{\mathbf{H}} - \omega^2\tilde{\mu}\tilde{\epsilon}\tilde{\mathbf{H}} = \nabla \times \tilde{\mathbf{J}}^i + \nabla \times \tilde{\mathbf{J}}^c - j\omega\tilde{\epsilon}\tilde{\mathbf{J}}_m.$$

Using

$$\nabla \times \tilde{\mathbf{J}}^c = \nabla \times (\tilde{\sigma}\tilde{\mathbf{E}}) = \tilde{\sigma}\nabla \times \tilde{\mathbf{E}} = \tilde{\sigma}(-j\omega\tilde{\mathbf{B}} - \tilde{\mathbf{J}}_m)$$

and $\nabla \cdot \tilde{\mathbf{H}} = \tilde{\rho}_m/\tilde{\mu}$ we then get

$$(\nabla^2 + k^2)\tilde{\mathbf{H}} = -\nabla \times \tilde{\mathbf{J}}^i + j\omega\tilde{\epsilon}^c\tilde{\mathbf{J}}_m + \frac{1}{\tilde{\mu}}\nabla\tilde{\rho}_m, \qquad (4.207)$$

which is the vector Helmholtz equation for $\tilde{\mathbf{H}}$.

4.11.2 Field relationships and the wave equation for two-dimensional fields

Many important canonical problems are two-dimensional in nature, with the sources and fields invariant along one direction. Two-dimensional fields have a simple structure compared to three-dimensional fields, and this structure often allows a decomposition into even simpler field structures.

Consider a homogeneous region of space characterized by the permittivity $\tilde{\epsilon}$, permeability $\tilde{\mu}$, and conductivity $\tilde{\sigma}$. We assume that all sources and fields are z-invariant, and wish to find the relationship between the various components of the frequency-domain fields in a source-free region. It is useful to define the transverse vector component of an arbitrary vector $\mathbf{A}$ as the component of $\mathbf{A}$ perpendicular to the axis of invariance:

$$\mathbf{A}_t = \mathbf{A} - \hat{\mathbf{z}}(\hat{\mathbf{z}} \cdot \mathbf{A}).$$

For the position vector $\mathbf{r}$, this component is the transverse position vector $\mathbf{r}_t = \boldsymbol{\rho}$. For instance we have

$$\boldsymbol{\rho} = \hat{\mathbf{x}}x + \hat{\mathbf{y}}y, \qquad \boldsymbol{\rho} = \hat{\boldsymbol{\rho}}\rho,$$

in the rectangular and cylindrical coordinate systems, respectively.

Because the region is source-free, the fields $\tilde{\mathbf{E}}$ and $\tilde{\mathbf{H}}$ obey the homogeneous Helmholtz equations

$$(\nabla^2 + k^2) \begin{Bmatrix} \tilde{\mathbf{E}} \\ \tilde{\mathbf{H}} \end{Bmatrix} = 0.$$

Writing the fields in terms of rectangular components, we find that each component must obey a homogeneous scalar Helmholtz equation. In particular, we have for the *axial components* $\tilde{E}_z$ and $\tilde{H}_z$,

$$(\nabla^2 + k^2) \begin{Bmatrix} \tilde{E}_z \\ \tilde{H}_z \end{Bmatrix} = 0.$$

But since the fields are independent of z we may also write

$$(\nabla_t^2 + k^2) \begin{Bmatrix} \tilde{E}_z \\ \tilde{H}_z \end{Bmatrix} = 0 \tag{4.208}$$

where ∇_t^2 is the transverse Laplacian operator

$$\nabla_t^2 = \nabla^2 - \hat{\mathbf{z}}\frac{\partial^2}{\partial z^2}. \tag{4.209}$$

In rectangular coordinates we have

$$\nabla_t^2 = \frac{\partial^2}{\partial x^2} + \frac{\partial^2}{\partial y^2},$$

while in circular cylindrical coordinates

$$\nabla_t^2 = \frac{\partial^2}{\partial \rho^2} + \frac{1}{\rho}\frac{\partial}{\partial \rho} + \frac{1}{\rho^2}\frac{\partial^2}{\partial \phi^2}. \tag{4.210}$$

With our condition on z-independence we can relate the transverse fields $\tilde{\mathbf{E}}_t$ and $\tilde{\mathbf{H}}_t$ to $\tilde{E}_z$ and $\tilde{H}_z$. By Faraday's law we have

$$\nabla \times \tilde{\mathbf{E}}(\boldsymbol{\rho}, \omega) = -j\omega\tilde{\mu}\tilde{\mathbf{H}}(\boldsymbol{\rho}, \omega)$$

and thus

$$\tilde{\mathbf{H}}_t = -\frac{1}{j\omega\tilde{\mu}}\left[\nabla \times \tilde{\mathbf{E}}\right]_t.$$

The transverse portion of the curl is merely

$$\left[\nabla \times \tilde{\mathbf{E}}\right]_t = \hat{\mathbf{x}}\left[\frac{\partial \tilde{E}_z}{\partial y} - \frac{\partial \tilde{E}_y}{\partial z}\right] + \hat{\mathbf{y}}\left[\frac{\partial \tilde{E}_x}{\partial z} - \frac{\partial \tilde{E}_z}{\partial x}\right] = -\hat{\mathbf{z}} \times \left[\hat{\mathbf{x}}\frac{\partial \tilde{E}_z}{\partial x} + \hat{\mathbf{y}}\frac{\partial \tilde{E}_z}{\partial y}\right]$$

since the derivatives with respect to z vanish. The term in brackets is the transverse gradient of $\tilde{E}_z$, where the transverse gradient operator is

$$\nabla_t = \nabla - \hat{\mathbf{z}}\frac{\partial}{\partial z}.$$

In circular cylindrical coordinates this operator becomes

$$\nabla_t = \hat{\boldsymbol{\rho}}\frac{\partial}{\partial \rho} + \hat{\boldsymbol{\phi}}\frac{1}{\rho}\frac{\partial}{\partial \phi}. \tag{4.211}$$

Thus we have

$$\tilde{\mathbf{H}}_t(\boldsymbol{\rho}, \omega) = \frac{1}{j\omega\tilde{\mu}}\hat{\mathbf{z}} \times \nabla_t \tilde{E}_z(\boldsymbol{\rho}, \omega).$$

Similarly, the source-free Ampere's law yields

$$\tilde{\mathbf{E}}_t(\boldsymbol{\rho}, \omega) = -\frac{1}{j\omega\tilde{\epsilon}^c}\hat{\mathbf{z}} \times \nabla_t \tilde{H}_z(\boldsymbol{\rho}, \omega).$$

These results suggest that we can solve a two-dimensional problem by superposition. We first consider the case where $\tilde{E}_z \neq 0$ and $\tilde{H}_z = 0$, called *electric polarization.* This case is also called *TM* or *transverse magnetic* polarization because the magnetic field is transverse to the z-direction (TM_z). We have

$$(\nabla_t^2 + k^2)\tilde{E}_z = 0, \qquad \tilde{\mathbf{H}}_t(\boldsymbol{\rho}, \omega) = \frac{1}{j\omega\tilde{\mu}}\hat{\mathbf{z}} \times \nabla_t \tilde{E}_z(\boldsymbol{\rho}, \omega). \tag{4.212}$$

Once we have solved the Helmholtz equation for $\tilde{E}_z$, the remaining field components follow by simple differentiation. We next consider the case where $\tilde{H}_z \neq 0$ and $\tilde{E}_z = 0$. This is the case of *magnetic polarization*, also called *TE* or *transverse electric* polarization (TE_z). In this case

$$(\nabla_t^2 + k^2)\tilde{H}_z = 0, \qquad \tilde{\mathbf{E}}_t(\boldsymbol{\rho}, \omega) = -\frac{1}{j\omega\tilde{\epsilon}^c}\hat{\mathbf{z}} \times \nabla_t \tilde{H}_z(\boldsymbol{\rho}, \omega). \tag{4.213}$$

A problem involving both $\tilde{E}_z$ and $\tilde{H}_z$ is solved by adding the results for the individual TE_z and TM_z cases.

Note that we can obtain the expression for the TE fields from the expression for the TM fields, and vice versa, using duality. For instance, knowing that the TM fields obey (4.212) we may replace $\tilde{\mathbf{H}}_t$ with $\tilde{\mathbf{E}}_t/\eta$ and $\tilde{E}_z$ with $-\eta\tilde{H}_z$ to obtain

$$\frac{\tilde{\mathbf{E}}_t(\boldsymbol{\rho}, \omega)}{\eta} = \frac{1}{j\omega\tilde{\mu}}\hat{\mathbf{z}} \times \nabla_t[-\eta\tilde{H}_z(\boldsymbol{\rho}, \omega)],$$

which reproduces (4.213).

4.11.3 Plane waves in a homogeneous, isotropic, lossy material

The plane-wave field. In later sections we will solve the frequency-domain wave equation with an arbitrary source distribution. At this point we are more interested in the general behavior of EM waves in the frequency domain, so we seek simple solutions to the homogeneous equation

$$(\nabla^2 + k^2)\tilde{\mathbf{E}}(\mathbf{r}, \omega) = 0 \tag{4.214}$$

that governs the fields in source-free regions of space. Here

$$[k(\omega)]^2 = \omega^2 \tilde{\mu}(\omega)\tilde{\epsilon}^c(\omega).$$

Many properties of plane waves are best understood by considering the behavior of a monochromatic field oscillating at a single frequency $\check{\omega}$. In these cases we merely make the replacements

$$\omega \to \check{\omega}, \qquad \tilde{\mathbf{E}}(\mathbf{r}, \omega) \to \check{\mathbf{E}}(\mathbf{r}),$$

and apply the rules developed in § 4.7 for the manipulation of phasor fields.

For our first solutions we choose those that demonstrate rectangular symmetry. *Plane waves* have planar spatial phase loci. That is, the spatial surfaces over which the phase of the complex frequency-domain field is constant are planes. Solutions of this type may be obtained using separation of variables in rectangular coordinates. Writing

$$\tilde{\mathbf{E}}(\mathbf{r}, \omega) = \hat{\mathbf{x}}\tilde{E}_x(\mathbf{r}, \omega) + \hat{\mathbf{y}}\tilde{E}_y(\mathbf{r}, \omega) + \hat{\mathbf{z}}\tilde{E}_z(\mathbf{r}, \omega)$$

we find that (4.214) reduces to three scalar equations of the form

$$(\nabla^2 + k^2)\tilde{\psi}(\mathbf{r}, \omega) = 0$$

where $\tilde{\psi}$ is representative of $\tilde{E}_x$, $\tilde{E}_y$, and $\tilde{E}_z$. This is called the homogeneous scalar Helmholtz equation. Product solutions to this equation are considered in § A.4. In rectangular coordinates

$$\tilde{\psi}(\mathbf{r}, \omega) = X(x, \omega)Y(y, \omega)Z(z, \omega)$$

where X, Y, and Z are chosen from the list (A.102). Since the exponentials describe propagating wave functions, we choose

$$\tilde{\psi}(\mathbf{r}, \omega) = A(\omega)e^{\pm jk_x(\omega)x}e^{\pm jk_y(\omega)y}e^{\pm jk_z(\omega)z}$$

where A is the *amplitude spectrum* of the plane wave and $k_x^2 + k_y^2 + k_z^2 = k^2$. Using this solution to represent each component of $\tilde{\mathbf{E}}$, we have a propagating-wave solution to the homogeneous vector Helmholtz equation:

$$\tilde{\mathbf{E}}(\mathbf{r}, \omega) = \tilde{\mathbf{E}}_0(\omega)e^{\pm jk_x(\omega)x}e^{\pm jk_y(\omega)y}e^{\pm jk_z(\omega)z}, \tag{4.215}$$

where $\mathbf{E}_0(\omega)$ is the vector amplitude spectrum. If we define the *wave vector*

$$\mathbf{k}(\omega) = \hat{\mathbf{x}}k_x(\omega) + \hat{\mathbf{y}}k_y(\omega) + \hat{\mathbf{z}}k_z(\omega),$$

then we can write (4.215) as

$$\tilde{\mathbf{E}}(\mathbf{r}, \omega) = \tilde{\mathbf{E}}_0(\omega)e^{-j\mathbf{k}(\omega)\cdot\mathbf{r}}. \tag{4.216}$$

Note that we choose the negative sign in the exponential function and allow the vector components of $\mathbf{k}$ to be either positive or negative as required by the physical nature of a specific problem. Also note that the magnitude of the wave vector is the wavenumber: $|\mathbf{k}| = k$.

We may always write the wave vector as a sum of real and imaginary vector components

$$\mathbf{k} = \mathbf{k}' + j\mathbf{k}'' \tag{4.217}$$

which must obey

$$\mathbf{k} \cdot \mathbf{k} = k^2 = k'^2 - k''^2 + 2j\mathbf{k}' \cdot \mathbf{k}''. \tag{4.218}$$

When the real and imaginary components are collinear, (4.216) describes a *uniform plane wave* with

$$\mathbf{k} = \hat{\mathbf{k}}(k' + jk'').$$

When $\mathbf{k}'$ and $\mathbf{k}''$ have different directions, (4.216) describes a *nonuniform plane wave.* We shall find in § 4.13 that any frequency-domain electromagnetic field in free space may be represented as a continuous superposition of elemental plane-wave components of the type (4.216), but that both uniform and nonuniform terms are required.

The TEM nature of a uniform plane wave. Given the plane-wave solution to the wave equation for the electric field, it is straightforward to find the magnetic field. Substitution of (4.216) into Faraday's law gives

$$\nabla \times \left[\tilde{\mathbf{E}}_0(\omega)e^{-j\mathbf{k}(\omega)\cdot\mathbf{r}}\right] = -j\omega\tilde{\mathbf{B}}(\mathbf{r}, \omega).$$

Computation of the curl is straightforward and easily done in rectangular coordinates. This and similar derivatives often appear when manipulating plane-wave solutions; see the tabulation in Appendix B, By (B.78) we have

$$\tilde{\mathbf{H}} = \frac{\mathbf{k} \times \tilde{\mathbf{E}}}{\omega\tilde{\mu}}. \tag{4.219}$$

Taking the cross product of this expression with $\mathbf{k}$, we also have

$$\mathbf{k} \times \tilde{\mathbf{H}} = \frac{\mathbf{k} \times (\mathbf{k} \times \tilde{\mathbf{E}})}{\omega\tilde{\mu}} = \frac{\mathbf{k}(\mathbf{k} \cdot \tilde{\mathbf{E}}) - \tilde{\mathbf{E}}(\mathbf{k} \cdot \mathbf{k})}{\omega\tilde{\mu}}. \tag{4.220}$$

We can show that $\mathbf{k} \cdot \tilde{\mathbf{E}} = 0$ by examining Gauss' law and employing (B.77):

$$\nabla \cdot \tilde{\mathbf{E}} = -j\mathbf{k} \cdot \tilde{\mathbf{E}}e^{-j\mathbf{k}\cdot\mathbf{r}} = \frac{\tilde{\rho}}{\tilde{\epsilon}} = 0. \tag{4.221}$$

Using this and $\mathbf{k} \cdot \mathbf{k} = k^2 = \omega^2\tilde{\mu}\tilde{\epsilon}^c$, we obtain from (4.220)

$$\tilde{\mathbf{E}} = -\frac{\mathbf{k} \times \tilde{\mathbf{H}}}{\omega\tilde{\epsilon}^c}. \tag{4.222}$$

Now for a uniform plane wave $\mathbf{k} = \hat{\mathbf{k}}k$, so we can also write (4.219) as

$$\tilde{\mathbf{H}} = \frac{\hat{\mathbf{k}} \times \tilde{\mathbf{E}}}{\eta} = \frac{\hat{\mathbf{k}} \times \tilde{\mathbf{E}}_0}{\eta}e^{-j\mathbf{k}\cdot\mathbf{r}} \tag{4.223}$$

and (4.222) as

$$\tilde{\mathbf{E}} = -\eta\hat{\mathbf{k}} \times \tilde{\mathbf{H}}.$$

Here

$$\eta = \frac{\omega\tilde{\mu}}{k} = \sqrt{\frac{\tilde{\mu}}{\tilde{\epsilon}^c}}$$

is the complex intrinsic impedance of the medium.

Equations (4.223) and (4.221) show that the electric and magnetic fields and the wave vector are mutually orthogonal. The wave is said to be *transverse electromagnetic* or *TEM* to the direction of propagation.

The phase and attenuation constants of a uniform plane wave. For a uniform plane wave we may write

$$\mathbf{k} = k'\hat{\mathbf{k}} + jk''\hat{\mathbf{k}} = k\hat{\mathbf{k}} = (\beta - j\alpha)\hat{\mathbf{k}}$$

where $k' = \beta$ and $k'' = -\alpha$. Here α is called the *attenuation constant* and β is the *phase constant*. Since k is defined through (4.206), we have

$$k^2 = (\beta - j\alpha)^2 = \beta^2 - 2j\alpha\beta - \alpha^2 = \omega^2\tilde{\mu}\tilde{\epsilon}^c = \omega^2(\tilde{\mu}' + j\tilde{\mu}'')(\tilde{\epsilon}^{c\prime} + j\tilde{\epsilon}^{c\prime\prime}).$$

Equating real and imaginary parts we have

$$\beta^2 - \alpha^2 = \omega^2[\tilde{\mu}'\tilde{\epsilon}^{c\prime} - \tilde{\mu}''\tilde{\epsilon}^{c\prime\prime}], \qquad -2\alpha\beta = \omega^2[\tilde{\mu}''\tilde{\epsilon}^{c\prime} + \tilde{\mu}'\tilde{\epsilon}^{c\prime\prime}].$$

We assume the material is passive so that $\tilde{\mu}'' \le 0$, $\tilde{\epsilon}^{c\prime\prime} \le 0$. Letting

$$\beta^2 - \alpha^2 = \omega^2[\tilde{\mu}'\tilde{\epsilon}^{c\prime} - \tilde{\mu}''\tilde{\epsilon}^{c\prime\prime}] = A, \qquad 2\alpha\beta = \omega^2[|\tilde{\mu}''|\tilde{\epsilon}^{c\prime} + \tilde{\mu}'|\tilde{\epsilon}^{c\prime\prime}|] = B,$$

we may solve simultaneously to find that

$$\beta^2 = \frac{1}{2}\left[A + \sqrt{A^2 + B^2}\right], \qquad \alpha^2 = \frac{1}{2}\left[-A + \sqrt{A^2 + B^2}\right].$$

Since $A^2 + B^2 = \omega^4(\tilde{\epsilon}^{c\prime 2} + \tilde{\epsilon}^{c\prime\prime 2})(\tilde{\mu}'^2 + \tilde{\mu}''^2)$, we have

$$\beta = \omega\sqrt{\tilde{\mu}'\tilde{\epsilon}^{c\prime}}\sqrt{\frac{1}{2}\left[\sqrt{\left(1 + \frac{\tilde{\epsilon}^{c\prime\prime 2}}{\tilde{\epsilon}^{c\prime 2}}\right)\left(1 + \frac{\tilde{\mu}''^2}{\tilde{\mu}'^2}\right)} + \left(1 - \frac{\tilde{\mu}''}{\tilde{\mu}'}\frac{\tilde{\epsilon}^{c\prime\prime}}{\tilde{\epsilon}^{c\prime}}\right)\right]}, \tag{4.224}$$

$$\alpha = \omega\sqrt{\tilde{\mu}'\tilde{\epsilon}^{c\prime}}\sqrt{\frac{1}{2}\left[\sqrt{\left(1 + \frac{\tilde{\epsilon}^{c\prime\prime 2}}{\tilde{\epsilon}^{c\prime 2}}\right)\left(1 + \frac{\tilde{\mu}''^2}{\tilde{\mu}'^2}\right)} - \left(1 - \frac{\tilde{\mu}''}{\tilde{\mu}'}\frac{\tilde{\epsilon}^{c\prime\prime}}{\tilde{\epsilon}^{c\prime}}\right)\right]}, \tag{4.225}$$

where $\tilde{\epsilon}^c$ and $\tilde{\mu}$ are functions of ω. If $\tilde{\epsilon}(\omega) = \epsilon$, $\tilde{\mu}(\omega) = \mu$, and $\tilde{\sigma}(\omega) = \sigma$ are real and frequency independent, then

$$\alpha = \omega\sqrt{\mu\epsilon}\sqrt{\frac{1}{2}\left[\sqrt{1 + \left(\frac{\sigma}{\omega\epsilon}\right)^2} - 1\right]}, \tag{4.226}$$

$$\beta = \omega\sqrt{\mu\epsilon}\sqrt{\frac{1}{2}\left[\sqrt{1 + \left(\frac{\sigma}{\omega\epsilon}\right)^2} + 1\right]}. \tag{4.227}$$

These values of α and β are valid for $\omega > 0$. For negative frequencies we must be more careful in evaluating the square root in $k = \omega(\tilde{\mu}\tilde{\epsilon}^c)^{1/2}$. Writing

$$\tilde{\mu}(\omega) = \tilde{\mu}'(\omega) + j\tilde{\mu}''(\omega) = |\tilde{\mu}(\omega)|e^{j\xi^\mu(\omega)},$$
$$\tilde{\epsilon}^c(\omega) = \tilde{\epsilon}^{c\prime}(\omega) + j\tilde{\epsilon}^{c\prime\prime}(\omega) = |\tilde{\epsilon}^c(\omega)|e^{j\xi^\epsilon(\omega)},$$

we have

$$k(\omega) = \beta(\omega) - j\alpha(\omega) = \omega\sqrt{\tilde{\mu}(\omega)\tilde{\epsilon}^c(\omega)} = \omega\sqrt{|\tilde{\mu}(\omega)||\tilde{\epsilon}^c(\omega)|}e^{j\frac{1}{2}[\xi^\mu(\omega)+\xi^\epsilon(\omega)]}.$$

Now for passive materials we must have, by (4.48), $\tilde{\mu}'' < 0$ and $\tilde{\epsilon}^{c\prime\prime} < 0$ for $\omega > 0$. Since we also have $\tilde{\mu}' > 0$ and $\tilde{\epsilon}^{c\prime} > 0$ for $\omega > 0$, we find that $-\pi/2 < \xi^\mu < 0$ and $-\pi/2 < \xi^\epsilon < 0$, and thus $-\pi/2 < (\xi^\mu + \xi^\epsilon)/2 < 0$. Thus we must have $\beta > 0$ and $\alpha > 0$ for $\omega > 0$. For $\omega < 0$ we have by (4.44) and (4.45) that $\tilde{\mu}'' > 0$, $\tilde{\epsilon}^{c\prime\prime} > 0$, $\tilde{\mu}' > 0$, and $\tilde{\epsilon}^{c\prime} > 0$. Thus $\pi/2 > (\xi^\mu + \xi^\epsilon)/2 > 0$, and so $\beta < 0$ and $\alpha > 0$ for $\omega < 0$. In summary, $\alpha(\omega)$ is an even function of frequency and $\beta(\omega)$ is an odd function of frequency:

$$\beta(\omega) = -\beta(-\omega), \qquad \alpha(\omega) = \alpha(-\omega), \tag{4.228}$$

where $\beta(\omega) > 0, \alpha(\omega) > 0$ when $\omega > 0$. From this we find a condition on $\tilde{\mathbf{E}}_0$ in (4.216). Since by (4.47) we must have $\tilde{\mathbf{E}}(\omega) = \tilde{\mathbf{E}}^*(-\omega)$, we see that the uniform plane-wave field obeys

$$\tilde{\mathbf{E}}_0(\omega)e^{[-j\beta(\omega)-\alpha(\omega)]\hat{\mathbf{k}}\cdot\mathbf{r}} = \tilde{\mathbf{E}}_0^*(-\omega)e^{[+j\beta(-\omega)-\alpha(-\omega)]\hat{\mathbf{k}}\cdot\mathbf{r}}$$

or

$$\tilde{\mathbf{E}}_0(\omega) = \tilde{\mathbf{E}}_0^*(-\omega),$$

since $\beta(-\omega) = -\beta(\omega)$ and $\alpha(-\omega) = \alpha(\omega)$.

Propagation of a uniform plane wave: the group and phase velocities. We have derived the plane-wave solution to the wave equation in the frequency domain, but can discover the wave nature of the solution only by examining its behavior in the time domain. Unfortunately, the explicit form of the time-domain field is highly dependent on the frequency behavior of the constitutive parameters. Even the simplest case in which ϵ, μ, and σ are frequency independent is quite complicated, as we discovered in § 2.10.6. To overcome this difficulty, it is helpful to examine the behavior of a narrowband (but non-monochromatic) signal in a lossy medium with arbitrary constitutive parameters. We will find that the time-domain wave field propagates as a disturbance through the surrounding medium with a velocity determined by the constitutive parameters of the medium. The temporal wave shape does not change as the wave propagates, but the amplitude of the wave attenuates at a rate dependent on the constitutive parameters.

For clarity of presentation we shall assume a linearly polarized plane wave (§ **??**) with

$$\tilde{\mathbf{E}}(\mathbf{r},\omega) = \hat{\mathbf{e}}\tilde{E}_0(\omega)e^{-j\mathbf{k}(\omega)\cdot\mathbf{r}}. \tag{4.229}$$

Here $\tilde{E}_0(\omega)$ is the spectrum of the temporal dependence of the wave. For the temporal dependence we choose the narrowband signal

$$E_0(t) = E_0 f(t)\cos(\omega_0 t)$$

where $f(t)$ has a narrowband spectrum centered about $\omega = 0$ (and is therefore called a *baseband signal*). An appropriate choice for $f(t)$ is the Gaussian function used in (4.52):

$$f(t) = e^{-a^2t^2} \leftrightarrow \tilde{F}(\omega) = \sqrt{\frac{\pi}{a^2}}e^{-\frac{\omega^2}{4a^2}},$$

producing

$$E_0(t) = E_0 e^{-a^2t^2}\cos(\omega_0 t). \tag{4.230}$$

We think of $f(t)$ as *modulating* the single-frequency cosine *carrier wave*, thus providing the *envelope*. By using a large value of a we obtain a narrowband signal whose spectrum is centered about $\pm\omega_0$. Later we shall let $a \to 0$, thereby driving the width of $f(t)$ to infinity and producing a monochromatic waveform.

By (1) we have

$$\tilde{E}_0(\omega) = E_0\frac{1}{2}\left[\tilde{F}(\omega-\omega_0) + \tilde{F}(\omega+\omega_0)\right]$$

where $f(t) \leftrightarrow \tilde{F}(\omega)$. A plot of this spectrum is shown in Figure 4.2. We see that the narrowband signal is centered at $\omega = \pm\omega_0$. Substituting into (4.229) and using $\mathbf{k} = (\beta - j\alpha)\hat{\mathbf{k}}$ for a uniform plane wave, we have the frequency-domain field

$$\tilde{\mathbf{E}}(\mathbf{r},\omega) = \hat{\mathbf{e}}E_0\frac{1}{2}\left[\tilde{F}(\omega-\omega_0)e^{-j[\beta(\omega)-j\alpha(\omega)]\hat{\mathbf{k}}\cdot\mathbf{r}} + \tilde{F}(\omega+\omega_0)e^{-j[\beta(\omega)-j\alpha(\omega)]\hat{\mathbf{k}}\cdot\mathbf{r}}\right]. \tag{4.231}$$

The field at any time t and position $\mathbf{r}$ can now be found by inversion:

$$\hat{\mathbf{e}}E(\mathbf{r},t) = \frac{1}{2\pi}\int_{-\infty}^{\infty}\hat{\mathbf{e}}E_0\frac{1}{2}\left[\tilde{F}(\omega-\omega_0)e^{-j[\beta(\omega)-j\alpha(\omega)]\hat{\mathbf{k}}\cdot\mathbf{r}} + \right.$$
$$\left. + \;\tilde{F}(\omega+\omega_0)e^{-j[\beta(\omega)-j\alpha(\omega)]\hat{\mathbf{k}}\cdot\mathbf{r}}\right]e^{j\omega t}\,d\omega. \tag{4.232}$$

We assume that $\beta(\omega)$ and $\alpha(\omega)$ vary slowly within the band occupied by $\tilde{E}_0(\omega)$. With this assumption we can expand β and α near $\omega = \omega_0$ as

$$\beta(\omega) = \beta(\omega_0) + \beta'(\omega_0)(\omega-\omega_0) + \frac{1}{2}\beta''(\omega_0)(\omega-\omega_0)^2 + \cdots,$$
$$\alpha(\omega) = \alpha(\omega_0) + \alpha'(\omega_0)(\omega-\omega_0) + \frac{1}{2}\alpha''(\omega_0)(\omega-\omega_0)^2 + \cdots,$$

where $\beta'(\omega) = d\beta(\omega)/d\omega$, $\beta''(\omega) = d^2\beta(\omega)/d\omega^2$, and so on. In a similar manner we can expand β and α near $\omega = -\omega_0$:

$$\beta(\omega) = \beta(-\omega_0) + \beta'(-\omega_0)(\omega+\omega_0) + \frac{1}{2}\beta''(-\omega_0)(\omega+\omega_0)^2 + \cdots,$$
$$\alpha(\omega) = \alpha(-\omega_0) + \alpha'(-\omega_0)(\omega+\omega_0) + \frac{1}{2}\alpha''(-\omega_0)(\omega+\omega_0)^2 + \cdots.$$

Since we are most interested in the propagation velocity, we need not approximate α with great accuracy, and thus use $\alpha(\omega) \approx \alpha(\pm\omega_0)$ within the narrow band. We must consider β to greater accuracy to uncover the propagating nature of the wave, and thus use

$$\beta(\omega) \approx \beta(\omega_0) + \beta'(\omega_0)(\omega-\omega_0) \tag{4.233}$$

near $\omega = \omega_0$ and

$$\beta(\omega) \approx \beta(-\omega_0) + \beta'(-\omega_0)(\omega+\omega_0) \tag{4.234}$$

near $\omega = -\omega_0$. Substituting these approximations into (4.232) we find

$$\hat{\mathbf{e}}E(\mathbf{r},t) = \frac{1}{2\pi}\int_{-\infty}^{\infty}\hat{\mathbf{e}}E_0\frac{1}{2}\left[\tilde{F}(\omega-\omega_0)e^{-j[\beta(\omega_0)+\beta'(\omega_0)(\omega-\omega_0)]\hat{\mathbf{k}}\cdot\mathbf{r}}e^{-[\alpha(\omega_0)]\hat{\mathbf{k}}\cdot\mathbf{r}} + \right.$$
$$\left. + \;\tilde{F}(\omega+\omega_0)e^{-j[\beta(-\omega_0)+\beta'(-\omega_0)(\omega+\omega_0)]\hat{\mathbf{k}}\cdot\mathbf{r}}e^{-[\alpha(-\omega_0)]\hat{\mathbf{k}}\cdot\mathbf{r}}\right]e^{j\omega t}\,d\omega. \tag{4.235}$$

By (4.228) we know that α is even in ω and β is odd in ω. Since the derivative of an odd function is an even function, we also know that β' is even in ω. We can therefore write (4.235) as

$$\hat{\mathbf{e}}E(\mathbf{r},t) = \hat{\mathbf{e}}E_0 e^{-\alpha(\omega_0)\hat{\mathbf{k}}\cdot\mathbf{r}} \frac{1}{2\pi}\int_{-\infty}^{\infty} \frac{1}{2}\Big[\tilde{F}(\omega-\omega_0)e^{-j\beta(\omega_0)\hat{\mathbf{k}}\cdot\mathbf{r}} e^{-j\beta'(\omega_0)(\omega-\omega_0)\hat{\mathbf{k}}\cdot\mathbf{r}} + \\ + \tilde{F}(\omega+\omega_0)e^{j\beta(\omega_0)\hat{\mathbf{k}}\cdot\mathbf{r}} e^{-j\beta'(\omega_0)(\omega+\omega_0)\hat{\mathbf{k}}\cdot\mathbf{r}}\Big] e^{j\omega t}\, d\omega.$$

Multiplying and dividing by $e^{j\omega_0 t}$ and rearranging, we have

$$\hat{\mathbf{e}}E(\mathbf{r},t) = \hat{\mathbf{e}}E_0 e^{-\alpha(\omega_0)\hat{\mathbf{k}}\cdot\mathbf{r}} \frac{1}{2\pi}\int_{-\infty}^{\infty} \frac{1}{2}\big[\tilde{F}(\omega-\omega_0)e^{j\phi}e^{j(\omega-\omega_0)[t-\tau]} + \\ + \tilde{F}(\omega+\omega_0)e^{-j\phi}e^{j(\omega+\omega_0)[t-\tau]}\big]\, d\omega$$

where

$$\phi = \omega_0 t - \beta(\omega_0)\hat{\mathbf{k}}\cdot\mathbf{r}, \qquad \tau = \beta'(\omega_0)\hat{\mathbf{k}}\cdot\mathbf{r}.$$

Setting $u = \omega - \omega_0$ in the first term and $u = \omega + \omega_0$ in the second term we have

$$\hat{\mathbf{e}}E(\mathbf{r},t) = \hat{\mathbf{e}}E_0 e^{-\alpha(\omega_0)\hat{\mathbf{k}}\cdot\mathbf{r}} \cos\phi \frac{1}{2\pi}\int_{-\infty}^{\infty} \tilde{F}(u)e^{ju(t-\tau)}\, du.$$

Finally, the time-shifting theorem (A.3) gives us the time-domain wave field

$$\hat{\mathbf{e}}E(\mathbf{r},t) = \hat{\mathbf{e}}E_0 e^{-\alpha(\omega_0)\hat{\mathbf{k}}\cdot\mathbf{r}} \cos\left(\omega_0\left[t - \hat{\mathbf{k}}\cdot\mathbf{r}/v_p(\omega_0)\right]\right) f\left(t - \hat{\mathbf{k}}\cdot\mathbf{r}/v_g(\omega_0)\right) \tag{4.236}$$

where

$$v_g(\omega) = d\omega/d\beta = [d\beta/d\omega]^{-1} \tag{4.237}$$

is called the *group velocity* and

$$v_p(\omega) = \omega/\beta$$

is called the *phase velocity*.

To interpret (4.236), we note that at any given time t the field is constant over the surface described by

$$\hat{\mathbf{k}}\cdot\mathbf{r} = C \tag{4.238}$$

where C is some constant. This surface is a plane, as shown in Figure 4.10, with its normal along $\hat{\mathbf{k}}$. It is easy to verify that any point $\mathbf{r}$ on this plane satisfies (4.238). Let $\mathbf{r}_0 = r_0\hat{\mathbf{k}}$ describe the point on the plane with position vector in the direction of $\hat{\mathbf{k}}$, and let $\mathbf{d}$ be a displacement vector from this point to any other point on the plane. Then

$$\hat{\mathbf{k}}\cdot\mathbf{r} = \hat{\mathbf{k}}\cdot(\mathbf{r}_0 + \mathbf{d}) = r_0(\hat{\mathbf{k}}\cdot\hat{\mathbf{k}}) + \hat{\mathbf{k}}\cdot\mathbf{d}.$$

But $\hat{\mathbf{k}}\cdot\mathbf{d} = 0$, so

$$\hat{\mathbf{k}}\cdot\mathbf{r} = r_0, \tag{4.239}$$

which is a fixed distance, so (238) holds.

Let us identify the plane over which the envelope f takes on a certain value, and follow its motion as time progresses. The value of r_0 associated with this plane must increase with increasing time in such a way that the argument of f remains constant:

$$t - r_0/v_g(\omega_0) = C.$$

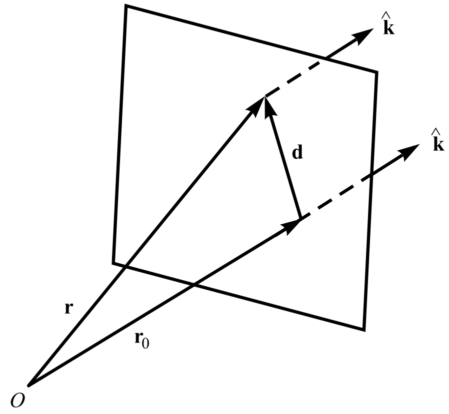

Figure 4.10: Surface of constant $\hat{\mathbf{k}} \cdot \mathbf{r}$.

Differentiation gives

$$\frac{dr_0}{dt} = v_g = \frac{d\omega}{d\beta}. \tag{4.240}$$

So the envelope propagates along $\hat{\mathbf{k}}$ at a rate given by the group velocity v_g. Associated with this propagation is an *attenuation* described by the factor $e^{-\alpha(\omega_0)\hat{\mathbf{k}}\cdot\mathbf{r}}$. This accounts for energy transfer into the lossy medium through Joule heating.

Similarly, we can identify a plane over which the phase of the carrier is constant; this will be parallel to the plane of constant envelope described above. We now set

$$\omega_0 \left[t - \hat{\mathbf{k}} \cdot \mathbf{r}/v_p(\omega_0)\right] = C$$

and differentiate to get

$$\frac{dr_0}{dt} = v_p = \frac{\omega}{\beta}. \tag{4.241}$$

This shows that surfaces of constant carrier phase propagate along $\hat{\mathbf{k}}$ with velocity v_p.

Caution must be exercised in interpreting the two velocities v_g and v_p; in particular, we must be careful not to associate the propagation velocities of energy or information with v_p. Since envelope propagation represents the actual progression of the disturbance, v_g has the recognizable physical meaning of energy velocity. Kraus and Fleisch [105] suggest that we think of a strolling caterpillar: the speed (v_p) of the undulations along the caterpillar's back (representing the carrier wave) may be much faster than the speed (v_g) of the caterpillar's body (representing the envelope of the disturbance).

In fact, v_g is the velocity of energy propagation even for a monochromatic wave (§ **??**). However, for purely monochromatic waves v_g cannot be identified from the time-domain field, whereas v_p can. This leads to some unfortunate misconceptions, especially when v_p exceeds the speed of light. Since v_p is not the velocity of propagation of a physical quantity, but is rather the rate of change of a phase reference point, Einstein's postulate of c as the limiting velocity is not violated.

We can obtain interesting relationships between v_p and v_g by manipulating (4.237) and (4.241). For instance, if we compute

$$\frac{dv_p}{d\omega} = \frac{d}{d\omega}\left(\frac{\omega}{\beta}\right) = \frac{\beta - \omega\frac{d\beta}{d\omega}}{\beta^2}$$

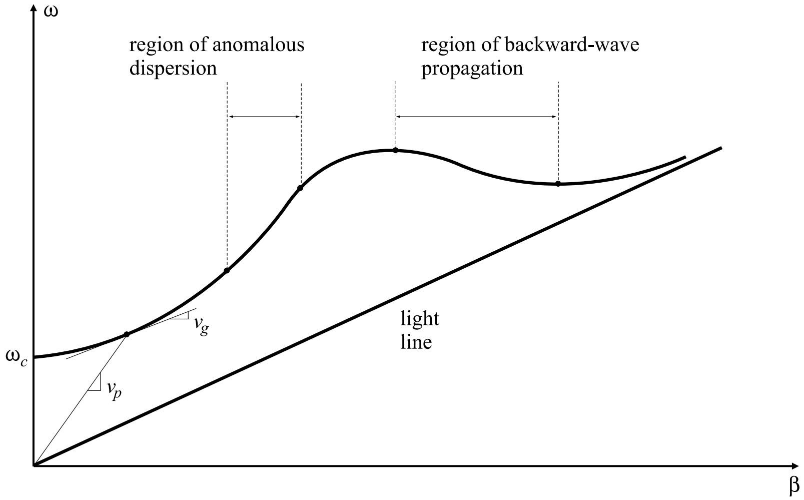

Figure 4.11: An ω–β diagram for a fictitious material.

we find that

$$\frac{v_p}{v_g} = 1 - \beta \frac{dv_p}{d\omega}. \tag{4.242}$$

Hence in frequency ranges where v_p decreases with increasing frequency, we have $v_g < v_p$. These are known as regions of *normal dispersion*. In frequency ranges where v_p increases with increasing frequency, we have $v_g > v_p$. These are known as regions of *anomalous dispersion*. As mentioned in § 4.6.3, the word "anomalous" does not imply that this type of dispersion is unusual.

The propagation of a uniform plane wave through a lossless medium provides a particularly simple example. In a lossless medium we have

$$\beta(\omega) = \omega\sqrt{\mu\epsilon}, \qquad \alpha(\omega) = 0.$$

In this case (4.233) becomes

$$\beta(\omega) = \omega_0\sqrt{\mu\epsilon} + \sqrt{\mu\epsilon}(\omega - \omega_0) = \omega\sqrt{\mu\epsilon}$$

and (4.236) becomes

$$\hat{\mathbf{e}}E(\mathbf{r}, t) = \hat{\mathbf{e}}E_0 \cos\left(\omega_0\left[t - \hat{\mathbf{k}}\cdot\mathbf{r}/v_p(\omega_0)\right]\right) f\left(t - \hat{\mathbf{k}}\cdot\mathbf{r}/v_g(\omega_0)\right).$$

Since the linear approximation to the phase constant β is in this case exact, the wave packet truly propagates without distortion, with a group velocity identical to the phase velocity:

$$v_g = \left[\frac{d}{d\omega}\omega\sqrt{\mu\epsilon}\right]^{-1} = \frac{1}{\sqrt{\mu\epsilon}} = \frac{\omega}{\beta} = v_p.$$

Examples of wave propagation in various media; the ω–β diagram. A plot of ω versus $\beta(\omega)$ can be useful for displaying the dispersive properties of a material. Figure 4.11 shows such an *ω–β plot*, or *dispersion diagram*, for a fictitious material. The

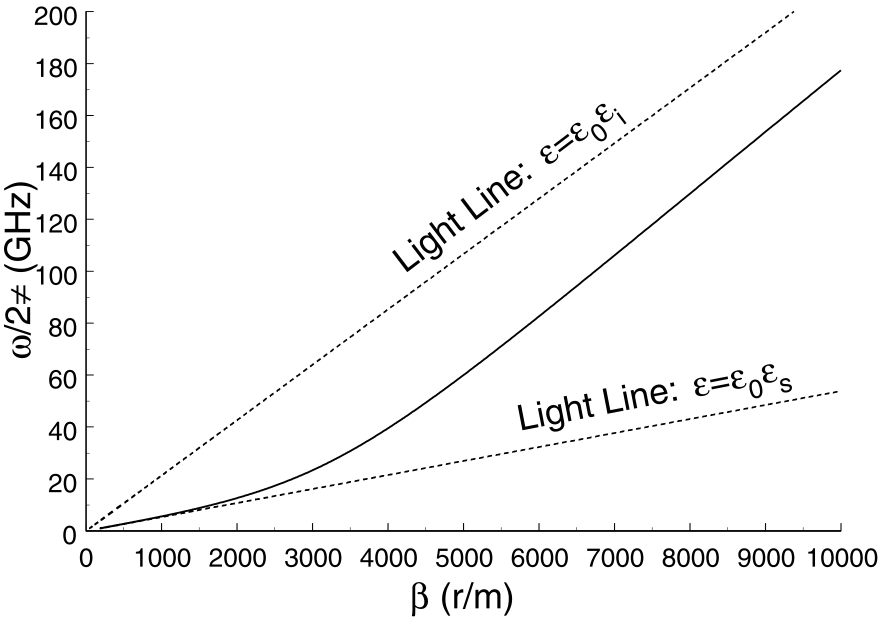

Figure 4.12: Dispersion plot for water computed using the Debye relaxation formula.

slope of the line from the origin to a point (β, ω) is the phase velocity, while the slope of the line tangent to the curve at that point is the group velocity. This plot shows many of the different characteristics of electromagnetic waves (although not necessarily of plane waves). For instance, there may be a minimum frequency ω_c called the *cutoff frequency* at which $\beta = 0$ and below which the wave cannot propagate. This behavior is characteristic of a plane wave propagating in a plasma (as shown below) or of a wave in a hollow pipe waveguide (§ 5.4.3). Over most values of β we have $v_g < v_p$ so the material demonstrates normal dispersion. However, over a small region we do have anomalous dispersion. In another range the slope of the curve is actually negative and thus $v_g < 0$; here the directions of energy and phase front propagation are opposite. Such *backward waves* are encountered in certain guided-wave structures used in microwave oscillators. The ω–β plot also includes the *light line* as a reference curve. For all points on this line $v_g = v_p$; it is generally used to represent propagation within the material under special circumstances, such as when the loss is zero or the material occupies unbounded space. It may also be used to represent propagation within a vacuum.

As an example for which the constitutive parameters depend on frequency, let us consider the relaxation effects of water. By the Debye formula (4.106) we have

$$\tilde{\epsilon}(\omega) = \epsilon_\infty + \frac{\epsilon_s - \epsilon_\infty}{1 + j\omega\tau}.$$

Assuming $\epsilon_\infty = 5\epsilon_0$, $\epsilon_s = 78.3\epsilon_0$, and $\tau = 9.6 \times 10^{-12}$ s [49], we obtain the relaxation spectrum shown in Figure 4.5. If we also assume that $\mu = \mu_0$, we may compute β as a function of ω and construct the ω–β plot. This is shown in Figure 4.12. Since ϵ' varies with frequency, we show both the light line for zero frequency found using $\epsilon_s = 78.3\epsilon_0$, and the light line for infinite frequency found using $\epsilon_i = 5\epsilon_0$. We see that at low values of frequency the dispersion curve follows the low-frequency light line very closely, and thus $v_p \approx v_g \approx c/\sqrt{78.3}$. As the frequency increases, the dispersion curve rises up and

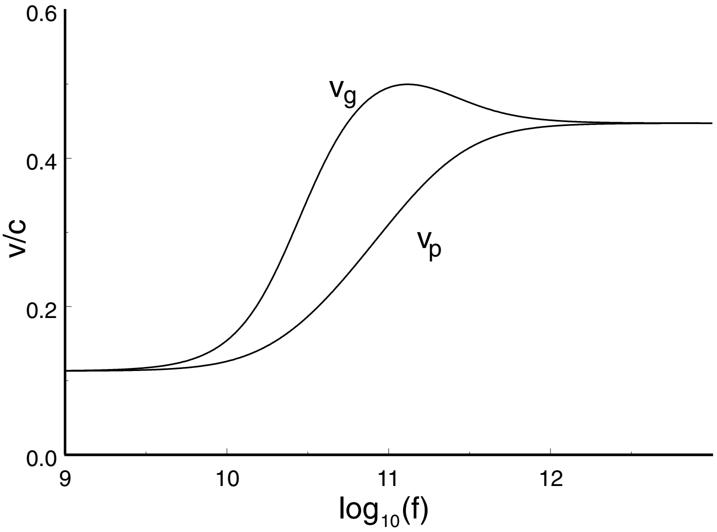

Figure 4.13: Phase and group velocities for water computed using the Debye relaxation formula.

eventually becomes asymptotic with the high-frequency light line. Plots of v_p and v_g shown in Figure 4.13 verify that the velocities start out at $c/\sqrt{78.3}$ for low frequencies, and approach $c/\sqrt{5}$ for high frequencies. Because $v_g > v_p$ at all frequencies, this model of water demonstrates anomalous dispersion.

Another interesting example is that of a non-magnetized plasma. For a collisionless plasma we may set $\nu = 0$ in (4.76) to find

$$k = \begin{cases} \frac{\omega}{c}\sqrt{1 - \frac{\omega_p^2}{\omega^2}}, & \omega > \omega_p, \\ -j\frac{\omega}{c}\sqrt{\frac{\omega_p^2}{\omega^2} - 1}, & \omega < \omega_p. \end{cases}$$

Thus, when $\omega > \omega_p$ we have

$$\tilde{\mathbf{E}}(\mathbf{r}, \omega) = \tilde{E}_0(\omega)e^{-j\beta(\omega)\hat{\mathbf{k}}\cdot\mathbf{r}}$$

and so

$$\beta = \frac{\omega}{c}\sqrt{1 - \frac{\omega_p^2}{\omega^2}}, \qquad \alpha = 0.$$

In this case a plane wave propagates through the plasma without attenuation. However, when $\omega < \omega_p$ we have

$$\tilde{\mathbf{E}}(\mathbf{r}, \omega) = \tilde{E}_0(\omega)e^{-\alpha(\omega)\hat{\mathbf{k}}\cdot\mathbf{r}}$$

with

$$\alpha = \frac{\omega}{c}\sqrt{\frac{\omega_p^2}{\omega^2} - 1}, \qquad \beta = 0,$$

and a plane wave does not propagate, but only attenuates. Such a wave is called an *evanescent wave*. We say that for frequencies below ω_p the wave is *cut off*, and call ω_p the *cutoff frequency*.

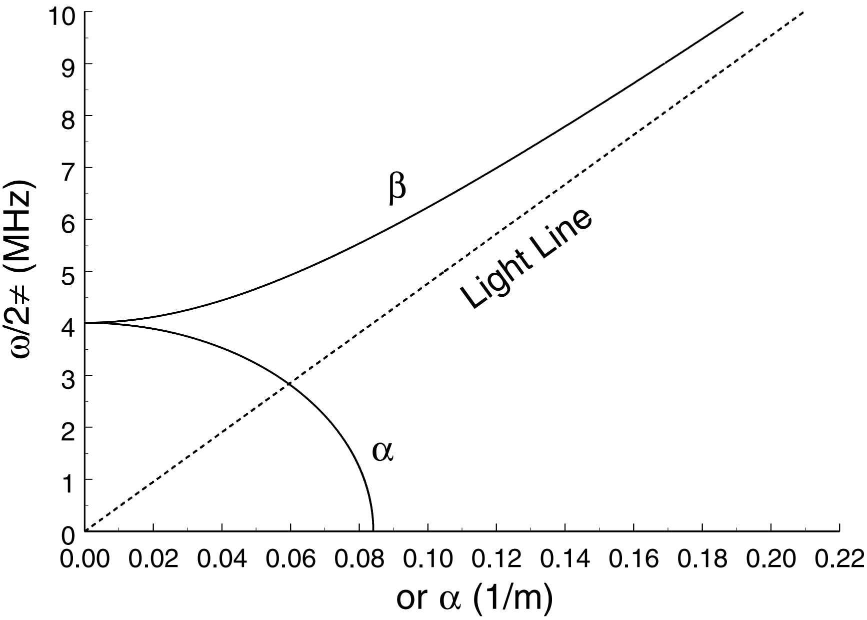

Figure 4.14: Dispersion plot for the ionosphere computed using $N_e = 2 \times 10^{11} m^{-3}$, $\nu = 0$. Light line computed using $\epsilon = \epsilon_0$, $\mu = \mu_0$.

Consider, for instance, a plane wave propagating in the earth's ionosphere. Both the electron density and the collision frequency are highly dependent on such factors as altitude, time of day, and latitude. However, except at the very lowest altitudes, the collision frequency is low enough that the ionosphere may be considered lossless. For instance, at a height of 200 km (the F_1 layer of the ionosphere), as measured for a mid-latitude region, we find that during the day the electron density is approximately $N_e = 2 \times 10^{11} m^{-3}$, while the collision frequency is only $\nu = 100 s^{-1}$ [16]. The attenuation is so small in this case that the ionosphere may be considered essentially lossless above the cutoff frequency (we will develop an approximate formula for the attenuation constant below). Figure 4.14 shows the ω–β diagram for the ionosphere assuming $\nu = 0$, along with the light line $v_p = c$. We see that above the cutoff frequency of $f_p = \omega_p/2\pi = 4.0$ MHz the wave propagates and that $v_g < c$ while $v_p > c$. Below the cutoff frequency the wave does not propagate and the field decays very rapidly because α is large.

A formula for the phase velocity of a plane wave in a lossless plasma is easily derived:

$$v_p = \frac{\omega}{\beta} = \frac{c}{\sqrt{1 - \frac{\omega_p^2}{\omega^2}}} > c.$$

Thus, our observation from the ω–β plot that $v_p > c$ is verified. Similarly, we find that

$$v_g = \left(\frac{d\beta}{d\omega}\right)^{-1} = \left(\frac{1}{c}\sqrt{1 - \frac{\omega_p^2}{\omega^2}} + \frac{1}{c}\frac{\omega_p^2/\omega^2}{\sqrt{1 - \frac{\omega_p^2}{\omega^2}}}\right)^{-1} = c\sqrt{1 - \frac{\omega_p^2}{\omega^2}} < c$$

and our observation that $v_g < c$ is also verified. Interestingly, we find that in this case of an unmagnetized collisionless plasma

$$v_p v_g = c^2.$$

Since $v_p > v_g$, this model of a plasma demonstrates normal dispersion at all frequencies above cutoff.

For the case of a plasma with collisions we retain ν in (4.76) and find that

$$k = \frac{\omega}{c}\sqrt{\left[1 - \frac{\omega_p^2}{\omega^2 + \nu^2}\right] - j\nu\frac{\omega_p^2}{\omega(\omega^2 + \nu^2)}}.$$

When $\nu \neq 0$ a true cutoff effect is not present and the wave may propagate at all frequencies. However, when $\nu \ll \omega_p$ the attenuation for propagating waves of frequency $\omega < \omega_p$ is quite severe, and for all practical purposes the wave is cut off. For waves of frequency $\omega > \omega_p$ there is attenuation. Assuming that $\nu \ll \omega_p$ and that $\nu \ll \omega$, we may approximate the square root with the first two terms of a binomial expansion, and find that to first order

$$\beta = \frac{\omega}{c}\sqrt{1 - \frac{\omega_p^2}{\omega^2}}, \qquad \alpha = \frac{1}{2}\frac{\nu}{c}\frac{\omega_p^2/\omega^2}{\sqrt{1 - \frac{\omega_p^2}{\omega^2}}}.$$

Hence the phase and group velocities above cutoff are essentially those of a lossless plasma, while the attenuation constant is directly proportional to ν.

4.11.4 Monochromatic plane waves in a lossy medium

Many properties of monochromatic plane waves are particularly simple. In fact, certain properties, such as wavelength, only have meaning for monochromatic fields. And since monochromatic or nearly monochromatic waves are employed extensively in radar, communications, and energy transport, it is useful to simplify the results of the preceding section for the special case in which the spectrum of the plane-wave signal consists of a single frequency component. In addition, plane waves of more general time dependence can be viewed as superpositions of individual single-frequency components (through the inverse Fourier transform), and thus we may regard monochromatic waves as building blocks for more complicated plane waves.

We can view the monochromatic field as a specialization of (4.230) for $a \to 0$. This results in $\tilde{F}(\omega) \to \delta(\omega)$, so the linearly-polarized plane wave expression (4.232) reduces to

$$\hat{\mathbf{e}}E(\mathbf{r}, t) = \hat{\mathbf{e}}E_0 e^{-\alpha(\omega_0)[\hat{\mathbf{k}}\cdot\mathbf{r}]}\cos(\omega_0 t - j\beta(\omega_0)[\hat{\mathbf{k}}\cdot\mathbf{r}]). \tag{4.243}$$

It is convenient to represent monochromatic fields with frequency $\omega = \check{\omega}$ in phasor form. The phasor form of (4.243) is

$$\check{\mathbf{E}}(\mathbf{r}) = \hat{\mathbf{e}}E_0 e^{-j\beta(\hat{\mathbf{k}}\cdot\mathbf{r})}e^{-\alpha(\hat{\mathbf{k}}\cdot\mathbf{r})} \tag{4.244}$$

where $\beta = \beta(\check{\omega})$ and $\alpha = \alpha(\check{\omega})$. We can identify a surface of constant phase as a locus of points obeying

$$\check{\omega}t - \beta(\hat{\mathbf{k}}\cdot\mathbf{r}) = C_P \tag{4.245}$$

for some constant C_P. This surface is a plane, as shown in Figure 4.10, with its normal in the direction of $\hat{\mathbf{k}}$. It is easy to verify that any point $\mathbf{r}$ on this plane satisfies (4.245). Let $\mathbf{r}_0 = r_0\hat{\mathbf{k}}$ describe the point on the plane with position vector in the $\hat{\mathbf{k}}$ direction, and let $\mathbf{d}$ be a displacement vector from this point to any other point on the plane. Then

$$\hat{\mathbf{k}}\cdot\mathbf{r} = \hat{\mathbf{k}}\cdot(\mathbf{r}_0 + \mathbf{d}) = r_0(\hat{\mathbf{k}}\cdot\hat{\mathbf{k}}) + \hat{\mathbf{k}}\cdot\mathbf{d}.$$

But $\hat{\mathbf{k}} \cdot \mathbf{d} = 0$, so

$$\hat{\mathbf{k}} \cdot \mathbf{r} = r_0, \tag{4.246}$$

which is a spatial constant, hence (4.245) holds for any t. The planar surfaces described by (4.245) are *wavefronts*.

Note that surfaces of constant amplitude are determined by

$$\alpha(\hat{\mathbf{k}} \cdot \mathbf{r}) = C_A$$

where C_A is some constant. As with the phase term, this requires that $\hat{\mathbf{k}} \cdot \mathbf{r} =$ constant, and thus surfaces of constant phase and surfaces of constant amplitude are coplanar. This is a property of uniform plane waves. We shall see later that nonuniform plane waves have planar surfaces that are not parallel.

The cosine term in (4.243) represents a *traveling wave*. As t increases, the argument of the cosine function remains unchanged as long as $\hat{\mathbf{k}} \cdot \mathbf{r}$ increases correspondingly. Thus the planar wavefronts propagate along $\hat{\mathbf{k}}$. As the wavefront progresses, the wave is attenuated because of the factor $e^{-\alpha(\hat{\mathbf{k}} \cdot \mathbf{r})}$. This accounts for energy transferred from the propagating wave to the surrounding medium via Joule heating.

Phase velocity of a uniform plane wave. The propagation velocity of the progressing wavefront is found by differentiating (4.245) to get

$$\check{\omega} - \beta \hat{\mathbf{k}} \cdot \frac{d\mathbf{r}}{dt} = 0.$$

By (4.246) we have

$$v_p = \frac{dr_0}{dt} = \frac{\check{\omega}}{\beta}, \tag{4.247}$$

where the phase velocity v_p represents the propagation speed of the constant-phase surfaces. For the case of a lossy medium with frequency-independent constitutive parameters, (4.227) shows that

$$v_p \leq \frac{1}{\sqrt{\mu \epsilon}},$$

hence the phase velocity in a conducting medium cannot exceed that in a lossless medium with the same parameters μ and ϵ. We cannot draw this conclusion for a medium with frequency-dependent $\tilde{\mu}$ and $\tilde{\epsilon}^c$, since by (4.224) the value of $\check{\omega}/\beta$ might be greater or less than $1/\sqrt{\tilde{\mu}' \tilde{\epsilon}^{c\prime}}$, depending on the ratios $\tilde{\mu}''/\tilde{\mu}'$ and $\tilde{\epsilon}^{c\prime\prime}/\tilde{\epsilon}^{c\prime}$.

Wavelength of a uniform plane wave. Another important property of a uniform plane wave is the distance between adjacent wavefronts that produce the same value of the cosine function in (4.243). Note that the field amplitude may not be the same on these two surfaces because of possible attenuation of the wave. Let $\mathbf{r}_1$ and $\mathbf{r}_2$ be points on adjacent wavefronts. We require

$$\beta(\hat{\mathbf{k}} \cdot \mathbf{r}_1) = \beta(\hat{\mathbf{k}} \cdot \mathbf{r}_2) - 2\pi$$

or

$$\lambda = \hat{\mathbf{k}} \cdot (\mathbf{r}_2 - \mathbf{r}_1) = r_{02} - r_{01} = 2\pi/\beta.$$

We call λ the *wavelength*.

Polarization of a uniform plane wave. Plane-wave *polarization* describes the temporal evolution of the vector direction of the electric field, which depends on the manner in which the wave is generated. *Completely polarized* waves are produced by antennas or other equipment; these have a deterministic polarization state which may be described completely by three parameters as discussed below. *Randomly polarized* waves are emitted by some natural sources. *Partially polarized* waves, such as those produced by cosmic radio sources, contain both completely polarized and randomly polarized components. We shall concentrate on the description of completely polarized waves.

The polarization state of a completely polarized monochromatic plane wave propagating in a homogeneous, isotropic region may be described by superposing two simpler plane waves that propagate along the same direction but with different phases and spatially orthogonal electric fields. Without loss of generality we may study propagation along the z-axis and choose the orthogonal field directions to be along $\hat{\mathbf{x}}$ and $\hat{\mathbf{y}}$. So we are interested in the behavior of a wave with electric field

$$\check{\mathbf{E}}(\mathbf{r}) = \hat{\mathbf{x}} E_{x0} e^{j\phi_x} e^{-jkz} + \hat{\mathbf{y}} E_{y0} e^{j\phi_y} e^{-jkz}. \tag{4.248}$$

The time evolution of the direction of $\mathbf{E}$ must be examined in the time domain where we have

$$\mathbf{E}(\mathbf{r}, t) = \mathrm{Re}\left\{\check{\mathbf{E}} e^{j\omega t}\right\} = \hat{\mathbf{x}} E_{x0} \cos(\omega t - kz + \phi_x) + \hat{\mathbf{y}} E_{y0} \cos(\omega t - kz + \phi_y)$$

and thus, by the identity $\cos(x + y) \equiv \cos x \cos y - \sin x \sin y$,

$$\begin{aligned} E_x &= E_{x0} \left[\cos(\omega t - kz)\cos(\phi_x) - \sin(\omega t - kz)\sin(\phi_x)\right], \\ E_y &= E_{y0} \left[\cos(\omega t - kz)\cos(\phi_y) - \sin(\omega t - kz)\sin(\phi_y)\right]. \end{aligned}$$

The tip of the vector $\mathbf{E}$ moves cyclically in the xy-plane with temporal period $T = \omega/2\pi$. Its locus may be found by eliminating the parameter t to obtain a relationship between E_{x0} and E_{y0}. Letting $\delta = \phi_y - \phi_x$ we note that

$$\begin{aligned} \frac{E_x}{E_{x0}} \sin\phi_y - \frac{E_y}{E_{y0}} \sin\phi_x &= \cos(\omega t - kz)\sin\delta, \\ \frac{E_x}{E_{x0}} \cos\phi_y - \frac{E_y}{E_{y0}} \cos\phi_x &= \sin(\omega t - kz)\sin\delta; \end{aligned}$$

squaring these terms we find that

$$\left(\frac{E_x}{E_{x0}}\right)^2 + \left(\frac{E_y}{E_{y0}}\right)^2 - 2\frac{E_x}{E_{x0}}\frac{E_y}{E_{y0}}\cos\delta = \sin^2\delta,$$

which is the equation for the ellipse shown in Figure 4.15. By (4.223) the magnetic field of the plane wave is

$$\check{\mathbf{H}} = \frac{\hat{\mathbf{z}} \times \check{\mathbf{E}}}{\eta},$$

hence its tip also traces an ellipse in the xy-plane.

The tip of the electric field vector cycles around the *polarization ellipse* in the xy-plane once every T seconds. The sense of rotation is determined by the sign of δ, and is described by the terms *clockwise/counterclockwise* or *right-hand/left-hand*. There is some disagreement about how to do this. We shall adopt the IEEE definitions (IEEE Standard 145-1983 [189]) and associate with $\delta < 0$ rotation in the *right-hand sense*: if

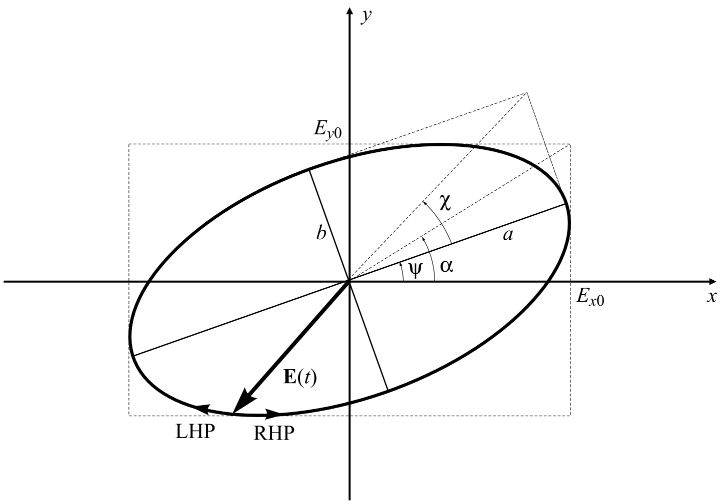

Figure 4.15: Polarization ellipse for a monochromatic plane wave.

the right thumb points in the direction of wave propagation then the fingers curl in the direction of field rotation for increasing time. This is *right-hand polarization* (*RHP*). We associate $\delta > 0$ with *left-hand polarization* (*LHP*).

The polarization ellipse is contained within a rectangle of sides $2E_{x0}$ and $2E_{y0}$, and has its major axis rotated from the x-axis by the *tilt angle* ψ, $0 \le \psi \le \pi$. The ratio of E_{y0} to E_{x0} determines an angle α, $0 \le \alpha \le \pi/2$:

$$E_{y0}/E_{x0} = \tan\alpha.$$

The shape of the ellipse is determined by the three parameters E_{x0}, E_{y0}, and δ, while the sense of polarization is described by the sign of δ. These may not, however, be the most convenient parameters for describing the polarization of a wave. We can also inscribe the ellipse within a box measuring $2a$ by $2b$, where a and b are the lengths of the semimajor and semiminor axes. Then b/a determines an angle χ, $-\pi/4 \le \chi \le \pi/4$, that is analogous to α:

$$\pm b/a = \tan\chi.$$

Here the algebraic sign of χ is used to indicate the sense of polarization: $\chi > 0$ for LHP, $\chi < 0$ for RHP.

The quantities a, b, ψ can also be used to describe the polarization ellipse. When we use the procedure outlined in Born and Wolf [19] to relate the quantities (a, b, ψ) to (E_{x0}, E_{y0}, δ), we find that

$$\begin{aligned} a^2 + b^2 &= E_{x0}^2 + E_{y0}^2, \\ \tan 2\psi &= (\tan 2\alpha)\cos\delta = \frac{2E_{x0}E_{y0}}{E_{x0}^2 - E_{y0}^2}\cos\delta, \\ \sin 2\chi &= (\sin 2\alpha)\sin\delta = \frac{2E_{x0}E_{y0}}{E_{x0}^2 + E_{y0}^2}\sin\delta. \end{aligned}$$

Alternatively, we can describe the polarization ellipse by the angles ψ and χ and one of the amplitudes E_{x0} or E_{y0}.

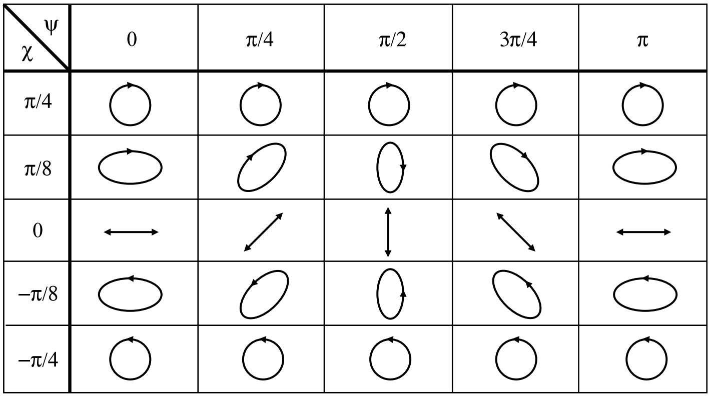

Figure 4.16: Polarization states as a function of tilt angle ψ and ellipse aspect ratio angle χ. Left-hand polarization for $\chi > 0$, right-hand for $\chi < 0$.

Each of these parameter sets is somewhat inconvenient since in each case the units differ among the parameters. In 1852 G. Stokes introduced a system of three independent quantities with identical dimension that can be used to describe plane-wave polarization. Various normalizations of these *Stokes parameters* are employed; when the parameters are chosen to have the dimension of power density we may write them as

$$s_0 = \frac{1}{2\eta}\left[E_{x0}^2 + E_{y0}^2\right], \tag{4.249}$$

$$s_1 = \frac{1}{2\eta}\left[E_{x0}^2 - E_{y0}^2\right] = s_0 \cos(2\chi)\cos(2\psi), \tag{4.250}$$

$$s_2 = \frac{1}{\eta} E_{x0} E_{y0} \cos\delta = s_0 \cos(2\chi)\sin(2\psi), \tag{4.251}$$

$$s_3 = \frac{1}{\eta} E_{x0} E_{y0} \sin\delta = s_0 \sin(2\chi). \tag{4.252}$$

Only three of these four parameters are independent since $s_0^2 = s_1^2 + s_2^2 + s_3^2$. Often the Stokes parameters are designated (I, Q, U, V) rather than (s_0, s_1, s_2, s_3).

Figure 4.16 summarizes various polarization states as a function of the angles ψ and χ. Two interesting special cases occur when $\chi = 0$ and $\chi = \pm\pi/4$. The case $\chi = 0$ corresponds to $b = 0$ and thus $\delta = 0$. In this case the electric vector traces out a straight line and we call the polarization *linear*. Here

$$\mathbf{E} = \left(\hat{\mathbf{x}} E_{x0} + \hat{\mathbf{y}} E_{y0}\right)\cos(\omega t - kz + \phi_x).$$

When $\psi = 0$ we have $E_{y0} = 0$ and refer to this as *horizontal linear polarization* (HLP); when $\psi = \pi/2$ we have $E_{x0} = 0$ and *vertical linear polarization* (VLP).

The case $\chi = \pm\pi/4$ corresponds to $b = a$ and $\delta = \pm\pi/2$. Thus $E_{x0} = E_{y0}$, and $\mathbf{E}$ traces out a circle regardless of the value of ψ. If $\chi = -\pi/4$ we have right-hand rotation of $\mathbf{E}$ and thus refer to this case as *right-hand circular polarization* (RHCP). If $\chi = \pi/4$ we have *left-hand circular polarization* (LHCP). For these cases

$$\mathbf{E} = E_{x0}\left[\hat{\mathbf{x}}\cos(\omega t - kz) \mp \hat{\mathbf{y}}\sin(\omega t - kz)\right],$$

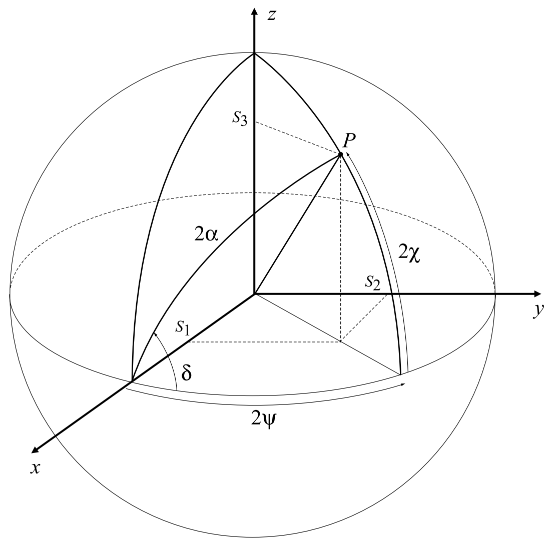

Figure 4.17: Graphical representation of the polarization of a monochromatic plane wave using the Poincaré sphere.

where the upper and lower signs correspond to LHCP and RHCP, respectively. All other values of χ result in the general cases of left-hand or right-hand *elliptical polarization.*

The French mathematician H. Poincaré realized that the Stokes parameters (s_1, s_2, s_3) describe a point on a sphere of radius s_0, and that this *Poincaré sphere* is useful for visualizing the various polarization states. Each state corresponds uniquely to one point on the sphere, and by (4.250)–(4.252) the angles 2χ and 2ψ are the spherical angular coordinates of the point as shown in Figure 4.17. We may therefore map the polarization states shown in Figure 4.16 directly onto the sphere: left- and right-hand polarizations appear in the upper and lower hemispheres, respectively; circular polarization appears at the poles $(2\chi = \pm\pi/2)$; linear polarization appears on the equator $(2\chi = 0)$, with HLP at $2\psi = 0$ and VLP at $2\psi = \pi$. The angles α and δ also have geometrical interpretations on the Poincaré sphere. The spherical angle of the great-circle route between the point of HLP and a point on the sphere is 2α, while the angle between the great-circle path and the equator is δ.

Uniform plane waves in a good dielectric. We may base some useful plane-wave approximations on whether the real or imaginary part of $\tilde{\epsilon}^c$ dominates at the frequency of operation. We assume that $\tilde{\mu}(\omega) = \mu$ is independent of frequency and use the notation $\epsilon^c = \tilde{\epsilon}^c(\check{\omega})$, $\sigma = \tilde{\sigma}(\check{\omega})$, etc. Remember that

$$\epsilon^c = \left(\epsilon' + j\epsilon''\right) + \frac{\sigma}{j\check{\omega}} = \epsilon' + j\left(\epsilon'' - \frac{\sigma}{\check{\omega}}\right) = \epsilon^{c\prime} + j\epsilon^{c\prime\prime}.$$

By definition, a "good dielectric" obeys

$$\tan\delta_c = -\frac{\epsilon^{c\prime\prime}}{\epsilon^{c\prime}} = \frac{\sigma}{\check{\omega}\epsilon'} - \frac{\epsilon''}{\epsilon'} \ll 1. \tag{4.253}$$

Here $\tan\delta_c$ is the *loss tangent* of the material, as first described in (4.107) for a material without conductivity. For a good dielectric we have

$$k = \beta - j\alpha = \check{\omega}\sqrt{\mu\epsilon^c} = \check{\omega}\sqrt{\mu\left[\epsilon' + j\epsilon^{c''}\right]} = \check{\omega}\sqrt{\mu\epsilon'}\sqrt{1 - j\tan\delta_c},$$

hence

$$k \approx \check{\omega}\sqrt{\mu\epsilon'}\left[1 - j\frac{1}{2}\tan\delta_c\right] \tag{4.254}$$

by the binomial approximation for the square root. Therefore

$$\beta \approx \check{\omega}\sqrt{\mu\epsilon'} \tag{4.255}$$

and

$$\alpha \approx \frac{\beta}{2}\tan\delta_c = \frac{\sigma}{2}\sqrt{\frac{\mu}{\epsilon'}}\left[1 - \frac{\check{\omega}\epsilon''}{\sigma}\right]. \tag{4.256}$$

We conclude that $\alpha \ll \beta$. Using this and the binomial approximation we establish

$$\eta = \frac{\check{\omega}\mu}{k} = \frac{\check{\omega}\mu}{\beta}\frac{1}{1 - j\alpha/\beta} \approx \frac{\check{\omega}\mu}{\beta}\left(1 + j\frac{\alpha}{\beta}\right).$$

Finally,

$$v_p = \frac{\check{\omega}}{\beta} \approx \frac{1}{\sqrt{\mu\epsilon'}}$$

and

$$v_g = \left[\frac{d\beta}{d\omega}\right]^{-1} \approx \frac{1}{\sqrt{\mu\epsilon'}}.$$

To first order, the phase constant, phase velocity, and group velocity are the same as those of a lossless medium.

Uniform plane waves in a good conductor. We classify a material as a "good conductor" if

$$\tan\delta_c \approx \frac{\sigma}{\check{\omega}\epsilon} \gg 1.$$

In a good conductor the conduction current $\sigma\check{\mathbf{E}}$ is much greater than the displacement current $j\check{\omega}\epsilon'\check{\mathbf{E}}$, and ϵ'' is usually ignored. Now we may approximate

$$k = \beta - j\alpha = \check{\omega}\sqrt{\mu\epsilon'}\sqrt{1 - j\tan\delta_c} \approx \check{\omega}\sqrt{\mu\epsilon'}\sqrt{-j\tan\delta_c}.$$

Since $\sqrt{-j} = (1-j)/\sqrt{2}$ we find that

$$\beta = \alpha \approx \sqrt{\pi f\mu\sigma}. \tag{4.257}$$

Hence

$$v_p = \frac{\check{\omega}}{\beta} \approx \sqrt{\frac{2\check{\omega}}{\mu\sigma}} = \frac{1}{\sqrt{\mu\epsilon'}}\sqrt{\frac{2}{\tan\delta_c}}.$$

To find v_g we must replace $\check{\omega}$ by ω and differentiate, obtaining

$$v_g = \left[\frac{d\beta}{d\omega}\right]^{-1}\Bigg|_{\omega=\check{\omega}} \approx \left[\frac{1}{2}\sqrt{\frac{\mu\sigma}{2\check{\omega}}}\right]^{-1} = 2\sqrt{\frac{2\check{\omega}}{\mu\sigma}} = 2v_p.$$

In a good conductor the group velocity is approximately twice the phase velocity. We could have found this relation from the phase velocity using (4.242). Indeed, noting that

$$\frac{dv_p}{d\omega} = \frac{d}{d\omega}\sqrt{\frac{2\omega}{\mu\sigma}} = \frac{1}{2}\sqrt{\frac{2}{\omega\mu\sigma}}$$

and

$$\beta\frac{dv_p}{d\omega} = \sqrt{\frac{\omega\mu\sigma}{2}}\frac{1}{2}\sqrt{\frac{2}{\omega\mu\sigma}} = \frac{1}{2},$$

we see that

$$\frac{v_p}{v_g} = 1 - \frac{1}{2} = \frac{1}{2}.$$

Note that the phase and group velocities may be only small fractions of the free-space light velocity. For example, in copper ($\sigma = 5.8 \times 10^7$ S/m, $\mu = \mu_0$, $\epsilon = \epsilon_0$) at 1 MHz, we have $v_p = 415$ m/s.

A factor often used to judge the quality of a conductor is the distance required for a propagating uniform plane wave to decrease in amplitude by the factor $1/e$. By (4.244) this distance is given by

$$\delta = \frac{1}{\alpha} = \frac{1}{\sqrt{\pi f \mu\sigma}}. \tag{4.258}$$

We call δ the *skin depth*. A good conductor is characterized by a small skin depth. For example, copper at 1 MHz has $\delta = 0.066$ mm.

Power carried by a uniform plane wave. Since a plane wavefront is infinite in extent, we usually speak of the *power density* carried by the wave. This is identical to the time-average Poynting flux. Substitution from (4.223) and (4.244) gives

$$\mathbf{S}_{av} = \frac{1}{2}\,\mathrm{Re}\{\check{\mathbf{E}} \times \check{\mathbf{H}}^*\} = \frac{1}{2}\,\mathrm{Re}\left\{\check{\mathbf{E}} \times \left(\frac{\hat{\mathbf{k}} \times \check{\mathbf{E}}}{\eta}\right)^*\right\}. \tag{4.259}$$

Expanding the cross products and remembering that $\mathbf{k} \cdot \check{\mathbf{E}} = 0$, we get

$$\mathbf{S}_{av} = \frac{1}{2}\hat{\mathbf{k}}\,\mathrm{Re}\left\{\frac{|\check{\mathbf{E}}|^2}{\eta^*}\right\} = \hat{\mathbf{k}}\,\mathrm{Re}\left\{\frac{E_0^2}{2\eta^*}\right\} e^{-2\alpha\hat{\mathbf{k}}\cdot\mathbf{r}}.$$

Hence a uniform plane wave propagating in an isotropic medium carries power in the direction of wavefront propagation.

Velocity of energy transport. The group velocity (4.237) has an additional interpretation as the velocity of energy transport. If the time-average volume density of energy is given by

$$\langle w_{em}\rangle = \langle w_e\rangle + \langle w_m\rangle$$

and the time-average volume density of energy flow is given by the Poynting flux density

$$\mathbf{S}_{av} = \frac{1}{2}\,\mathrm{Re}\left\{\check{\mathbf{E}}(\mathbf{r}) \times \check{\mathbf{H}}^*(\mathbf{r})\right\} = \frac{1}{4}\left[\check{\mathbf{E}}(\mathbf{r}) \times \check{\mathbf{H}}^*(\mathbf{r}) + \check{\mathbf{E}}^*(\mathbf{r}) \times \check{\mathbf{H}}(\mathbf{r})\right], \tag{4.260}$$

then the velocity of energy flow, $\mathbf{v}_e$, is defined by

$$\mathbf{S}_{av} = \langle w_{em}\rangle \mathbf{v}_e. \tag{4.261}$$

Let us calculate $\mathbf{v}_e$ for a plane wave propagating in a lossless, source-free medium where $\mathbf{k} = \hat{\mathbf{k}}\omega\sqrt{\mu\epsilon}$. By (4.216) and (4.223) we have

$$\tilde{\mathbf{E}}(\mathbf{r},\omega) = \tilde{\mathbf{E}}_0(\omega)e^{-j\beta\hat{\mathbf{k}}\cdot\mathbf{r}}, \tag{4.262}$$

$$\tilde{\mathbf{H}}(\mathbf{r},\omega) = \left(\frac{\hat{\mathbf{k}}\times\tilde{\mathbf{E}}_0(\omega)}{\eta}\right)e^{-j\beta\hat{\mathbf{k}}\cdot\mathbf{r}} = \tilde{\mathbf{H}}_0(\omega)e^{-j\beta\hat{\mathbf{k}}\cdot\mathbf{r}}. \tag{4.263}$$

We can compute the time-average stored energy density using the energy theorem (4.68). In point form we have

$$-\nabla\cdot\left(\tilde{\mathbf{E}}^*\times\frac{\partial\tilde{\mathbf{H}}}{\partial\omega}+\frac{\partial\tilde{\mathbf{E}}}{\partial\omega}\times\tilde{\mathbf{H}}^*\right)\bigg|_{\omega=\check{\omega}} = 4j\langle w_{em}\rangle. \tag{4.264}$$

Upon substitution of (4.262) and (4.263) we find that we need to compute the frequency derivatives of $\tilde{\mathbf{E}}$ and $\tilde{\mathbf{H}}$. Using

$$\frac{\partial}{\partial\omega}e^{-j\beta\hat{\mathbf{k}}\cdot\mathbf{r}} = \left(\frac{\partial}{\partial\beta}e^{-j\beta\hat{\mathbf{k}}\cdot\mathbf{r}}\right)\frac{d\beta}{d\omega} = -j\hat{\mathbf{k}}\cdot\mathbf{r}\frac{d\beta}{d\omega}e^{-j\beta\hat{\mathbf{k}}\cdot\mathbf{r}}$$

and remembering that $\mathbf{k} = \hat{\mathbf{k}}\beta$, we have

$$\frac{\partial\tilde{\mathbf{E}}(\mathbf{r},\omega)}{\partial\omega} = \frac{d\tilde{\mathbf{E}}_0(\omega)}{d\omega}e^{-j\mathbf{k}\cdot\mathbf{r}} + \tilde{\mathbf{E}}_0(\omega)\left(-j\mathbf{r}\cdot\frac{d\mathbf{k}}{d\omega}\right)e^{-j\mathbf{k}\cdot\mathbf{r}},$$

$$\frac{\partial\tilde{\mathbf{H}}(\mathbf{r},\omega)}{\partial\omega} = \frac{d\tilde{\mathbf{H}}_0(\omega)}{d\omega}e^{-j\mathbf{k}\cdot\mathbf{r}} + \tilde{\mathbf{H}}_0(\omega)\left(-j\mathbf{r}\cdot\frac{d\mathbf{k}}{d\omega}\right)e^{-j\mathbf{k}\cdot\mathbf{r}}.$$

Equation (4.264) becomes

$$-\nabla\cdot\left\{\tilde{\mathbf{E}}_0^*(\omega)\times\frac{d\tilde{\mathbf{H}}_0(\omega)}{d\omega}+\frac{d\tilde{\mathbf{E}}_0(\omega)}{d\omega}\times\tilde{\mathbf{H}}_0^*(\omega)- \right.$$
$$\left. -j\mathbf{r}\cdot\frac{d\mathbf{k}}{d\omega}\left[\tilde{\mathbf{E}}_0^*(\omega)\times\tilde{\mathbf{H}}_0(\omega)+\tilde{\mathbf{E}}_0(\omega)\times\tilde{\mathbf{H}}_0^*(\omega)\right]\right\}\bigg|_{\omega=\check{\omega}} = 4j\langle w_{em}\rangle.$$

The first two terms on the left-hand side have zero divergence, since these terms do not depend on $\mathbf{r}$. By the product rule (B.42) we have

$$\left[\tilde{\mathbf{E}}_0^*(\check{\omega})\times\tilde{\mathbf{H}}_0(\check{\omega})+\tilde{\mathbf{E}}_0(\check{\omega})\times\tilde{\mathbf{H}}_0^*(\check{\omega})\right]\cdot\nabla\left(\mathbf{r}\cdot\frac{d\mathbf{k}}{d\omega}\right)\bigg|_{\omega=\check{\omega}} = 4\langle w_{em}\rangle.$$

The gradient term is merely

$$\nabla\left(\mathbf{r}\cdot\frac{d\mathbf{k}}{d\omega}\right)\bigg|_{\omega=\check{\omega}} = \nabla\left(x\frac{dk_x}{d\omega}+y\frac{dk_y}{d\omega}+z\frac{dk_z}{d\omega}\right)\bigg|_{\omega=\check{\omega}} = \frac{d\mathbf{k}}{d\omega}\bigg|_{\omega=\check{\omega}},$$

hence

$$\left[\tilde{\mathbf{E}}_0^*(\check{\omega})\times\tilde{\mathbf{H}}_0(\check{\omega})+\tilde{\mathbf{E}}_0(\check{\omega})\times\tilde{\mathbf{H}}_0^*(\check{\omega})\right]\cdot\frac{d\mathbf{k}}{d\omega}\bigg|_{\omega=\check{\omega}} = 4\langle w_{em}\rangle. \tag{4.265}$$

Finally, the left-hand side of this expression can be written in terms of the time-average Poynting vector. By (4.260) we have

$$\mathbf{S}_{av} = \frac{1}{2}\operatorname{Re}\left\{\check{\mathbf{E}}\times\check{\mathbf{H}}^*\right\} = \frac{1}{4}\left[\tilde{\mathbf{E}}_0(\check{\omega})\times\tilde{\mathbf{H}}_0^*(\check{\omega})+\tilde{\mathbf{E}}_0^*(\check{\omega})\times\tilde{\mathbf{H}}_0(\check{\omega})\right]$$

and thus we can write (4.265) as

$$\mathbf{S}_{av} \cdot \left.\frac{d\mathbf{k}}{d\omega}\right|_{\omega=\check{\omega}} = \langle w_{em} \rangle.$$

Since for a uniform plane wave in an isotropic medium $\mathbf{k}$ and $\mathbf{S}_{av}$ are in the same direction, we have

$$\mathbf{S}_{av} = \hat{\mathbf{k}} \left.\frac{d\omega}{d\beta}\right|_{\omega=\check{\omega}} \langle w_{em} \rangle$$

and the velocity of energy transport for a plane wave of frequency $\check{\omega}$ is then

$$\mathbf{v}_e = \hat{\mathbf{k}} \left.\frac{d\omega}{d\beta}\right|_{\omega=\check{\omega}}.$$

Thus, for a uniform plane wave in a lossless medium the velocity of energy transport is identical to the group velocity.

Nonuniform plane waves. A nonuniform plane wave has the same form (4.216) as a uniform plane wave, but the vectors $\mathbf{k}'$ and $\mathbf{k}''$ described in (4.217) are not aligned. Thus

$$\check{\mathbf{E}}(\mathbf{r}) = \mathbf{E}_0 e^{-j\mathbf{k}'\cdot\mathbf{r}} e^{\mathbf{k}''\cdot\mathbf{r}}.$$

In the time domain this becomes

$$\check{\mathbf{E}}(\mathbf{r}) = \mathbf{E}_0 e^{\mathbf{k}''\cdot\mathbf{r}} \cos[\check{\omega}t - k'(\hat{\mathbf{k}}' \cdot \mathbf{r})]$$

where $\mathbf{k}' = \hat{\mathbf{k}}'k'$. The surfaces of constant phase are planes perpendicular to $\mathbf{k}'$ and propagating in the direction of $\hat{\mathbf{k}}'$. The phase velocity is now

$$v_p = \check{\omega}/k'$$

and the wavelength is

$$\lambda = 2\pi/k'.$$

In contrast, surfaces of constant amplitude must obey

$$\mathbf{k}'' \cdot \mathbf{r} = C$$

and thus are planes perpendicular to $\mathbf{k}''$.

In a nonuniform plane wave the TEM nature of the fields is lost. This is easily seen by calculating $\check{\mathbf{H}}$ from (4.219):

$$\check{\mathbf{H}}(\mathbf{r}) = \frac{\mathbf{k} \times \check{\mathbf{E}}(\mathbf{r})}{\check{\omega}\mu} = \frac{\mathbf{k}' \times \check{\mathbf{E}}(\mathbf{r})}{\check{\omega}\mu} + j\frac{\mathbf{k}'' \times \check{\mathbf{E}}(\mathbf{r})}{\check{\omega}\mu}.$$

Thus, $\check{\mathbf{H}}$ is no longer perpendicular to the direction of propagation of the phase front. The power carried by the wave also differs from that of the uniform case. The time-average Poynting vector

$$\mathbf{S}_{av} = \frac{1}{2} \mathrm{Re} \left\{ \check{\mathbf{E}} \times \left(\frac{\mathbf{k} \times \check{\mathbf{E}}}{\check{\omega}\mu} \right)^* \right\}$$

can be expanded using the identity (B.7):

$$\mathbf{S}_{av} = \frac{1}{2} \mathrm{Re} \left\{ \frac{1}{\check{\omega}\mu^*} \left[\mathbf{k}^* \times (\check{\mathbf{E}} \times \check{\mathbf{E}}^*) + \check{\mathbf{E}}^* \times (\mathbf{k}^* \times \check{\mathbf{E}}) \right] \right\}. \tag{4.266}$$

Since we still have $\mathbf{k} \cdot \mathbf{E} = 0$, we may use the rest of (B.7) to write

$$\check{\mathbf{E}}^* \times (\mathbf{k}^* \times \check{\mathbf{E}}) = \mathbf{k}^*(\check{\mathbf{E}} \cdot \check{\mathbf{E}}^*) + \check{\mathbf{E}}(\mathbf{k} \cdot \check{\mathbf{E}})^* = \mathbf{k}^*(\check{\mathbf{E}} \cdot \check{\mathbf{E}}^*).$$

Substituting this into (4.266), and noting that $\check{\mathbf{E}} \times \check{\mathbf{E}}^*$ is purely imaginary, we find

$$\mathbf{S}_{av} = \frac{1}{2} \operatorname{Re} \left\{ \frac{1}{\check{\omega}\mu^*} \left[j\mathbf{k}^* \times \operatorname{Im}\left\{\check{\mathbf{E}} \times \check{\mathbf{E}}^*\right\} + \mathbf{k}^*|\check{\mathbf{E}}|^2 \right] \right\}. \tag{4.267}$$

Thus the vector direction of $\mathbf{S}_{av}$ is not generally in the direction of propagation of the plane wavefronts.

Let us examine the special case of nonuniform plane waves propagating in a lossless material. It is intriguing that $\mathbf{k}$ may be complex when k is real, and the implication is important for the plane-wave expansion of complicated fields in free space. By (4.218), real k requires that if $k'' \neq 0$ then

$$\mathbf{k}' \cdot \mathbf{k}'' = 0.$$

Thus, for a nonuniform plane wave in a lossless material the surfaces of constant phase and the surfaces of constant amplitude are orthogonal. To specialize the time-average power to the lossless case we note that μ is purely real and that

$$\mathbf{E} \times \mathbf{E}^* = (\mathbf{E}_0 \times \mathbf{E}_0^*)e^{2\mathbf{k}''\cdot\mathbf{r}}.$$

Then (4.267) becomes

$$\mathbf{S}_{av} = \frac{1}{2\check{\omega}\mu} e^{2\mathbf{k}''\cdot\mathbf{r}} \operatorname{Re}\left\{ j(\mathbf{k}' - j\mathbf{k}'') \times \operatorname{Im}\left\{\mathbf{E}_0 \times \mathbf{E}_0^*\right\} + (\mathbf{k}' - j\mathbf{k}'')|\check{\mathbf{E}}|^2 \right\}$$

or

$$\mathbf{S}_{av} = \frac{1}{2\check{\omega}\mu} e^{2\mathbf{k}''\cdot\mathbf{r}} \left[\mathbf{k}'' \times \operatorname{Im}\left\{\mathbf{E}_0 \times \mathbf{E}_0^*\right\} + \mathbf{k}'\check{\mathbf{E}}|^2 \right].$$

We see that in a lossless medium the direction of energy propagation is perpendicular to the surfaces of constant amplitude (since $\mathbf{k}'' \cdot \mathbf{S}_{av} = 0$), but the direction of energy propagation is not generally in the direction of propagation of the phase planes.

We shall encounter nonuniform plane waves when we study the reflection and refraction of a plane wave from a planar interface in the next section. We shall also find in § 4.13 that nonuniform plane waves are a necessary constituent of the angular spectrum representation of an arbitrary wave field.

4.11.5 Plane waves in layered media

A useful canonical problem in wave propagation involves the reflection of plane waves by planar interfaces between differing material regions. This has many direct applications, from the design of optical coatings and microwave absorbers to the probing of underground oil-bearing rock layers. We shall begin by studying the reflection of a plane wave at a single interface and then extend the results to any number of material layers.

Reflection of a uniform plane wave at a planar material interface. Consider two lossy media separated by the $z = 0$ plane as shown in Figure 4.18. The media are assumed to be isotropic and homogeneous with permeability $\tilde{\mu}(\omega)$ and complex permittivity $\tilde{\epsilon}^c(\omega)$. Both $\tilde{\mu}$ and $\tilde{\epsilon}^c$ may be complex numbers describing magnetic and dielectric loss, respectively. We assume that a linearly-polarized plane-wave field of the form (4.216) is created within region 1 by a process that we shall not study here. We take this field to be the known "incident wave" produced by an impressed source, and wish to compute the total field in regions 1 and 2. Here we shall assume that the incident field is that of a uniform plane wave, and shall extend the analysis to certain types of nonuniform plane waves subsequently.

Since the incident field is uniform, we may write the wave vector associated with this field as

$$\mathbf{k}^i = \hat{\mathbf{k}}^i k^i = \hat{\mathbf{k}}^i (k^{i\prime} + jk^{i\prime\prime})$$

where

$$[k^i(\omega)]^2 = \omega^2 \tilde{\mu}_1(\omega)\tilde{\epsilon}_1^c(\omega).$$

We can assume without loss of generality that $\hat{\mathbf{k}}^i$ lies in the xz-plane and makes an angle θ_i with the interface normal as shown in Figure 4.18. We refer to θ_i as the *incidence angle* of the incident field, and note that it is the angle between the direction of propagation of the planar phase fronts and the normal to the interface. With this we have

$$\mathbf{k}^i = \hat{\mathbf{x}}k_1 \sin\theta_i + \hat{\mathbf{z}}k_1 \cos\theta_i = \hat{\mathbf{x}}k_x^i + \hat{\mathbf{z}}k_z^i.$$

Using $k_1 = \beta_1 - j\alpha_1$ we also have

$$k_x^i = (\beta_1 - j\alpha_1)\sin\theta_i.$$

The term k_z^i is written in a somewhat different form in order to make the result easily applicable to reflections from multiple interfaces. We write

$$k_z^i = (\beta_1 - j\alpha_1)\cos\theta_i = \tau^i e^{-j\gamma^i} = \tau^i \cos\gamma^i - j\tau^i \sin\gamma^i.$$

Thus,

$$\tau^i = \sqrt{\beta_1^2 + \alpha_1^2}\cos\theta_i, \qquad \gamma^i = \tan^{-1}(\alpha_1/\beta_1).$$

We solve for the fields in each region of space directly in the frequency domain. The incident electric field has the form of (4.216),

$$\tilde{\mathbf{E}}^i(\mathbf{r},\omega) = \tilde{\mathbf{E}}_0^i(\omega)e^{-j\mathbf{k}^i(\omega)\cdot\mathbf{r}}, \tag{4.268}$$

while the magnetic field is found from (4.219) to be

$$\tilde{\mathbf{H}}^i = \frac{\mathbf{k}^i \times \tilde{\mathbf{E}}^i}{\omega\tilde{\mu}_1}. \tag{4.269}$$

The incident field may be decomposed into two orthogonal components, one parallel to the plane of incidence (the plane containing $\hat{\mathbf{k}}$ and the interface normal $\hat{\mathbf{z}}$) and one perpendicular to this plane. We seek unique solutions for the fields in both regions, first for the case in which the incident electric field has only a parallel component, and then for the case in which it has only a perpendicular component. The total field is then determined by superposition of the individual solutions. For perpendicular polarization we have from (4.268) and (4.269)

$$\tilde{\mathbf{E}}_\perp^i = \hat{\mathbf{y}}\tilde{E}_\perp^i e^{-j(k_x^i x + k_z^i z)}, \tag{4.270}$$

$$\tilde{\mathbf{H}}_\perp^i = \frac{-\hat{\mathbf{x}}k_z^i + \hat{\mathbf{z}}k_x^i}{k_1}\frac{\tilde{E}_\perp^i}{\eta_1}e^{-j(k_x^i x + k_z^i z)}, \tag{4.271}$$

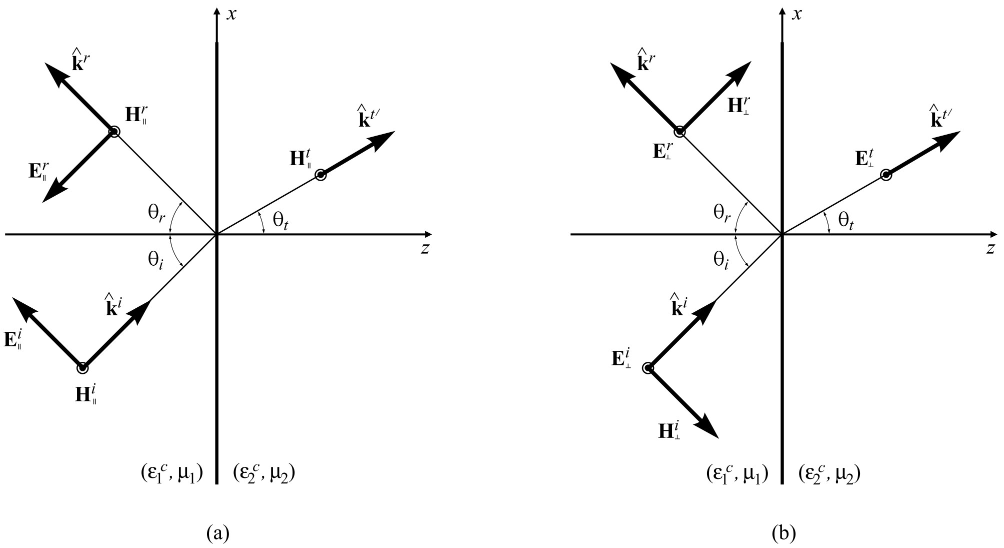

Figure 4.18: Uniform plane wave incident on planar interface between two lossy regions of space. (a) TM polarization, (b) TE polarization.

as shown graphically in Figure 4.18. Here $\eta_1 = (\tilde{\mu}_1/\tilde{\epsilon}_1^c)^{1/2}$ is the intrinsic impedance of medium 1. For parallel polarization, the direction of $\tilde{\mathbf{E}}$ is found by remembering that the wave must be TEM. Thus $\tilde{\mathbf{E}}_\parallel$ is perpendicular to $\mathbf{k}^i$. Since $\tilde{\mathbf{E}}_\parallel$ must also be perpendicular to $\tilde{\mathbf{E}}_\perp$, we have two possible directions for $\tilde{\mathbf{E}}_\parallel$. By convention we choose the one for which $\tilde{\mathbf{H}}$ lies in the same direction as did $\tilde{\mathbf{E}}$ for perpendicular polarization. Thus we have for parallel polarization

$$\tilde{\mathbf{H}}_\parallel^i = \hat{\mathbf{y}}\frac{\tilde{E}_\parallel^i}{\eta_1} e^{-j(k_x^i x + k_z^i z)}, \tag{4.272}$$

$$\tilde{\mathbf{E}}_\parallel^i = \frac{\hat{\mathbf{x}}k_z^i - \hat{\mathbf{z}}k_x^i}{k_1}\tilde{E}_\parallel^i e^{-j(k_x^i x + k_z^i z)}, \tag{4.273}$$

as shown in Figure 4.18. Because $\tilde{\mathbf{E}}$ lies transverse (normal) to the plane of incidence under perpendicular polarization, the field set is often described as *transverse electric* or *TE*. Because $\tilde{\mathbf{H}}$ lies transverse to the plane of incidence under parallel polarization, the fields in that case are *transverse magnetic* or *TM*.

Uniqueness requires that the total field obey the boundary conditions at the planar interface. We hypothesize that the total field within region 1 consists of the incident field superposed with a "reflected" plane-wave field having wave vector $\mathbf{k}^r$, while the field in region 2 consists of a single "transmitted" plane-wave field having wave vector $\mathbf{k}^t$. We cannot at the outset make any assumption regarding whether either of these fields are uniform plane waves. However, we do note that the reflected and transmitted fields cannot have vector components not present in the incident field; extra components would preclude satisfaction of the boundary conditions. Letting $\tilde{E}^r$ be the amplitude of the reflected plane-wave field we may write

$$\tilde{\mathbf{E}}_\perp^r = \hat{\mathbf{y}}\tilde{E}_\perp^r e^{-j(k_x^r x + k_z^r z)}, \qquad \tilde{\mathbf{H}}_\perp^r = \frac{-\hat{\mathbf{x}}k_z^r + \hat{\mathbf{z}}k_x^r}{k_1}\frac{\tilde{E}_\perp^r}{\eta_1} e^{-j(k_x^r x + k_z^r z)},$$

$$\tilde{\mathbf{H}}_\parallel^r = \hat{\mathbf{y}}\frac{\tilde{E}_\parallel^r}{\eta_1}e^{-j(k_x^r x + k_z^r z)}, \qquad \tilde{\mathbf{E}}_\parallel^r = \frac{\hat{\mathbf{x}}k_z^r - \hat{\mathbf{z}}k_x^r}{k_1}\tilde{E}_\parallel^r e^{-j(k_x^r x + k_z^r z)},$$

where $(k_x^r)^2 + (k_z^r)^2 = k_1^2$. Similarly, letting $\tilde{E}^t$ be the amplitude of the transmitted field we have

$$\tilde{\mathbf{E}}_\perp^t = \hat{\mathbf{y}}\tilde{E}_\perp^t e^{-j(k_x^t x + k_z^t z)}, \qquad \tilde{\mathbf{H}}_\perp^t = \frac{-\hat{\mathbf{x}}k_z^t + \hat{\mathbf{z}}k_x^t}{k_2}\frac{\tilde{E}_\perp^t}{\eta_2}e^{-j(k_x^t x + k_z^t z)},$$
$$\tilde{\mathbf{H}}_\parallel^t = \hat{\mathbf{y}}\frac{\tilde{E}_\parallel^t}{\eta_2}e^{-j(k_x^t x + k_z^t z)}, \qquad \tilde{\mathbf{E}}_\parallel^t = \frac{\hat{\mathbf{x}}k_z^t - \hat{\mathbf{z}}k_x^t}{k_2}\tilde{E}_\parallel^t e^{-j(k_x^t x + k_z^t z)},$$

where $(k_x^t)^2 + (k_z^t)^2 = k_2^2$.

The relationships between the field amplitudes $\tilde{E}^i$, $\tilde{E}^r$, $\tilde{E}^t$, and between the components of the reflected and transmitted wave vectors $\mathbf{k}^r$ and $\mathbf{k}^t$, can be found by applying the boundary conditions. The tangential electric and magnetic fields are continuous across the interface at $z = 0$:

$$\hat{\mathbf{z}} \times (\tilde{\mathbf{E}}^i + \tilde{\mathbf{E}}^r)|_{z=0} = \hat{\mathbf{z}} \times \tilde{\mathbf{E}}^t|_{z=0},$$
$$\hat{\mathbf{z}} \times (\tilde{\mathbf{H}}^i + \tilde{\mathbf{H}}^r)|_{z=0} = \hat{\mathbf{z}} \times \tilde{\mathbf{H}}^t|_{z=0}.$$

Substituting the field expressions, we find that for perpendicular polarization the two boundary conditions require

$$\tilde{E}_\perp^i e^{-jk_x^i x} + \tilde{E}_\perp^r e^{-jk_x^r x} = \tilde{E}_\perp^t e^{-jk_x^t x}, \tag{4.274}$$
$$\frac{k_z^i}{k_1}\frac{\tilde{E}_\perp^i}{\eta_1}e^{-jk_x^i x} + \frac{k_z^r}{k_1}\frac{\tilde{E}_\perp^r}{\eta_1}e^{-jk_x^r x} = \frac{k_z^t}{k_2}\frac{\tilde{E}_\perp^t}{\eta_2}e^{-jk_x^t x}, \tag{4.275}$$

while for parallel polarization they require

$$\frac{k_z^i}{k_1}\tilde{E}_\parallel^i e^{-jk_x^i x} + \frac{k_z^r}{k_1}\tilde{E}_\parallel^r e^{-jk_x^r x} = \frac{k_z^t}{k_2}\tilde{E}_\parallel^t e^{-jk_x^t x}, \tag{4.276}$$
$$\frac{\tilde{E}_\parallel^i}{\eta_1}e^{-jk_x^i x} + \frac{\tilde{E}_\parallel^r}{\eta_1}e^{-jk_x^r x} = \frac{\tilde{E}_\parallel^t}{\eta_2}e^{-jk_x^t x}. \tag{4.277}$$

For the above to hold for all x we must have the exponential terms equal. This requires

$$k_x^i = k_x^r = k_x^t, \tag{4.278}$$

and also establishes a relation between k_z^i, k_z^r, and k_z^t. Since $(k_x^i)^2 + (k_z^i)^2 = (k_x^r)^2 + (k_z^r)^2 = k_1^2$, we must have $k_z^r = \pm k_z^i$. In order to make the reflected wavefronts propagate away from the interface we select $k_z^r = -k_z^i$. Letting $k_x^i = k_x^r = k_x^t = k_{1x}$ and $k_z^i = -k_z^r = k_{1z}$, we may write the wave vectors in region 1 as

$$\mathbf{k}^i = \hat{\mathbf{x}}k_{1x} + \hat{\mathbf{z}}k_{1z}, \qquad \mathbf{k}^r = \hat{\mathbf{x}}k_{1x} - \hat{\mathbf{z}}k_{1z}.$$

Since $(k_x^t)^2 + (k_z^t)^2 = k_2^2$, letting $k_2 = \beta_2 - j\alpha_2$ we have

$$k_z^t = \sqrt{k_2^2 - k_{1x}^2} = \sqrt{(\beta_2 - j\alpha_2)^2 - (\beta_1 - j\alpha_1)^2\sin^2\theta_i} = \tau^t e^{-j\gamma^t}.$$

Squaring out the above relation, we have

$$A - jB = (\tau^t)^2\cos 2\gamma^t - j(\tau^t)^2\sin 2\gamma^t$$

where

$$A = \beta_2^2 - \alpha_2^2 - (\beta_1^2 - \alpha_1^2)\sin^2\theta_i, \qquad B = 2(\beta_2\alpha_2 - \beta_1\alpha_1 \sin^2\theta_i). \tag{4.279}$$

Thus

$$\tau^t = \left(A^2 + B^2\right)^{1/4}, \qquad \gamma^t = \frac{1}{2}\tan^{-1}\frac{B}{A}. \tag{4.280}$$

Renaming k_z^t as k_{2z}, we may write the transmitted wave vector as

$$\mathbf{k}^t = \hat{\mathbf{x}}k_{1x} + \hat{\mathbf{z}}k_{2z} = \mathbf{k}_2' + j\mathbf{k}_2''$$

where

$$\mathbf{k}_2' = \hat{\mathbf{x}}\beta_1 \sin\theta_i + \hat{\mathbf{z}}\tau^t \cos\gamma^t, \qquad \mathbf{k}_2'' = -\hat{\mathbf{x}}\alpha_1 \sin\theta_i - \hat{\mathbf{z}}\tau^t \sin\gamma^t.$$

Since the direction of propagation of the transmitted field phase fronts is perpendicular to $\mathbf{k}_2'$, a unit vector in the direction of propagation is

$$\hat{\mathbf{k}}_2' = \frac{\hat{\mathbf{x}}\beta_1 \sin\theta_i + \hat{\mathbf{z}}\tau^t \cos\gamma^t}{\sqrt{\beta_1^2 \sin^2\theta_i + (\tau^t)^2 \cos^2\theta_i}}. \tag{4.281}$$

Similarly, a unit vector perpendicular to planar surfaces of constant amplitude is given by

$$\hat{\mathbf{k}}_2'' = \frac{\hat{\mathbf{x}}\alpha_1 \sin\theta_i + \hat{\mathbf{z}}\tau^t \sin\gamma^t}{\sqrt{\alpha_1^2 \sin^2\theta_i + (\tau^t)^2 \sin^2\gamma^t}}. \tag{4.282}$$

In general $\hat{\mathbf{k}}'$ is not aligned with $\hat{\mathbf{k}}''$ and thus the transmitted field is a nonuniform plane wave.

With these definitions of k_{1x}, k_{1z}, k_{2z}, equations (4.274) and (4.275) can be solved simultaneously and we have

$$\tilde{E}_\perp^r = \tilde{\Gamma}_\perp \tilde{E}_\perp^i, \qquad \tilde{E}_\perp^t = \tilde{T}_\perp \tilde{E}_\perp^i,$$

where

$$\tilde{\Gamma}_\perp = \frac{Z_{2\perp} - Z_{1\perp}}{Z_{2\perp} + Z_{1\perp}}, \qquad \tilde{T}_\perp = 1 + \tilde{\Gamma}_\perp = \frac{2Z_{2\perp}}{Z_{2\perp} + Z_{1\perp}}, \tag{4.283}$$

with

$$Z_{1\perp} = \frac{k_1\eta_1}{k_{1z}}, \qquad Z_{2\perp} = \frac{k_2\eta_2}{k_{2z}}.$$

Here $\tilde{\Gamma}$ is a frequency-dependent *reflection coefficient* that relates the tangential components of the incident and reflected electric fields, and $\tilde{T}$ is a frequency-dependent *transmission coefficient* that relates the tangential components of the incident and transmitted electric fields. These coefficients are also called the *Fresnel coefficients*.

For the case of parallel polarization we solve (4.276) and (4.277) to find

$$\frac{\tilde{E}_{\parallel,x}^r}{\tilde{E}_{\parallel,x}^i} = \frac{k_x^r}{k_x^i}\frac{\tilde{E}_\parallel^r}{\tilde{E}_\parallel^i} = -\frac{\tilde{E}_\parallel^r}{\tilde{E}_\parallel^i} = \tilde{\Gamma}_\parallel, \qquad \frac{\tilde{E}_{\parallel,x}^t}{\tilde{E}_{\parallel,x}^i} = \frac{(k_z^t/k_2)\tilde{E}_\parallel^t}{(k_z^i/k_1)\tilde{E}_\parallel^i} = \tilde{T}_\parallel.$$

Here

$$\tilde{\Gamma}_\parallel = \frac{Z_{2\parallel} - Z_{1\parallel}}{Z_{2\parallel} + Z_{1\parallel}}, \qquad \tilde{T}_\parallel = 1 + \tilde{\Gamma}_\parallel = \frac{2Z_{2\parallel}}{Z_{2\parallel} + Z_{1\parallel}}, \tag{4.284}$$

with

$$Z_{1\parallel} = \frac{k_{1z}\eta_1}{k_1}, \qquad Z_{2\parallel} = \frac{k_{2z}\eta_2}{k_2}.$$

Note that we may also write

$$\tilde{E}^r_\parallel = -\tilde{\Gamma}_\parallel \tilde{E}^i_\parallel, \qquad \tilde{E}^t_\parallel = \tilde{T}_\parallel \tilde{E}^i_\parallel \left(\frac{k^i_z}{k_1}\frac{k_2}{k^t_z}\right).$$

Let us summarize the fields in each region. For perpendicular polarization we have

$$\begin{aligned} \tilde{\mathbf{E}}^i_\perp &= \hat{\mathbf{y}}\tilde{E}^i_\perp e^{-j\mathbf{k}^i\cdot\mathbf{r}}, \\ \tilde{\mathbf{E}}^r_\perp &= \hat{\mathbf{y}}\tilde{\Gamma}_\perp \tilde{E}^i_\perp e^{-j\mathbf{k}^r\cdot\mathbf{r}}, \\ \tilde{\mathbf{E}}^t_\perp &= \hat{\mathbf{y}}\tilde{T}_\perp \tilde{E}^i_\perp e^{-j\mathbf{k}^t\cdot\mathbf{r}}, \end{aligned} \tag{4.285}$$

and

$$\tilde{\mathbf{H}}^i_\perp = \frac{\mathbf{k}^i \times \tilde{\mathbf{E}}^i_\perp}{k_1\eta_1}, \quad \tilde{\mathbf{H}}^r_\perp = \frac{\mathbf{k}^r \times \tilde{\mathbf{E}}^r_\perp}{k_1\eta_1}, \quad \tilde{\mathbf{H}}^t_\perp = \frac{\mathbf{k}^t \times \tilde{\mathbf{E}}^t_\perp}{k_2\eta_2}. \tag{4.286}$$

For parallel polarization we have

$$\begin{aligned} \tilde{\mathbf{E}}^i_\parallel &= -\eta_1 \frac{\mathbf{k}^i \times \tilde{\mathbf{H}}^i_\parallel}{k_1} e^{-j\mathbf{k}^i\cdot\mathbf{r}}, \\ \tilde{\mathbf{E}}^r_\parallel &= -\eta_1 \frac{\mathbf{k}^r \times \tilde{\mathbf{H}}^r_\parallel}{k_1} e^{-j\mathbf{k}^r\cdot\mathbf{r}}, \\ \tilde{\mathbf{E}}^t_\parallel &= -\eta_2 \frac{\mathbf{k}^t \times \tilde{\mathbf{H}}^t_\parallel}{k_2} e^{-j\mathbf{k}^t\cdot\mathbf{r}}, \end{aligned} \tag{4.287}$$

and

$$\begin{aligned} \tilde{\mathbf{H}}^i_\parallel &= \hat{\mathbf{y}} \frac{\tilde{E}^i_\parallel}{\eta_1} e^{-j\mathbf{k}^i\cdot\mathbf{r}}, \\ \tilde{\mathbf{H}}^r_\parallel &= -\hat{\mathbf{y}} \frac{\tilde{\Gamma}_\parallel \tilde{E}^i_\parallel}{\eta_1} e^{-j\mathbf{k}^r\cdot\mathbf{r}}, \\ \tilde{\mathbf{H}}^t_\parallel &= \hat{\mathbf{y}} \frac{\tilde{T}_\parallel \tilde{E}^i_\parallel}{\eta_2} \left(\frac{k^i_z}{k_1}\frac{k_2}{k^t_z}\right) e^{-j\mathbf{k}^t\cdot\mathbf{r}}. \end{aligned} \tag{4.288}$$

The wave vectors are given by

$$\mathbf{k}^i = (\hat{\mathbf{x}}\beta_1 \sin\theta_i + \hat{\mathbf{z}}\tau^i \cos\gamma^i) - j(\hat{\mathbf{x}}\alpha_1 \sin\theta_i + \hat{\mathbf{z}}\tau^i \sin\gamma^i), \tag{4.289}$$

$$\mathbf{k}^r = (\hat{\mathbf{x}}\beta_1 \sin\theta_i - \hat{\mathbf{z}}\tau^i \cos\gamma^i) - j(\hat{\mathbf{x}}\alpha_1 \sin\theta_i - \hat{\mathbf{z}}\tau^i \sin\gamma^i), \tag{4.290}$$

$$\mathbf{k}^t = (\hat{\mathbf{x}}\beta_1 \sin\theta_i + \hat{\mathbf{z}}\tau^t \cos\gamma^t) - j(\hat{\mathbf{x}}\alpha_1 \sin\theta_i + \hat{\mathbf{z}}\tau^t \sin\gamma^t). \tag{4.291}$$

We see that the reflected wave must, like the incident wave, be a uniform plane wave. We define the unsigned *reflection angle* θ_r as the angle between the surface normal and the direction of propagation of the reflected wavefronts (Figure 4.18). Since

$$\mathbf{k}^i \cdot \hat{\mathbf{z}} = k_1 \cos\theta_i = -\mathbf{k}^r \cdot \hat{\mathbf{z}} = k_1 \cos\theta_r$$

and

$$\mathbf{k}^i \cdot \hat{\mathbf{x}} = k_1 \sin\theta_i = \mathbf{k}^r \cdot \hat{\mathbf{x}} = k_1 \sin\theta_r$$

we must have

$$\theta_i = \theta_r.$$

This is known as *Snell's law of reflection.* We can similarly define the *transmission angle* to be the angle between the direction of propagation of the transmitted wavefronts and the interface normal. Noting that $\hat{\mathbf{k}}_2' \cdot \hat{\mathbf{z}} = \cos\theta_t$ and $\hat{\mathbf{k}}_2' \cdot \hat{\mathbf{x}} = \sin\theta_t$, we have from (4.281) and (4.282)

$$\cos\theta_t = \frac{\tau^t \cos\gamma^t}{\sqrt{\beta_1^2 \sin^2\theta_i + (\tau^t)^2 \cos^2\gamma^t}}, \tag{4.292}$$

$$\sin\theta_t = \frac{\beta_1 \sin\theta_i}{\sqrt{\beta_1^2 \sin^2\theta_i + (\tau^t)^2 \cos^2\gamma^t}}, \tag{4.293}$$

and thus

$$\theta_t = \tan^{-1}\left(\frac{\beta_1}{\tau^t}\frac{\sin\theta_i}{\cos\gamma^t}\right). \tag{4.294}$$

Depending on the properties of the media, at a certain incidence angle θ_c, called the *critical angle*, the angle of transmission becomes $\pi/2$. Under this condition $\hat{\mathbf{k}}_2'$ has only an x-component. Thus, surfaces of constant phase propagate parallel to the interface. Later we shall see that for low-loss (or lossless) media, this implies that no time-average power is carried by a monochromatic transmitted wave into the second medium.

We also see that although the transmitted field may be a nonuniform plane wave, its mathematical form is that of the incident plane wave. This allows us to easily generalize the single-interface reflection problem to one involving many layers.

Uniform plane-wave reflection for lossless media. We can specialize the preceding results to the case for which both regions are lossless with $\tilde{\mu} = \mu$ and $\tilde{\epsilon}^c = \epsilon$ real and frequency-independent. By (4.224) we have

$$\beta = \omega\sqrt{\mu\epsilon},$$

while (4.225) gives

$$\alpha = 0.$$

We can easily show that the transmitted wave must be uniform unless the incidence angle exceeds the critical angle. By (4.279) we have

$$A = \beta_2^2 - \beta_1^2 \sin^2\theta_i, \qquad B = 0, \tag{4.295}$$

while (4.280) gives

$$\tau = \left[A^2\right]^{1/4} = \sqrt{|\beta_2^2 - \beta_1^2 \sin^2\theta_i|}$$

and

$$\gamma^t = \frac{1}{2}\tan^{-1}(0).$$

We have several possible choices for γ^t. To choose properly we note that γ^t represents the negative of the phase of the quantity $k_z^t = \sqrt{A}$. If $A > 0$ the phase of the square root is 0. If $A < 0$ the phase of the square root is $-\pi/2$ and thus $\gamma^t = +\pi/2$. Here we choose the plus sign on γ^t to ensure that the transmitted field decays as z increases. We note that if $A = 0$ then $\tau^t = 0$ and from (4.293) we have $\theta_t = \pi/2$. This defines the critical angle, which from (4.295) is

$$\theta_c = \sin^{-1}\left(\frac{\beta_2^2}{\beta_1^2}\right) = \sin^{-1}\left(\frac{\mu_2\epsilon_2}{\mu_1\epsilon_1}\right).$$

Therefore

$$\gamma^t = \begin{cases} 0, & \theta_i < \theta_c, \\ \pi/2, & \theta_i > \theta_c. \end{cases}$$

Using these we can write down the transmitted wave vector from (4.291):

$$\mathbf{k}^t = \mathbf{k}^{t\prime} + j\mathbf{k}^{t\prime\prime} = \begin{cases} \hat{\mathbf{x}}\beta_1 \sin\theta_i + \hat{\mathbf{z}}\sqrt{|A|}, & \theta_i < \theta_c, \\ \hat{\mathbf{x}}\beta_1 \sin\theta_i - j\hat{\mathbf{z}}\sqrt{|A|}, & \theta_i > \theta_c. \end{cases} \tag{4.296}$$

By (4.293) we have

$$\sin\theta_t = \frac{\beta_1 \sin\theta_i}{\sqrt{\beta_1^2 \sin^2\theta_i + \beta_2^2 - \beta_1^2 \sin^2\theta_i}} = \frac{\beta_1 \sin\theta_i}{\beta_2}$$

or

$$\beta_2 \sin\theta_t = \beta_1 \sin\theta_i. \tag{4.297}$$

This is known as *Snell's law of refraction*. With this we can write for $\theta_i < \theta_c$

$$A = \beta_2^2 - \beta_1^2 \sin^2\theta_i = \beta_2^2 \cos^2\theta_t.$$

Using this and substituting $\beta_2 \sin\theta_t$ for $\beta_1 \sin\theta_i$, we may rewrite (4.296) for $\theta_i < \theta_c$ as

$$\mathbf{k}^t = \mathbf{k}^{t\prime} + j\mathbf{k}^{t\prime\prime} = \hat{\mathbf{x}}\beta_2 \sin\theta_t + \hat{\mathbf{z}}\beta_2 \cos\theta_t. \tag{4.298}$$

Hence the transmitted plane wave is uniform with $\mathbf{k}^{t\prime\prime} = 0$. When $\theta_i > \theta_c$ we have from (4.296)

$$\mathbf{k}^{t\prime} = \hat{\mathbf{x}}\beta_1 \sin\theta_i, \qquad \mathbf{k}^{t\prime\prime} = -\hat{\mathbf{z}}\sqrt{\beta_1^2 \sin^2\theta_i - \beta_2^2}.$$

Since $\mathbf{k}^{t\prime}$ and $\mathbf{k}^{t\prime\prime}$ are not collinear, the plane wave is nonuniform. Let us examine the cases $\theta_i < \theta_c$ and $\theta_i > \theta_c$ in greater detail.

Case 1: $\theta_i < \theta_c$. By (4.289)–(4.290) and (4.298) the wave vectors are

$$\begin{aligned} \mathbf{k}^i &= \hat{\mathbf{x}}\beta_1 \sin\theta_i + \hat{\mathbf{z}}\beta_1 \cos\theta_i, \\ \mathbf{k}^r &= \hat{\mathbf{x}}\beta_1 \sin\theta_i - \hat{\mathbf{z}}\beta_1 \cos\theta_i, \\ \mathbf{k}^t &= \hat{\mathbf{x}}\beta_2 \sin\theta_t + \hat{\mathbf{z}}\beta_2 \cos\theta_t, \end{aligned}$$

and the wave impedances are

$$Z_{1\perp} = \frac{\eta_1}{\cos\theta_i}, \qquad Z_{2\perp} = \frac{\eta_2}{\cos\theta_t},$$
$$Z_{1\parallel} = \eta_1 \cos\theta_i, \qquad Z_{2\parallel} = \eta_2 \cos\theta_t.$$

The reflection coefficients are

$$\tilde{\Gamma}_\perp = \frac{\eta_2 \cos\theta_i - \eta_1 \cos\theta_t}{\eta_2 \cos\theta_i + \eta_1 \cos\theta_t}, \qquad \tilde{\Gamma}_\parallel = \frac{\eta_2 \cos\theta_t - \eta_1 \cos\theta_i}{\eta_2 \cos\theta_t + \eta_1 \cos\theta_i}. \tag{4.299}$$

So the reflection coefficients are purely real, with signs dependent on the constitutive parameters of the media. We can write

$$\tilde{\Gamma}_\perp = \rho_\perp e^{j\phi_\perp}, \qquad \tilde{\Gamma}_\parallel = \rho_\parallel e^{j\phi_\parallel},$$

where ρ and ϕ are real, and where $\phi = 0$ or π.

Under certain conditions the reflection coefficients vanish. For a given set of constitutive parameters we may achieve $\tilde{\Gamma} = 0$ at an incidence angle θ_B, known as the *Brewster* or *polarizing angle*. A wave with an arbitrary combination of perpendicular and parallel polarized components incident at this angle produces a reflected field with a single component. A wave incident with only the appropriate single component produces no reflected field, regardless of its amplitude.

For perpendicular polarization we set $\tilde{\Gamma}_\perp = 0$, requiring

$$\eta_2 \cos\theta_i - \eta_1 \cos\theta_t = 0$$

or equivalently

$$\frac{\mu_2}{\epsilon_2}(1 - \sin^2\theta_i) = \frac{\mu_1}{\epsilon_1}(1 - \sin^2\theta_t).$$

By (4.297) we may put

$$\sin^2\theta_t = \frac{\mu_1\epsilon_1}{\mu_2\epsilon_2}\sin^2\theta_i,$$

resulting in

$$\sin^2\theta_i = \frac{\mu_2}{\epsilon_1}\frac{\epsilon_2\mu_1 - \epsilon_1\mu_2}{\mu_1^2 - \mu_2^2}.$$

The value of θ_i that satisfies this equation must be the Brewster angle, and thus

$$\theta_{B\perp} = \sin^{-1}\sqrt{\frac{\mu_2}{\epsilon_1}\frac{\epsilon_2\mu_1 - \epsilon_1\mu_2}{\mu_1^2 - \mu_2^2}}.$$

When $\mu_1 = \mu_2$ there is no solution to this equation, hence the reflection coefficient cannot vanish. When $\epsilon_1 = \epsilon_2$ we have

$$\theta_{B\perp} = \sin^{-1}\sqrt{\frac{\mu_2}{\mu_1 + \mu_2}} = \tan^{-1}\sqrt{\frac{\mu_2}{\mu_1}}.$$

For parallel polarization we set $\tilde{\Gamma}_\parallel = 0$ and have

$$\eta_2 \cos\theta_t = \eta_1 \cos\theta_i.$$

Proceeding as above we find that

$$\theta_{B\parallel} = \sin^{-1}\sqrt{\frac{\epsilon_2}{\mu_1}\frac{\epsilon_1\mu_2 - \epsilon_2\mu_1}{\epsilon_1^2 - \epsilon_2^2}}.$$

This expression has no solution when $\epsilon_1 = \epsilon_2$, and thus the reflection coefficient cannot vanish under this condition. When $\mu_1 = \mu_2$ we have

$$\theta_{B\parallel} = \sin^{-1}\sqrt{\frac{\epsilon_2}{\epsilon_1 + \epsilon_2}} = \tan^{-1}\sqrt{\frac{\epsilon_2}{\epsilon_1}}.$$

We find that when $\theta_i < \theta_c$ the total field in region 1 behaves as a traveling wave along x, but has characteristics of both a standing wave and a traveling wave along z (Problem 4.7). The traveling-wave component is associated with a Poynting power flux, while the standing-wave component is not. This flux is carried across the boundary into region 2 where the transmitted field consists only of a traveling wave. By (4.161) the normal component of time-average Poynting flux is continuous across the boundary, demonstrating that the time-average power carried by the wave into the interface from region 1 passes out through the interface into region 2 (Problem 4.8).

Case 2: $\theta_i < \theta_c$**.** The wave vectors are, from (4.289)–(4.290) and (4.296),

$$\begin{aligned}
\mathbf{k}^i &= \hat{\mathbf{x}}\beta_1 \sin\theta_i + \hat{\mathbf{z}}\beta_1 \cos\theta_i, \\
\mathbf{k}^r &= \hat{\mathbf{x}}\beta_1 \sin\theta_i - \hat{\mathbf{z}}\beta_1 \cos\theta_i, \\
\mathbf{k}^t &= \hat{\mathbf{x}}\beta_1 \sin\theta_i - j\hat{\mathbf{z}}\alpha_c,
\end{aligned}$$

where

$$\alpha_c = \sqrt{\beta_1^2 \sin^2\theta_i - \beta_2^2}$$

is the *critical angle attenuation constant.* The wave impedances are

$$\begin{aligned}
Z_{1\perp} &= \frac{\eta_1}{\cos\theta_i}, \qquad & Z_{2\perp} &= j\frac{\beta_2\eta_2}{\alpha_c}, \\
Z_{1\parallel} &= \eta_1 \cos\theta_i, \qquad & Z_{2\parallel} &= -j\frac{\alpha_c\eta_2}{\beta_2}.
\end{aligned}$$

Substituting these into (4.283) and (4.284), we find that the reflection coefficients are the complex quantities

$$\begin{aligned}
\tilde{\Gamma}_\perp &= \frac{\beta_2\eta_2\cos\theta_i + j\eta_1\alpha_c}{\beta_2\eta_2\cos\theta_i - j\eta_1\alpha_c} = e^{j\phi_\perp}, \\
\tilde{\Gamma}_\parallel &= -\frac{\beta_2\eta_1\cos\theta_i + j\eta_2\alpha_c}{\beta_2\eta_1\cos\theta_i - j\eta_2\alpha_c} = e^{j\phi_\parallel},
\end{aligned}$$

where

$$\phi_\perp = 2\tan^{-1}\left(\frac{\eta_1\alpha_c}{\beta_2\eta_2\cos\theta_i}\right), \qquad \phi_\parallel = \pi + 2\tan^{-1}\left(\frac{\eta_2\alpha_c}{\beta_2\eta_1\cos\theta_i}\right).$$

We note with interest that $\rho_\perp = \rho_\parallel = 1$. So the amplitudes of the reflected waves are identical to those of the incident waves, and we call this the case of *total internal reflection.* The phase of the reflected wave at the interface is changed from that of the incident wave by an amount $\phi_\perp$ or $\phi_\parallel$. The phase shift incurred by the reflected wave upon total internal reflection is called the *Goos–Hänchen shift.*

In the case of total internal reflection the field in region 1 is a pure standing wave while the field in region 2 decays exponentially in the z-direction and is evanescent (Problem 4.9). Since a standing wave transports no power, there is no Poynting flux into region 2. We find that the evanescent wave also carries no power and thus the boundary condition on power flux at the interface is satisfied (Problem 4.10). We note that for any incident angle except $\theta_i = 0$ (normal incidence) the wave in region 1 does transport power in the x-direction.

Reflection of time-domain uniform plane waves. Solution for the fields reflected and transmitted at an interface shows us the properties of the fields for a certain single excitation frequency and allows us to obtain time-domain fields by Fourier inversion. Under certain conditions it is possible to do the inversion analytically, providing physical insight into the temporal behavior of the fields.

As a simple example, consider a perpendicularly-polarized, uniform plane wave incident from free space at an angle θ_i on the planar surface of a conducting material (Figure 4.18). The material is assumed to have frequency-independent constitutive parameters $\tilde{\mu} = \mu_0$, $\tilde{\epsilon} = \epsilon$, and $\tilde{\sigma} = \sigma$. By (4.285) we have the reflected field

$$\tilde{\mathbf{E}}^r_\perp(\mathbf{r}, \omega) = \hat{\mathbf{y}}\tilde{\Gamma}_\perp(\omega)\tilde{E}^i_\perp(\omega)e^{-j\mathbf{k}^r(\omega)\cdot\mathbf{r}} = \hat{\mathbf{y}}\tilde{E}^r(\omega)e^{-j\omega\frac{\hat{\mathbf{k}}^r\cdot\mathbf{r}}{c}} \tag{4.300}$$

where $\tilde{E}^r = \tilde{\Gamma}_\perp\tilde{E}^i_\perp$. We can use the time-shifting theorem (A.3)to invert the transform and obtain

$$\mathbf{E}^r_\perp(\mathbf{r}, t) = \mathcal{F}^{-1}\left\{\tilde{\mathbf{E}}^r_\perp(\mathbf{r}, \omega)\right\} = \hat{\mathbf{y}}E^r\left(t - \frac{\hat{\mathbf{k}}^r\cdot\mathbf{r}}{c}\right) \tag{4.301}$$

where we have by the convolution theorem (12)

$$E^r(t) = \mathcal{F}^{-1}\left\{\tilde{E}^r(\omega)\right\} = \Gamma_\perp(t) * E_\perp(t).$$

Here

$$E_\perp(t) = \mathcal{F}^{-1}\left\{\tilde{E}^i_\perp(\omega)\right\}$$

is the time waveform of the incident plane wave, while

$$\Gamma_\perp(t) = \mathcal{F}^{-1}\left\{\tilde{\Gamma}_\perp(\omega)\right\}$$

is the time-domain reflection coefficient.

By (4.301) the reflected time-domain field propagates along the direction $\hat{\mathbf{k}}^r$ at the speed of light. The time waveform of the field is the convolution of the waveform of the incident field with the time-domain reflection coefficient $\Gamma_\perp(t)$. In the lossless case ($\sigma = 0$), $\Gamma_\perp(t)$ is a δ-function and thus the waveforms of the reflected and incident fields are identical. With the introduction of loss $\Gamma_\perp(t)$ broadens and thus the reflected field waveform becomes a convolution-broadened version of the incident field waveform. To understand the waveform of the reflected field we must compute $\Gamma_\perp(t)$. Note that by choosing the permittivity of region 2 to exceed that of region 1 we preclude total internal reflection.

We can specialize the frequency-domain reflection coefficient (4.283) for our problem by noting that

$$k_{1z} = \beta_1\cos\theta_i, \qquad k_{2z} = \sqrt{k_2^2 - k_{1x}^2} = \omega\sqrt{\mu_0}\sqrt{\epsilon + \frac{\sigma}{j\omega} - \epsilon_0\sin^2\theta_i},$$

and thus

$$Z_{1\perp} = \frac{\eta_0}{\cos\theta_i}, \qquad Z_{2\perp} = \frac{\eta_0}{\sqrt{\epsilon_r + \frac{\sigma}{j\omega\epsilon_0} - \sin^2\theta_i}},$$

where $\epsilon_r = \epsilon/\epsilon_0$ and $\eta_0 = \sqrt{\mu_0/\epsilon_0}$. We thus obtain

$$\tilde{\Gamma}_\perp = \frac{\sqrt{s} - \sqrt{Ds + B}}{\sqrt{s} + \sqrt{Ds + B}} \tag{4.302}$$

where $s = j\omega$ and

$$D = \frac{\epsilon_r - \sin^2\theta_i}{\cos^2\theta_i}, \qquad B = \frac{\sigma}{\epsilon_0 \cos^2\theta_i}.$$

We can put (4.302) into a better form for inversion. We begin by subtracting $\Gamma_{\perp\infty}$, the high-frequency limit of $\tilde{\Gamma}_\perp$. Noting that

$$\lim_{\omega\to\infty} \tilde{\Gamma}_\perp(\omega) = \Gamma_{\perp\infty} = \frac{1-\sqrt{D}}{1+\sqrt{D}},$$

we can form

$$\tilde{\Gamma}^0_\perp(\omega) = \tilde{\Gamma}_\perp(\omega) - \Gamma_{\perp\infty} = \frac{\sqrt{s} - \sqrt{Ds+B}}{\sqrt{s}+\sqrt{Ds+B}} - \frac{1-\sqrt{D}}{1+\sqrt{D}}$$
$$= 2\frac{\sqrt{D}}{1+\sqrt{D}}\left[\frac{\sqrt{s}-\sqrt{s+B/D}}{\sqrt{s}+\sqrt{D}\sqrt{s+D/B}}\right].$$

With a bit of algebra this becomes

$$\tilde{\Gamma}^0_\perp(\omega) = -\frac{2\sqrt{D}}{D-1}\left(\frac{s}{s+\frac{B}{D-1}}\right)\left(1-\sqrt{\frac{s+\frac{B}{D}}{s}}\right) - \frac{2B}{\left(1+\sqrt{D}\right)(D-1)}\left(\frac{1}{s+\frac{B}{D-1}}\right).$$

Now we can apply (C.12), (C.18), and (C.19) to obtain

$$\Gamma^0_\perp(t) = \mathcal{F}^{-1}\left\{\tilde{\Gamma}^0_\perp(\omega)\right\} = f_1(t) + f_2(t) + f_3(t) \tag{4.303}$$

where

$$f_1(t) = -\frac{2B}{(1+\sqrt{D})(D-1)} e^{-\frac{Bt}{D-1}} U(t),$$
$$f_2(t) = -\frac{B^2}{\sqrt{D}(D-1)^2} U(t) \int_0^t e^{-\frac{B(t-x)}{D-1}} I\left(\frac{Bx}{2D}\right) dx,$$
$$f_3(t) = \frac{B}{\sqrt{D}(D-1)} I\left(\frac{Bt}{2D}\right) U(t).$$

Here

$$I(x) = e^{-x}\left[I_0(x) + I_1(x)\right]$$

where $I_0(x)$ and $I_1(x)$ are modified Bessel functions of the first kind. Setting $u = Bx/2D$ we can also write

$$f_2(t) = -\frac{2B\sqrt{D}}{(D-1)^2} U(t) \int_0^{\frac{Bt}{2D}} e^{-\frac{Bt-2Du}{D-1}} I(u)\, du.$$

Polynomial approximations for $I(x)$ may be found in Abramowitz and Stegun [**?**], making the computation of $\Gamma^0_\perp(t)$ straightforward.

The complete time-domain reflection coefficient is

$$\Gamma_\perp(t) = \frac{1-\sqrt{D}}{1+\sqrt{D}}\delta(t) + \Gamma^0_\perp(t).$$

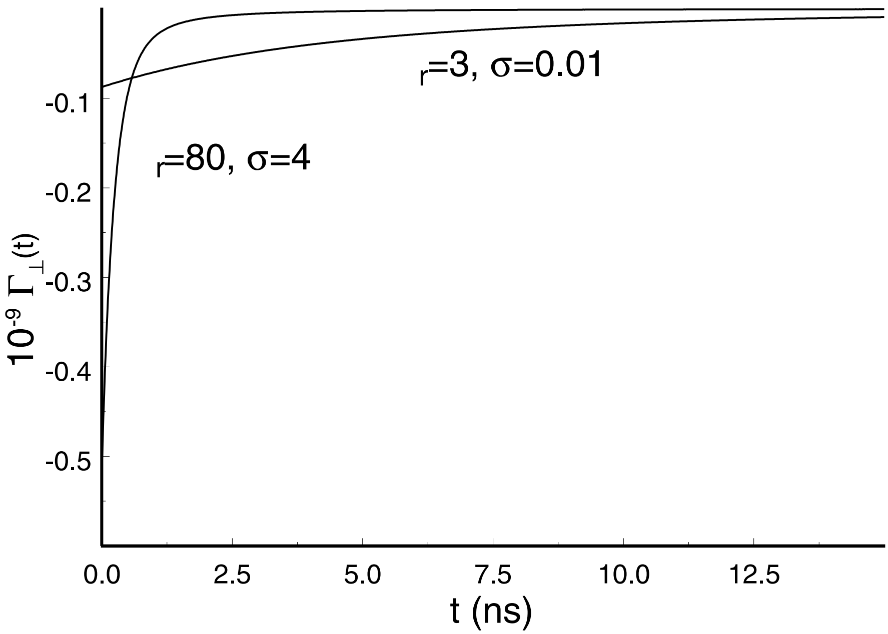

Figure 4.19: Time-domain reflection coefficients.

If $\sigma = 0$ then $\Gamma^0_\perp(t) = 0$ and the reflection coefficient reduces to a single δ-function. Since convolution with this term does not alter wave shape, the reflected field has the same waveform as the incident field.

A plot of $\Gamma^0_\perp(t)$ for normal incidence ($\theta_i = 0^0$) is shown in Figure 4.19. Here two material cases are displayed: $\epsilon_r = 3$, $\sigma = 0.01$ S/m, which is representative of dry water ice, and $\epsilon_r = 80$, $\sigma = 4$ S/m, which is representative of sea water. We see that a pulse waveform experiences more temporal spreading upon reflection from ice than from sea water, but that the amplitude of the dispersive component is less than that for sea water.

Reflection of a nonuniform plane wave from a planar interface. Describing the interaction of a general nonuniform plane wave with a planar interface is problematic because of the non-TEM behavior of the incident wave. We cannot decompose the fields into two mutually orthogonal cases as we did with uniform waves, and thus the analysis is more difficult. However, we found in the last section that when a uniform wave is incident on a planar interface, the transmitted wave, even if nonuniform in nature, takes on the same mathematical form and may be decomposed in the same manner as the incident wave. Thus, we may study the case in which this refracted wave is incident on a successive interface using exactly the same analysis as with a uniform incident wave. This is helpful in the case of multi-layered media, which we shall examine next.

Interaction of a plane wave with multi-layered, planar materials. Consider $N + 1$ regions of space separated by N planar interfaces as shown in Figure 4.20, and assume that a uniform plane wave is incident on the first interface at angle θ_i. Each region is assumed isotropic and homogeneous with a frequency-dependent complex permittivity and permeability. We can easily generalize the previous analysis regarding reflection from a single interface by realizing that in order to satisfy the boundary conditions each

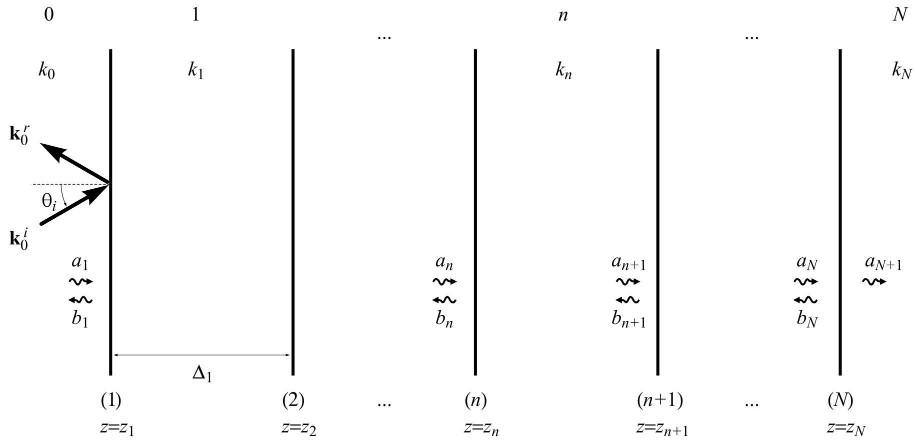

Figure 4.20: Interaction of a uniform plane wave with a multi-layered material.

region, except region N, contains an incident-type wave of the form

$$\tilde{\mathbf{E}}^i(\mathbf{r},\omega) = \tilde{\mathbf{E}}_0^i e^{-j\mathbf{k}^i\cdot\mathbf{r}}$$

and a reflected-type wave of the form

$$\tilde{\mathbf{E}}^r(\mathbf{r},\omega) = \tilde{\mathbf{E}}_0^r e^{-j\mathbf{k}^r\cdot\mathbf{r}}.$$

In region n we may write the wave vectors describing these waves as

$$\mathbf{k}_n^i = \hat{\mathbf{x}}k_{x,n} + \hat{\mathbf{z}}k_{z,n}, \qquad \mathbf{k}_n^r = \hat{\mathbf{x}}k_{x,n} - \hat{\mathbf{z}}k_{z,n},$$

where

$$k_{x,n}^2 + k_{z,n}^2 = k_n^2, \qquad k_n^2 = \omega^2\tilde{\mu}_n\tilde{\epsilon}_n^c = (\beta_n - j\alpha_n)^2.$$

We note at the outset that, as with the single interface case, the boundary conditions are only satisfied when Snell's law of reflection holds, and thus

$$k_{x,n} = k_{x,0} = k_0 \sin\theta_i \tag{4.304}$$

where $k_0 = \omega(\tilde{\mu}_0\tilde{\epsilon}_0^c)^{1/2}$ is the wavenumber of the 0th region (not necessarily free space). From this condition we have

$$k_{z,n} = \sqrt{k_n^2 - k_{x,0}^2} = \tau_n e^{-j\gamma_n}$$

where

$$\tau_n = (A_n^2 + B_n^2)^{1/4}, \qquad \gamma_n = \frac{1}{2}\tan^{-1}\left(\frac{B_n}{A_n}\right),$$

and

$$A_n = \beta_n^2 - \alpha_n^2 - (\beta_0^2 - \alpha_0^2)\sin^2\theta_i, \qquad B_n = 2(\beta_n\alpha_n - \beta_0\alpha_0\sin^2\theta_i).$$

Provided that the incident wave is uniform, we can decompose the fields in every region into cases of perpendicular and parallel polarization. This is true even when the waves in certain layers are nonuniform. For the case of perpendicular polarization we can write the electric field in region n, $0 \le n \le N-1$, as $\tilde{\mathbf{E}}_{\perp n} = \tilde{\mathbf{E}}^i_{\perp n} + \tilde{\mathbf{E}}^r_{\perp n}$ where

$$\tilde{\mathbf{E}}^i_{\perp n} = \hat{\mathbf{y}} a_{n+1} e^{-jk_{x,n}x} e^{-jk_{z,n}(z-z_{n+1})},$$
$$\tilde{\mathbf{E}}^r_{\perp n} = \hat{\mathbf{y}} b_{n+1} e^{-jk_{x,n}x} e^{+jk_{z,n}(z-z_{n+1})},$$

and the magnetic field as $\tilde{\mathbf{H}}_{\perp n} = \tilde{\mathbf{H}}^i_{\perp n} + \mathbf{H}^r_{\perp n}$ where

$$\tilde{\mathbf{H}}^i_{\perp n} = \frac{-\hat{\mathbf{x}}k_{z,n} + \hat{\mathbf{z}}k_{x,n}}{k_n \eta_n} a_{n+1} e^{-jk_{x,n}x} e^{-jk_{z,n}(z-z_{n+1})},$$
$$\tilde{\mathbf{H}}^r_{\perp n} = \frac{+\hat{\mathbf{x}}k_{z,n} + \hat{\mathbf{z}}k_{x,n}}{k_n \eta_n} b_{n+1} e^{-jk_{x,n}x} e^{+jk_{z,n}(z-z_{n+1})}.$$

When $n = N$ there is no reflected wave; in this region we write

$$\tilde{\mathbf{E}}_{\perp N} = \hat{\mathbf{y}} a_{N+1} e^{-jk_{x,N}x} e^{-jk_{z,N}(z-z_N)},$$
$$\tilde{\mathbf{H}}_{\perp N} = \frac{-\hat{\mathbf{x}}k_{z,N} + \hat{\mathbf{z}}k_{x,N}}{k_N \eta_N} a_{N+1} e^{-jk_{x,N}x} e^{-jk_{z,N}(z-z_N)}.$$

Since a_1 is the known amplitude of the incident wave, there are $2N$ unknown wave amplitudes. We obtain the necessary $2N$ simultaneous equations by applying the boundary conditions at each of the interfaces. At interface n located at $z = z_n$, $1 \le n \le N-1$, we have from the continuity of tangential electric field

$$a_n + b_n = a_{n+1} e^{-jk_{z,n}(z_n - z_{n+1})} + b_{n+1} e^{+jk_{z,n}(z_n - z_{n+1})}$$

while from the continuity of magnetic field

$$-a_n \frac{k_{z,n-1}}{k_{n-1}\eta_{n-1}} + b_n \frac{k_{z,n-1}}{k_{n-1}\eta_{n-1}} = -a_{n+1} \frac{k_{z,n}}{k_n \eta_n} e^{-jk_{z,n}(z_n - z_{n+1})} + b_{n+1} \frac{k_{z,n}}{k_n \eta_n} e^{+jk_{z,n}(z_n - z_{n+1})}.$$

Noting that the wave impedance of region n is

$$Z_{\perp n} = \frac{k_n \eta_n}{k_{z,n}}$$

and defining the region n propagation factor as

$$\tilde{P}_n = e^{-jk_{z,n}\Delta_n}$$

where $\Delta_n = z_{n+1} - z_n$, we can write

$$a_n \tilde{P}_n + b_n \tilde{P}_n = a_{n+1} + b_{n+1} \tilde{P}_n^2, \tag{4.305}$$
$$-a_n \tilde{P}_n + b_n \tilde{P}_n = -a_{n+1} \frac{Z_{\perp n-1}}{Z_{\perp n}} + b_{n+1} \frac{Z_{\perp n-1}}{Z_{\perp n}} \tilde{P}_n^2. \tag{4.306}$$

We must still apply the boundary conditions at $z = z_N$. Proceeding as above, we find that (4.305) and (4.306) hold for $n = N$ if we set $b_{N+1} = 0$ and $\tilde{P}_N = 1$.

The $2N$ simultaneous equations (4.305)–(4.306) may be solved using standard matrix methods. However, through a little manipulation we can put the equations into a form easily solved by recursion, providing a very nice physical picture of the multiple reflections that occur within the layered medium. We begin by eliminating b_n by subtracting (4.306) from (4.305):

$$2a_n \tilde{P}_n = a_{n+1} \left[1 + \frac{Z_{\perp n-1}}{Z_{\perp n}}\right] + b_{n+1} \tilde{P}_n^2 \left[1 - \frac{Z_{\perp n-1}}{Z_{\perp n}}\right]. \tag{4.307}$$

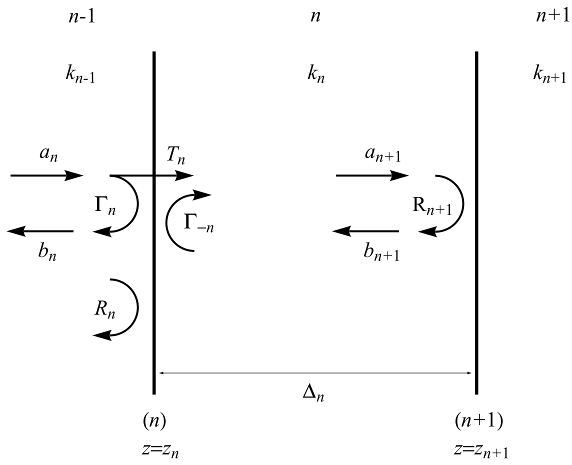

Figure 4.21: Wave flow diagram showing interaction of incident and reflected waves for region n.

Defining

$$\tilde{\Gamma}_n = \frac{Z_{\perp n} - Z_{\perp n-1}}{Z_{\perp n} + Z_{\perp n-1}} \tag{4.308}$$

as the *interfacial reflection coefficient* for interface n (i.e., the reflection coefficient assuming a single interface as in (4.283)), and

$$\tilde{T}_n = \frac{2Z_{\perp n}}{Z_{\perp n} + Z_{\perp n-1}} = 1 + \tilde{\Gamma}_n$$

as the *interfacial transmission coefficient* for interface n, we can write (4.307) as

$$a_{n+1} = a_n \tilde{T}_n \tilde{P}_n + b_{n+1} \tilde{P}_n (-\tilde{\Gamma}_n) \tilde{P}_n.$$

Finally, if we define the *global* reflection coefficient R_n for region n as the ratio of the amplitudes of the reflected and incident waves,

$$\tilde{R}_n = b_n / a_n,$$

we can write

$$a_{n+1} = a_n \tilde{T}_n \tilde{P}_n + a_{n+1} \tilde{R}_{n+1} \tilde{P}_n (-\tilde{\Gamma}_n) \tilde{P}_n. \tag{4.309}$$

For $n = N$ we merely set $R_{N+1} = 0$ to find

$$a_{N+1} = a_N \tilde{T}_N \tilde{P}_N. \tag{4.310}$$

If we choose to eliminate a_{n+1} from (4.305) and (4.306) we find that

$$b_n = a_n \tilde{\Gamma}_n + \tilde{R}_{n+1} \tilde{P}_n (1 - \tilde{\Gamma}_n) a_{n+1}. \tag{4.311}$$

For $n = N$ this reduces to

$$b_N = a_N \tilde{\Gamma}_N. \tag{4.312}$$

Equations (4.309) and (4.311) have nice physical interpretations. Consider Figure 4.21, which shows the wave amplitudes for region n. We may think of the wave incident on interface $n+1$ with amplitude a_{n+1} as consisting of two terms. The first term is the wave transmitted through interface n (at $z = z_n$). This wave must propagate through a distance Δ_n to reach interface $n+1$ and thus has an amplitude $a_n \tilde{T}_n \tilde{P}_n$. The second term is the reflection at interface n of the wave traveling in the $-z$ direction within region n. The amplitude of the wave before reflection is merely $b_{n+1}\tilde{P}_n$, where the term $\tilde{P}_n$ results from the propagation of the negatively-traveling wave from interface $n+1$ to interface n. Now, since the interfacial reflection coefficient at interface n for a wave incident from region n is the negative of that for a wave incident from region $n-1$ (since the wave is traveling in the reverse direction), and since the reflected wave must travel through a distance Δ_n from interface n back to interface $n+1$, the amplitude of the second term is $b_{n+1}\tilde{P}_n(-\Gamma_n)\tilde{P}_n$. Finally, remembering that $b_{n+1} = \tilde{R}_{n+1}a_{n+1}$, we can write

$$a_{n+1} = a_n \tilde{T}_n \tilde{P}_n + a_{n+1}\tilde{R}_{n+1}\tilde{P}_n(-\tilde{\Gamma}_n)\tilde{P}_n.$$

This equation is exactly the same as (4.309) which was found using the boundary conditions. By similar reasoning, we may say that the wave traveling in the $-z$ direction in region $n-1$ consists of a term reflected from the interface and a term transmitted through the interface. The amplitude of the reflected term is merely $a_n\tilde{\Gamma}_n$. The amplitude of the transmitted term is found by considering $b_{n+1} = \tilde{R}_{n+1}a_{n+1}$ propagated through a distance Δ_n and then transmitted backwards through interface n. Since the transmission coefficient for a wave going from region n to region $n-1$ is $1 + (-\tilde{\Gamma}_n)$, the amplitude of the transmitted term is $\tilde{R}_{n+1}\tilde{P}_n(1-\tilde{\Gamma}_n)a_{n+1}$. Thus we have

$$b_n = \tilde{\Gamma}_n a_n + \tilde{R}_{n+1}\tilde{P}_n(1-\tilde{\Gamma}_n)a_{n+1},$$

which is identical to (4.311).

We are still left with the task of solving for the various field amplitudes. This can be done using a simple recursive technique. Using $\tilde{T}_n = 1 + \tilde{\Gamma}_n$ we find from (4.309) that

$$a_{n+1} = \frac{(1+\tilde{\Gamma}_n)\tilde{P}_n}{1+\tilde{\Gamma}_n\tilde{R}_{n+1}\tilde{P}_n^2}a_n. \tag{4.313}$$

Substituting this into (4.311) we find

$$b_n = \frac{\tilde{\Gamma}_n + \tilde{R}_{n+1}\tilde{P}_n^2}{1+\tilde{\Gamma}_n\tilde{R}_{n+1}\tilde{P}_n^2}a_n. \tag{4.314}$$

Using this expression we find a recursive relationship for the global reflection coefficient:

$$\tilde{R}_n = \frac{b_n}{a_n} = \frac{\tilde{\Gamma}_n + \tilde{R}_{n+1}\tilde{P}_n^2}{1+\tilde{\Gamma}_n\tilde{R}_{n+1}\tilde{P}_n^2}. \tag{4.315}$$

The procedure is now as follows. The global reflection coefficient for interface N is, from (4.312),

$$\tilde{R}_N = b_N/a_N = \tilde{\Gamma}_N. \tag{4.316}$$

This is also obtained from (4.315) with $\tilde{R}_{N+1} = 0$. We next use (4.315) to find $\tilde{R}_{N-1}$:

$$\tilde{R}_{N-1} = \frac{\tilde{\Gamma}_{N-1} + \tilde{R}_N\tilde{P}_{N-1}^2}{1+\tilde{\Gamma}_{N-1}\tilde{R}_N\tilde{P}_{N-1}^2}.$$

This process is repeated until reaching $\tilde{R}_1$, whereupon all of the global reflection coefficients are known. We then find the amplitudes beginning with a_1, which is the known incident field amplitude. From (4.315) we find $b_1 = a_1\tilde{R}_1$, and from (4.313) we find

$$a_2 = \frac{(1+\tilde{\Gamma}_1)\tilde{P}_1}{1+\tilde{\Gamma}_1\tilde{R}_2\tilde{P}_1^2}a_1.$$

This process is repeated until all field amplitudes are known.

We note that the process outlined above holds equally well for parallel polarization as long as we use the parallel wave impedances

$$Z_{\parallel n} = \frac{k_{z,n}\eta_n}{k_n}$$

when computing the interfacial reflection coefficients. See Problem **??**.

As a simple example, consider a slab of material of thickness Δ sandwiched between two lossless dielectrics. A time-harmonic uniform plane wave of frequency $\omega = \check{\omega}$ is normally incident onto interface 1, and we wish to compute the amplitude of the wave reflected by interface 1 and determine the conditions under which the reflected wave vanishes. In this case we have $N = 2$, with two interfaces and three regions. By (4.316) we have $R_2 = \Gamma_2$, where $R_2 = \tilde{R}_2(\check{\omega})$, $\Gamma_2 = \tilde{\Gamma}_2(\check{\omega})$, etc. Then by (4.315) we find

$$R_1 = \frac{\Gamma_1 + R_2P_1^2}{1+\Gamma_1R_2P_1^2} = \frac{\Gamma_1+\Gamma_2P_1^2}{1+\Gamma_1\Gamma_2P_1^2}.$$

Hence the reflected wave vanishes when

$$\Gamma_1 + \Gamma_2P_1^2 = 0.$$

Since the field in region 0 is normally incident we have

$$k_{z,n} = k_n = \beta_n = \check{\omega}\sqrt{\mu_n\epsilon_n}.$$

If we choose $P_1^2 = -1$, then $\Gamma_1 = \Gamma_2$ results in no reflected wave. This requires

$$\frac{Z_1 - Z_0}{Z_1+Z_0} = \frac{Z_2-Z_1}{Z_2+Z_1}.$$

Clearing the denominator we find that $2Z_1^2 = 2Z_0Z_2$ or

$$Z_1 = \sqrt{Z_0Z_2}.$$

This condition makes the reflected field vanish if we can ensure that $P_1^2 = -1$. To do this we need

$$e^{-j\beta_1 2\Delta} = -1.$$

The minimum thickness that satisfies this condition is $\beta_1 2\Delta = \pi$. Since $\beta = 2\pi/\lambda$, this is equivalent to

$$\Delta = \lambda/4.$$

A layer of this type is called a *quarter-wave transformer*. Since no wave is reflected from the initial interface, and since all the regions are assumed lossless, all of the power carried by the incident wave in the first region is transferred into the third region. Thus, two regions of differing materials may be "matched" by inserting an appropriate slab between

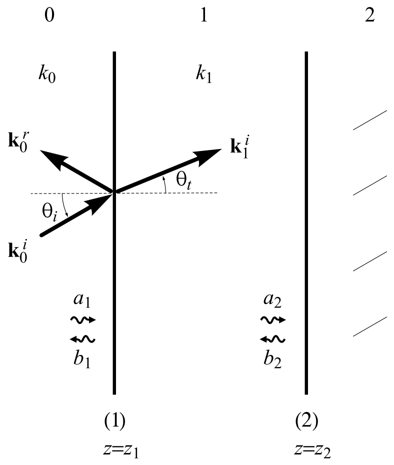

Figure 4.22: Interaction of a uniform plane wave with a conductor-backed dielectric slab.

them. This technique finds use in optical coatings for lenses and for reducing the radar reflectivity of objects.

As a second example, consider a lossless dielectric slab with $\tilde{\epsilon} = \epsilon_1 = \epsilon_{1r}\epsilon_0$, and $\tilde{\mu} = \mu_0$, backed by a perfect conductor and immersed in free space as shown in Figure 4.22. A perpendicularly polarized uniform plane wave is incident on the slab from free space and we wish to find the temporal response of the reflected wave by first calculating the frequency-domain reflected field. Since $\epsilon_0 < \epsilon_1$, total internal reflection cannot occur. Thus the wave vectors in region 1 have real components and can be written as

$$\mathbf{k}_1^i = k_{x,1}\hat{\mathbf{x}} + k_{z,1}\hat{\mathbf{z}}, \qquad \mathbf{k}_1^r = k_{x,1}\hat{\mathbf{x}} - k_{z,1}\hat{\mathbf{z}}.$$

From Snell's law of refraction we know that

$$k_{x,1} = k_0 \sin\theta_i = k_1 \sin\theta_t$$

and so

$$k_{z,1} = \sqrt{k_1^2 - k_{x,1}^2} = \frac{\omega}{c}\sqrt{\epsilon_{1r} - \sin^2\theta_i} = k_1\cos\theta_t$$

where θ_t is the transmission angle in region 1. Since region 2 is a perfect conductor we have $\tilde{R}_2 = -1$. By (4.315) we have

$$\tilde{R}_1(\omega) = \frac{\Gamma_1 - \tilde{P}_1^2(\omega)}{1 - \Gamma_1\tilde{P}_1^2(\omega)}, \tag{4.317}$$

where from (4.308)

$$\Gamma_1 = \frac{Z_1 - Z_0}{Z_1 + Z_0}$$

is not a function of frequency. By the approach we used to obtain (4.300) we write

$$\tilde{\mathbf{E}}_\perp^r(\mathbf{r},\omega) = \hat{\mathbf{y}}\tilde{R}_1(\omega)\tilde{E}_\perp^i(\omega)e^{-j\mathbf{k}_1^r(\omega)\cdot\mathbf{r}}.$$

So

$$\mathbf{E}_\perp^r(\mathbf{r},t) = \hat{\mathbf{y}}E^r\left(t - \frac{\hat{\mathbf{k}}_1^r\cdot\mathbf{r}}{c}\right)$$

where by the convolution theorem

$$E^r(t) = R_1(t) * E_\perp^i(t). \tag{4.318}$$

Here

$$E_\perp^i(t) = \mathcal{F}^{-1}\left\{\tilde{E}_\perp^i(\omega)\right\}$$

is the time waveform of the incident plane wave, while

$$R_1(t) = \mathcal{F}^{-1}\left\{\tilde{R}_1(\omega)\right\}$$

is the global time-domain reflection coefficient.

To invert $\tilde{R}_1(\omega)$, we use the binomial expansion $(1-x)^{-1} = 1 + x + x^2 + x^3 + \cdots$ on the denominator of (4.317), giving

$$\begin{aligned}\tilde{R}_1(\omega) &= [\Gamma_1 - \tilde{P}_1^2(\omega)]\left\{1 + [\Gamma_1\tilde{P}_1^2(\omega)] + [\Gamma_1\tilde{P}_1^2(\omega)]^2 + [\Gamma_1\tilde{P}_1^2(\omega)]^3 + \ldots\right\} \\ &= \Gamma_1 - [1-\Gamma_1^2]\tilde{P}_1^2(\omega) - [1-\Gamma_1^2]\Gamma_1\tilde{P}_1^4(\omega) - [1-\Gamma_1^2]\Gamma_1^2\tilde{P}_1^6(\omega) - \cdots. \end{aligned} \tag{4.319}$$

Thus we need the inverse transform of

$$\tilde{P}_1^{2n}(\omega) = e^{-j2nk_{z,1}\Delta_1} = e^{-j2nk_1\Delta_1\cos\theta_t}.$$

Writing $k_1 = \omega/v_1$, where $v_1 = 1/(\mu_0\epsilon_1)^{1/2}$ is the phase velocity of the wave in region 1, and using $1 \leftrightarrow \delta(t)$ along with the time-shifting theorem (A.3) we have

$$\tilde{P}_1^{2n}(\omega) = e^{-j\omega 2n\tau} \leftrightarrow \delta(t - 2n\tau)$$

where $\tau = \Delta_1\cos\theta_t/v_1$. With this the inverse transform of $\tilde{R}_1$ in (4.319) is

$$R_1(t) = \Gamma_1\delta(t) - (1+\Gamma_1)(1-\Gamma_1)\delta(t-2\tau) - (1+\Gamma_1)(1-\Gamma_1)\Gamma_1\delta(t-4\tau) - \cdots$$

and thus from (4.318)

$$E^r(t) = \Gamma_1 E_\perp^i(t) - (1+\Gamma_1)(1-\Gamma_1)E_\perp^i(t-2\tau) - (1+\Gamma_1)(1-\Gamma_1)\Gamma_1 E_\perp^i(t-4\tau) - \cdots.$$

The reflected field consists of time-shifted and amplitude-scaled versions of the incident field waveform. These terms can be interpreted as multiple reflections of the incident wave. Consider Figure 4.23. The first term is the direct reflection from interface 1 and thus has its amplitude multiplied by Γ_1. The next term represents a wave that penetrates the interface (and thus has its amplitude multiplied by the transmission coefficient $1+\Gamma_1$), propagates to and reflects from the conductor (and thus has its amplitude multiplied by -1), and then propagates back to the interface and passes through in the opposite direction (and thus has its amplitude multiplied by the transmission coefficient for passage from region 1 to region 0, $1-\Gamma_1$). The time delay between this wave and the initially-reflected wave is given by 2τ, as discussed in detail below. The third term represents a wave that penetrates the interface, reflects from the conductor, returns to and reflects from the interface a second time, again reflects from the conductor, and then passes through the interface in the opposite direction. Its amplitude has an additional multiplicative factor of $-\Gamma_1$ to account for reflection from the interface and an additional factor of -1 to account for the second reflection from the conductor, and is time-delayed by an additional 2τ. Subsequent terms account for additional reflections;

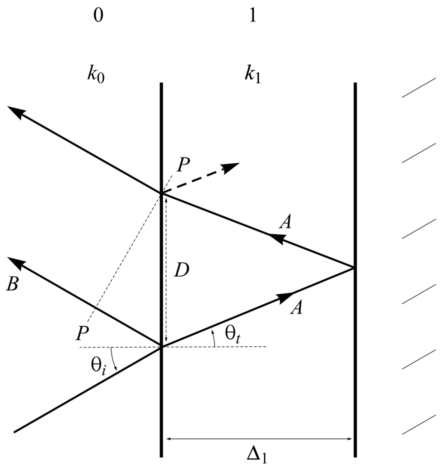

Figure 4.23: Timing diagram for multiple reflections from a conductor-backed dielectric slab.

the nth reflected wave amplitude is multiplied by an additional $(-1)^n$ and $(-\Gamma_1)^n$ and is time-delayed by an additional $2n\tau$.

It is important to understand that the time delay 2τ is *not* just the propagation time for the wave to travel through the slab. To properly describe the timing between the initially-reflected wave and the waves that reflect from the conductor we must consider the field over identical observation planes as shown in Figure 4.23. For example, consider the observation plane designated P-P intersecting the first "exit point" on interface 1. To arrive at this plane the initially-reflected wave takes the path labeled B, arriving at a time

$$\frac{D\sin\theta_i}{v_0}$$

after the time of initial reflection, where $v_0 = c$ is the velocity in region 0. To arrive at this same plane the wave that penetrates the surface takes the path labeled A, arriving at a time

$$\frac{2\Delta_1}{v_1\cos\theta_t}$$

where v_1 is the wave velocity in region 1 and θ_t is the transmission angle. Noting that $D = 2\Delta_1\tan\theta_t$, the time delay between the arrival of the two waves at the plane P-P is

$$T = \frac{2\Delta_1}{v_1\cos\theta_t} - \frac{D\sin\theta_i}{v_0} = \frac{2\Delta_1}{v_1\cos\theta_t}\left[1 - \frac{\sin\theta_t\sin\theta_i}{v_0/v_1}\right].$$

By Snell's law of refraction (4.297) we can write

$$\frac{v_0}{v_1} = \frac{\sin\theta_i}{\sin\theta_t},$$

which, upon substitution, gives

$$T = 2\frac{\Delta_1\cos\theta_t}{v_1}.$$

This is exactly the time delay 2τ.

4.11.6 Plane-wave propagation in an anisotropic ferrite medium

Several interesting properties of plane waves, such as Faraday rotation and the existence of stopbands, appear only when the waves propagate through anisotropic media. We shall study the behavior of waves propagating in a magnetized ferrite medium, and note that this behavior is shared by waves propagating in a magnetized plasma, because of the similarity in the dyadic constitutive parameters of the two media.

Consider a uniform ferrite material having scalar permittivity $\tilde{\epsilon} = \epsilon$ and dyadic permeability $\tilde{\bar{\boldsymbol{\mu}}}$. We assume that the ferrite is lossless and magnetized along the z-direction. By (4.115)– (4.117) the permeability of the medium is

$$[\tilde{\bar{\boldsymbol{\mu}}}(\omega)] = \begin{bmatrix} \mu_1 & j\mu_2 & 0 \\ -j\mu_2 & \mu_1 & 0 \\ 0 & 0 & \mu_0 \end{bmatrix}$$

where

$$\mu_1 = \mu_0 \left[1 + \frac{\omega_M \omega_0}{\omega_0^2 - \omega^2} \right], \qquad \mu_2 = \mu_0 \frac{\omega \omega_M}{\omega_0^2 - \omega^2}.$$

The source-free frequency-domain wave equation can be found using (4.201) with $\tilde{\bar{\boldsymbol{\zeta}}} = \tilde{\bar{\boldsymbol{\xi}}} = 0$ and $\tilde{\bar{\boldsymbol{\epsilon}}} = \epsilon \bar{\mathbf{I}}$:

$$\left[\bar{\nabla} \cdot \left(\bar{\mathbf{I}} \frac{1}{\epsilon} \right) \cdot \bar{\nabla} - \omega^2 \tilde{\bar{\boldsymbol{\mu}}} \right] \cdot \tilde{\mathbf{H}} = 0$$

or, since $\bar{\nabla} \cdot \mathbf{A} = \nabla \times \mathbf{A}$,

$$\frac{1}{\epsilon} \nabla \times \left(\nabla \times \tilde{\mathbf{H}} \right) - \omega^2 \tilde{\bar{\boldsymbol{\mu}}} \cdot \tilde{\mathbf{H}} = 0. \tag{4.320}$$

The simplest solutions to the wave equation for this anisotropic medium are TEM plane waves that propagate along the applied dc magnetic field. We thus seek solutions of the form

$$\tilde{\mathbf{H}}(\mathbf{r}, \omega) = \tilde{\mathbf{H}}_0(\omega) e^{-j\mathbf{k}\cdot\mathbf{r}} \tag{4.321}$$

where $\mathbf{k} = \hat{\mathbf{z}}\beta$ and $\hat{\mathbf{z}} \cdot \tilde{\mathbf{H}}_0 = 0$. We can find β by enforcing (4.320). From (B.7) we find that

$$\nabla \times \tilde{\mathbf{H}} = -j\beta \hat{\mathbf{z}} \times \tilde{\mathbf{H}}_0 e^{-j\beta z}.$$

By Ampere's law we have

$$\tilde{\mathbf{E}} = \frac{\nabla \times \tilde{\mathbf{H}}}{j\omega\epsilon} = -Z_{TEM} \hat{\mathbf{z}} \times \tilde{\mathbf{H}}, \tag{4.322}$$

where

$$Z_{TEM} = \beta / \omega\epsilon$$

is the wave impedance. Note that the wave is indeed TEM. The second curl is found to be

$$\nabla \times \left(\nabla \times \tilde{\mathbf{H}} \right) = -j\beta \nabla \times \left[\hat{\mathbf{z}} \times \tilde{\mathbf{H}}_0 e^{-j\beta z} \right].$$

After an application of (B.43) this becomes

$$\nabla \times \left(\nabla \times \tilde{\mathbf{H}} \right) = -j\beta \left[e^{-j\beta z} \nabla \times (\hat{\mathbf{z}} \times \tilde{\mathbf{H}}_0) - (\hat{\mathbf{z}} \times \tilde{\mathbf{H}}_0) \times \nabla e^{-j\beta z} \right].$$

The first term on the right-hand side is zero, and thus using (B.76) we have

$$\nabla \times \left(\nabla \times \tilde{\mathbf{H}}\right) = \left[-j\beta e^{-j\beta z}\hat{\mathbf{z}} \times (\hat{\mathbf{z}} \times \tilde{\mathbf{H}}_0)\right](-j\beta)$$

or, using (B.7),

$$\nabla \times \left(\nabla \times \tilde{\mathbf{H}}\right) = \beta^2 e^{-j\beta z}\tilde{\mathbf{H}}_0$$

since $\hat{\mathbf{z}} \cdot \tilde{\mathbf{H}}_0 = 0$. With this (4.320) becomes

$$\beta^2\tilde{\mathbf{H}}_0 = \omega^2\epsilon\tilde{\bar{\boldsymbol{\mu}}} \cdot \tilde{\mathbf{H}}_0. \tag{4.323}$$

We can solve (4.323) for β by writing the vector equation in component form:

$$\beta^2 H_{0x} = \omega^2\epsilon\left[\mu_1 H_{0x} + j\mu_2 H_{0y}\right],$$
$$\beta^2 H_{0y} = \omega^2\epsilon\left[-j\mu_2 H_{0x} + \mu_1 H_{0y}\right].$$

In matrix form these are

$$\begin{bmatrix} \beta^2 - \omega^2\epsilon\mu_1 & -j\omega^2\epsilon\mu_2 \\ j\omega^2\epsilon\mu_2 & \beta^2 - \omega^2\epsilon\mu_1 \end{bmatrix}\begin{bmatrix} H_{0x} \\ H_{0y} \end{bmatrix} = \begin{bmatrix} 0 \\ 0 \end{bmatrix}, \tag{4.324}$$

and nontrivial solutions occur only if

$$\begin{vmatrix} \beta^2 - \omega^2\epsilon\mu_1 & -j\omega^2\epsilon\mu_2 \\ j\omega^2\epsilon\mu_2 & \beta^2 - \omega^2\epsilon\mu_1 \end{vmatrix} = 0.$$

Expansion yields the two solutions

$$\beta_\pm = \omega\sqrt{\epsilon\mu_\pm} \tag{4.325}$$

where

$$\mu_\pm = \mu_1 \pm \mu_2 = \mu_0\left[1 + \frac{\omega_M}{\omega_0 \mp \omega}\right]. \tag{4.326}$$

So the propagation properties of the plane wave are the same as those in a medium with an equivalent scalar permeability given by $\mu_\pm$.

Associated with each of these solutions is a relationship between H_{0x} and H_{0y} that can be found from (4.324). Substituting β_+ into the first equation we have

$$\omega^2\epsilon\mu_2 H_{0x} - j\omega^2\epsilon\mu_2 H_{0y} = 0$$

or $H_{0x} = jH_{0y}$. Similarly, substitution of β_- produces $H_{0x} = -jH_{0y}$. Thus, by (4.321) the magnetic field may be expressed as

$$\tilde{\mathbf{H}}(\mathbf{r}, \omega) = H_{0y}[\pm j\hat{\mathbf{x}} + \hat{\mathbf{y}}]e^{-j\beta_\pm z}.$$

By (4.322) we also have the electric field

$$\tilde{\mathbf{E}}(\mathbf{r}, \omega) = Z_{TEM} H_{0y}[\hat{\mathbf{x}} + e^{\mp j\frac{\pi}{2}}\hat{\mathbf{y}}]e^{-j\beta_\pm z}.$$

This field has the form of (4.248). For β_+ we have $\phi_y - \phi_x = -\pi/2$ and thus the wave exhibits RHCP. For β_- we have $\phi_y - \phi_x = \pi/2$ and the wave exhibits LHCP.

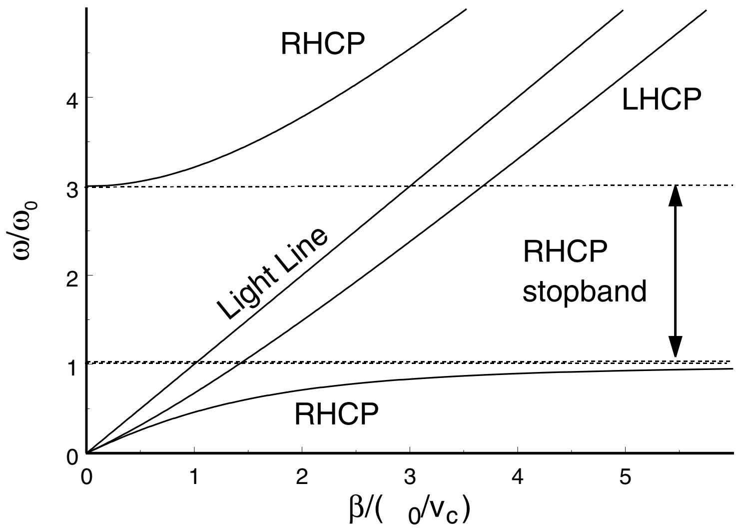

Figure 4.24: Dispersion plot for unmagnetized ferrite with $\omega_M = 2\omega_0$. Light line shows $\omega/\beta = v_c = 1/(\mu_0\epsilon)^{1/2}$.

The dispersion diagram for each polarization case is shown in Figure 4.24, where we have arbitrarily chosen $\omega_M = 2\omega_0$. Here we have combined (4.325) and (4.326) to produce the normalized expression

$$\frac{\beta_\pm}{\omega_0/v_c} = \frac{\omega}{\omega_0}\sqrt{1 + \frac{\omega_M/\omega_0}{1 \mp \omega/\omega_0}}$$

where $v_c = 1/(\mu_0\epsilon)^{1/2}$. Except at low frequencies, an LHCP plane wave passes through the ferrite as if the permeability is close to that of free space. Over all frequencies we have $v_p < v_c$ and $v_g < v_c$. In contrast, an RHCP wave excites the electrons in the ferrite and a resonance occurs at $\omega = \omega_0$. For all frequencies below ω_0 we have $v_p < v_c$ and $v_g < v_c$ and both v_p and v_g reduce to zero as $\omega \to \omega_0$. Because the ferrite is lossless, frequencies between $\omega = \omega_0$ and $\omega = \omega_0 + \omega_M$ result in β being purely imaginary and thus the wave being evanescent. We thus call the frequency range $\omega_0 < \omega < \omega_0 + \omega_M$ a *stopband*; within this band the plane wave cannot transport energy. For frequencies above $\omega_0 + \omega_M$ the RHCP wave propagates as if it is in a medium with permeability less than that of free space. Here we have $v_p > v_c$ and $v_g < v_c$, with $v_p \to v_c$ and $v_g \to v_c$ as $\omega \to \infty$.

Faraday rotation. The solutions to the wave equation found above do not allow the existence of linearly polarized plane waves. However, by superposing LHCP and RHCP waves we can obtain a wave with the appearance of linear polarization. That is, over any z-plane the electric field vector may be written as $\tilde{\mathbf{E}} = K(E_{x0}\hat{\mathbf{x}} + E_{y0}\hat{\mathbf{y}})$ where E_{x0} and E_{y0} are real (although K may be complex). To see this let us examine

$$\tilde{\mathbf{E}} = \tilde{\mathbf{E}}^+ + \tilde{\mathbf{E}}^- = \frac{E_0}{2}[\hat{\mathbf{x}} - j\hat{\mathbf{y}}]e^{-j\beta_+ z} + \frac{E_0}{2}[\hat{\mathbf{x}} + j\hat{\mathbf{y}}]e^{-j\beta_- z}$$

$$= \frac{E_0}{2}\left[\hat{\mathbf{x}}\left(e^{-j\beta_+ z} + e^{-j\beta_- z}\right) + j\hat{\mathbf{y}}\left(-e^{-j\beta_+ z} + e^{-j\beta_- z}\right)\right]$$
$$= E_0 e^{-j\frac{1}{2}(\beta_+ + \beta_-)z}\left[\hat{\mathbf{x}}\cos\frac{1}{2}(\beta_+ - \beta_-)z + \hat{\mathbf{y}}\sin\frac{1}{2}(\beta_+ - \beta_-)z\right]$$

or

$$\tilde{\mathbf{E}} = E_0 e^{-j\frac{1}{2}(\beta_+ + \beta_-)z}\left[\hat{\mathbf{x}}\cos\theta(z) + \hat{\mathbf{y}}\sin\theta(z)\right]$$

where $\theta(z) = (\beta_+ - \beta_-)z/2$. Because $\beta_+ \neq \beta_-$, the velocities of the two circularly polarized waves differ and the waves superpose to form a linearly polarized wave with a polarization that depends on the observation plane z-value. We may think of the wave as undergoing a phase shift of $(\beta_+ + \beta_-)z/2$ radians as it propagates, while the direction of $\tilde{\mathbf{E}}$ rotates to an angle $\theta(z) = (\beta_+ - \beta_-)z/2$ as the wave propagates. *Faraday rotation* can only occur at frequencies where both the LHCP and RHCP waves propagate, and therefore not within the stopband $\omega_0 < \omega < \omega_0 + \omega_M$.

Faraday rotation is non-reciprocal. That is, if a wave that has undergone a rotation of θ_0 radians by propagating through a distance z_0 is made to propagate an equal distance back in the direction from whence it came, the polarization does not return to its initial state but rather incurs an additional rotation of θ_0. Thus, the polarization angle of the wave when it returns to the starting point is not zero, but $2\theta_0$. This effect is employed in a number of microwave devices including gyrators, isolators, and circulators. The interested reader should see Collin [40], Elliott [67], or Liao [111] for details. We note that for $\omega \gg \omega_M$ we can approximate the rotation angle as

$$\theta(z) = (\beta_+ - \beta_-)z/2 = \frac{1}{2}\omega z\sqrt{\epsilon\mu_0}\left[\sqrt{1 + \frac{\omega_M}{\omega_0 - \omega}} - \sqrt{1 + \frac{\omega_M}{\omega_0 + \omega}}\right] \approx -\frac{1}{2}z\omega_M\sqrt{\epsilon\mu_0},$$

which is independent of frequency. So it is possible to construct Faraday rotation-based ferrite devices that maintain their properties over wide bandwidths.

It is straightforward to extend the above analysis to the case of a lossy ferrite. We find that for typical ferrites the attenuation constant associated with μ_- is small for all frequencies, but the attenuation constant associated with μ_+ is large near the resonant frequency ($\omega \approx \omega_0$) [40]. See Problem 4.16.

4.11.7 Propagation of cylindrical waves

By studying plane waves we have gained insight into the basic behavior of frequency-domain and time-harmonic waves. However, these solutions do not display the fundamental property that waves in space must diverge from their sources. To understand this behavior we shall treat waves having cylindrical and spherical symmetries.

Uniform cylindrical waves. In § 2.10.7 we studied the temporal behavior of cylindrical waves in a homogeneous, lossless medium and found that they diverge from a line source located along the z-axis. Here we shall extend the analysis to lossy media and investigate the behavior of the waves in the frequency domain.

Consider a homogeneous region of space described by the permittivity $\tilde{\epsilon}(\omega)$, permeability $\tilde{\mu}(\omega)$, and conductivity $\tilde{\sigma}(\omega)$. We seek solutions that are invariant over a cylindrical surface: $\tilde{\mathbf{E}}(\mathbf{r},\omega) = \tilde{\mathbf{E}}(\rho,\omega)$, $\tilde{\mathbf{H}}(\mathbf{r},\omega) = \tilde{\mathbf{H}}(\rho,\omega)$. Such waves are called *uniform cylindrical waves*. Since the fields are z-independent we may decompose them into TE and TM sets as described in § 4.11.2. For TM polarization we may insert (4.211) into (4.212) to find

$$\tilde{H}_\phi(\rho,\omega) = \frac{1}{j\omega\tilde{\mu}(\omega)}\frac{\partial\tilde{E}_z(\rho,\omega)}{\partial\rho}. \quad (4.327)$$

For TE polarization we have from (4.213)

$$\tilde{E}_\phi(\rho,\omega) = -\frac{1}{j\omega\tilde{\epsilon}^c(\omega)}\frac{\partial \tilde{H}_z(\rho,\omega)}{\partial\rho} \tag{4.328}$$

where $\tilde{\epsilon}^c = \tilde{\epsilon} + \tilde{\sigma}/j\omega$ is the complex permittivity introduced in § 4.4.1. Since $\tilde{\mathbf{E}} = \hat{\boldsymbol{\phi}}\tilde{E}_\phi + \hat{\mathbf{z}}\tilde{E}_z$ and $\tilde{\mathbf{H}} = \hat{\boldsymbol{\phi}}\tilde{H}_\phi + \hat{\mathbf{z}}\tilde{H}_z$, we can always decompose a cylindrical electromagnetic wave into cases of electric and magnetic polarization. In each case the resulting field is TEM_ρ since $\tilde{\mathbf{E}}$, $\tilde{\mathbf{H}}$, and $\hat{\boldsymbol{\rho}}$ are mutually orthogonal.

Wave equations for $\tilde{E}_z$ in the electric polarization case and for $\tilde{H}_z$ in the magnetic polarization case can be derived by substituting (4.210) into (4.208):

$$\left(\frac{\partial^2}{\partial\rho^2} + \frac{1}{\rho}\frac{\partial}{\partial\rho} + k^2\right)\left\{\begin{array}{c}\tilde{E}_z\\ \tilde{H}_z\end{array}\right\} = 0.$$

Thus the electric field must obey the ordinary differential equation

$$\frac{d^2\tilde{E}_z}{d\rho^2} + \frac{1}{\rho}\frac{d\tilde{E}_z}{d\rho} + k^2\tilde{E}z = 0. \tag{4.329}$$

This is merely Bessel's equation (A.124). It is a second-order equation with two independent solutions chosen from the list

$$J_0(k\rho), \quad Y_0(k\rho), \quad H_0^{(1)}(k\rho), \quad H_0^{(2)}(k\rho).$$

We find that $J_0(k\rho)$ and $Y_0(k\rho)$ are useful for describing standing waves between boundaries, while $H_0^{(1)}(k\rho)$ and $H_0^{(2)}(k\rho)$ are useful for describing waves propagating in the ρ-direction. Of these, $H_0^{(1)}(k\rho)$ represents waves traveling inward while $H_0^{(2)}(k\rho)$ represents waves traveling outward. At this point we are interested in studying the behavior of outward propagating waves and so we choose

$$\tilde{E}_z(\rho,\omega) = -\frac{j}{4}\tilde{E}_{z0}(\omega)H_0^{(2)}(k\rho). \tag{4.330}$$

As explained in § 2.10.7, $\tilde{E}_{z0}(\omega)$ is the amplitude spectrum of the wave, while the term $-j/4$ is included to make the conversion to the time domain more convenient. By (4.327) we have

$$\tilde{H}_\phi = \frac{1}{j\omega\tilde{\mu}}\frac{\partial\tilde{E}_z}{\partial\rho} = \frac{1}{j\omega\tilde{\mu}}\frac{\partial}{\partial\rho}\left[-\frac{j}{4}\tilde{E}_{z0}H_0^{(2)}(k\rho)\right]. \tag{4.331}$$

Using $dH_0^{(2)}(x)/dx = -H_1^{(2)}(x)$ we find that

$$\tilde{H}_\phi = \frac{1}{Z_{TM}}\frac{\tilde{E}_{z0}}{4}H_1^{(2)}(k\rho) \tag{4.332}$$

where

$$Z_{TM} = \frac{\omega\tilde{\mu}}{k}$$

is called the *TM wave impedance.*

For the case of magnetic polarization, the field $\tilde{H}_z$ must satisfy Bessel's equation (4.329). Thus we choose

$$\tilde{H}_z(\rho,\omega) = -\frac{j}{4}\tilde{H}_{z0}(\omega)H_0^{(2)}(k\rho). \tag{4.333}$$

From (4.328) we find the electric field associated with the wave:

$$\tilde{E}_\phi = -Z_{TE}\frac{\tilde{H}_{z0}}{4}H_1^{(2)}(k\rho), \tag{4.334}$$

where

$$Z_{TE} = \frac{k}{\omega\tilde{\epsilon}^c}$$

is the *TE wave impedance.*

It is not readily apparent that the terms $H_0^{(2)}(k\rho)$ or $H_1^{(2)}(k\rho)$ describe outward propagating waves. We shall see later that the cylindrical wave may be written as a superposition of plane waves, both uniform and evanescent, propagating in all possible directions. Each of these components does have the expected wave behavior, but it is still not obvious that the sum of such waves is outward propagating.

We saw in § 2.10.7 that when examined in the time domain, a cylindrical wave of the form $H_0^{(2)}(k\rho)$ does indeed propagate outward, and that for lossless media the velocity of propagation of its wavefronts is $v = 1/(\mu\epsilon)^{1/2}$. For time-harmonic fields, the cylindrical wave takes on a familiar behavior when the observation point is sufficiently removed from the source. We may specialize (4.330) to the time-harmonic case by setting $\omega = \check{\omega}$ and using phasors, giving

$$\check{E}_z(\rho) = -\frac{j}{4}\check{E}_{z0}H_0^{(2)}(k\rho).$$

If $|k\rho| \gg 1$ we can use the asymptotic representation (E.62) for the Hankel function

$$H_\nu^{(2)}(z) \sim \sqrt{\frac{2}{\pi z}}e^{-j(z-\pi/4-\nu\pi/2)}, \qquad |z| \gg 1, \quad -2\pi < \arg(z) < \pi,$$

to obtain

$$\check{E}_z(\rho) \sim \check{E}_{z0}\frac{e^{-jk\rho}}{\sqrt{8j\pi k\rho}} \tag{4.335}$$

and

$$\check{H}_\phi(\rho) \sim -\check{E}_{z0}\frac{1}{Z_{TM}}\frac{e^{-jk\rho}}{\sqrt{8j\pi k\rho}} \tag{4.336}$$

for $|k\rho| \gg 1$. Except for the $\sqrt{\rho}$ term in the denominator, the wave has very much the same form as the plane waves encountered earlier. For the case of magnetic polarization, we can approximate (4.333) and (4.334) to obtain

$$\check{H}_z(\rho) \sim \check{H}_{z0}\frac{e^{-jk\rho}}{\sqrt{8j\pi k\rho}} \tag{4.337}$$

and

$$\check{E}_\phi(\rho) \sim Z_{TE}\check{H}_{z0}\frac{e^{-jk\rho}}{\sqrt{8j\pi k\rho}} \tag{4.338}$$

for $|k\rho| \gg 1$.

To interpret the wave nature of the field (4.335) let us substitute $k = \beta - j\alpha$ into the exponential function, where β is the phase constant (4.224) and α is the attenuation constant (4.225). Then

$$\check{E}_z(\rho) \sim \check{E}_{z0}\frac{1}{\sqrt{8j\pi k\rho}}e^{-\alpha\rho}e^{-j\beta\rho}.$$

Assuming $\check{E}_{z0} = |E_{z0}|e^{j\xi^E}$, the time-domain representation is found from (4.126):

$$E_z(\rho, t) = \frac{|E_{z0}|}{\sqrt{8\pi k\rho}} e^{-\alpha\rho} \cos[\check{\omega}t - \beta\rho - \pi/4 + \xi^E]. \tag{4.339}$$

We can identify a surface of constant phase as a locus of points obeying

$$\check{\omega}t - \beta\rho - \pi/4 + \xi^E = C_P \tag{4.340}$$

where C_P is some constant. These surfaces are cylinders coaxial with the z-axis, and are called *cylindrical wavefronts*. Note that surfaces of constant amplitude, as determined by

$$\frac{e^{-\alpha\rho}}{\sqrt{\rho}} = C_A$$

where C_A is some constant, are also cylinders.

The cosine term in (4.339) represents a traveling wave. As t is increased the argument of the cosine function remains fixed as long as ρ is increased correspondingly. Hence the cylindrical wavefronts propagate outward as time progresses. As the wavefront travels outward, the field is attenuated because of the factor $e^{-\alpha\rho}$. The velocity of propagation of the phase fronts may be computed by a now familiar technique. Differentiating (4.340) with respect to t we find that

$$\check{\omega} - \beta\frac{d\rho}{dt} = 0,$$

and thus have the phase velocity v_p of the outward expanding phase fronts:

$$v_p = \frac{d\rho}{dt} = \frac{\check{\omega}}{\beta}.$$

Calculation of wavelength also proceeds as before. Examining the two adjacent wavefronts that produce the same value of the cosine function in (4.339), we find $\beta\rho_1 = \beta\rho_2 - 2\pi$ or

$$\lambda = \rho_2 - \rho_1 = 2\pi/\beta.$$

Computation of the power carried by a cylindrical wave is straightforward. Since a cylindrical wavefront is infinite in extent, we usually speak of the *power per unit length* carried by the wave. This is found by integrating the time-average Poynting flux given in (4.157). For electric polarization we find the time-average power flux density using (4.330) and (4.331):

$$\mathbf{S}_{av} = \frac{1}{2}\,\text{Re}\{\check{E}_z\hat{\mathbf{z}} \times \check{H}_\phi^*\hat{\boldsymbol{\phi}}\} = \frac{1}{2}\,\text{Re}\left\{\hat{\boldsymbol{\rho}}\frac{j}{16Z_{TM}^*}|\check{E}_{z0}|^2 H_0^{(2)}(k\rho)H_1^{(2)*}(k\rho)\right\}. \tag{4.341}$$

For magnetic polarization we use (4.333) and (4.334):

$$\mathbf{S}_{av} = \frac{1}{2}\,\text{Re}\{\check{E}_\phi\hat{\boldsymbol{\phi}} \times \check{H}_z^*\hat{\mathbf{z}}\} = \frac{1}{2}\,\text{Re}\left\{-\hat{\boldsymbol{\rho}}\frac{jZ_{TE}}{16}|\check{H}_{z0}|^2 H_0^{(2)*}(k\rho)H_1^{(2)}(k\rho)\right\}.$$

For a lossless medium these expressions can be greatly simplified. By (E.5) we can write

$$jH_0^{(2)}(k\rho)H_1^{(2)*}(k\rho) = j[J_0(k\rho) - jN_0(k\rho)][J_1(k\rho) + jN_1(k\rho)],$$

hence

$$jH_0^{(2)}(k\rho)H_1^{(2)*}(k\rho) = [N_0(k\rho)J_1(k\rho) - J_0(k\rho)N_1(k\rho)] + j[J_0(k\rho)J_1(k\rho) + N_0(k\rho)N_1(k\rho)].$$

Substituting this into (4.341) and remembering that $Z_{TM} = \eta = (\mu/\epsilon)^{1/2}$ is real for lossless media, we have

$$\mathbf{S}_{av} = \hat{\boldsymbol{\rho}}\frac{1}{32\eta}|\check{E}_{z0}|^2[N_0(k\rho)J_1(k\rho) - J_0(k\rho)N_1(k\rho)].$$

By the Wronskian relation (E.88) we have

$$\mathbf{S}_{av} = \hat{\boldsymbol{\rho}}\frac{|\check{E}_{z0}|^2}{16\pi k\rho\eta}.$$

The power density is inversely proportional to ρ. When we compute the total time-average power per unit length passing through a cylinder of radius ρ, this factor cancels with the ρ-dependence of the surface area to give a result independent of radius:

$$P_{av}/l = \int_0^{2\pi} \mathbf{S}_{av} \cdot \hat{\boldsymbol{\rho}}\rho \, d\phi = \frac{|\check{E}_{z0}|^2}{8k\eta}. \tag{4.342}$$

For a lossless medium there is no mechanism to dissipate the power and so the wave propagates unabated. A similar calculation for the case of magnetic polarization (Problem **??**) gives

$$\mathbf{S}_{av} = \hat{\boldsymbol{\rho}}\frac{\eta|\check{H}_{z0}|^2}{16\pi k\rho}$$

and

$$P_{av}/l = \frac{\eta|\check{H}_{z0}|^2}{8k}.$$

For a lossy medium the expressions are more difficult to evaluate. In this case we expect the total power passing through a cylinder to depend on the radius of the cylinder, since the fields decay exponentially with distance and thus give up power as they propagate. If we assume that the observation point is far from the z-axis with $|k\rho| \gg 1$, then we can use (4.335) and (4.336) for the electric polarization case to obtain

$$\mathbf{S}_{av} = \frac{1}{2}\,\mathrm{Re}\{\check{E}_z\hat{\mathbf{z}} \times \check{H}_\phi^*\hat{\boldsymbol{\phi}}\} = \frac{1}{2}\,\mathrm{Re}\left\{\hat{\boldsymbol{\rho}}\frac{e^{-2\alpha\rho}}{8\pi\rho|k|Z_{TM}^*}|\check{E}_{z0}|^2\right\}.$$

Therefore

$$P_{av}/l = \int_0^{2\pi} \mathbf{S}_{av} \cdot \hat{\boldsymbol{\rho}}\rho \, d\phi = \mathrm{Re}\left\{\frac{1}{Z_{TM}^*}\right\}|\check{E}_{z0}|^2\frac{e^{-2\alpha\rho}}{8|k|}.$$

We note that for a lossless material $Z_{TM} = \eta$ and $\alpha = 0$, and the expression reduces to (4.342) as expected. Thus for lossy materials the power depends on the radius of the cylinder. In the case of magnetic polarization we use (4.337) and (4.338) to get

$$\mathbf{S}_{av} = \frac{1}{2}\,\mathrm{Re}\{\check{E}_\phi\hat{\boldsymbol{\phi}} \times \check{H}_z^*\hat{\mathbf{z}}\} = \frac{1}{2}\,\mathrm{Re}\left\{\hat{\boldsymbol{\rho}}Z_{TE}^*\frac{e^{-2\alpha\rho}}{8\pi\rho|k|}|\check{H}_{z0}|^2\right\}$$

and

$$P_{av}/l = \mathrm{Re}\left\{Z_{TE}^*\right\}|\check{H}_{z0}|^2\frac{e^{-2\alpha\rho}}{8|k|}.$$

Example of uniform cylindrical waves: fields of a line source. The simplest example of a uniform cylindrical wave is that produced by an electric or magnetic line source. Consider first an infinite electric line current of amplitude $\tilde{I}(\omega)$ on the z-axis, immersed within a medium of permittivity $\tilde{\epsilon}(\omega)$, permeability $\tilde{\mu}(\omega)$, and conductivity $\tilde{\sigma}(\omega)$. We assume that the current does not vary in the z-direction, and thus the problem is two-dimensional. We can decompose the field produced by the line source into TE and TM cases according to § 4.11.2. It turns out that an electric line source only excites TM fields, as we shall show in § 5.4, and thus we need only $\tilde{E}_z$ to completely describe the fields.

By symmetry the fields are ϕ-independent and thus the wave produced by the line source is a uniform cylindrical wave. Since the wave propagates outward from the line source we have the electric field from (4.330),

$$\tilde{E}_z(\rho, \omega) = -\frac{j}{4}\tilde{E}_{z0}(\omega)H_0^{(2)}(k\rho), \tag{4.343}$$

and the magnetic field from (4.332),

$$\tilde{H}_\phi(\rho, \omega) = \frac{k}{\omega\tilde{\mu}}\frac{\tilde{E}_{z0}(\omega)}{4}H_1^{(2)}(k\rho).$$

We can find $\tilde{E}_{z0}$ by using Ampere's law:

$$\oint_\Gamma \tilde{\mathbf{H}} \cdot \mathbf{dl} = \int_S \tilde{\mathbf{J}} \cdot \mathbf{dS} + j\omega \int_S \tilde{\mathbf{D}} \cdot \mathbf{dS}.$$

Since $\tilde{\mathbf{J}}$ is the sum of the impressed current $\tilde{I}$ and the secondary conduction current $\tilde{\sigma}\tilde{\mathbf{E}}$, we can also write

$$\oint_\Gamma \tilde{\mathbf{H}} \cdot \mathbf{dl} = \tilde{I} + \int_S (\tilde{\sigma} + j\omega\tilde{\epsilon})\tilde{\mathbf{E}} \cdot \mathbf{dS} = \tilde{I} + j\omega\tilde{\epsilon}^c \int_S \tilde{\mathbf{E}} \cdot \mathbf{dS}.$$

Choosing our path of integration as a circle of radius a in the $z = 0$ plane and substituting for $\tilde{E}_z$ and $\tilde{H}_\phi$, we find that

$$\frac{k}{\omega\tilde{\mu}}\frac{\tilde{E}_{z0}}{4}H_1^{(2)}(ka)2\pi a = \tilde{I} + j\omega\tilde{\epsilon}^c 2\pi \frac{-j\tilde{E}_{z0}}{4} \lim_{\delta\to 0}\int_\delta^a H_0^{(2)}(k\rho)\rho\, d\rho. \tag{4.344}$$

The limit operation is required because $H_0^{(2)}(k\rho)$ diverges as $\rho \to 0$. By (E.104) the integral is

$$\lim_{\delta\to 0}\int_\delta^a H_0^{(2)}(k\rho)\rho\, d\rho = \frac{a}{k}H_1^{(2)}(ka) - \frac{1}{k}\lim_{\delta\to 0}\delta H_1^{(2)}(k\delta).$$

The limit may be found by using $H_1^{(2)}(x) = J_1(x) - jN_1(x)$ and the small argument approximations (E.50) and (E.53):

$$\lim_{\delta\to 0}\delta H_1^{(2)}(\delta) = \lim_{\delta\to 0}\delta\left[\frac{k\delta}{2} - j\left(-\frac{1}{\pi}\frac{2}{k\delta}\right)\right] = j\frac{2}{\pi k}.$$

Substituting these expressions into (4.344) we obtain

$$\frac{k}{\omega\tilde{\mu}}\frac{\tilde{E}_{z0}}{4}H_1^{(2)}(ka)2\pi a = \tilde{I} + j\omega\tilde{\epsilon}^c 2\pi \frac{-j\tilde{E}_{z0}}{4}\left[\frac{a}{k}H_1^{(2)}(ka) - j\frac{2}{\pi k^2}\right].$$

Using $k^2 = \omega^2 \tilde{\mu} \tilde{\epsilon}^c$ we find that the two Hankel function terms cancel. Solving for $\tilde{E}_{z0}$ we have

$$\tilde{E}_{z0} = -j\omega\tilde{\mu}\tilde{I}$$

and therefore

$$\tilde{E}_z(\rho, \omega) = -\frac{\omega\tilde{\mu}}{4}\tilde{I}(\omega)H_0^{(2)}(k\rho) = -j\omega\tilde{\mu}\tilde{I}(\omega)\tilde{G}(x, y|0, 0; \omega). \tag{4.345}$$

Here $\tilde{G}$ is called the *two-dimensional Green's function* and is given by

$$\tilde{G}(x, y|x', y'; \omega) = \frac{1}{4j}H_0^{(2)}\left(k\sqrt{(x - x')^2 + (y - y')^2}\right). \tag{4.346}$$

Green's functions are examined in greater detail in Chapter 5

It is also possible to determine the field amplitude by evaluating

$$\lim_{a\to 0}\oint_C \tilde{\mathbf{H}} \cdot \mathbf{dl}.$$

This produces an identical result and is a bit simpler since it can be argued that the surface integral of $\tilde{E}_z$ vanishes as $a \to 0$ without having to perform the calculation directly [83, 8].

For a magnetic line source $\tilde{I}_m(\omega)$ aligned along the z-axis we proceed as above, but note that the source only produces TE fields. By (4.333) and (4.334) we have

$$\tilde{H}_z(\rho, \omega) = -\frac{j}{4}\tilde{H}_{z0}(\omega)H_0^{(2)}(k\rho), \qquad \tilde{E}_\phi = -\frac{k}{\omega\tilde{\epsilon}^c}\frac{\tilde{H}_{0z}}{4}H_1^{(2)}(k\rho).$$

We can find $\tilde{H}_{z0}$ by applying Faraday's law

$$\oint_C \tilde{\mathbf{E}} \cdot \mathbf{dl} = -\int_S \tilde{\mathbf{J}}_m \cdot \mathbf{dS} - j\omega\int_S \tilde{\mathbf{B}} \cdot \mathbf{dS}$$

about a circle of radius a in the $z = 0$ plane. We have

$$-\frac{k}{\omega\tilde{\epsilon}^c}\frac{\tilde{H}_{z0}}{4}H_1^{(2)}(ka)2\pi a = -\tilde{I}_m - j\omega\tilde{\mu}\left[-\frac{j}{4}\right]\tilde{H}_{z0}2\pi\lim_{\delta\to 0}\int_\delta^a H_0^{(2)}(k\rho)\rho\,d\rho.$$

Proceeding as above we find that

$$\tilde{H}_{z0} = j\omega\tilde{\epsilon}^c\tilde{I}_m$$

hence

$$\tilde{H}_z(\rho, \omega) = -\frac{\omega\tilde{\epsilon}^c}{4}\tilde{I}_m(\omega)H_0^{(2)}(k\rho) = -j\omega\tilde{\epsilon}^c\tilde{I}_m(\omega)\tilde{G}(x, y|0, 0; \omega). \tag{4.347}$$

Note that we could have solved for the magnetic field of a magnetic line current by using the field of an electric line current and the principle of duality. Letting the magnetic current be equal to $-\eta$ times the electric current and using (4.198), we find that

$$\tilde{H}_{z0} = \left(-\frac{1}{\eta}\frac{\tilde{I}_m(\omega)}{\tilde{I}(\omega)}\right)\left(-\frac{1}{\eta}\left[-\frac{\omega\tilde{\mu}}{4}\tilde{I}(\omega)H_0^{(2)}(k\rho)\right]\right) = -\tilde{I}_m(\omega)\frac{\omega\tilde{\epsilon}^c}{4}H_0^{(2)}(k\rho) \tag{4.348}$$

as in (4.347).

Nonuniform cylindrical waves. When we solve two-dimensional boundary value problems we encounter cylindrical waves that are z-independent but ϕ-dependent. Although such waves propagate outward, they have a more complicated structure than those considered above.

For the case of TM polarization we have, by (4.212),

$$\tilde{H}_\rho = \frac{j}{Z_{TM}k}\frac{1}{\rho}\frac{\partial \tilde{E}_z}{\partial \phi}, \tag{4.349}$$

$$\tilde{H}_\phi = -\frac{j}{Z_{TM}k}\frac{\partial \tilde{E}_z}{\partial \rho}, \tag{4.350}$$

where $Z_{TM} = \omega\tilde{\mu}/k$. For the TE case we have, by (4.213),

$$\tilde{E}_\rho = -\frac{jZ_{TE}}{k}\frac{1}{\rho}\frac{\partial \tilde{H}_z}{\partial \phi}, \tag{4.351}$$

$$\tilde{E}_\phi = \frac{jZ_{TE}}{k}\frac{\partial \tilde{H}_z}{\partial \rho}, \tag{4.352}$$

where $Z_{TE} = k/\omega\tilde{\epsilon}^c$. By (4.208) the wave equations are

$$\left(\frac{\partial^2}{\partial\rho^2} + \frac{1}{\rho}\frac{\partial}{\partial\rho} + \frac{1}{\rho^2}\frac{\partial^2}{\partial\phi^2} + k^2\right)\left\{\begin{matrix}\tilde{E}_z\\ \tilde{H}_z\end{matrix}\right\} = 0.$$

Because this has the form of A.177 with $\partial/\partial z \to 0$, we have

$$\left\{\begin{matrix}\tilde{E}_z(\rho,\phi,\omega)\\ \tilde{H}_z(\rho,\phi,\omega)\end{matrix}\right\} = P(\rho,\omega)\Phi(\phi,\omega) \tag{4.353}$$

where

$$\Phi(\phi,\omega) = A_\phi(\omega)\sin k_\phi\phi + B_\phi(\omega)\cos k_\phi\phi, \tag{4.354}$$

$$P(\rho) = A_\rho(\omega)B^{(1)}_{k_\phi}(k\rho) + B_\rho(\omega)B^{(2)}_{k_\phi}(k\rho), \tag{4.355}$$

and where $B^{(1)}_\nu(z)$ and $B^{(2)}_\nu(z)$ are any two independent Bessel functions chosen from the set

$$J_\nu(z), \quad N_\nu(z), \quad H^{(1)}_\nu(z), \quad H^{(2)}_\nu(z).$$

In bounded regions we generally use the oscillatory functions $J_\nu(z)$ and $N_\nu(z)$ to represent standing waves. In unbounded regions we generally use $H^{(2)}_\nu(z)$ and $H^{(1)}_\nu(z)$ to represent outward and inward propagating waves, respectively.

Boundary value problems in cylindrical coordinates: scattering by a material cylinder. A variety of problems can be solved using nonuniform cylindrical waves. We shall examine two interesting cases in which an external field is impressed on a two-dimensional object. The impressed field creates secondary sources within or on the object, and these in turn create a secondary field. Our goal is to determine the secondary field by applying appropriate boundary conditions.

As a first example, consider a material cylinder of radius a, complex permittivity $\tilde{\epsilon}^c$, and permeability $\tilde{\mu}$, aligned along the z-axis in free space (Figure 4.25). An incident plane wave propagating in the x-direction is impressed on the cylinder, inducing secondary polarization and conduction currents within the cylinder. These in turn produce

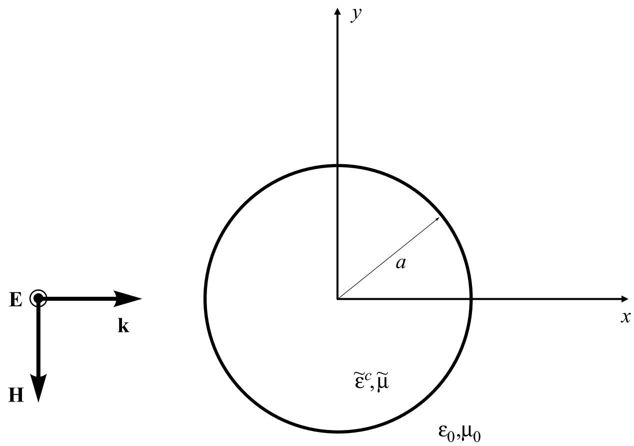

Figure 4.25: TM plane-wave field incident on a material cylinder.

secondary or scattered fields, which are standing waves within the cylinder and outward traveling waves external to the cylinder. Although we have not yet learned how to write the secondary fields in terms of the impressed sources, we can solve for the fields as a boundary value problem. The total field must obey the boundary conditions on tangential components at the interface between the cylinder and surrounding free space. We need not worry about the effect of the secondary sources on the source of the primary field, since by definition impressed sources cannot be influenced by secondary fields.

The scattered field can be found using superposition. When excited by a TM impressed field, the secondary field is also TM. The situation for TE excitation is similar. By decomposing the impressed field into TE and TM components, we may solve for the scattered field in each case and then superpose the results to determine the complete solution.

We first consider the TM case. The impressed electric field may be written as

$$\tilde{\mathbf{E}}^i(\mathbf{r}, \omega) = \hat{\mathbf{z}}\tilde{E}_0(\omega)e^{-jk_0 x} = \hat{\mathbf{z}}\tilde{E}_0(\omega)e^{-jk_0\rho\cos\phi} \tag{4.356}$$

while the magnetic field is, by (4.223),

$$\tilde{\mathbf{H}}^i(\mathbf{r}, \omega) = -\hat{\mathbf{y}}\frac{\tilde{E}_0(\omega)}{\eta_0}e^{-jk_0 x} = -(\hat{\boldsymbol{\rho}}\sin\phi + \hat{\boldsymbol{\phi}}\cos\phi)\frac{\tilde{E}_0(\omega)}{\eta_0}e^{-jk_0\rho\cos\phi}.$$

Here $k_0 = \omega(\mu_0\epsilon_0)^{1/2}$ and $\eta_0 = (\mu_0/\epsilon_0)^{1/2}$. The scattered electric field takes the form of a nonuniform cylindrical wave (4.353). Periodicity in ϕ implies that k_ϕ is an integer, say $k_\phi = n$. Within the cylinder we cannot use any of the functions $N_n(k\rho)$, $H_n^{(2)}(k\rho)$, or $H_n^{(1)}(k\rho)$ to represent the radial dependence of the field, since each is singular at the origin. So we choose $B_n^{(1)}(k\rho) = J_n(k\rho)$ and $B_\rho(\omega) = 0$ in (4.355). Physically, $J_n(k\rho)$ represents the standing wave created by the interaction of outward and inward propagating waves. External to the cylinder we use $H_n^{(2)}(k\rho)$ to represent the radial dependence of the secondary field components: we avoid $N_n(k\rho)$ and $J_n(k\rho)$ since these represent standing waves, and avoid $H_n^{(1)}(k\rho)$ since there are no external secondary sources to create an inward traveling wave.

Any attempt to satisfy the boundary conditions by using a single nonuniform wave fails. This is because the sinusoidal dependence on ϕ of each individual nonuniform wave cannot match the more complicated dependence of the impressed field (4.356). Since the sinusoids are complete, an infinite series of the functions (4.353) can be used to represent the scattered field. So we have internal to the cylinder

$$\tilde{E}_z^s(\mathbf{r}, \omega) = \sum_{n=0}^{\infty} [A_n(\omega) \sin n\phi + B_n(\omega) \cos n\phi] \, J_n(k\rho)$$

where $k = \omega(\tilde{\mu}\tilde{\epsilon}^c)^{1/2}$. External to the cylinder we have free space and thus

$$\tilde{E}_z^s(\mathbf{r}, \omega) = \sum_{n=0}^{\infty} [C_n(\omega) \sin n\phi + D_n(\omega) \cos n\phi] \, H_n^{(2)}(k_0\rho).$$

Equations (4.349) and (4.350) yield the magnetic field internal to the cylinder:

$$\tilde{H}_\rho^s = \sum_{n=0}^{\infty} \frac{jn}{Z_{TM}k} \frac{1}{\rho} [A_n(\omega) \cos n\phi - B_n(\omega) \sin n\phi] \, J_n(k\rho),$$

$$\tilde{H}_\phi^s = -\sum_{n=0}^{\infty} \frac{j}{Z_{TM}} [A_n(\omega) \sin n\phi + B_n(\omega) \cos n\phi] \, J_n'(k\rho),$$

where $Z_{TM} = \omega\tilde{\mu}/k$. Outside the cylinder

$$\tilde{H}_\rho^s = \sum_{n=0}^{\infty} \frac{jn}{\eta_0 k_0} \frac{1}{\rho} [C_n(\omega) \cos n\phi - D_n(\omega) \sin n\phi] \, H_n^{(2)}(k_0\rho),$$

$$\tilde{H}_\phi^s = -\sum_{n=0}^{\infty} \frac{j}{\eta_0} [C_n(\omega) \sin n\phi + D_n(\omega) \cos n\phi] \, H_n^{(2)\prime}(k_0\rho),$$

where $J_n'(z) = dJ_n(z)/dz$ and $H_n^{(2)\prime}(z) = dH_n^{(2)}(z)/dz$.

We have two sets of unknown spectral amplitudes (A_n, B_n) and (C_n, D_n). These can be determined by applying the boundary conditions at the interface. Since the total field outside the cylinder is the sum of the impressed and scattered terms, an application of continuity of the tangential electric field at $\rho = a$ gives us

$$\sum_{n=0}^{\infty} [A_n \sin n\phi + B_n \cos n\phi] \, J_n(ka) =$$
$$\sum_{n=0}^{\infty} [C_n \sin n\phi + D_n \cos n\phi] \, H_n^{(2)}(k_0a) + \tilde{E}_0 e^{-jk_0a\cos\phi},$$

which must hold for all $-\pi \le \phi \le \pi$. To remove the coefficients from the sum we apply orthogonality. Multiplying both sides by $\sin m\phi$, integrating over $[-\pi, \pi]$, and using the orthogonality conditions (A.129)–(A.131) we obtain

$$\pi A_m J_m(ka) - \pi C_m H_m^{(2)}(k_0a) = \tilde{E}_0 \int_{-\pi}^{\pi} \sin m\phi e^{-jk_0a\cos\phi} \, d\phi = 0. \tag{4.357}$$

Multiplying by $\cos m\phi$ and integrating, we find that

$$\begin{aligned} 2\pi B_m J_m(ka) - 2\pi D_m H_m^{(2)}(k_0a) &= \tilde{E}_0 \epsilon_m \int_{-\pi}^{\pi} \cos m\phi e^{-jk_0a\cos\phi} \, d\phi \\ &= 2\pi \tilde{E}_0 \epsilon_m j^{-m} J_m(k_0a) \end{aligned} \tag{4.358}$$

where ϵ_n is Neumann's number (A.132) and where we have used (E.83) and (E.39) to evaluate the integral.

We must also have continuity of the tangential magnetic field $\tilde{H}_\phi$ at $\rho = a$. Thus

$$-\sum_{n=0}^{\infty} \frac{j}{Z_{TM}} [A_n \sin n\phi + B_n \cos n\phi] J_n'(ka) =$$
$$-\sum_{n=0}^{\infty} \frac{j}{\eta_0} [C_n \sin n\phi + D_n \cos n\phi] H_n^{(2)\prime}(k_0 a) - \cos\phi \frac{\tilde{E}_0}{\eta_0} e^{-jk_0 a \cos\phi}$$

must hold for all $-\pi \le \phi \le \pi$. By orthogonality

$$\pi \frac{j}{Z_{TM}} A_m J_m'(ka) - \pi \frac{j}{\eta_0} C_m H_m^{(2)\prime}(k_0 a) = \frac{\tilde{E}_0}{\eta_0} \int_{-\pi}^{\pi} \sin m\phi \cos\phi e^{-jk_0 a \cos\phi}\, d\phi = 0 \qquad (4.359)$$

and

$$2\pi \frac{j}{Z_{TM}} B_m J_m'(ka) - 2\pi \frac{j}{\eta_0} D_m H_m^{(2)\prime}(k_0 a) = \epsilon_m \frac{\tilde{E}_0}{\eta_0} \int_{-\pi}^{\pi} \cos m\phi \cos\phi e^{-jk_0 a \cos\phi}\, d\phi.$$

The integral may be computed as

$$\int_{-\pi}^{\pi} \cos m\phi \cos\phi e^{-jk_0 a \cos\phi}\, d\phi = j \frac{d}{d(k_0 a)} \int_{-\pi}^{\pi} \cos m\phi e^{-jk_0 a \cos\phi}\, d\phi = j 2\pi j^{-m} J_m'(k_0 a)$$

and thus

$$\frac{1}{Z_{TM}} B_m J_m'(ka) - \frac{1}{\eta_0} D_m H_m^{(2)\prime}(k_0 a) = \frac{\tilde{E}_0}{\eta_0} \epsilon_m j^{-m} J_m'(k_0 a). \qquad (4.360)$$

We now have four equations for the coefficients A_n, B_n, C_n, D_n. We may write (4.357) and (4.359) as

$$\begin{bmatrix} J_m(ka) & -H_m^{(2)}(k_0 a) \\ \frac{\eta_0}{Z_{TM}} J_m'(ka) & -H_m^{(2)\prime}(k_0 a) \end{bmatrix} \begin{bmatrix} A_m \\ C_m \end{bmatrix} = 0, \qquad (4.361)$$

and (4.358) and (4.360) as

$$\begin{bmatrix} J_m(ka) & -H_m^{(2)}(k_0 a) \\ \frac{\eta_0}{Z_{TM}} J_m'(ka) & -H_m^{(2)\prime}(k_0 a) \end{bmatrix} \begin{bmatrix} B_m \\ D_m \end{bmatrix} = \begin{bmatrix} \tilde{E}_0 \epsilon_m j^{-m} J_m(k_0 a) \\ \tilde{E}_0 \epsilon_m j^{-m} J_m'(k_0 a) \end{bmatrix}. \qquad (4.362)$$

Matrix equations (4.361) and (4.362) cannot hold simultaneously unless $A_m = C_m = 0$. Then the solution to (4.362) is

$$B_m = \tilde{E}_0 \epsilon_m j^{-m} \left[\frac{H_m^{(2)}(k_0 a) J_m'(k_0 a) - J_m(k_0 a) H_m^{(2)\prime}(k_0 a)}{\frac{\eta_0}{Z_{TM}} J_m'(ka) H_m^{(2)}(k_0 a) - H_m^{(2)\prime}(k_0 a) J_m(ka)} \right], \qquad (4.363)$$

$$D_m = -\tilde{E}_0 \epsilon_m j^{-m} \left[\frac{\frac{\eta_0}{Z_{TM}} J_m'(ka) J_m(k_0 a) - J_m'(k_0 a) J_m(ka)}{\frac{\eta_0}{Z_{TM}} J_m'(ka) H_m^{(2)}(k_0 a) - H_m^{(2)\prime}(k_0 a) J_m(ka)} \right]. \qquad (4.364)$$

With these coefficients we can calculate the field inside the cylinder ($\rho \le a$) from

$$\tilde{E}_z(\mathbf{r}, \omega) = \sum_{n=0}^{\infty} B_n(\omega) J_n(k\rho) \cos n\phi,$$

$$\tilde{H}_\rho(\mathbf{r},\omega) = -\sum_{n=0}^{\infty} \frac{jn}{Z_{TM}k}\frac{1}{\rho} B_n(\omega) J_n(k\rho)\sin n\phi,$$

$$\tilde{H}_\phi(\mathbf{r},\omega) = -\sum_{n=0}^{\infty} \frac{j}{Z_{TM}} B_n(\omega) J_n'(k\rho)\cos n\phi,$$

and the field outside the cylinder ($\rho > a$) from

$$\tilde{E}_z(\mathbf{r},\omega) = \tilde{E}_0(\omega) e^{-jk_0\rho\cos\phi} + \sum_{n=0}^{\infty} D_n(\omega) H_n^{(2)}(k_0\rho)\cos n\phi,$$

$$\tilde{H}_\rho(\mathbf{r},\omega) = -\sin\phi \frac{\tilde{E}_0(\omega)}{\eta_0} e^{-jk_0\rho\cos\phi} - \sum_{n=0}^{\infty} \frac{jn}{\eta_0 k_0}\frac{1}{\rho} D_n(\omega) H_n^{(2)}(k_0\rho)\sin n\phi,$$

$$\tilde{H}_\phi(\mathbf{r},\omega) = -\cos\phi \frac{\tilde{E}_0(\omega)}{\eta_0} e^{-jk_0\rho\cos\phi} - \sum_{n=0}^{\infty} \frac{j}{\eta_0} D_n(\omega) H_n^{(2)\prime}(k_0\rho)\cos n\phi.$$

We can easily specialize these results to the case of a perfectly conducting cylinder by allowing $\tilde{\sigma} \to \infty$. Then

$$\frac{\eta_0}{Z_{TM}} = \sqrt{\frac{\mu_0\tilde{\epsilon}^c}{\tilde{\mu}\epsilon_0}} \to \infty$$

and

$$B_n \to 0, \qquad D_n \to -\tilde{E}_0 \epsilon_m j^{-m} \frac{J_m(k_0 a)}{H_m^{(2)}(k_0 a)}.$$

In this case it is convenient to combine the formulas for the impressed and scattered fields when forming the total fields. Since the impressed field is z-independent and obeys the homogeneous Helmholtz equation, we may represent it in terms of nonuniform cylindrical waves:

$$\tilde{E}_z^i = \tilde{E}_0 e^{-jk_0\rho\cos\phi} = \sum_{n=0}^{\infty} \left[E_n \sin n\phi + F_n \cos n\phi\right] J_n(k_0\rho),$$

where we have chosen the Bessel function $J_n(k_0\rho)$ since the field is finite at the origin and periodic in ϕ. Applying orthogonality we see immediately that $E_n = 0$ and that

$$\frac{2\pi}{\epsilon_m} F_m J_m(k_0\rho) = \tilde{E}_0 \int_{-\pi}^{\pi} \cos m\phi e^{-jk_0\rho\cos\phi}\, d\phi = \tilde{E}_0 2\pi j^{-m} J_m(k_0\rho).$$

Thus, $F_n = \tilde{E}_0 \epsilon_n j^{-n}$ and

$$\tilde{E}_z^i = \sum_{n=0}^{\infty} \tilde{E}_0 \epsilon_n j^{-n} J_n(k_0\rho)\cos n\phi.$$

Adding this impressed field to the scattered field we have the total field outside the cylinder,

$$\tilde{E}_z = \tilde{E}_0 \sum_{n=0}^{\infty} \frac{\epsilon_n j^{-n}}{H_n^{(2)}(k_0 a)} \left[J_n(k_0\rho) H_n^{(2)}(k_0 a) - J_n(k_0 a) H_n^{(2)}(k_0\rho)\right]\cos n\phi,$$

while the field within the cylinder vanishes. Then, by (4.350),

$$\tilde{H}_\phi = -\frac{j}{\eta_0}\tilde{E}_0 \sum_{n=0}^{\infty} \frac{\epsilon_n j^{-n}}{H_n^{(2)}(k_0 a)} \left[J_n'(k_0\rho) H_n^{(2)}(k_0 a) - J_n(k_0 a) H_n^{(2)\prime}(k_0\rho)\right]\cos n\phi.$$

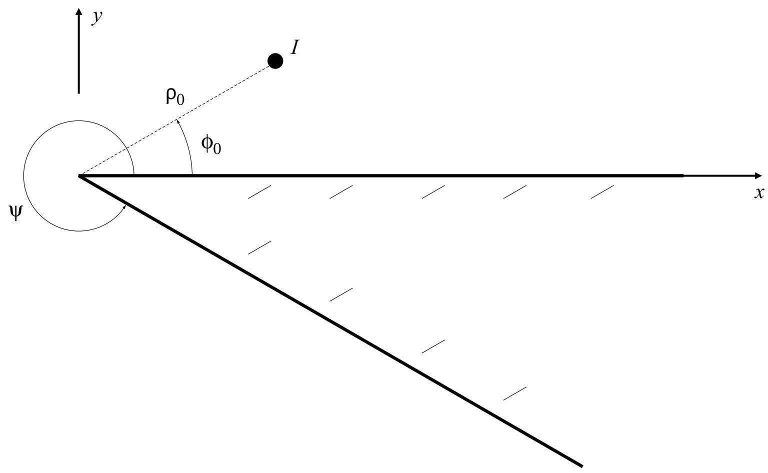

Figure 4.26: Geometry of a perfectly conducting wedge illuminated by a line source.

This in turn gives us the surface current induced on the cylinder. From the boundary condition $\tilde{\mathbf{J}}_s = \hat{\mathbf{n}} \times \tilde{\mathbf{H}}|_{\rho=a} = \hat{\boldsymbol{\rho}} \times [\hat{\boldsymbol{\rho}}\tilde{H}_\rho + \hat{\boldsymbol{\phi}}\tilde{H}_\phi]|_{\rho=a} = \hat{\mathbf{z}}\tilde{H}_\phi|_{\rho=a}$ we have

$$\mathbf{J}_s(\phi,\omega) = -\frac{j}{\eta_0}\hat{\mathbf{z}}\tilde{E}_0 \sum_{n=0}^{\infty} \frac{\epsilon_n j^{-n}}{H_n^{(2)}(k_0 a)} \left[J_n'(k_0 a)H_n^{(2)}(k_0 a) - J_n(k_0 a)H_n^{(2)\prime}(k_0 a)\right] \cos n\phi,$$

and an application of (E.93) gives us

$$\mathbf{J}_s(\phi,\omega) = \hat{\mathbf{z}}\frac{2\tilde{E}_0}{\eta_0 k_0 \pi a} \sum_{n=0}^{\infty} \frac{\epsilon_n j^{-n}}{H_n^{(2)}(k_0 a)} \cos n\phi. \tag{4.365}$$

Computation of the scattered field for a magnetically-polarized impressed field proceeds in the same manner. The impressed electric and magnetic fields are assumed to be

$$\tilde{\mathbf{E}}^i(\mathbf{r},\omega) = \hat{\mathbf{y}}\tilde{E}_0(\omega)e^{-jk_0 x} = (\hat{\boldsymbol{\rho}}\sin\phi + \hat{\boldsymbol{\phi}}\cos\phi)\tilde{E}_0(\omega)e^{-jk_0\rho\cos\phi},$$
$$\tilde{\mathbf{H}}^i(\mathbf{r},\omega) = \hat{\mathbf{z}}\frac{\tilde{E}_0(\omega)}{\eta_0}e^{-jk_0 x} = \hat{\mathbf{z}}\frac{\tilde{E}_0(\omega)}{\eta_0}e^{-jk_0\rho\cos\phi}.$$

For a perfectly conducting cylinder, the total magnetic field is

$$\tilde{H}_z = \frac{\tilde{E}_0}{\eta_0} \sum_{n=0}^{\infty} \frac{\epsilon_n j^{-n}}{H_n^{(2)\prime}(k_0 a)} \left[J_n(k_0\rho)H_n^{(2)\prime}(k_0 a) - J_n'(k_0 a)H_n^{(2)}(k_0\rho)\right] \cos n\phi. \tag{4.366}$$

The details are left as an exercise.

Boundary value problems in cylindrical coordinates: scattering by a perfectly conducting wedge. As a second example, consider a perfectly conducting wedge immersed in free space and illuminated by a line source (Figure 4.26) carrying current $\tilde{I}(\omega)$ and located at (ρ_0, ϕ_0). The current, which is assumed to be z-invariant, induces a secondary current on the surface of the wedge which in turn produces a secondary (scattered) field. This scattered field, also z-invariant, can be found by solving a boundary value problem. We do this by separating space into the two regions $\rho < \rho_0$ and $\rho > \rho_0$, $0 < \phi < \psi$. Each of these is source-free, so we can represent the total field using nonuniform cylindrical waves of the type (4.353). The line source is brought into the problem by applying the boundary condition on the tangential magnetic field across the cylindrical surface $\rho = \rho_0$.

Since the impressed electric field has only a z-component, so do the scattered and total electric fields. We wish to represent the total field $\tilde{E}_z$ in terms of nonuniform cylindrical waves of the type (4.353). Since the field is not periodic in ϕ, the separation constant k_ϕ need not be an integer; instead, its value is determined by the positions of the wedge boundaries. For the region $\rho < \rho_0$ we represent the radial dependence of the field using the functions J_ν since the field must be finite at the origin. For $\rho > \rho_0$ we use the outward-propagating wave functions $H_\delta^{(2)}$. Thus

$$\tilde{E}_z(\rho, \phi, \omega) = \begin{cases} \sum_\nu \left[A_\nu \sin \nu\phi + B_\nu \cos \nu\phi\right] J_\nu(k_0\rho), & \rho < \rho_0, \\ \sum_\delta \left[C_\delta \sin \delta\phi + D_\delta \cos \delta\phi\right] H_\delta^{(2)}(k_0\rho), & \rho > \rho_0. \end{cases} \tag{4.367}$$

The coefficients $A_\nu, B_\nu, C_\delta, D_\delta$ and separation constants ν, δ may be found by applying the boundary conditions on the fields at the surface of the wedge and across the surface $\rho = \rho_0$. On the wedge face at $\phi = 0$ we must have $\tilde{E}_z = 0$, hence $B_\nu = D_\delta = 0$. On the wedge face at $\phi = \psi$ we must also have $\tilde{E}_z = 0$, requiring $\sin \nu\psi = \sin \delta\psi = 0$ and therefore

$$\nu = \delta = \nu_n = n\pi/\psi, \qquad n = 1, 2, \ldots.$$

So

$$\tilde{E}_z = \begin{cases} \sum_{n=0}^\infty A_n \sin \nu_n\phi J_{\nu_n}(k_0\rho), & \rho < \rho_0, \\ \sum_{n=0}^\infty C_n \sin \nu_n\phi H_{\nu_n}^{(2)}(k_0\rho), & \rho > \rho_0. \end{cases} \tag{4.368}$$

The magnetic field can be found from (4.349)–(4.350):

$$\tilde{H}_\rho = \begin{cases} \sum_{n=0}^\infty A_n \frac{j}{\eta_0 k_0} \frac{\nu_n}{\rho} \cos \nu_n\phi J_{\nu_n}(k_0\rho), & \rho < \rho_0, \\ \sum_{n=0}^\infty C_n \frac{j}{\eta_0 k_0} \frac{\nu_n}{\rho} \cos \nu_n\phi H_{\nu_n}^{(2)}(k_0\rho), & \rho > \rho_0, \end{cases} \tag{4.369}$$

$$\tilde{H}_\phi = \begin{cases} -\sum_{n=0}^\infty A_n \frac{j}{\eta_0} \sin \nu_n\phi J'_{\nu_n}(k_0\rho), & \rho < \rho_0, \\ -\sum_{n=0}^\infty C_n \frac{j}{\eta_0} \sin \nu_n\phi H_{\nu_n}^{(2)\prime}(k_0\rho), & \rho > \rho_0. \end{cases} \tag{4.370}$$

The coefficients A_n and C_n are found by applying the boundary conditions at $\rho = \rho_0$. By continuity of the tangential electric field

$$\sum_{n=0}^\infty A_n \sin \nu_n\phi J_{\nu_n}(k_0\rho_0) = \sum_{n=0}^\infty C_n \sin \nu_n\phi H_{\nu_n}^{(2)}(k_0\rho_0).$$

We now apply orthogonality over the interval $[0, \psi]$. Multiplying by $\sin \nu_m\phi$ and integrating we have

$$\sum_{n=0}^\infty A_n J_{\nu_n}(k_0\rho_0) \int_0^\psi \sin \nu_n\phi \sin \nu_m\phi \, d\phi = \sum_{n=0}^\infty C_n H_{\nu_n}^{(2)}(k_0\rho_0) \int_0^\psi \sin \nu_n\phi \sin \nu_m\phi \, d\phi.$$

Setting $u = \phi\pi/\psi$ we have

$$\int_0^\psi \sin \nu_n\phi \sin \nu_m\phi \, d\phi = \frac{\psi}{\pi} \int_0^\pi \sin nu \sin mu \, du = \frac{\psi}{2}\delta_{mn},$$

thus

$$A_m J_{\nu_m}(k_0\rho_0) = C_m H^{(2)}_{\nu_m}(k_0\rho_0). \tag{4.371}$$

The boundary condition $\hat{\mathbf{n}}_{12} \times (\tilde{\mathbf{H}}_1 - \tilde{\mathbf{H}}_2) = \tilde{\mathbf{J}}_s$ requires the surface current at $\rho = \rho_0$. We can write the line current in terms of a surface current density using the δ-function:

$$\tilde{\mathbf{J}}_s = \hat{\mathbf{z}}\tilde{I}\frac{\delta(\phi - \phi_0)}{\rho_0}.$$

This is easily verified as the correct expression since the integral of this density along the circular arc at $\rho = \rho_0$ returns the correct value $\tilde{I}$ for the total current. Thus the boundary condition requires

$$\tilde{H}_\phi(\rho_0^+, \phi, \omega) - \tilde{H}_\phi(\rho_0^-, \phi, \omega) = \tilde{I}\frac{\delta(\phi - \phi_0)}{\rho_0}.$$

By (4.370) we have

$$-\sum_{n=0}^{\infty} C_n \frac{j}{\eta_0} \sin \nu_n\phi H^{(2)\prime}_{\nu_n}(k_0\rho_0) + \sum_{n=0}^{\infty} A_n \frac{j}{\eta_0} \sin \nu_n\phi J'_{\nu_n}(k_0\rho_0) = \tilde{I}\frac{\delta(\phi - \phi_0)}{\rho_0}$$

and orthogonality yields

$$-C_m \frac{\psi}{2}\frac{j}{\eta_0} H^{(2)\prime}_{\nu_m}(k_0\rho_0) + A_m \frac{\psi}{2}\frac{j}{\eta_0} J'_{\nu_m}(k_0\rho_0) = \tilde{I}\frac{\sin \nu_m\phi_0}{\rho_0}. \tag{4.372}$$

The coefficients A_m and C_m thus obey the matrix equation

$$\begin{bmatrix} J_{\nu_m}(k_0\rho_0) & -H^{(2)}_{\nu_m}(k_0\rho_0) \\ J'_{\nu_m}(k_0\rho_0) & -H^{(2)\prime}_{\nu_m}(k_0\rho_0) \end{bmatrix} \begin{bmatrix} A_m \\ C_m \end{bmatrix} = \begin{bmatrix} 0 \\ -j2\tilde{I}\frac{\eta_0}{\psi}\frac{\sin \nu_m\phi_0}{\rho_0} \end{bmatrix}$$

and are

$$A_m = \frac{j2\tilde{I}\frac{\eta_0}{\psi}\frac{\sin \nu_m\phi_0}{\rho_0} H^{(2)}_{\nu_m}(k_0\rho_0)}{H^{(2)\prime}_{\nu_m}(k_0\rho_0) J_{\nu_m}(k_0\rho_0) - J'_{\nu_m}(k_0\rho_0) H^{(2)}_{\nu_m}(k_0\rho_0)},$$

$$C_m = \frac{j2\tilde{I}\frac{\eta_0}{\psi}\frac{\sin \nu_m\phi_0}{\rho_0} J_{\nu_m}(k_0\rho_0)}{H^{(2)\prime}_{\nu_m}(k_0\rho_0) J_{\nu_m}(k_0\rho_0) - J'_{\nu_m}(k_0\rho_0) H^{(2)}_{\nu_m}(k_0\rho_0)}.$$

Using the Wronskian relation (E.93), we replace the denominators in these expressions by $2/(j\pi k_0\rho_0)$:

$$A_m = -\tilde{I}\frac{\eta_0}{\psi}\pi k_0 \sin \nu_m\phi_0 H^{(2)}_{\nu_m}(k_0\rho_0),$$

$$C_m = -\tilde{I}\frac{\eta_0}{\psi}\pi k_0 \sin \nu_m\phi_0 J_{\nu_m}(k_0\rho_0).$$

Hence (4.368) gives

$$\tilde{E}_z(\rho, \phi, \omega) = \begin{cases} -\sum_{n=0}^{\infty} \tilde{I}\frac{\eta_0}{2\psi}\pi k_0\epsilon_n J_{\nu_n}(k_0\rho) H^{(2)}_{\nu_n}(k_0\rho_0) \sin \nu_n\phi \sin \nu_n\phi_0, & \rho < \rho_0, \\ -\sum_{n=0}^{\infty} \tilde{I}\frac{\eta_0}{2\psi}\pi k_0\epsilon_n H^{(2)}_{\nu_n}(k_0\rho) J_{\nu_n}(k_0\rho_0) \sin \nu_n\phi \sin \nu_n\phi_0, & \rho > \rho_0, \end{cases} \tag{4.373}$$

where ϵ_n is Neumann's number (A.132). The magnetic fields can also be found by substituting the coefficients into (4.369) and (4.370).

The fields produced by an impressed plane wave may now be obtained by letting the line source recede to infinity. For large ρ_0 we use the asymptotic form (E.62) and find that

$$\tilde{E}_z(\rho,\phi,\omega) = -\sum_{n=0}^{\infty} \tilde{I} \frac{\eta_0}{2\psi} \pi k_0 \epsilon_n J_{\nu_n}(k_0\rho) \left[\sqrt{\frac{2j}{\pi k_0 \rho_0}} j^{\nu_n} e^{-jk_0\rho_0} \right] \sin\nu_n\phi \sin\nu_n\phi_0, \qquad \rho < \rho_0. \tag{4.374}$$

Since the field of a line source falls off as $\rho_0^{-1/2}$, the amplitude of the impressed field approaches zero as $\rho_0 \to \infty$. We must compensate for the reduction in the impressed field by scaling the amplitude of the current source. To obtain the proper scale factor, we note that the electric field produced at a point $\boldsymbol{\rho}$ by a line source located at $\boldsymbol{\rho}_0$ may be found from (4.345):

$$\tilde{E}_z = -\tilde{I} \frac{k_0\eta_0}{4} H_0^{(2)}(k_0|\boldsymbol{\rho} - \boldsymbol{\rho}_0|) \approx -\tilde{I} \frac{k_0\eta_0}{4} \sqrt{\frac{2j}{\pi k_0 \rho_0}} e^{-jk_0\rho_0} e^{jk\rho\cos(\phi-\phi_0)}, \qquad k_0\rho_0 \gg 1.$$

But if we write this as

$$\tilde{E}_z \approx \tilde{E}_0 e^{j\mathbf{k}\cdot\boldsymbol{\rho}}$$

then the field looks exactly like that produced by a plane wave with amplitude $\tilde{E}_0$ traveling along the wave vector $\mathbf{k} = -k_0\hat{\mathbf{x}}\cos\phi_0 - k_0\hat{\mathbf{y}}\sin\phi_0$. Solving for $\tilde{I}$ in terms of $\tilde{E}_0$ and substituting it back into (4.374), we get the total electric field scattered from a wedge with an impressed TM plane-wave field:

$$\tilde{E}_z(\rho,\phi,\omega) = \frac{2\pi}{\psi} \tilde{E}_0 \sum_{n=0}^{\infty} \epsilon_n j^{\nu_n} J_{\nu_n}(k_0\rho) \sin\nu_n\phi \sin\nu_n\phi_0.$$

Here we interpret the angle ϕ_0 as the incidence angle of the plane wave.

To determine the field produced by an impressed TE plane-wave field, we use a magnetic line source $\tilde{I}_m$ located at ρ_0, ϕ_0 and proceed as above. By analogy with (4.367) we write

$$\tilde{H}_z(\rho,\phi,\omega) = \begin{cases} \sum_\nu \left[A_\nu \sin\nu\phi + B_\nu \cos\nu\phi\right] J_\nu(k_0\rho), & \rho < \rho_0, \\ \sum_\delta \left[C_\delta \sin\delta\phi + D_\delta \cos\delta\phi\right] H_\delta^{(2)}(k_0\rho), & \rho > \rho_0. \end{cases}$$

By (4.351) the tangential electric field is

$$\tilde{E}_\rho(\rho,\phi,\omega) = \begin{cases} -\sum_\nu \left[A_\nu \cos\nu\phi - B_\nu \sin\nu\phi\right] j\frac{Z_{TE}}{k}\frac{1}{\rho}\nu J_\nu(k_0\rho), & \rho < \rho_0, \\ -\sum_\delta \left[C_\delta \cos\delta\phi - D_\delta \sin\delta\phi\right] j\frac{Z_{TE}}{k}\frac{1}{\rho}\delta H_\delta^{(2)}(k_0\rho), & \rho > \rho_0. \end{cases}$$

Application of the boundary conditions on the tangential electric field at $\phi = 0, \psi$ results in $A_\nu = C_\delta = 0$ and $\nu = \delta = \nu_n = n\pi/\psi$, and thus $\tilde{H}_z$ becomes

$$\tilde{H}_z(\rho,\phi,\omega) = \begin{cases} \sum_{n=0}^{\infty} B_n \cos\nu_n\phi J_{\nu_n}(k_0\rho), & \rho < \rho_0, \\ \sum_{n=0}^{\infty} D_n \cos\nu_n\phi H_{\nu_n}^{(2)}(k_0\rho), & \rho > \rho_0. \end{cases} \tag{4.375}$$

Application of the boundary conditions on tangential electric and magnetic fields across the magnetic line source then leads directly to

$$\tilde{H}_z(\rho,\phi,\omega) = \begin{cases} -\sum_{n=0}^{\infty} \tilde{I}_m \frac{\eta_0}{2\psi}\pi k_0 \epsilon_n J_{\nu_n}(k_0\rho) H_{\nu_n}^{(2)}(k_0\rho_0) \cos\nu_n\phi \cos\nu_n\phi_0, & \rho < \rho_0 \\ -\sum_{n=0}^{\infty} \tilde{I}_m \frac{\eta_0}{2\psi}\pi k_0 \epsilon_n H_{\nu_n}^{(2)}(k_0\rho) J_{\nu_n}(k_0\rho_0) \cos\nu_n\phi \cos\nu_n\phi_0, & \rho > \rho_0. \end{cases} \tag{4.376}$$

For a plane-wave impressed field this reduces to

$$\tilde{H}_z(\rho,\phi,\omega) = \frac{2\pi}{\psi}\frac{\tilde{E}_0}{\eta_0}\sum_{n=0}^{\infty}\epsilon_n j^{\nu_n} J_{\nu_n}(k_0\rho)\cos\nu_n\phi\cos\nu_n\phi_0.$$

Behavior of current near a sharp edge. In § 3.2.9 we studied the behavior of static charge near a sharp conducting edge by modeling the edge as a wedge. We can follow the same procedure for frequency-domain fields. Assume that the perfectly conducting wedge shown in Figure 4.26 is immersed in a finite, z-independent impressed field of a sort that will not concern us. A current is induced on the surface of the wedge and we wish to study its behavior as we approach the edge.

Because the field is z-independent, we may consider the superposition of TM and TE fields as was done above to solve for the field scattered by a wedge. For TM polarization, if the source is not located near the edge we may write the total field (impressed plus scattered) in terms of nonuniform cylindrical waves. The form of the field that obeys the boundary conditions at $\phi = 0$ and $\phi = \psi$ is given by (4.368):

$$\tilde{E}_z = \sum_{n=0}^{\infty} A_n \sin\nu_n\phi\, J_{\nu_n}(k_0\rho),$$

where $\nu_n = n\pi/\psi$. Although the A_n depend on the impressed source, the general behavior of the current near the edge is determined by the properties of the Bessel functions. The current on the wedge face at $\phi = 0$ is given by

$$\tilde{\mathbf{J}}_s(\rho,\omega) = \hat{\boldsymbol{\phi}} \times [\hat{\boldsymbol{\phi}}\tilde{H}_\phi + \hat{\boldsymbol{\rho}}\tilde{H}_\rho]|_{\phi=0} = -\hat{\mathbf{z}}\tilde{H}_\rho(\rho,0,\omega).$$

By (4.349) we have the surface current

$$\tilde{\mathbf{J}}_s(\rho,\omega) = -\hat{\mathbf{z}}\frac{1}{Z_{TM}k_0}\sum_{n=0}^{\infty} A_n\frac{\nu_n}{\rho}J_{\nu_n}(k_0\rho).$$

For $\rho \to 0$ the small-argument approximation (E.51) yields

$$\tilde{\mathbf{J}}_s(\rho,\omega) \approx -\hat{\mathbf{z}}\frac{1}{Z_{TM}k_0}\sum_{n=0}^{\infty} A_n\nu_n\frac{1}{\Gamma(\nu_n+1)}\left(\frac{k_0}{2}\right)^{\nu_n}\rho^{\nu_n-1}.$$

The sum is dominated by the smallest power of ρ. Since the $n = 0$ term vanishes we have

$$\tilde{J}_s(\rho,\omega) \sim \rho^{\frac{\pi}{\psi}-1}, \qquad \rho \to 0.$$

For $\psi < \pi$ the current density, which runs parallel to the edge, is unbounded as $\rho \to 0$. A right-angle wedge ($\psi = 3\pi/2$) carries

$$\tilde{J}_s(\rho,\omega) \sim \rho^{-1/3}.$$

Another important case is that of a half-plane ($\psi = 2\pi$) where

$$\tilde{J}_s(\rho,\omega) \sim \frac{1}{\sqrt{\rho}}. \tag{4.377}$$

This square-root edge singularity dominates the behavior of the current flowing parallel to any flat edge, either straight or with curvature large compared to a wavelength, and is useful for modeling currents on complicated structures.

In the case of TE polarization the magnetic field near the edge is, by (4.375),

$$\tilde{H}_z(\rho,\phi,\omega) = \sum_{n=0}^{\infty} B_n \cos\nu_n\phi\, J_{\nu_n}(k_0\rho), \qquad \rho < \rho_0.$$

The current at $\phi = 0$ is

$$\tilde{\mathbf{J}}_s(\rho,\omega) = \hat{\boldsymbol{\phi}} \times \hat{\mathbf{z}}\tilde{H}_z|_{\phi=0} = \hat{\boldsymbol{\rho}}\tilde{H}_z(\rho,0,\omega)$$

or

$$\tilde{\mathbf{J}}_s(\rho,\omega) = \hat{\boldsymbol{\rho}} \sum_{n=0}^{\infty} B_n J_{\nu_n}(k_0\rho).$$

For $\rho \to 0$ we use (E.51) to write

$$\tilde{\mathbf{J}}_s(\rho,\omega) = \hat{\boldsymbol{\rho}} \sum_{n=0}^{\infty} B_n \frac{1}{\Gamma(\nu_n+1)} \left(\frac{k_0}{2}\right)^{\nu_n} \rho^{\nu_n}.$$

The $n = 0$ term gives a constant contribution, so we keep the first two terms to see how the current behaves near $\rho = 0$:

$$\tilde{J}_s \sim b_0 + b_1\rho^{\frac{\pi}{\psi}}.$$

Here b_0 and b_1 depend on the form of the impressed field. For a thin plate where $\psi = 2\pi$ this becomes

$$\tilde{J}_s \sim b_0 + b_1\sqrt{\rho}.$$

This is the companion square-root behavior to (4.377). When perpendicular to a sharp edge, the current grows away from the edge as $\rho^{1/2}$. In most cases $b_0 = 0$ since there is no mechanism to store charge along a sharp edge.

4.11.8 Propagation of spherical waves in a conducting medium

We cannot obtain uniform spherical wave solutions to Maxwell's equations. Any field dependent only on r produces the null field external to the source region, as shown in § 4.11.9. Nonuniform spherical waves are in general complicated and most easily handled using potentials. We consider here only the simple problem of fields dependent on r and θ. These waves display the fundamental properties of all spherical waves: they diverge from a localized source and expand with finite velocity.

Consider a homogeneous, source-free region characterized by $\tilde{\epsilon}(\omega)$, $\tilde{\mu}(\omega)$, and $\tilde{\sigma}(\omega)$. We seek wave solutions that are TEM$_r$ in spherical coordinates ($\tilde{H}_r = \tilde{E}_r = 0$) and ϕ-independent. Thus we write

$$\tilde{\mathbf{E}}(\mathbf{r},\omega) = \hat{\boldsymbol{\theta}}\tilde{E}_\theta(r,\theta,\omega) + \hat{\boldsymbol{\phi}}\tilde{E}_\phi(r,\theta,\omega),$$
$$\tilde{\mathbf{H}}(\mathbf{r},\omega) = \hat{\boldsymbol{\theta}}\tilde{H}_\theta(r,\theta,\omega) + \hat{\boldsymbol{\phi}}\tilde{H}_\phi(r,\theta,\omega).$$

To determine the behavior of these fields we first examine Faraday's law

$$\nabla \times \tilde{\mathbf{E}}(r,\theta,\omega) = \hat{\mathbf{r}}\frac{1}{r\sin\theta}\frac{\partial}{\partial\theta}[\sin\theta\,\tilde{E}_\phi(r,\theta,\omega)] - \hat{\boldsymbol{\theta}}\frac{1}{r}\frac{\partial}{\partial r}[r\tilde{E}_\phi(r,\theta,\omega)] + \hat{\boldsymbol{\phi}}\frac{1}{r}\frac{\partial}{\partial r}[r\tilde{E}_\theta(r,\theta,\omega)]$$
$$= -j\omega\tilde{\mu}\tilde{\mathbf{H}}(r,\theta,\omega). \qquad (4.378)$$

Since we require $\tilde{H}_r = 0$ we must have

$$\frac{\partial}{\partial \theta}[\sin\theta \tilde{E}_\phi(r,\theta,\omega)] = 0.$$

This implies that either $\tilde{E}_\phi \sim 1/\sin\theta$ or $\tilde{E}_\phi = 0$. We choose $\tilde{E}_\phi = 0$ and investigate whether the resulting fields satisfy the remaining Maxwell equations.

In a source-free, homogeneous region of space we have $\nabla\cdot\tilde{\mathbf{D}} = 0$ and thus also $\nabla\cdot\tilde{\mathbf{E}} = 0$. Since we have only a θ-component of the electric field, this requires

$$\frac{1}{r}\frac{\partial}{\partial \theta}\tilde{E}_\theta(r,\theta,\omega) + \frac{\cot\theta}{r}\tilde{E}_\theta(r,\theta,\omega) = 0.$$

From this we see that when $\tilde{E}_\phi = 0$, the field $\tilde{E}_\theta$ must obey

$$\tilde{E}_\theta(r,\theta,\omega) = \frac{\tilde{f}_E(r,\omega)}{\sin\theta}.$$

By (4.378) there is only a ϕ-component of magnetic field which obeys

$$\tilde{H}_\phi(r,\theta,\omega) = \frac{\tilde{f}_H(r,\omega)}{\sin\theta}$$

where

$$-j\omega\tilde{\mu}\tilde{f}_H(r,\omega) = \frac{1}{r}\frac{\partial}{\partial r}[r\tilde{f}_E(r,\omega)]. \tag{4.379}$$

So the spherical wave is TEM to the r-direction.

We can obtain a wave equation for $\tilde{f}_E$ by taking the curl of (4.378) and substituting from Ampere's law:

$$\nabla\times(\nabla\times\tilde{\mathbf{E}}) = -\hat{\boldsymbol{\theta}}\frac{1}{r}\frac{\partial^2}{\partial r^2}(r\tilde{E}_\theta) = \nabla\times\left(-j\omega\tilde{\mu}\tilde{\mathbf{H}}\right) = -j\omega\tilde{\mu}\left(\tilde{\sigma}\tilde{\mathbf{E}} + j\omega\tilde{\epsilon}\tilde{\mathbf{E}}\right),$$

hence

$$\frac{d^2}{dr^2}[r\tilde{f}_E(r,\omega)] + k^2[r\tilde{f}_E(r,\omega)] = 0. \tag{4.380}$$

Here $k = \omega(\tilde{\mu}\tilde{\epsilon}^c)^{1/2}$ is the complex wavenumber and $\tilde{\epsilon}^c = \tilde{\epsilon} + \tilde{\sigma}/j\omega$ is the complex permittivity. The equation for $\tilde{f}_H$ is identical.

The wave equation (4.380) is merely the second-order harmonic differential equation, with two independent solutions chosen from the list

$$\sin kr, \quad \cos kr, \quad e^{-jkr}, \quad e^{jkr}.$$

We find $\sin kr$ and $\cos kr$ useful for describing standing waves between boundaries, and e^{jkr} and e^{-jkr} useful for describing waves propagating in the r-direction. Of these, e^{jkr} represents waves traveling inward while e^{-jkr} represents waves traveling outward. At this point we choose $r\tilde{f}_E = e^{-jkr}$ and thus

$$\tilde{\mathbf{E}}(r,\theta,\omega) = \hat{\boldsymbol{\theta}}\tilde{E}_0(\omega)\frac{e^{-jkr}}{r\sin\theta}. \tag{4.381}$$

By (4.379) we have

$$\tilde{\mathbf{H}}(r,\theta,\omega) = \hat{\boldsymbol{\phi}}\frac{\tilde{E}_0(\omega)}{Z_{TEM}}\frac{e^{-jkr}}{r\sin\theta} \tag{4.382}$$

where $Z_{TEM} = (\tilde{\mu}/\epsilon^c)^{1/2}$ is the complex wave impedance. Since we can also write

$$\tilde{\mathbf{H}}(r,\theta,\omega) = \frac{\hat{\mathbf{r}} \times \tilde{\mathbf{E}}(r,\theta,\omega)}{Z_{TEM}},$$

the field is TEM to the r-direction, which is the direction of wave propagation as shown below.

The wave nature of the field is easily identified by considering the fields in the phasor domain. Letting $\omega \to \check{\omega}$ and setting $k = \beta - j\alpha$ in the exponential function we find that

$$\check{\mathbf{E}}(r,\theta) = \hat{\boldsymbol{\theta}}\check{E}_0 e^{-\alpha r}\frac{e^{-j\beta r}}{r\sin\theta}$$

where $\check{E}_0 = E_0 e^{j\xi^E}$. The time-domain representation may be found using (4.126):

$$\mathbf{E}(r,\theta,t) = \hat{\boldsymbol{\theta}}E_0\frac{e^{-\alpha r}}{r\sin\theta}\cos(\check{\omega}t - \beta r + \xi^E). \tag{4.383}$$

We can identify a surface of constant phase as a locus of points obeying

$$\check{\omega}t - \beta r + \xi^E = C_P \tag{4.384}$$

where C_P is some constant. These surfaces, which are spheres centered on the origin, are called *spherical wavefronts*. Note that surfaces of constant amplitude as determined by

$$\frac{e^{-\alpha r}}{r} = C_A,$$

where C_A is some constant, are also spheres.

The cosine term in (4.383) represents a traveling wave with spherical wavefronts that propagate outward as time progresses. Attenuation is caused by the factor $e^{-\alpha r}$. By differentiation we find that the phase velocity is

$$v_p = \check{\omega}/\beta.$$

The wavelength is given by $\lambda = 2\pi/\beta$.

Our solution is not appropriate for unbounded space since the fields have a singularity at $\theta = 0$. To exclude the z-axis we add conducting cones as mentioned on page 105. This results in a biconical structure that can be used as a transmission line or antenna.

To compute the power carried by a spherical wave, we use (4.381) and (4.382) to obtain the time-average Poynting flux

$$\mathbf{S}_{av} = \frac{1}{2}\operatorname{Re}\{\check{E}_\theta\hat{\boldsymbol{\theta}} \times \check{H}_\phi^*\hat{\boldsymbol{\phi}}\} = \frac{1}{2}\hat{\mathbf{r}}\operatorname{Re}\left\{\frac{1}{Z_{TEM}^*}\right\}\frac{E_0^2}{r^2\sin^2\theta}e^{-2\alpha r}.$$

The power flux is radial and has density inversely proportional to r^2. The time-average power carried by the wave through a spherical surface at r sandwiched between the cones at θ_1 and θ_2 is

$$P_{av}(r) = \frac{1}{2}\operatorname{Re}\left\{\frac{1}{Z_{TEM}^*}\right\}E_0^2 e^{-2\alpha r}\int_0^{2\pi}d\phi\int_{\theta_1}^{\theta_2}\frac{d\theta}{\sin\theta} = \pi F\operatorname{Re}\left\{\frac{1}{Z_{TEM}^*}\right\}E_0^2 e^{-2\alpha r}$$

where

$$F = \ln\left[\frac{\tan(\theta_2/2)}{\tan(\theta_1/2)}\right]. \tag{4.385}$$

This is independent of r when $\alpha = 0$. For lossy media the power decays exponentially because of Joule heating.

We can write the phasor electric field in terms of the transverse gradient of a scalar potential function $\check{\Phi}$:

$$\check{\mathbf{E}}(r,\theta) = \hat{\boldsymbol{\theta}}\check{E}_0 \frac{e^{-jkr}}{r\sin\theta} = -\nabla_t \check{\Phi}(\theta)$$

where

$$\check{\Phi}(\theta) = -\check{E}_0 e^{-jkr} \ln\left(\tan\frac{\theta}{2}\right).$$

By ∇_t we mean the gradient with the r-component excluded. It is easily verified that

$$\check{\mathbf{E}}(r,\theta) = -\nabla_t \check{\Phi}(\theta) = -\hat{\boldsymbol{\theta}}\check{E}_0 \frac{1}{r}\frac{\partial \check{\Phi}(\theta)}{\partial \theta} = \hat{\boldsymbol{\theta}}\check{E}_0 \frac{e^{-jkr}}{r\sin\theta}.$$

Because $\check{\mathbf{E}}$ and $\check{\Phi}$ are related by the gradient, we can define a unique potential difference between the two cones at any radial position r:

$$\check{V}(r) = -\int_{\theta_1}^{\theta_2} \check{\mathbf{E}} \cdot \mathbf{dl} = \check{\Phi}(\theta_2) - \check{\Phi}(\theta_1) = \check{E}_0 F e^{-jkr},$$

where F is given in (4.385). The existence of a unique voltage difference is a property of all transmission line structures operated in the TEM mode. We can similarly compute the current flowing outward on the cone surfaces. The surface current on the cone at $\theta = \theta_1$ is $\check{\mathbf{J}}_s = \hat{\mathbf{n}} \times \check{\mathbf{H}} = \hat{\boldsymbol{\theta}} \times \hat{\boldsymbol{\phi}}\check{H}_\phi = \hat{\mathbf{r}}\check{H}_\phi$, hence

$$\check{I}(r) = \int_0^{2\pi} \check{\mathbf{J}}_s \cdot \hat{\mathbf{r}} r\sin\theta\, d\phi = 2\pi \frac{\check{E}_0}{Z_{TEM}} e^{-jkr}.$$

The ratio of voltage to current at any radius r is the *characteristic impedance* of the biconical transmission line (or, equivalently, the *input impedance* of the biconical antenna):

$$Z = \frac{\check{V}(r)}{\check{I}(r)} = \frac{Z_{TEM}}{2\pi} F.$$

If the material between the cones is lossless (and thus $\tilde{\mu} = \mu$ and $\tilde{\epsilon}^c = \epsilon$ are real), this becomes

$$Z = \frac{\eta}{2\pi} F$$

where $\eta = (\mu/\epsilon)^{1/2}$. The frequency independence of this quantity makes biconical antennas (or their approximate representations) useful for broadband applications.

Finally, the time-average power carried by the wave may be found from

$$P_{av}(r) = \frac{1}{2}\operatorname{Re}\left\{\check{V}(r)\check{I}^*(r)\right\} = \pi F \operatorname{Re}\left\{\frac{1}{Z_{TEM}^*}\right\} E_0^2 e^{-2\alpha r}.$$

The complex power relationship $P = VI^*$ is also a property of TEM guided-wave structures.

4.11.9 Nonradiating sources

We showed in § 2.10.9 that not all time-varying sources produce electromagnetic waves. In fact, a subset of localized sources known as *nonradiating sources* produce no field external to the source region. Devaney and Wolf [54] have shown that all nonradiating time-harmonic sources in an unbounded homogeneous medium can be represented in the form

$$\check{\mathbf{J}}^{nr}(\mathbf{r}) = -\nabla \times \left[\nabla \times \check{\mathbf{f}}(\mathbf{r})\right] + k^2\check{\mathbf{f}}(\mathbf{r}) \tag{4.386}$$

where $\check{\mathbf{f}}$ is any vector field that is continuous, has partial derivatives up to third order, and vanishes outside some localized region V_s. In fact, $\check{\mathbf{E}}(\mathbf{r}) = j\check{\omega}\mu\check{\mathbf{f}}(\mathbf{r})$ is precisely the phasor electric field produced by $\check{\mathbf{J}}^{nr}(\mathbf{r})$. The reasoning is straightforward. Consider the Helmholtz equation (4.203):

$$\nabla \times (\nabla \times \check{\mathbf{E}}) - k^2\check{\mathbf{E}} = -j\check{\omega}\mu\check{\mathbf{J}}.$$

By (4.386) we have

$$\left(\nabla \times \nabla \times -k^2\right)\left[\check{\mathbf{E}} - j\check{\omega}\mu\check{\mathbf{f}}\right] = 0.$$

Since $\check{\mathbf{f}}$ is zero outside the source region it must vanish at infinity. $\check{\mathbf{E}}$ also vanishes at infinity by the radiation condition, and thus the quantity $\check{\mathbf{E}} - j\check{\omega}\mu\check{\mathbf{f}}$ obeys the radiation condition and is a unique solution to the Helmholtz equation throughout all space. Since the Helmholtz equation is homogeneous we have

$$\check{\mathbf{E}} - j\check{\omega}\mu\check{\mathbf{f}} = 0$$

everywhere; since $\check{\mathbf{f}}$ is zero outside the source region, so is $\check{\mathbf{E}}$ (and so is $\check{\mathbf{H}}$).

An interesting special case of nonradiating sources is

$$\check{\mathbf{f}} = \frac{\nabla\check{\Phi}}{k^2}$$

so that

$$\check{\mathbf{J}}^{nr} = -\left(\nabla \times \nabla \times -k^2\right)\frac{\nabla\check{\Phi}}{k^2} = \nabla\check{\Phi}.$$

Using $\check{\Phi}(\mathbf{r}) = \check{\Phi}(r)$, we see that this source describes the current produced by an oscillating spherical balloon of charge (cf., § 2.10.9). Radially-directed, spherically-symmetric sources cannot produce uniform spherical waves, since these sources are of the nonradiating type.

4.12 Interpretation of the spatial transform

Now that we understand the meaning of a Fourier transform on the time variable, let us consider a single transform involving one of the spatial variables. For a transform over z we shall use the notation

$$\psi^z(x, y, k_z, t) \leftrightarrow \psi(x, y, z, t).$$

Here the spatial frequency transform variable k_z has units of m^{-1}. The forward and inverse transform expressions are

$$\psi^z(x, y, k_z, t) = \int_{-\infty}^{\infty} \psi(x, y, z, t) e^{-jk_z z}\, dz, \tag{4.387}$$

$$\psi(x, y, z, t) = \frac{1}{2\pi} \int_{-\infty}^{\infty} \psi^z(x, y, k_z, t) e^{jk_z z}\, dk_z, \tag{4.388}$$

by (A.1) and (A.2).

We interpret (4.388) much as we interpreted the temporal inverse transform (4.2). Any vector component of the electromagnetic field can be decomposed into a continuous superposition of elemental spatial terms $e^{jk_z z}$ with weighting factors $\psi^z(x, y, k_z, t)$. In this case ψ^z is the *spatial frequency spectrum* of ψ. The elemental terms are spatial sinusoids along z with rapidity of variation described by k_z.

As with the temporal transform, ψ^z cannot be arbitrary since ψ must obey a scalar wave equation such as (2.327). For instance, for a source-free region of free space we must have

$$\left(\nabla^2 - \frac{1}{c^2}\frac{\partial}{\partial t^2}\right) \frac{1}{2\pi} \int_{-\infty}^{\infty} \psi^z(x, y, k_z, t) e^{jk_z z}\, dk_z = 0.$$

Decomposing the Laplacian operator as $\nabla^2 = \nabla_t^2 + \partial^2/\partial z^2$ and taking the derivatives into the integrand, we have

$$\frac{1}{2\pi} \int_{-\infty}^{\infty} \left[\left(\nabla_t^2 - k_z^2 - \frac{1}{c^2}\frac{\partial^2}{\partial t^2}\right) \psi^z(x, y, k_z, t)\right] e^{jk_z z}\, dk_z = 0.$$

Hence

$$\left(\nabla_t^2 - k_z^2 - \frac{1}{c^2}\frac{\partial^2}{\partial t^2}\right) \psi^z(x, y, k_z, t) = 0 \tag{4.389}$$

by the Fourier integral theorem.

The elemental component $e^{jk_z z}$ is spatially sinusoidal and occupies all of space. Because such an element could only be created by a source that spans all of space, it is nonphysical when taken by itself. Nonetheless it is often used to represent more complicated fields. If the elemental spatial term is to be used alone, it is best interpreted physically when combined with a temporal decomposition. That is, we consider a two-dimensional transform, with transforms over both time and space. Then the time-domain representation of the elemental component is

$$\phi(z, t) = \frac{1}{2\pi} \int_{-\infty}^{\infty} e^{jk_z z} e^{j\omega t}\, d\omega. \tag{4.390}$$

Before attempting to compute this transform, we should note that if the elemental term is to describe an EM field ψ in a source-free region, it must obey the homogeneous scalar wave equation. Substituting (4.390) into the homogeneous wave equation we have

$$\left(\nabla^2 - \frac{1}{c^2}\frac{\partial^2}{\partial t^2}\right) \frac{1}{2\pi} \int_{-\infty}^{\infty} e^{jk_z z} e^{j\omega t}\, d\omega = 0.$$

Differentiation under the integral sign gives

$$\frac{1}{2\pi} \int_{-\infty}^{\infty} \left[\left(-k_z^2 + \frac{\omega^2}{c^2}\right) e^{jk_z z}\right] e^{j\omega t}\, d\omega = 0$$

and thus

$$k_z^2 = \frac{\omega^2}{c^2} = k^2.$$

Substitution of $k_z = k$ into (4.390) gives the time-domain representation of the elemental component

$$\phi(z,t) = \frac{1}{2\pi}\int_{-\infty}^{\infty} e^{j\omega(t+z/c)}\, d\omega.$$

Finally, using the shifting theorem (A.3) along with (A.4), we have

$$\phi(z,t) = \delta\left(t + \frac{z}{c}\right), \tag{4.391}$$

which we recognize as a uniform plane wave propagating in the $-z$-direction with velocity c. There is no variation in the directions transverse to the direction of propagation and the surface describing a constant argument of the δ-function at any time t is a plane perpendicular to the direction of propagation.

We can also consider the elemental spatial component in tandem with a single sinusoidal steady-state elemental component. The phasor representation of the elemental spatial component is

$$\check{\phi}(z) = e^{jk_z z} = e^{jkz}.$$

This elemental term is a time-harmonic plane wave propagating in the $-z$-direction. Indeed, multiplying by $e^{j\check{\omega}t}$ and taking the real part we get

$$\phi(z,t) = \cos(\check{\omega}t + kz),$$

which is the sinusoidal steady-state analogue of (4.391).

Many authors choose to define the temporal and spatial transforms using differing sign conventions. The temporal transform is defined as in (4.1) and (4.2), but the spatial transform is defined through

$$\psi^z(x,y,k_z,t) = \int_{-\infty}^{\infty} \psi(x,y,z,t)e^{jk_z z}\, dz, \tag{4.392}$$

$$\psi(x,y,z,t) = \frac{1}{2\pi}\int_{-\infty}^{\infty} \psi^z(x,y,k_z,t)e^{-jk_z z}\, dk_z. \tag{4.393}$$

This employs a wave traveling in the positive z-direction as the elemental spatial component, which is quite useful for physical interpretation. We shall adopt this notation in § 4.13. The drawback is that we must alter the formulas from standard Fourier transform tables (replacing k by $-k$) to reflect this difference.

In the following sections we shall show how a spatial Fourier decomposition can be used to solve for the electromagnetic fields in a source-free region of space. By employing the spatial transform we may eliminate one or more spatial variables from Maxwell's equations, making the wave equation easier to solve. In the end we must perform an inversion to return to the space domain. This may be difficult or impossible to do analytically, requiring a numerical Fourier inversion.

4.13 Spatial Fourier decomposition of two-dimensional fields

Consider a homogeneous, source-free region characterized by $\tilde{\epsilon}(\omega)$, $\tilde{\mu}(\omega)$, and $\tilde{\sigma}(\omega)$. We seek z-independent solutions to the frequency-domain Maxwell's equations, using the Fourier transform to represent the spatial dependence. By § 4.11.2 a general two-dimensional field may be decomposed into fields TE and TM to the z-direction. In the TM case $\tilde{H}_z = 0$, and $\tilde{E}_z$ obeys the homogeneous scalar Helmholtz equation (4.208). In the TE case $\tilde{E}_z = 0$, and $\tilde{H}_z$ obeys the homogeneous scalar Helmholtz equation. Since each field component obeys the same equation, we let $\tilde{\psi}(x, y, \omega)$ represent either $\tilde{E}_z(x, y, \omega)$ or $\tilde{H}_z(x, y, \omega)$. Then $\tilde{\psi}$ obeys

$$(\nabla_t^2 + k^2)\tilde{\psi}(x, y, \omega) = 0 \tag{4.394}$$

where ∇_t^2 is the transverse Laplacian (4.209) and $k = \omega(\tilde{\mu}\tilde{\epsilon}^c)^{1/2}$ with $\tilde{\epsilon}^c$ the complex permittivity.

We may choose to represent $\tilde{\psi}(x, y, \omega)$ using Fourier transforms over one or both spatial variables. For application to problems in which boundary values or boundary conditions are specified at a constant value of a single variable (e.g., over a plane), one transform suffices. For instance, we may know the values of the field in the $y = 0$ plane (as we will, for example, when we solve the boundary value problems of § ??). Then we may transform over x and leave the y variable intact so that we may substitute the boundary values.

We adopt (4.392) since the result is more readily interpreted in terms of propagating plane waves. Choosing to transform over x we have

$$\tilde{\psi}^x(k_x, y, \omega) = \int_{-\infty}^{\infty} \tilde{\psi}(x, y, \omega)e^{jk_x x}\, dx, \tag{4.395}$$

$$\tilde{\psi}(x, y, \omega) = \frac{1}{2\pi}\int_{-\infty}^{\infty} \psi^x(k_x, y, \omega)e^{-jk_x x}\, dk_x. \tag{4.396}$$

For convenience in computation or interpretation of the inverse transform, we often regard k_x as a complex variable and perturb the inversion contour into the complex $k_x = k_{xr} + jk_{xi}$ plane. The integral is not altered if the contour is not moved past singularities such as poles or branch points. If the function being transformed has exponential (wave) behavior, then a pole exists in the complex plane; if we move the inversion contour across this pole, the inverse transform does not return the original function. We generally indicate the desire to interpret k_x as complex by indicating that the inversion contour is parallel to the real axis but located in the complex plane at $k_{xi} = \Delta$:

$$\tilde{\psi}(x, y, \omega) = \frac{1}{2\pi}\int_{-\infty+j\Delta}^{\infty+j\Delta} \tilde{\psi}^x(k_x, y, \omega)e^{-jk_x x}\, dk_x. \tag{4.397}$$

Additional perturbations of the contour are allowed provided that the contour is not moved through singularities.

As an example, consider the function

$$u(x) = \begin{cases} 0, & x < 0, \\ e^{-jkx}, & x > 0, \end{cases} \tag{4.398}$$

where $k = k_r + jk_i$ represents a wavenumber. This function has the form of a plane wave propagating in the x-direction and is thus relevant to our studies. If the material through which the wave is propagating is lossy, then $k_i < 0$. The Fourier transform of the function is

$$u^x(k_x) = \int_0^{\infty} e^{-jkx}e^{jk_x x}\, dx = \frac{1}{j(k_x - k)}\left[e^{j(k_{xr}-k_r)x}e^{-(k_{xi}-k_i)x}\right]\Big|_0^{\infty}.$$

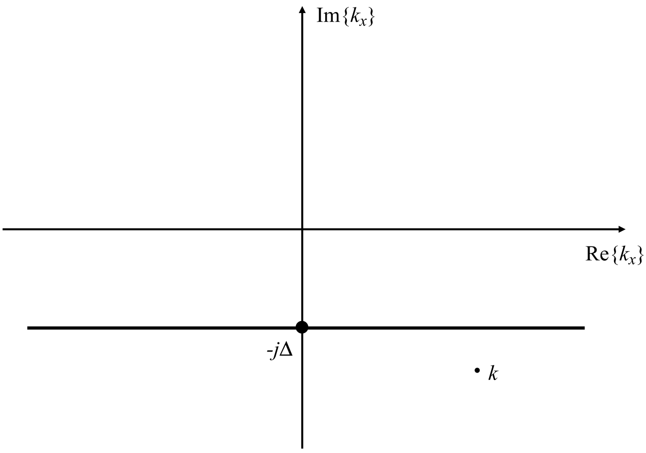

Figure 4.27: Inversion contour for evaluating the spectral integral for a plane wave.

The integral converges if $k_{xi} > k_i$, and the transform is

$$u^x(k_x) = -\frac{1}{j(k_x - k)}.$$

Since $u(x)$ is an exponential function, $u^x(k_x)$ has a pole at $k_x = k$ as anticipated.

To compute the inverse transform we use (4.397):

$$u(x) = \frac{1}{2\pi} \int_{-\infty+j\Delta}^{\infty+j\Delta} \left[-\frac{1}{j(k_x - k)} \right] e^{-jk_x x} \, dk_x. \tag{4.399}$$

We must be careful to choose Δ in such a way that all values of k_x along the inversion contour lead to a convergent forward Fourier transform. Since we must have $k_{xi} > k_i$, choosing $\Delta > k_i$ ensures proper convergence. This gives the inversion contour shown in Figure 4.27, a special case of which is the real axis. We compute the inversion integral using contour integration as in § A.1. We close the contour in the complex plane and use Cauchy's residue theorem (A.14) For $x > 0$ we take $0 > \Delta > k_i$ and close the contour in the lower half-plane using a semicircular contour C_R of radius R. Then the closed contour integral is equal to $-2\pi j$ times the residue at the pole $k_x = k$. As $R \to \infty$ we find that $k_{xi} \to -\infty$ at all points on the contour C_R. Thus the integrand, which varies as $e^{k_{xi}x}$, vanishes on C_R and there is no contribution to the integral. The inversion integral (4.399) is found from the residue at the pole:

$$u(x) = (-2\pi j)\frac{1}{2\pi} \text{Res}_{k_x=k} \left[-\frac{1}{j(k_x - k)} e^{-jk_x x} \right].$$

Since the residue is merely je^{-jkx} we have $u(x) = e^{-jkx}$. When $x < 0$ we choose $\Delta > 0$ and close the contour along a semicircle C_R of radius R in the upper half-plane. Again we find that on C_R the integrand vanishes as $R \to \infty$, and thus the inversion integral (4.399) is given by $2\pi j$ times the residues of the integrand at any poles within the closed contour. This time, however, there are no poles enclosed and thus $u(x) = 0$. We have recovered the original function (4.398) for both $x > 0$ and $x < 0$. Note that if we had erroneously chosen $\Delta < k_i$ we would not have properly enclosed the pole and would have obtained an incorrect inverse transform.

Now that we know how to represent the Fourier transform pair, let us apply the transform to solve (4.394). Our hope is that by representing $\tilde{\psi}$ in terms of a spatial Fourier integral we will make the equation easier to solve. We have

$$(\nabla_t^2 + k^2)\frac{1}{2\pi}\int_{-\infty+j\Delta}^{\infty+j\Delta} \tilde{\psi}^x(k_x, y, \omega)e^{-jk_x x}\, dk_x = 0.$$

Differentiation under the integral sign with subsequent application of the Fourier integral theorem implies that $\tilde{\psi}$ must obey the second-order harmonic differential equation

$$\left[\frac{d^2}{dy^2} + k_y^2\right]\tilde{\psi}^x(k_x, y, \omega) = 0$$

where we have defined the dependent parameter $k_y = k_{yr} + jk_{yi}$ through $k_x^2 + k_y^2 = k^2$. Two independent solutions to the differential equation are $e^{\mp jk_y y}$ and thus

$$\tilde{\psi}(k_x, y, \omega) = A(k_x, \omega)e^{\mp jk_y y}.$$

Substituting this into the inversion integral, we have the solution to the Helmholtz equation:

$$\tilde{\psi}(x, y, \omega) = \frac{1}{2\pi}\int_{-\infty+j\Delta}^{\infty+j\Delta} A(k_x, \omega)e^{-jk_x x}e^{\mp jk_y y}\, dk_x. \qquad (4.400)$$

If we define the wave vector $\mathbf{k} = \hat{\mathbf{x}}k_x \pm \hat{\mathbf{y}}k_y$, we can also write the solution in the form

$$\tilde{\psi}(x, y, \omega) = \frac{1}{2\pi}\int_{-\infty+j\Delta}^{\infty+j\Delta} A(k_x, \omega)e^{-j\mathbf{k}\cdot\boldsymbol{\rho}}\, dk_x \qquad (4.401)$$

where $\boldsymbol{\rho} = \hat{\mathbf{x}}x + \hat{\mathbf{y}}y$ is the two-dimensional position vector.

The solution (4.401) has an important physical interpretation. The exponential term looks exactly like a plane wave with its wave vector lying in the xy-plane. For lossy media the plane wave is nonuniform, and the surfaces of constant phase may not be aligned with the surfaces of constant amplitude (see § 4.11.4). For the special case of a lossless medium we have $k_i \to 0$ and can let $\Delta \to 0$ as long as $\Delta > k_i$. As we perform the inverse transform integral over k_x from $-\infty$ to ∞ we will encounter both the condition $k_x^2 > k^2$ and $k_x^2 \le k^2$. For $k_x^2 \le k^2$ we have

$$e^{-jk_x x}e^{\mp jk_y y} = e^{-jk_x x}e^{\mp j\sqrt{k^2-k_x^2}y}$$

where we choose the upper sign for $y > 0$ and the lower sign for $y < 0$ to ensure that the waves propagate in the $\pm y$-direction, respectively. Thus, in this regime the exponential represents a propagating wave that travels into the half-plane $y > 0$ along a direction which depends on k_x, making an angle ξ with the x-axis as shown in Figure 4.28. For k_x in $[-k, k]$, every possible wave direction is covered, and thus we may think of the inversion integral as constructing the solution to the two-dimensional Helmholtz equation from a continuous superposition of plane waves. The amplitude of each plane wave component is given by $A(k_x, \omega)$, which is often called the *angular spectrum* of the plane waves and

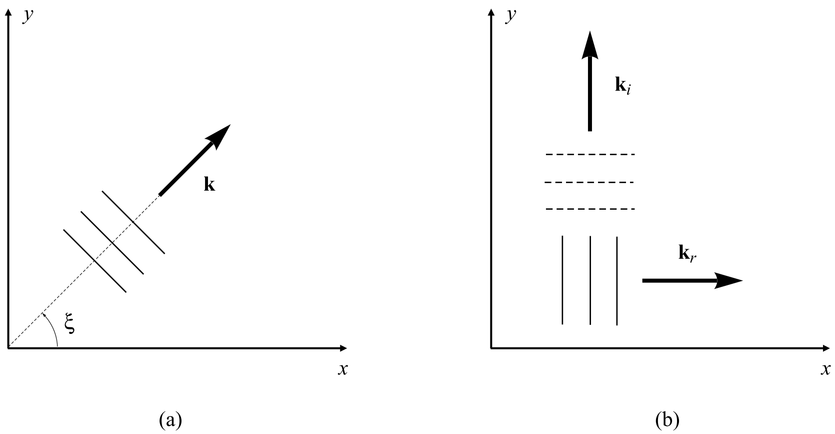

Figure 4.28: Propagation behavior of the angular spectrum for (a) $k_x^2 \le k^2$, (b) $k_x^2 > k^2$.

is determined by the values of the field over the boundaries of the solution region. But this is not the whole picture. The inverse transform integral also requires values of k_x in the intervals $[-\infty, k]$ and $[k, \infty]$. Here we have $k_x^2 > k^2$ and thus

$$e^{-jk_x x} e^{-jk_y y} = e^{-jk_x x} e^{\mp\sqrt{k_x^2 - k^2} y},$$

where we choose the upper sign for $y > 0$ and the lower sign for $y < 0$ to ensure that the field decays along the y-direction. In these regimes we have an evanescent wave, propagating along x but decaying along y, with surfaces of constant phase and amplitude mutually perpendicular (Figure 4.28). As k_x ranges out to ∞, evanescent waves of all possible decay constants also contribute to the plane-wave superposition.

We may summarize the plane-wave contributions by letting $\mathbf{k} = \hat{\mathbf{x}}k_x + \hat{\mathbf{y}}k_y = \mathbf{k}_r + j\mathbf{k}_i$ where

$$\mathbf{k}_r = \begin{cases} \hat{\mathbf{x}}k_x \pm \hat{\mathbf{y}}\sqrt{k^2 - k_x^2}, & k_x^2 < k^2, \\ \hat{\mathbf{x}}k_x, & k_x^2 > k^2, \end{cases}$$

$$\mathbf{k}_i = \begin{cases} 0, & k_x^2 < k^2, \\ \mp\hat{\mathbf{y}}\sqrt{k_x^2 - k^2}, & k_x^2 > k^2, \end{cases}$$

where the upper sign is used for $y > 0$ and the lower sign for $y < 0$.

In many applications, including the half-plane example considered later, it is useful to write the inversion integral in polar coordinates. Letting

$$k_x = k\cos\xi, \qquad k_y = \pm k\sin\xi,$$

where $\xi = \xi_r + j\xi_i$ is a new complex variable, we have $\mathbf{k}\cdot\boldsymbol{\rho} = kx\cos\xi \pm ky\sin\xi$ and $dk_x = -k\sin\xi\, d\xi$. With this change of variables (4.401) becomes

$$\tilde{\psi}(x, y, \omega) = \frac{k}{2\pi}\int_C A(k\cos\xi, \omega)e^{-jkx\cos\xi}e^{\pm jky\sin\xi}\sin\xi\, d\xi. \tag{4.402}$$

Since $A(k_x, \omega)$ is a function to be determined, we may introduce a new function

$$f(\xi, \omega) = \frac{k}{2\pi}A(k_x, \omega)\sin\xi$$

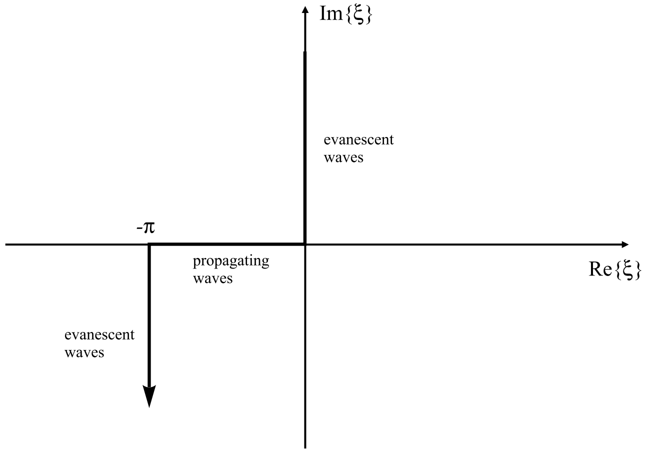

Figure 4.29: Inversion contour for the polar coordinate representation of the inverse Fourier transform.

so that (4.402) becomes

$$\tilde{\psi}(x, y, \omega) = \int_C f(\xi, \omega) e^{-jk\rho\cos(\phi \pm \xi)} \, d\xi \tag{4.403}$$

where $x = \rho\cos\phi$, $y = \rho\sin\phi$, and where the upper sign corresponds to $0 < \phi < \pi$ ($y > 0$) while the lower sign corresponds to $\pi < \phi < 2\pi$ ($y < 0$). In these expressions C is a contour in the complex ξ-plane to be determined. Values along this contour must produce identical values of the integrand as did the values of k_x over $[-\infty, \infty]$ in the original inversion integral. By the identities

$$\cos z = \cos(u + jv) = \cos u \cosh v - j \sin u \sinh v,$$
$$\sin z = \sin(u + jv) = \sin u \cosh v + j \cos u \sinh v,$$

we find that the contour shown in Figure 4.29 provides identical values of the integrand (Problem 4.24). The portions of the contour $[0 + j\infty, 0]$ and $[-\pi, -\pi - j\infty]$ together correspond to the regime of evanescent waves ($k < k_x < \infty$ and $-\infty < k_x < k$), while the segment $[0, -\pi]$ along the real axis corresponds to $-k < k_x < k$ and thus describes contributions from propagating plane waves. In this case ξ represents the propagation angle of the waves.

4.13.1 Boundary value problems using the spatial Fourier representation

The field of a line source. As a first example we calculate the Fourier representation of the field of an electric line source. Assume a uniform line current $\tilde{I}(\omega)$ is aligned along the z-axis in a medium characterized by complex permittivity $\tilde{\epsilon}^c(\omega)$ and permeability $\tilde{\mu}(\omega)$. We separate space into two source-free portions, $y > 0$ and $y < 0$, and write the field in each region in terms of an inverse spatial Fourier transform. Then, by applying the boundary conditions in the $y = 0$ plane, we solve for the angular spectrum of the line source.

Since this is a two-dimensional problem we may decompose the fields into TE and TM sets. For an electric line source we need only the TM set, and write E_z as a superposition of plane waves using (4.400). For $y \gtrless 0$ we represent the field in terms of plane waves traveling in the $\pm y$-direction. Thus

$$\tilde{E}_z(x, y, \omega) = \frac{1}{2\pi} \int_{-\infty+j\Delta}^{\infty+j\Delta} A^+(k_x, \omega) e^{-jk_x x} e^{-jk_y y} \, dk_x, \quad y > 0,$$

$$\tilde{E}_z(x, y, \omega) = \frac{1}{2\pi} \int_{-\infty+j\Delta}^{\infty+j\Delta} A^-(k_x, \omega) e^{-jk_x x} e^{+jk_y y} \, dk_x, \quad y < 0.$$

The transverse magnetic field may be found from the axial electric field using (4.212). We find

$$\tilde{H}_x = -\frac{1}{j\omega\tilde{\mu}} \frac{\partial \tilde{E}_z}{\partial y} \tag{4.404}$$

and thus

$$\tilde{H}_x(x, y, \omega) = \frac{1}{2\pi} \int_{-\infty+j\Delta}^{\infty+j\Delta} A^+(k_x, \omega) \left[\frac{k_y}{\omega\tilde{\mu}} \right] e^{-jk_x x} e^{-jk_y y} \, dk_x, \quad y > 0,$$

$$\tilde{H}_x(x, y, \omega) = \frac{1}{2\pi} \int_{-\infty+j\Delta}^{\infty+j\Delta} A^-(k_x, \omega) \left[-\frac{k_y}{\omega\tilde{\mu}} \right] e^{-jk_x x} e^{+jk_y y} \, dk_x, \quad y < 0.$$

To find the spectra $A^\pm(k_x, \omega)$ we apply the boundary conditions at $y = 0$. Since tangential $\tilde{\mathbf{E}}$ is continuous we have, after combining the integrals,

$$\frac{1}{2\pi} \int_{-\infty+j\Delta}^{\infty+j\Delta} \left[A^+(k_x, \omega) - A^-(k_x, \omega) \right] e^{-jk_x x} \, dk_x = 0,$$

and hence by the Fourier integral theorem

$$A^+(k_x, \omega) - A^-(k_x, \omega) = 0. \tag{4.405}$$

We must also apply $\hat{\mathbf{n}}_{12} \times (\tilde{\mathbf{H}}_1 - \tilde{\mathbf{H}}_2) = \tilde{\mathbf{J}}_s$. The line current may be written as a surface current density using the δ-function, giving

$$-\left[\tilde{H}_x(x, 0^+, \omega) - \tilde{H}_x(x, 0^-, \omega) \right] = \tilde{I}(\omega) \delta(x).$$

By (A.4)

$$\delta(x) = \frac{1}{2\pi} \int_{-\infty}^{\infty} e^{-jk_x x} dk_x.$$

Then, substituting for the fields and combining the integrands, we have

$$\frac{1}{2\pi} \int_{-\infty+j\Delta}^{\infty+j\Delta} \left[A^+(k_x, \omega) + A^-(k_x, \omega) + \frac{\omega\tilde{\mu}}{k_y} \tilde{I}(\omega) \right] e^{-jk_x x} = 0,$$

hence

$$A^+(k_x, \omega) + A^-(k_x, \omega) = -\frac{\omega\tilde{\mu}}{k_y}\tilde{I}(\omega). \tag{4.406}$$

Solution of (4.405) and (4.406) gives the angular spectra

$$A^+(k_x, \omega) = A^-(k_x, \omega) = -\frac{\omega\tilde{\mu}}{2k_y}\tilde{I}(\omega).$$

Substituting this into the field expressions and combining the cases for $y > 0$ and $y < 0$, we find

$$\tilde{E}_z(x, y, \omega) = -\frac{\omega\tilde{\mu}\tilde{I}(\omega)}{2\pi}\int_{-\infty+j\Delta}^{\infty+j\Delta}\frac{e^{-jk_y|y|}}{2k_y}e^{-jk_x x}\,dk_x = -j\omega\tilde{\mu}\tilde{I}(\omega)\tilde{G}(x, y|0, 0; \omega). \tag{4.407}$$

Here $\tilde{G}$ is the spectral representation of the two-dimensional Green's function first found in § 4.11.7, and is given by

$$\tilde{G}(x, y|x', y'; \omega) = \frac{1}{2\pi j}\int_{-\infty+j\Delta}^{\infty+j\Delta}\frac{e^{-jk_y|y-y'|}}{2k_y}e^{-jk_x(x-x')}\,dk_x. \tag{4.408}$$

By duality we have

$$\tilde{H}_z(x, y, \omega) = -\frac{\omega\tilde{\epsilon}^c\tilde{I}_m(\omega)}{2\pi}\int_{-\infty+j\Delta}^{\infty+j\Delta}\frac{e^{-jk_y|y|}}{2k_y}e^{-jk_x x}\,dk_x = -j\omega\tilde{\epsilon}^c\tilde{I}_m(\omega)G(x, y|0, 0; \omega) \tag{4.409}$$

for a magnetic line current $\tilde{I}_m(\omega)$ on the z-axis.

Note that since the earlier expression (4.346) should be equivalent to (4.408), we have the well known identity [33]

$$\frac{1}{\pi}\int_{-\infty+j\Delta}^{\infty+j\Delta}\frac{e^{-jk_y|y|}}{k_y}e^{-jk_x x}\,dk_x = H_0^{(2)}(k\rho).$$

We have not yet specified the contour appropriate for calculating the inverse transform (4.407). We must be careful because the denominator of (4.407) has branch points at $k_y = \sqrt{k^2 - k_x^2} = 0$, or equivalently, $k_x = \pm k = \pm(k_r + jk_i)$. For lossy materials we have $k_i < 0$ and $k_r > 0$, so the branch points appear as in Figure 4.30. We may take the branch cuts outward from these points, and thus choose the inversion contour to lie between the branch points so that the branch cuts are not traversed. This requires $k_i < \Delta < -k_i$. It is natural to choose $\Delta = 0$ and use the real axis as the inversion contour. We must be careful, though, when extending these arguments to the lossless case. If we consider the lossless case to be the limit of the lossy case as $k_i \to 0$, we find that the branch points migrate to the real axis and thus lie on the inversion contour. We can eliminate this problem by realizing that the inversion contour may be perturbed without affecting the value of the integral, as long as it is not made to pass through the branch cuts. If we perturb the inversion contour as shown in Figure 4.30, then as $k_i \to 0$ the branch points do not fall on the contour.

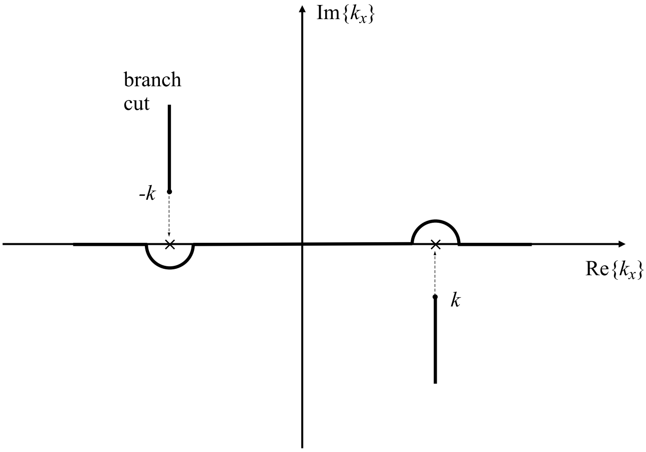

Figure 4.30: Inversion contour in complex k_x-plane for a line source. Dotted arrow shows migration of branch points to real axis as loss goes to zero.

There are many interesting techniques that may be used to compute the inversion integral appearing in (4.407) and in the other expressions we shall obtain in this section. These include direct real-axis integration and closed contour methods that use Cauchy's residue theorem to capture poles of the integrand (which often describe the properties of waves guided by surfaces). Often it is necessary to integrate around the branch cuts in order to meet the conditions for applying the residue theorem. When the observation point is far from the source we may use the method of steepest descents to obtain asymptotic forms for the fields. The interested reader should consult Chew [33], Kong [101], or Sommerfeld [184].

Field of a line source above an interface. Consider a z-directed electric line current located at $y = h$ within a medium having parameters $\tilde{\mu}_1(\omega)$ and $\tilde{\epsilon}_1^c(\omega)$. The $y = 0$ plane separates this region from a region having parameters $\tilde{\mu}_2(\omega)$ and $\tilde{\epsilon}_2^c(\omega)$. See Figure 4.31. The impressed line current source creates an electromagnetic field that induces secondary polarization and conduction currents in both regions. This current in turn produces a secondary field that adds to the primary field of the line source to satisfy the boundary conditions at the interface. We would like to solve for the secondary field and give its sources an image interpretation.

Since the fields are z-independent we may decompose the fields into sets TE and TM to z. For a z-directed impressed source there is a z-component of $\tilde{\mathbf{E}}$, but no z-component of $\tilde{\mathbf{H}}$; hence the fields are entirely specified by the TM set. The impressed source is unaffected by the secondary field, and we may represent the impressed electric field using (4.407):

$$\tilde{E}_z^i(x, y, \omega) = -\frac{\omega\tilde{\mu}_1\tilde{I}(\omega)}{2\pi}\int_{-\infty+j\Delta}^{\infty+j\Delta}\frac{e^{-jk_{y1}|y-h|}}{2k_{y1}}e^{-jk_x x}\,dk_x, \quad y \geq 0 \tag{4.410}$$

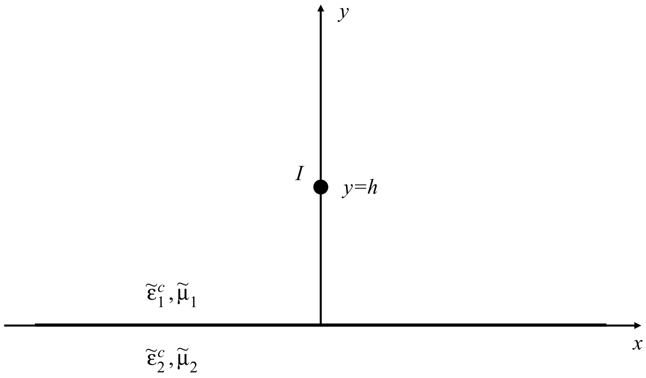

Figure 4.31: Geometry of a z-directed line source above an interface between two material regions.

where $k_{y1} = \sqrt{k_1^2 - k_x^2}$ and $k_1 = \omega(\tilde{\mu}_1\tilde{\epsilon}_1^c)^{1/2}$. From (4.404) we find that

$$\tilde{H}_x^i = -\frac{1}{j\omega\tilde{\mu}_1}\frac{\partial \tilde{E}_z^i}{\partial y} = \frac{\tilde{I}(\omega)}{2\pi}\int_{-\infty+j\Delta}^{\infty+j\Delta} \frac{e^{jk_{y1}(y-h)}}{2} e^{-jk_x x}\, dk_x, \quad 0 \le y < h.$$

The scattered field obeys the homogeneous Helmholtz equation for all $y > 0$, and thus may be written using (4.400) as a superposition of upward-traveling waves:

$$\tilde{E}_{z1}^s(x, y, \omega) = \frac{1}{2\pi}\int_{-\infty+j\Delta}^{\infty+j\Delta} A_1(k_x, \omega)e^{-jk_{y1}y}e^{-jk_x x}\, dk_x,$$

$$\tilde{H}_{x1}^s(x, y, \omega) = \frac{1}{2\pi}\int_{-\infty+j\Delta}^{\infty+j\Delta} \frac{k_{y1}}{\omega\tilde{\mu}_1} A_1(k_x, \omega)e^{-jk_{y1}y}e^{-jk_x x}\, dk_x.$$

Similarly, in region 2 the scattered field may be written as a superposition of downward-traveling waves:

$$\tilde{E}_{z2}^s(x, y, \omega) = \frac{1}{2\pi}\int_{-\infty+j\Delta}^{\infty+j\Delta} A_2(k_x, \omega)e^{jk_{y2}y}e^{-jk_x x}\, dk_x,$$

$$\tilde{H}_{x2}^s(x, y, \omega) = -\frac{1}{2\pi}\int_{-\infty+j\Delta}^{\infty+j\Delta} \frac{k_{y2}}{\omega\tilde{\mu}_2} A_2(k_x, \omega)e^{jk_{y2}y}e^{-jk_x x}\, dk_x,$$

where $k_{y2} = \sqrt{k_2^2 - k_x^2}$ and $k_2 = \omega(\tilde{\mu}_2\tilde{\epsilon}_2^c)^{1/2}$.

We can solve for the angular spectra A_1 and A_2 by applying the boundary conditions at the interface between the two media. From the continuity of total tangential electric field we find that

$$\frac{1}{2\pi}\int_{-\infty+j\Delta}^{\infty+j\Delta} \left[-\frac{\omega\tilde{\mu}_1\tilde{I}(\omega)}{2k_{y1}}e^{-jk_{y1}h} + A_1(k_x, \omega) - A_2(k_x, \omega)\right] e^{-jk_x x}\, dk_x = 0,$$

hence by the Fourier integral theorem

$$A_1(k_x,\omega) - A_2(k_x,\omega) = \frac{\omega\tilde{\mu}_1 \tilde{I}(\omega)}{2k_{y1}} e^{-jk_{y1}h}.$$

The boundary condition on the continuity of $\tilde{H}_x$ yields similarly

$$-\frac{\tilde{I}(\omega)}{2} e^{-jk_{y1}h} = \frac{k_{y1}}{\omega\tilde{\mu}_1} A_1(k_x,\omega) + \frac{k_{y2}}{\omega\tilde{\mu}_2} A_2(k_x,\omega).$$

We obtain

$$A_1(k_x,\omega) = \frac{\omega\tilde{\mu}_1 \tilde{I}(\omega)}{2k_{y1}} R_{TM}(k_x,\omega) e^{-jk_{y1}h},$$

$$A_2(k_x,\omega) = -\frac{\omega\tilde{\mu}_2 \tilde{I}(\omega)}{2k_{y2}} T_{TM}(k_x,\omega) e^{-jk_{y1}h}.$$

Here R_{TM} and $T_{TM} = 1 + R_{TM}$ are reflection and transmission coefficients given by

$$R_{TM}(k_x,\omega) = \frac{\tilde{\mu}_1 k_{y2} - \tilde{\mu}_2 k_{y1}}{\tilde{\mu}_1 k_{y2} + \tilde{\mu}_2 k_{y1}},$$

$$T_{TM}(k_x,\omega) = \frac{2\tilde{\mu}_1 k_{y2}}{\tilde{\mu}_1 k_{y2} + \tilde{\mu}_2 k_{y1}}.$$

These describe the reflection and transmission of each component of the plane-wave spectrum of the impressed field, and thus depend on the parameter k_x. The scattered fields are

$$\tilde{E}^s_{z1}(x,y,\omega) = \frac{\omega\tilde{\mu}_1 \tilde{I}(\omega)}{2\pi} \int_{-\infty+j\Delta}^{\infty+j\Delta} \frac{e^{-jk_{y1}(y+h)}}{2k_{y1}} R_{TM}(k_x,\omega) e^{-jk_x x}\, dk_x, \tag{4.411}$$

$$\tilde{E}^s_{z2}(x,y,\omega) = -\frac{\omega\tilde{\mu}_2 \tilde{I}(\omega)}{2\pi} \int_{-\infty+j\Delta}^{\infty+j\Delta} \frac{e^{jk_{y2}(y-hk_{y1}/k_{y2})}}{2k_{y2}} T_{TM}(k_x,\omega) e^{-jk_x x}\, dk_x. \tag{4.412}$$

We may now obtain the field produced by an electric line source above a perfect conductor. Letting $\tilde{\sigma}_2 \to \infty$ we have $k_{y2} = \sqrt{k_2^2 - k_x^2} \to \infty$ and

$$R_{TM} \to 1, \qquad T_{TM} \to 2.$$

With these, the scattered fields (4.411) and (4.412) become

$$\tilde{E}^s_{z1}(x,y,\omega) = \frac{\omega\tilde{\mu}_1 \tilde{I}(\omega)}{2\pi} \int_{-\infty+j\Delta}^{\infty+j\Delta} \frac{e^{-jk_{y1}(y+h)}}{2k_{y1}} e^{-jk_x x}\, dk_x, \tag{4.413}$$

$$\tilde{E}^s_{z2}(x,y,\omega) = 0. \tag{4.414}$$

Comparing (4.413) to (4.410) we see that the scattered field is exactly the same as that produced by a line source of amplitude $-\tilde{I}(\omega)$ located at $y = -h$. We call this line source the image of the impressed source, and say that the problem of two line sources located

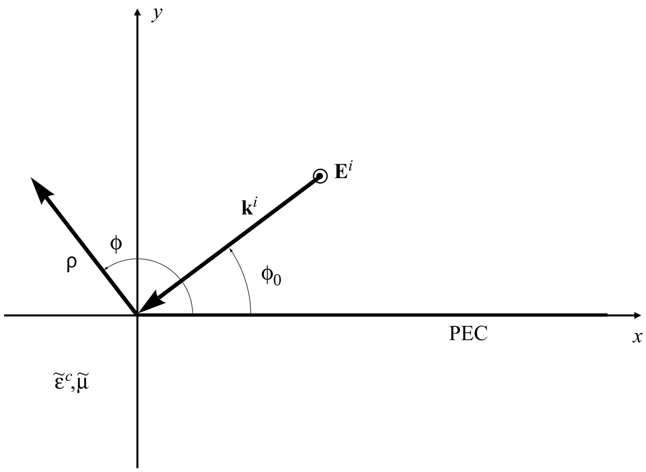

Figure 4.32: Geometry for scattering of a TM plane wave by a conducting half-plane.

symmetrically on the y-axis is equivalent for $y > 0$ to the problem of the line source above a ground plane. The total field is the sum of the impressed and scattered fields:

$$\tilde{E}_z(x, y, \omega) = -\frac{\omega\tilde{\mu}_1\tilde{I}(\omega)}{2\pi} \int_{-\infty+j\Delta}^{\infty+j\Delta} \frac{e^{-jk_{y1}|y-h|} - e^{-jk_{y1}(y+h)}}{2k_{y1}} e^{-jk_x x}\, dk_x, \quad y \geq 0.$$

We can write this in another form using the Hankel-function representation of the line source (4.345):

$$\tilde{E}_z(x, y, \omega) = -\frac{\omega\tilde{\mu}}{4}\tilde{I}(\omega)H_0^{(2)}(k|\boldsymbol{\rho} - \hat{\mathbf{y}}h|) + \frac{\omega\tilde{\mu}}{4}\tilde{I}(\omega)H_0^{(2)}(k|\boldsymbol{\rho} + \hat{\mathbf{y}}h|)$$

where $|\boldsymbol{\rho} \pm \hat{\mathbf{y}}h| = |\rho\hat{\boldsymbol{\rho}} \pm \hat{\mathbf{y}}h| = \sqrt{x^2 + (y \pm h)^2}$.

Interpreting the general case in terms of images is more difficult. Comparing (4.411) and (4.412) with (4.410), we see that each spectral component of the field in region 1 has the form of an image line source located at $y = -h$ in region 2, but that the amplitude of the line source, $R_{TM}\tilde{I}$, depends on k_x. Similarly, the field in region 2 is composed of spectral components that seem to originate from line sources with amplitudes $-T_{TM}\tilde{I}$ located at $y = hk_{y1}/k_{y2}$ in region 1. In this case the amplitude and position of the image line source producing a spectral component are both dependent on k_x.

The field scattered by a half-plane. Consider a thin planar conductor that occupies the half-plane $y = 0$, $x > 0$. We assume the half-plane lies within a slightly lossy medium having parameters $\tilde{\mu}(\omega)$ and $\tilde{\epsilon}^c(\omega)$, and may consider the case of free space as a lossless limit. The half-plane is illuminated by an impressed uniform plane wave with a z-directed electric field (Figure 4.32). The primary field induces a secondary current on the conductor and this in turn produces a secondary field. The total field must obey the boundary conditions at $y = 0$.

Because the z-directed incident field induces a z-directed secondary current, the fields may be described entirely in terms of a TM set. The impressed plane wave may be written as

$$\tilde{\mathbf{E}}^i(\mathbf{r}, \omega) = \hat{\mathbf{z}}\tilde{E}_0(\omega)e^{jk(x\cos\phi_0 + y\sin\phi_0)}$$

where ϕ_0 is the angle between the incident wave vector and the x-axis. By (4.223) we also have

$$\tilde{\mathbf{H}}^i(\mathbf{r},\omega) = \frac{\tilde{E}_0(\omega)}{\eta}(\hat{\mathbf{y}}\cos\phi_0 - \hat{\mathbf{x}}\sin\phi_0)e^{jk(x\cos\phi_0 + y\sin\phi_0)}.$$

The scattered fields may be written in terms of the Fourier transform solution to the Helmholtz equation. It is convenient to use the polar coordinate representation (4.403) to develop the necessary equations. Thus, for the scattered electric field we can write

$$\tilde{E}_z^s(x,y,\omega) = \int_C f(\xi,\omega)e^{-jk\rho\cos(\phi\pm\xi)}\,d\xi. \tag{4.415}$$

By (4.404) the x-component of the magnetic field is

$$\begin{aligned}\tilde{H}_x^s(x,y,\omega) = -\frac{1}{j\omega\tilde{\mu}}\frac{\partial\tilde{E}_z^s}{\partial y} &= -\frac{1}{j\omega\tilde{\mu}}\int_C f(\xi,\omega)\frac{\partial}{\partial y}\left(e^{-jkx\cos\xi}e^{\pm jky\sin\xi}\right)\\ &= -\frac{1}{j\omega\tilde{\mu}}(\pm jk)\int_C f(\xi,\omega)\sin\xi\, e^{-jk\rho\cos(\phi\pm\xi)}\,d\xi.\end{aligned}$$

To find the angular spectrum $f(\xi,\omega)$ and ensure uniqueness of solution, we must apply the boundary conditions over the entire $y = 0$ plane. For $x > 0$ where the conductor resides, the total tangential electric field must vanish. Setting the sum of the incident and scattered fields to zero at $\phi = 0$ we have

$$\int_C f(\xi,\omega)e^{-jkx\cos\xi}\,d\xi = -\tilde{E}_0 e^{jkx\cos\phi_0}, \quad x > 0. \tag{4.416}$$

To find the boundary condition for $x < 0$ we note that by symmetry $\tilde{E}_z^s$ is even about $y = 0$ while $\tilde{H}_x^s$, as the y-derivative of $\tilde{E}_z^s$, is odd. Since no current can be induced in the $y = 0$ plane for $x < 0$, the x-directed scattered magnetic field must be continuous and thus equal to zero there. Hence our second condition is

$$\int_C f(\xi,\omega)\sin\xi\, e^{-jkx\cos\xi}\,d\xi = 0, \quad x < 0. \tag{4.417}$$

Now that we have developed the two equations that describe $f(\xi,\omega)$, it is convenient to return to a rectangular-coordinate-based spectral integral to analyze them. Writing $\xi = \cos^{-1}(k_x/k)$ we have

$$\frac{d}{d\xi}(k\cos\xi) = -k\sin\xi = \frac{dk_x}{d\xi}$$

and

$$d\xi = -\frac{dk_x}{k\sin\xi} = -\frac{dk_x}{k\sqrt{1-\cos^2\xi}} = -\frac{dk_x}{\sqrt{k^2-k_x^2}}.$$

Upon substitution of these relations, the inversion contour returns to the real k_x axis (which may then be perturbed by $j\Delta$). Thus, (4.416) and (4.417) may be written as

$$\int_{-\infty+j\Delta}^{\infty+j\Delta} \frac{f\left(\cos^{-1}\frac{k_x}{k}\right)}{\sqrt{k^2-k_x^2}}e^{-jk_x x}\,dk_x = -\tilde{E}_0 e^{jk_{x0}x}, \quad x > 0, \tag{4.418}$$

$$\int_{-\infty+j\Delta}^{\infty+j\Delta} f\left(\cos^{-1}\frac{k_x}{k}\right)e^{-jk_x x}\,dk_x = 0, \quad x < 0, \tag{4.419}$$

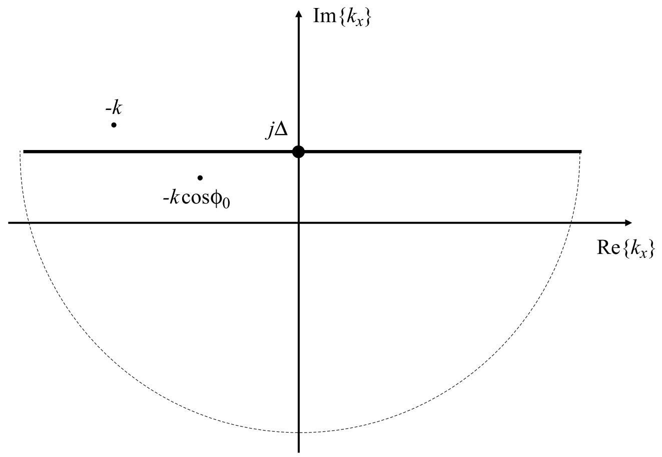

Figure 4.33: Integration contour used to evaluate the function $F(x)$.

where $k_{x0} = k\cos\phi_0$. Equations (4.418) and (4.419) comprise *dual integral equations* for f. We may solve these using an approach called the *Wiener–Hopf technique.*

We begin by considering (4.419). If we close the integration contour in the upper half-plane using a semicircle C_R of radius R where $R \to \infty$, we find that the contribution from the semicircle is

$$\lim_{R\to\infty} \int_{C_R} f\left(\cos^{-1}\frac{k_x}{k}\right) e^{-|x|k_{xi}} e^{j|x|k_{xr}}\, dk_x = 0$$

since $x < 0$. This assumes that f does not grow exponentially with R. Thus

$$\oint_C f\left(\cos^{-1}\frac{k_x}{k}\right) e^{-jk_x x}\, dk_x = 0$$

where C now encloses the portion of the upper half-plane $k_{xi} > \Delta$. By Morera's theorem [110],%citeLePage, the above relation holds if f is regular (contains no singularities or branch points) in this portion of the upper half-plane. We shall assume this and investigate the other properties of f that follow from (4.418).

In (4.418) we have an integral equated to an exponential function. To understand the implications of the equality it is helpful to write the exponential function as an integral as well. Consider the integral

$$F(x) = \frac{1}{2j\pi}\int_{-\infty+j\Delta}^{\infty+j\Delta} \frac{h(k_x)}{h(-k_{x0})}\frac{1}{k_x + k_{x0}} e^{-jk_x x}\, dk_x.$$

Here $h(k_x)$ is some function regular in the region $k_{xi} < \Delta$, with $h(k_x) \to 0$ as $k_x \to \infty$. If we choose Δ so that $-k_{xi} > \Delta > -k_{xi}\cos\theta_0$ and close the contour with a semicircle in the lower half-plane (Figure 4.33), then the contribution from the semicircle vanishes for large radius and thus, by Cauchy's residue theorem, $F(x) = -e^{jk_{x0}x}$. Using this (4.418) can be written as

$$\int_{-\infty+j\Delta}^{\infty+j\Delta} \left[\frac{f\left(\cos^{-1}\frac{k_x}{k}\right)}{\sqrt{k^2 - k_x^2}} - \frac{\tilde{E}_0}{2j\pi}\frac{h(k_x)}{h(-k_{x0})}\frac{1}{k_x + k_{x0}}\right] e^{-jk_x x}\, dk_x = 0.$$

Setting the integrand to zero and using $\sqrt{k^2 - k_x^2} = \sqrt{k - k_x}\sqrt{k + k_x}$, we have

$$\frac{f\left(\cos^{-1}\frac{k_x}{k}\right)}{\sqrt{k - k_x}}(k_x + k_{x0}) = \frac{\tilde{E}_0}{2j\pi}\sqrt{k + k_x}\frac{h(k_x)}{h(-k_{x0})}. \tag{4.420}$$

The left member has a branch point at $k_x = k$ while the right member has a branch point at $k_x = -k$. If we choose the branch cuts as in Figure 4.30 then since f is regular in the region $k_{xi} > \Delta$ the left side of (4.420) is regular there. Also, since $h(k_x)$ is regular in the region $k_{xi} < \Delta$, the right side is regular there. We assert that since the two sides are equal, both sides must be regular in the entire complex plane. By Liouville's theorem [35] if a function is entire (regular in the entire plane) and bounded, then it must be constant. So

$$\frac{f\left(\cos^{-1}\frac{k_x}{k}\right)}{\sqrt{k - k_x}}(k_x + k_{x0}) = \frac{\tilde{E}_0}{2j\pi}\sqrt{k + k_x}\frac{h(k_x)}{h(-k_{x0})} = \text{constant}.$$

We may evaluate the constant by inserting any value of k_x. Using $k_x = -k_{x0}$ on the right we find that

$$\frac{f\left(\cos^{-1}\frac{k_x}{k}\right)}{\sqrt{k - k_x}}(k_x + k_{x0}) = \frac{\tilde{E}_0}{2j\pi}\sqrt{k - k_{x0}}.$$

Substituting $k_x = k\cos\xi$ and $k_{x0} = k\cos\phi_0$ we have

$$f(\xi) = \frac{\tilde{E}_0}{2j\pi}\frac{\sqrt{1 - \cos\phi_0}\sqrt{1 - \cos\xi}}{\cos\xi + \cos\phi_0}.$$

Since $\sin(x/2) = \sqrt{(1 - \cos x)/2}$, we may also write

$$f(\xi) = \frac{\tilde{E}_0}{j\pi}\frac{\sin\frac{\phi_0}{2}\sin\frac{\xi}{2}}{\cos\xi + \cos\phi_0}.$$

Finally, substituting this into (4.415) we have the spectral representation for the field scattered by a half-plane:

$$\tilde{E}_z^s(\rho, \phi, \omega) = \frac{\tilde{E}_0(\omega)}{j\pi}\int_C \frac{\sin\frac{\phi_0}{2}\sin\frac{\xi}{2}}{\cos\xi + \cos\phi_0}e^{-jk\rho\cos(\phi\pm\xi)}\,d\xi. \tag{4.421}$$

The scattered field inversion integral in (4.421) may be rewritten in such a way as to separate geometrical optics (plane-wave) terms from diffraction terms. The diffraction terms may be written using standard functions (modified Fresnel integrals) and for large values of ρ appear as cylindrical waves emanating from a line source at the edge of the half-plane. Interested readers should see James [92] for details.

4.14 Periodic fields and Floquet's theorem

In several practical situations EM waves interact with, or are radiated by, structures spatially periodic along one or more directions. Periodic symmetry simplifies field computation, since boundary conditions need only be applied within one period, or *cell*, of the structure. Examples of situations that lead to periodic fields include the guiding of waves in slow-wave structures such as helices and meander lines, the scattering of plane waves from gratings, and the radiation of waves by antenna arrays. In this section we will study the representation of fields with infinite periodicity as spatial Fourier series.

4.14.1 Floquet's theorem

Consider an environment having spatial periodicity along the z-direction. In this environment the frequency-domain field may be represented in terms of a periodic function $\tilde{\psi}_p$ that obeys

$$\tilde{\psi}_p(x, y, z \pm mL, \omega) = \tilde{\psi}_p(x, y, z, \omega)$$

where m is an integer and L is the spatial period. According to *Floquet's theorem*, if $\tilde{\psi}$ represents some vector component of the field, then the field obeys

$$\tilde{\psi}(x, y, z, \omega) = e^{-j\kappa z}\tilde{\psi}_p(x, y, z, \omega). \tag{4.422}$$

Here $\kappa = \beta - j\alpha$ is a complex wavenumber describing the phase shift and attenuation of the field between the various cells of the environment. The phase shift and attenuation may arise from a wave propagating through a lossy periodic medium (see example below) or may be impressed by a plane wave as it scatters from a periodic surface, or may be produced by the excitation of an antenna array by a distributed terminal voltage. It is also possible to have $\kappa = 0$ as when, for example, a periodic antenna array is driven with all elements in phase.

Because $\tilde{\psi}_p$ is periodic we may expand it in a Fourier series

$$\tilde{\psi}_p(x, y, z, \omega) = \sum_{n=-\infty}^{\infty} \tilde{\psi}_n(x, y, \omega)e^{-j2\pi nz/L}$$

where the $\tilde{\psi}_n$ are found by orthogonality:

$$\tilde{\psi}_n(x, y, \omega) = \frac{1}{L}\int_{-L/2}^{L/2} \tilde{\psi}_p(x, y, z, \omega)e^{j2\pi nz/L}\,dz.$$

Substituting this into (4.422), we have a representation for the field as a Fourier series:

$$\tilde{\psi}(x, y, z, \omega) = \sum_{n=-\infty}^{\infty} \tilde{\psi}_n(x, y, \omega)e^{-j\kappa_n z}$$

where

$$\kappa_n = \beta + 2\pi n/L + j\alpha = \beta_n - j\alpha.$$

We see that within each cell the field consists of a number of constituents called *space harmonics* or *Hartree harmonics*, each with the property of a propagating or evanescent wave. Each has phase velocity

$$v_{pn} = \frac{\omega}{\beta_n} = \frac{\omega}{\beta + 2\pi n/L}.$$

A number of the space harmonics have phase velocities in the $+z$-direction while the remainder have phase velocities in the $-z$-direction, depending on the value of β. However, all of the space harmonics have the same group velocity

$$v_{gn} = \frac{d\omega}{d\beta} = \left(\frac{d\beta_n}{d\omega}\right)^{-1} = \left(\frac{d\beta}{d\omega}\right)^{-1} = v_g.$$

Those space harmonics for which the group and phase velocities are in opposite directions are referred to as *backward waves*, and form the basis of operation of microwave tubes known as "backward wave oscillators."

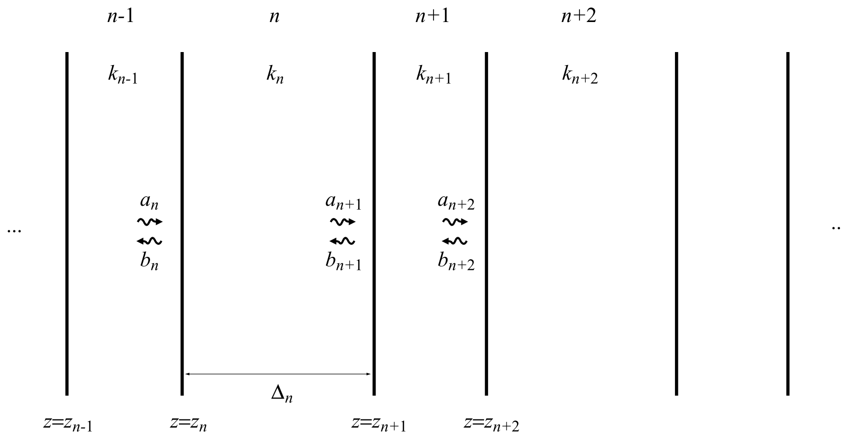

Figure 4.34: Geometry of a periodic stratified medium with each cell consisting of two material layers.

4.14.2 Examples of periodic systems

Plane-wave propagation within a periodically stratified medium. As an example of wave propagation in a periodic structure, let us consider a plane wave propagating within a layered medium consisting of two material layers repeated periodically as shown in Figure 4.34. Each section of two layers is a cell within the periodic medium, and we seek an expression for the propagation constant within the cells, κ.

We developed the necessary tools for studying plane waves within an arbitrary layered medium in § 4.11.5, and can apply them to the case of a periodic medium. In equations (4.305) and (4.306) we have expressions for the wave amplitudes in any region in terms of the amplitudes in the region immediately preceding it. We may write these in matrix form by eliminating one of the variables a_n or b_n from each equation:

$$\begin{bmatrix} T_{11}^{(n)} & T_{12}^{(n)} \\ T_{21}^{(n)} & T_{22}^{(n)} \end{bmatrix} \begin{bmatrix} a_{n+1} \\ b_{n+1} \end{bmatrix} = \begin{bmatrix} a_n \\ b_n \end{bmatrix} \tag{4.423}$$

where

$$\begin{aligned} T_{11}^{(n)} &= \frac{1}{2}\frac{Z_n + Z_{n-1}}{Z_n}\tilde{P}_n^{-1}, \\ T_{12}^{(n)} &= \frac{1}{2}\frac{Z_n - Z_{n-1}}{Z_n}\tilde{P}_n, \\ T_{21}^{(n)} &= \frac{1}{2}\frac{Z_n - Z_{n-1}}{Z_n}\tilde{P}_n^{-1}, \\ T_{22}^{(n)} &= \frac{1}{2}\frac{Z_n + Z_{n-1}}{Z_n}\tilde{P}_n. \end{aligned}$$

Here Z_n represents $Z_{n\perp}$ for perpendicular polarization and $Z_{n\parallel}$ for parallel polarization. The matrix entries are often called *transmission parameters*, and are similar to the parameters used to describe microwave networks, except that in network theory the wave amplitudes are often normalized using the wave impedances.We may use these parameters to describe the cascaded system of two layers:

$$\begin{bmatrix} T_{11}^{(n)} & T_{12}^{(n)} \\ T_{21}^{(n)} & T_{22}^{(n)} \end{bmatrix} \begin{bmatrix} T_{11}^{(n+1)} & T_{12}^{(n+1)} \\ T_{21}^{(n+1)} & T_{22}^{(n+1)} \end{bmatrix} \begin{bmatrix} a_{n+2} \\ b_{n+2} \end{bmatrix} = \begin{bmatrix} a_n \\ b_n \end{bmatrix}.$$

Since for a periodic layered medium the wave amplitudes should obey (4.422), we have

$$\begin{bmatrix} T_{11} & T_{12} \\ T_{21} & T_{22} \end{bmatrix} \begin{bmatrix} a_{n+2} \\ b_{n+2} \end{bmatrix} = \begin{bmatrix} a_n \\ b_n \end{bmatrix} = e^{j\kappa L} \begin{bmatrix} a_{n+2} \\ b_{n+2} \end{bmatrix} \tag{4.424}$$

where $L = \Delta_n + \Delta_{n+1}$ is the period of the structure and

$$\begin{bmatrix} T_{11} & T_{12} \\ T_{21} & T_{22} \end{bmatrix} = \begin{bmatrix} T_{11}^{(n)} & T_{12}^{(n)} \\ T_{21}^{(n)} & T_{22}^{(n)} \end{bmatrix} \begin{bmatrix} T_{11}^{(n+1)} & T_{12}^{(n+1)} \\ T_{21}^{(n+1)} & T_{22}^{(n+1)} \end{bmatrix}.$$

Equation (4.424) is an eigenvalue equation for κ and can be rewritten as

$$\begin{bmatrix} T_{11} - e^{j\kappa L} & T_{12} \\ T_{21} & T_{22} - e^{j\kappa L} \end{bmatrix} \begin{bmatrix} a_{n+2} \\ b_{n+2} \end{bmatrix} = \begin{bmatrix} 0 \\ 0 \end{bmatrix}.$$

This equation only has solutions when the determinant of the matrix vanishes. Expansion of the determinant gives

$$T_{11}T_{22} - T_{12}T_{21} - e^{j\kappa L}(T_{11} + T_{22}) + e^{j2\kappa L} = 0. \tag{4.425}$$

The first two terms are merely

$$T_{11}T_{22} - T_{12}T_{21} = \begin{vmatrix} T_{11} & T_{12} \\ T_{21} & T_{22} \end{vmatrix} = \begin{vmatrix} T_{11}^{(n)} & T_{12}^{(n)} \\ T_{21}^{(n)} & T_{22}^{(n)} \end{vmatrix} \begin{vmatrix} T_{11}^{(n+1)} & T_{12}^{(n+1)} \\ T_{21}^{(n+1)} & T_{22}^{(n+1)} \end{vmatrix}.$$

Since we can show that

$$\begin{vmatrix} T_{11}^{(n)} & T_{12}^{(n)} \\ T_{21}^{(n)} & T_{22}^{(n)} \end{vmatrix} = \frac{Z_{n-1}}{Z_n},$$

we have

$$T_{11}T_{22} - T_{12}T_{21} = \frac{Z_{n-1}}{Z_n}\frac{Z_n}{Z_{n+1}} = 1$$

where we have used $Z_{n-1} = Z_{n+1}$ because of the periodicity of the medium. With this, (4.425) becomes

$$\cos\kappa L = \frac{T_{11} + T_{22}}{2}.$$

Finally, computing the matrix product and simplifying to find $T_{11} + T_{22}$, we have

$$\cos\kappa L = \cos(k_{z,n}\Delta_n)\cos(k_{k,n-1}\Delta_{n-1}) - \\ - \frac{1}{2}\left(\frac{Z_{n-1}}{Z_n} + \frac{Z_n}{Z_{n-1}}\right)\sin(k_{z,n}\Delta_n)\sin(k_{z,n-1}\Delta_{n-1}) \tag{4.426}$$

or equivalently

$$\cos\kappa L = \frac{1}{4}\frac{(Z_{n-1} + Z_n)^2}{Z_n Z_{n-1}}\cos(k_{z,n}\Delta_n + k_{z,n-1}\Delta_{n-1}) - \\ - \frac{1}{4}\frac{(Z_{n-1} - Z_n)^2}{Z_n Z_{n-1}}\cos(k_{z,n}\Delta_n - k_{z,n-1}\Delta_{n-1}). \tag{4.427}$$

Note that both $\pm\kappa$ satisfy this equation, allowing waves with phase front propagation in both the $\pm z$-directions.

We see in (4.426) that even for lossless materials certain values of ω result in $\cos\kappa L > 1$, causing κL to be imaginary and producing evanescent waves. We refer to the frequency ranges over which $\cos\kappa L > 1$ as *stopbands*, and those over which $\cos\kappa L < 1$ as *passbands*. This terminology is used in filter analysis and, indeed, waves propagating in periodic media experience effects similar to those experienced by signals passing through filters.

Field produced by an infinite array of line sources. As a second example, consider an infinite number of z-directed line sources within a homogeneous medium of complex permittivity $\tilde{\epsilon}^c(\omega)$ and permeability $\tilde{\mu}(\omega)$, aligned along the x-axis with separation L such that

$$\tilde{\mathbf{J}}(\mathbf{r},\omega) = \sum_{n=-\infty}^{\infty} \hat{\mathbf{z}}\tilde{I}_n\delta(y)\delta(x-nL).$$

The current on each element is allowed to show a progressive phase shift and attenuation. (Such progression may result from a particular method of driving primary currents on successive elements, or, if the currents are secondary, from their excitation by an impressed field such as a plane wave.) Thus we write

$$\tilde{I}_n = \tilde{I}_0 e^{-j\kappa nL} \tag{4.428}$$

where κ is a complex constant.

We may represent the field produced by the source array as a superposition of the fields of individual line sources found earlier. In particular we may use the Hankel function representation (4.345) or the Fourier transform representation (4.407). Using the latter we have

$$\tilde{E}_z(x,y,\omega) = \sum_{n=-\infty}^{\infty} e^{-j\kappa nL}\left[-\frac{\omega\tilde{\mu}\tilde{I}_0(\omega)}{2\pi}\int_{-\infty+j\Delta}^{\infty+j\Delta}\frac{e^{-jk_y|y|}}{2k_y}e^{-jk_x(x-nL)}\,dk_x\right].$$

Interchanging the order of summation and integration we have

$$\tilde{E}_z(x,y,\omega) = -\frac{\omega\tilde{\mu}\tilde{I}_0(\omega)}{2\pi}\int_{-\infty+j\Delta}^{\infty+j\Delta}\frac{e^{-jk_y|y|}}{2k_y}\left[\sum_{n=-\infty}^{\infty} e^{jn(k_x-\kappa)L}\right]e^{-jk_x x}\,dk_x. \tag{4.429}$$

We can rewrite the sum in this expression using Poisson's sum formula [142].

$$\sum_{n=-\infty}^{\infty} f(x-nD) = \frac{1}{D}\sum_{n=-\infty}^{\infty} F(nk_0)e^{jnk_0x},$$

where $k_0 = 2\pi/D$. Letting $f(x) = \delta(x-x_0)$ in that expression we have

$$\sum_{n=-\infty}^{\infty}\delta\left(x-x_0-n\frac{2\pi}{L}\right) = \frac{L}{2\pi}\sum_{n=-\infty}^{\infty} e^{jnL(x-x_0)}.$$

Substituting this into (4.429) we have

$$\tilde{E}_z(x,y,\omega) = -\frac{\omega\tilde{\mu}\tilde{I}_0(\omega)}{2\pi}\int_{-\infty+j\Delta}^{\infty+j\Delta}\frac{e^{-jk_y|y|}}{2k_y}\left[\sum_{n=-\infty}^{\infty}\frac{2\pi}{L}\delta\left(k_x-\kappa-n\frac{2\pi}{L}\right)\right]e^{-jk_x x}\,dk_x.$$

Carrying out the integral we replace k_x with $\kappa_n = \kappa + 2n\pi/L$, giving

$$\begin{aligned}\tilde{E}_z(x, y, \omega) &= -\omega\tilde{\mu}\tilde{I}_0(\omega) \sum_{n=-\infty}^{\infty} \frac{e^{-jk_{y,n}|y|}e^{-j\kappa_n x}}{2Lk_{y,n}} \\ &= -j\omega\tilde{\mu}\tilde{I}_0(\omega)\tilde{G}_\infty(x, y|0, 0, \omega) \end{aligned} \tag{4.430}$$

where $k_{y,n} = \sqrt{k^2 - \kappa_n^2}$, and where

$$\tilde{G}_\infty(x, y|x', y', \omega) = \sum_{n=-\infty}^{\infty} \frac{e^{-jk_{y,n}|y-y'|}e^{-j\kappa_n(x-x')}}{2jLk_{y,n}} \tag{4.431}$$

is called the *periodic Green's function.*

We may also find the field produced by an infinite array of line sources in terms of the Hankel function representation of a single line source (4.345). Using the current representation (4.428) and summing over the sources, we obtain

$$\tilde{E}_z(\rho, \omega) = -\frac{\omega\tilde{\mu}}{4} \sum_{n=-\infty}^{\infty} \tilde{I}_0(\omega)e^{-j\kappa nL} H_0^{(2)}(k|\boldsymbol{\rho} - \boldsymbol{\rho}_n|) = -j\omega\tilde{\mu}\tilde{I}_0(\omega)\tilde{G}_\infty(x, y|0, 0, \omega)$$

where

$$|\boldsymbol{\rho} - \boldsymbol{\rho}_n| = |\hat{\mathbf{y}}y + \hat{\mathbf{x}}(x - nL)| = \sqrt{y^2 + (x - nL)^2}$$

and where $\tilde{G}_\infty$ is an alternative form of the periodic Green's function

$$\tilde{G}_\infty(x, y|x', y', \omega) = \frac{1}{4j} \sum_{n=-\infty}^{\infty} e^{-j\kappa nL} H_0^{(2)}\left(k\sqrt{(y - y')^2 + (x - nL - x')^2}\right). \tag{4.432}$$

The periodic Green's functions (4.431) and (4.432) produce identical results, but are each appropriate for certain applications. For example, (4.431) is useful for situations in which boundary conditions at constant values of y are to be applied. Both forms are difficult to compute under certain circumstances, and variants of these forms have been introduced in the literature [203].

4.15 Problems

4.1 Beginning with the Kronig–Kramers formulas (4.35)–(4.36), use the even–odd behavior of the real and imaginary parts of $\tilde{\epsilon}^c$ to derive the alternative relations (4.37)–(4.38).

4.2 Consider the complex permittivity dyadic of a magnetized plasma given by (4.88)–(4.91). Show that we may decompose $[\tilde{\bar{\boldsymbol{\epsilon}}}^c]$ as the sum of two matrices

$$[\tilde{\bar{\boldsymbol{\epsilon}}}^c] = [\tilde{\bar{\boldsymbol{\epsilon}}}] + \frac{[\tilde{\bar{\boldsymbol{\sigma}}}]}{j\omega}$$

where $[\tilde{\bar{\boldsymbol{\epsilon}}}]$ and $[\tilde{\bar{\boldsymbol{\sigma}}}]$ are hermitian.

4.3 Show that the Debye permittivity formulas

$$\tilde{\epsilon}'(\omega) - \epsilon_\infty = \frac{\epsilon_s - \epsilon_\infty}{1 + \omega^2\tau^2}, \qquad \tilde{\epsilon}''(\omega) = -\frac{\omega\tau(\epsilon_s - \epsilon_\infty)}{1 + \omega^2\tau^2},$$

obey the Kronig–Kramers relations.

4.4 The frequency-domain duality transformations for the constitutive parameters of an anisotropic medium are given in (4.197). Determine the analogous transformations for the constitutive parameters of a bianisotropic medium.

4.5 Establish the plane-wave identities (B.76)–(B.79) by direct differentiation in rectangular coordinates.

4.6 Assume that sea water has the parameters $\epsilon = 80\epsilon_0$, $\mu = \mu_0$, $\sigma = 4$ S/m, and that these parameters are frequency-independent. Plot the ω–β diagram for a plane wave propagating in this medium and compare to Figure 4.12. Describe the dispersion: is it normal or anomalous? Also plot the phase and group velocities and compare to Figure 4.13. How does the relaxation phenomenon affect the velocity of a wave in this medium?

4.7 Consider a uniform plane wave incident at angle θ_i onto an interface separating two lossless media (Figure 4.18). Assuming perpendicular polarization, write the explicit forms of the total fields in each region under the condition $\theta_i < \theta_c$, where θ_c is the critical angle. Show that the total field in region 1 can be decomposed into a portion that is a pure standing wave in the z-direction and a portion that is a pure traveling wave in the z-direction. Also show that the field in region 2 is a pure traveling wave. Repeat for parallel polarization.

4.8 Consider a uniform plane wave incident at angle θ_i onto an interface separating two lossless media (Figure 4.18). Assuming perpendicular polarization, use the total fields from Problem 4.7 to show that under the condition $\theta_i < \theta_c$ the normal component of the time-average Poynting vector is continuous across the interface. Here θ_c is the critical angle. Repeat for parallel polarization.

4.9 Consider a uniform plane wave incident at angle θ_i onto an interface separating two lossless media (Figure 4.18). Assuming perpendicular polarization, write the explicit forms of the total fields in each region under the condition $\theta_i > \theta_c$, where θ_c is the critical angle. Show that the field in region 1 is a pure standing wave in the z-direction and that the field in region 2 is an evanescent wave. Repeat for parallel polarization.

4.10 Consider a uniform plane wave incident at angle θ_i onto an interface separating two lossless media (Figure 4.18). Assuming perpendicular polarization, use the fields from Problem 4.9 to show that under the condition $\theta_i > \theta_c$ the field in region 1 carries no time-average power in the z-direction, while the field in region 2 carries no time-average power. Here θ_c is the critical angle. Repeat for parallel polarization.

4.11 Consider a uniform plane wave incident at angle θ_i from a lossless material onto a good conductor (Figure 4.18). The conductor has permittivity ϵ_0, permeability μ_0, and conductivity σ. Show that the transmission angle is $\theta_t \approx 0$ and thus the wave in the conductor propagates normal to the interface. Also show that for perpendicular polarization the current per unit width induced by the wave in region 2 is

$$\tilde{\mathbf{K}}(\omega) = \hat{\mathbf{y}}\sigma\tilde{T}_\perp(\omega)\tilde{E}_\perp(\omega)\frac{1-j}{2\beta_2}$$

and that this is identical to the tangential magnetic field at the surface:

$$\tilde{\mathbf{K}}(\omega) = -\hat{\mathbf{z}} \times \tilde{\mathbf{H}}^t|_{z=0}.$$

If we define the *surface impedance* $Z_s(\omega)$ of the conductor as the ratio of tangential electric and magnetic fields at the interface, show that

$$Z_s(\omega) = \frac{1+j}{\sigma\delta} = R_s(\omega) + jX_s(\omega).$$

Then show that the time-average power flux entering region 2 for a monochromatic wave of frequency $\check{\omega}$ is simply

$$\mathbf{S}_{av,2} = \hat{\mathbf{z}}\frac{1}{2}(\check{\mathbf{K}} \cdot \check{\mathbf{K}}^*)R_s.$$

Note that the since the surface impedance is also the ratio of tangential electric field to induced current per unit width in region 2, it is also called the *internal impedance*.

4.12 Consider a parallel-polarized plane wave obliquely incident from a lossless medium onto a multi-layered material as shown in Figure 4.20. Writing the fields in each region n, $0 \le n \le N-1$, as $\tilde{\mathbf{H}}_{\|n} = \tilde{\mathbf{H}}^i_{\|n} + \tilde{\mathbf{H}}^r_{\|n}$ where

$$\tilde{\mathbf{H}}^i_{\|n} = \hat{\mathbf{y}}a_{n+1}e^{-jk_{x,n}x}e^{-jk_{z,n}(z-z_{n+1})},$$
$$\tilde{\mathbf{H}}^r_{\|n} = -\hat{\mathbf{y}}b_{n+1}e^{-jk_{x,n}x}e^{+jk_{z,n}(z-z_{n+1})},$$

and the field in region N as

$$\tilde{\mathbf{H}}_{\|N} = \hat{\mathbf{y}}a_{N+1}e^{-jk_{x,N}x}e^{-jk_{z,N}(z-z_N)},$$

apply the boundary conditions to solve for the wave amplitudes a_{n+1} and b_n in terms of a global reflection coefficient $\tilde{R}_n$, an interfacial reflection coefficient $\Gamma_{n\|}$, and the wave amplitude a_n. Compare your results to those found for perpendicular polarization (4.313) and (4.314).

4.13 Consider a slab of lossless material with permittivity $\epsilon = \epsilon_r\epsilon_0$ and permeability $\mu = \mu_r\mu_0$ located in free space between the planes $z = z_1$ and $z = z_2$. A right-hand circularly-polarized plane wave is incident on the slab at angle θ_i as shown in Figure 4.22. Determine the conditions (if any) under which the reflected wave is: (a) linearly polarized; (b) right-hand or left-hand circularly polarized; (c) right-hand or left-hand elliptically polarized. Repeat for the transmitted wave.

4.14 Consider a slab of lossless material with permittivity $\epsilon = \epsilon_r\epsilon_0$ and permeability μ_0 located in free space between the planes $z = z_1$ and $z = z_2$. A transient, perpendicularly-polarized plane wave is obliquely incident on the slab as shown in Figure 4.22. If the temporal waveform of the incident wave is $E^i_\perp(t)$, find the transient reflected field in region 0 and the transient transmitted field in region 2 in terms of an infinite superposition of amplitude-scaled, time-shifted versions of the incident wave. Interpret each of the first four terms in the reflected and transmitted fields in terms of multiple reflection within the slab.

4.15 Consider a free-space gap embedded between the planes $z = z_1$ and $z = z_2$ in an infinite, lossless dielectric medium of permittivity $\epsilon_r\epsilon_0$ and permeability μ_0. A perpendicularly-polarized plane wave is incident on the gap at angle $\theta_i > \theta_c$ as shown in Figure 4.22. Here θ_c is the critical angle for a plane wave incident on the *single* interface between a lossless dielectric of permittivity $\epsilon_r\epsilon_0$ and free space. Apply the boundary conditions and find the fields in each of the three regions. Find the time-average Poynting vector in region 0 at $z = z_1$, in region 1 at $z = z_2$, and in region 2 at $z = z_2$. Is conservation of energy obeyed?

4.16 A uniform ferrite material has scalar permittivity $\tilde{\epsilon} = \epsilon$ and dyadic permeability $\tilde{\bar{\boldsymbol{\mu}}}$. Assume the ferrite is magnetized along the z-direction and has losses so that its permeability dyadic is given by (4.118). Show that the wave equation for a TEM plane wave of the form

$$\tilde{H}(\mathbf{r}, \omega) = \tilde{H}_0(\omega)e^{-jk_z z}$$

is

$$k_z^2 \tilde{H}_0 = \omega^2 \epsilon \tilde{\bar{\boldsymbol{\mu}}} \cdot \tilde{H}_0$$

where $k_z = \beta - j\alpha$. Find explicit formulas for the two solutions $k_{z\pm} = \beta_\pm - j\alpha_\pm$. Show that when the damping parameter $\alpha \ll 1$, near resonance $\alpha_+ \gg \alpha_-$.

4.17 A time-harmonic, TE-polarized, uniform cylindrical wave propagates in a lossy medium. Assuming $|k\rho| \gg 1$, show that the power per unit length passing through a cylinder of radius ρ is given by

$$P_{av}/l = \text{Re}\left\{Z_{TE}^*\right\} |\check{H}_{z0}|^2 \frac{e^{-2\alpha\rho}}{8|k|}.$$

If the material is lossless, show that the power per unit length passing through a cylinder is independent of the radius and is given by

$$P_{av}/l = \frac{\eta|\check{H}_{z0}|^2}{8k}.$$

4.18 A TM-polarized plane wave is incident on a cylinder made from a perfect electric conductor such that the current induced on the cylinder is given by (4.365). When the cylinder radius is large compared to the wavelength of the incident wave, we may approximate the current using the principle of *physical optics*. This states that the induced current is zero in the "shadow region" where the cylinder is not directly illuminated by the incident wave. Elsewhere, in the "illuminated region," the induced current is given by

$$\tilde{\mathbf{J}}_s = 2\hat{\mathbf{n}} \times \tilde{\mathbf{H}}^i.$$

Plot the current from (4.365) for various values of $k_0 a$ and compare to the current computed from physical optics. How large must $k_0 a$ be for the shadowing effect to be significant?

4.19 The *radar cross section* of a two-dimensional object illuminated by a TM-polarized plane wave is defined by

$$\sigma_{2-D}(\omega, \phi) = \lim_{\rho\to\infty} 2\pi\rho \frac{|\tilde{E}_z^s|^2}{|\tilde{E}_z^i|^2}.$$

This quantity has units of meters and is sometimes called the "scattering width" of the object. Using the asymptotic form of the Hankel function, determine the formula for the radar cross section of a TM-illuminated cylinder made of perfect electric conductor.

Show that when the cylinder radius is small compared to a wavelength the radar cross section may be approximated as

$$\sigma_{2-D}(\omega, \phi) = a\frac{\pi^2}{k_0 a}\frac{1}{\ln^2(0.89k_0 a)}$$

and is thus independent of the observation angle ϕ.

4.20 A TE-polarized plane wave is incident on a material cylinder with complex permittivity $\tilde{\epsilon}^c(\omega)$ and permeability $\tilde{\mu}(\omega)$, aligned along the z-axis in free space. Apply the boundary conditions on the surface of the cylinder and determine the total field both internal and external to the cylinder. Show that as $\tilde{\sigma} \to \infty$ the magnetic field external to the cylinder reduces to (4.366).

4.21 A TM-polarized plane wave is incident on a PEC cylinder of radius a aligned along the z-axis in free space. The cylinder is coated with a material layer of radius b with complex permittivity $\tilde{\epsilon}^c(\omega)$ and permeability $\tilde{\mu}(\omega)$. Apply the boundary conditions on the surface of the cylinder and across the interface between the material and free space and determine the total field both internal and external to the material layer.

4.22 A PEC cylinder of radius a, aligned along the z-axis in free space, is illuminated by a z-directed electric line source $\tilde{I}(\omega)$ located at (ρ_0, ϕ_0). Expand the fields in the regions $a < \rho < \rho_0$ and $\rho > \rho_0$ in terms of nonuniform cylindrical waves, and apply the boundary conditions at $\rho = a$ and $\rho = \rho_0$ to determine the fields everywhere.

4.23 Repeat Problem 4.22 for the case of a cylinder illuminated by a magnetic line source.

4.24 Assuming

$$f(\xi, \omega) = \frac{k}{2\pi}A(k_x, \omega)\sin\xi,$$

use the relations

$$\cos z = \cos(u + jv) = \cos u \cosh v - j \sin u \sinh v,$$
$$\sin z = \sin(u + jv) = \sin u \cosh v + j \cos u \sinh v,$$

to show that the contour in Figure 4.29 provides identical values of the integrand in

$$\tilde{\psi}(x, y, \omega) = \int_C f(\xi, \omega)e^{-jk\rho\cos(\phi\pm\xi)}\,d\xi$$

as does the contour $[-\infty + j\Delta, \infty + j\Delta]$ in

$$\tilde{\psi}(x, y, \omega) = \frac{1}{2\pi}\int_{-\infty+j\Delta}^{\infty+j\Delta} A(k_x, \omega)e^{-jk_x x}e^{\mp jk_y y}\,dk_x. \qquad (4.433)$$

4.25 Verify (4.409) by writing the TE fields in terms of Fourier transforms and applying boundary conditions.

4.26 Consider a z-directed electric line source $\tilde{I}(\omega)$ located on the y-axis at $y = h$. The region $y < 0$ contains a perfect electric conductor. Write the fields in the regions $0 < y < h$ and $y > h$ in terms of the Fourier transform solution to the homogeneous Helmholtz equation. Note that in the region $0 < y < h$ terms representing waves traveling in *both* the $\pm y$-directions are needed, while in the region $y > h$ only terms traveling in the y-direction are needed. Apply the boundary conditions at $y = 0, h$ to determine the spectral amplitudes. Show that the total field may be decomposed into an impressed term identical to (4.410) and a scattered term identical to (4.413).

4.27 Consider a z-directed magnetic line source $\tilde{I}_m(\omega)$ located on the y-axis at $y = h$. The region $y > 0$ contains a material with parameters $\tilde{\epsilon}_1^c(\omega)$ and $\tilde{\mu}_1(\omega)$, while the region $y < 0$ contains a material with parameters $\tilde{\epsilon}_2^c(\omega)$ and $\tilde{\mu}_2(\omega)$. Using the Fourier transform solution to the Helmholtz equation, write the total field for $y > 0$ as the sum of an impressed field of the magnetic line source and a scattered field, and write the field for $y < 0$ as a scattered field. Apply the boundary conditions at $y = 0$ to determine the spectral amplitudes. Can you interpret the scattered fields in terms of images of the line source?

4.28 Consider a TE-polarized plane wave incident on a PEC half-plane located at $y = 0$, $x > 0$. If the incident magnetic field is given by

$$\tilde{\mathbf{H}}^i(\mathbf{r}, \omega) = \hat{\mathbf{z}}\tilde{H}_0(\omega)e^{jk(x\cos\phi_0 + y\sin\phi_0)},$$

determine the appropriate boundary conditions on the fields at $y = 0$. Solve for the scattered magnetic field using the Fourier transform approach.

4.29 Consider the layered medium of Figure 4.34 with alternating layers of free space and perfect dielectric. The dielectric layer has permittivity $4\epsilon_0$ and thickness Δ while the free space layer has thickness 2Δ. Assuming a normally-incident plane wave, solve for $k_0\Delta$ in terms of $\kappa\Delta$, and plot k_0 versus κ, identifying the stop and pass bands. This type of ω–β plot for a periodic medium is named a *Brillouin diagram*, after L. Brillouin who investigated energy bands in periodic crystal lattices [23].

4.30 Consider a periodic layered medium as in Figure 4.34, but with each cell consisting of three different layers. Derive an eigenvalue equation similar to (4.427) for the propagation constant.